

## **INFORMATION TO USERS**

The most advanced technology has been used to photograph and reproduce this manuscript from the microfilm master. UMI films the text directly from the original or copy submitted. Thus, some thesis and dissertation copies are in typewriter face, while others may be from any type of computer printer.

**The quality of this reproduction is dependent upon the quality of the copy submitted.** Broken or indistinct print, colored or poor quality illustrations and photographs, print bleedthrough, substandard margins, and improper alignment can adversely affect reproduction.

In the unlikely event that the author did not send UMI a complete manuscript and there are missing pages, these will be noted. Also, if unauthorized copyright material had to be removed, a note will indicate the deletion.

Oversize materials (e.g., maps, drawings, charts) are reproduced by sectioning the original, beginning at the upper left-hand corner and continuing from left to right in equal sections with small overlaps. Each original is also photographed in one exposure and is included in reduced form at the back of the book.

Photographs included in the original manuscript have been reproduced xerographically in this copy. Higher quality 6" x 9" black and white photographic prints are available for any photographs or illustrations appearing in this copy for an additional charge. Contact UMI directly to order.

# **U·M·I**

University Microfilms International  
A Bell & Howell Information Company  
300 North Zeeb Road, Ann Arbor, MI 48106-1346 USA  
313/761-4700 800/521-0600



**Order Number 9114176**

**The effects of the tubulin-binding drug, colchicine, on the  
electrophysiological aspects of phototransduction in toad rod  
photoreceptors**

**Bert, Robert James, Ph.D.**

**University of Illinois at Urbana-Champaign, 1990**

**Copyright ©1990 by Bert, Robert James. All rights reserved.**

**U·M·I**  
300 N. Zeeb Rd.  
Ann Arbor, MI 48106



**THE EFFECTS OF THE TUBULIN-BINDING DRUG, COLCHICINE,  
ON THE ELECTROPHYSIOLOGICAL ASPECTS OF  
PHOTOTRANSDUCTION IN TOAD ROD PHOTORECEPTORS**

**BY**

**ROBERT JAMES BERT**

**B.S., University of Missouri, 1976**

**THESIS**

**Submitted in partial fulfillment of the requirements  
for the degree of Doctor of Philosophy in Biology  
in the Graduate College of the  
University of Illinois at Urbana-Champaign, 1990**

**Urbana, Illinois**

UNIVERSITY OF ILLINOIS AT URBANA-CHAMPAIGN

THE GRADUATE COLLEGE

JANUARY 1990

WE HEREBY RECOMMEND THAT THE THESIS BY

ROBERT JAMES BERT

ENTITLED THE EFFECTS OF THE TUBULIN-BINDING DRUG, COLCHICINE,  
ON THE ELECTROPHYSIOLOGICAL ASPECTS OF  
PHOTOTRANSDUCTION IN TOAD ROD PHOTORECEPTORS

BE ACCEPTED IN PARTIAL FULFILLMENT OF THE REQUIREMENTS FOR  
THE DEGREE OF DOCTOR OF PHILOSOPHY

*Burles Oakley II*

Director of Thesis Research

*Stanley Fuchs*

Head of Department

Committee on Final Examination†

*Burles Oakley II*

Chairperson

*James M. Royal*

*RA GIMM*

*Joseph S. Margolis*

† Required for doctor's degree but not for master's.

© Copyright by Robert James Bert, 1990

## ABSTRACT

### **The Effects of the Tubulin-binding Drug, Colchicine, on the Electrophysiological Aspects of Phototransduction in Toad Rod Photoreceptors.**

The drug colchicine is well-known in science for its antimitotic activity, and it is well-known in the clinic as a long-standing treatment for acute gout. Colchicine's antimitotic effects are known to result from its specific binding to soluble monomers of tubulin, a cellular protein which polymerizes to form microtubules. Microtubules, in turn, are fundamental to the mitotic process and to cell motility. Tubulin-colchicine binding inhibits stable microtubule formation. Inhibition of microtubule formation resulting in reduced inflammatory cell motility is thought to underlie colchicine's ability to reduce gouty inflammation. At higher concentrations, however, colchicine is also known to affect membrane conductances in neurons and certain cilia. Recent studies have focused on the possibility that this action results from colchicine binding to a unique form of tubulin which is membrane bound, and which may play a role in regulating transduction processes.

The effects of colchicine on toad rod photoreceptor physiology have been studied here, after the chance finding that colchicine affects phototransduction in rods. Colchicine superfusion onto intact retinas hyperpolarized rods, increased their membrane resistance and altered the kinetics of voltage responses to flashes of light. These effects persisted in the presence of pharmacologic agents known to block rod inner segment conductances. Blocking the light-sensitive conductance of rods with bright steps of light alone, however, nearly eliminated the effects of colchicine. It is concluded that colchicine blocks the light-sensitive conductance in toad rod photoreceptors.

Applying colchicine during and after light-stimulation of rods did not stop post-stimulus voltage recovery. Furthermore, colchicine did not block typical rod depolarizations evoked by injecting 3',5'-cyclic guanosine monophosphate, which directly activates the light-sensitive conductance. The effects of colchicine are more consistent with altering  $[cGMP]_i$  levels than with direct deactivation of cGMP-activated channels.

Colchicine alters some aspects of photoreceptor electrophysiology in a manner analogous to intracellular free calcium,  $[Ca^{2+}]_i$ : both increase in the time-to-peak of voltage photoresponses and both block the light-sensitive conductance by lowering  $[cGMP]_i$ . Data presented here show that both colchicine and increased  $[Ca^{2+}]_i$  cause similar changes in the rate of voltage recovery to intracellularly injected cGMP, implying that both produce similar changes in enzyme activity controlling the light-sensitive



conductance. It is hypothesized, then, that colchicine's effects result partly from a colchicine-evoked increase in  $[Ca^{2+}]_i$ .

Data are presented which test this hypothesis. Lowering  $[Ca^{2+}]_i$ , either by injecting large amounts of the  $Ca^{2+}$  buffer, EGTA, or by lowering  $[Ca^{2+}]_o$  in the presence of colchicine, reversed the hyperpolarizing effects, but not the desensitizing effects of colchicine. Conversely, colchicine reversed most of the effects of lowered  $[Ca^{2+}]_o$ . Adding colchicine to low- $Ca^{2+}$  superfusates reversed the effects of  $[Ca^{2+}]_o$  lowered to  $10^{-5}$  -  $10^{-6}$  M, but only partially and transiently reversed the typical desensitization that resulted from lowering  $[Ca^{2+}]_o$  to  $10^{-7}$  -  $10^{-8}$  M. Colchicine did, however, inhibit desensitization when superfused simultaneously with  $10^{-7.5}$  M  $Ca^{2+}$ . Injecting the  $Ca^{2+}$  buffer, EGTA, into photoreceptors is known to depolarize rods. Colchicine superfusion reversibly attenuated this effect. These results are consistent with colchicine's effects resulting from a  $Ca^{2+}$ -agonistic action of the drug or a colchicine-evoked increase in  $[Ca^{2+}]_i$ .

Measurements of  $[Ca^{2+}]_o$  during colchicine superfusion demonstrated colchicine-evoked increases in  $[Ca^{2+}]_o$ , consistent with a colchicine-evoked release of  $Ca^{2+}$  from rod stores. Control solutions known to increase rod  $Ca^{2+}$  permeability or to block  $Ca^{2+}$  extrusion, other plausible explanations for a colchicine-evoked increase in  $[Ca^{2+}]_i$ , caused  $[Ca^{2+}]_o$  to decrease. Calcium permeates the light-sensitive conductance, and the closure of this conductance leads to a transient increase in  $[Ca^{2+}]_o$ . This effect was distinguished from the effects of colchicine by comparing changes evoked by steps of light and steps of light followed by colchicine superfusion. Colchicine produced an additional small increase in  $[Ca^{2+}]_o$  during light steps, consistent with a colchicine-evoked release of intracellular  $Ca^{2+}$ .

The concentration-dependency of colchicine's effects was studied, and the effects of other tubulin-binding drugs were compared to colchicine's. Colchicine's effects were discernible over the range  $10^{-4}$  -  $10^{-2}$  M. Application of 0.5 mM  $\beta$ -lumicolchicine, a low affinity colchicine analog, produced effects similar to colchicine's. The poor solubility of  $\beta$ -lumicolchicine did not permit accurate analysis of higher concentrations. Low doses of the tubulin-binding drug, vincristine, had effects apparently opposite to those of colchicine. These data are inconsistent with microtubule disruption mediating colchicine's effects, but it is still plausible that membrane tubulin may mediate colchicine's effects on rods, as it does in  $\beta$ -adrenergic-sensitive heart and brain cells.

**A dedication.....**

**This thesis is dedicated to the lasting memory of the late Rev. Janis Hopkins. Her tragic suicide on June 21, 1981, scarred me emotionally in countless, untold ways, yet the inspiration she gave me during our years of friendship has carried me this far.**

## ACKNOWLEDGEMENTS

I wish to thank my dedicated wife for her Macintosh wizardry and patience in helping me prepare many of the illustrations and figures of this thesis. As always, I am indebted to her for her support and love.

I thank William McNeil, Wanda Elliot, Joseph Cobb and Robert Cicone for their technical assistance and fighting Illini spirit.

I extend special thanks to Dr. Harold Swartz, Dr. Rhanor Gillette, Dr. William T. Greenough and Peggy Harris for recruiting me to the University of Illinois and the Medical Scholars Program, and I thank Dr. Diane Gottheil for helping me to survive it. I also wish to thank Dr. Gillette for serving as one of my favorite scientific consultants; for serving on my advisory, preliminary exam and thesis committees; for his considerable help and insights; and for his scientific inspiration. I am greatly indebted to him. I wish to thank Dr. Ivan Siegel and Dr. Joseph Malpeli for serving on my thesis committee and for their efforts and comments, which have helped to improve this thesis. I must also thank Dr. John Willis and Dr. Thomas Ebrey for serving on my preliminary exam committee and for their scientific discussions, comments and insights, which not only helped improve this thesis, but also helped me to grow academically. I also extend thanks to Dr. Peter Stein and Dr. Jim Clack at Yale University for their original suggestion that I test colchicine for effects on rod physiology, and for their continued scientific exchange and support.

I wish to thank my advisor, Dr. Burks Oakley, for allowing me to carry out this research in his lab, for several semesters of research assistantships which afforded me the opportunity to pursue this work and my degree, for his many useful comments which have helped improve this work, and for his patience during my years of medical training.

I wish to extend a special thanks to Dr. Fred Delcomyn, whose friendship gave me the strength to carry on through troubled times, and for helping me to keep alive a fascination with science during times when the politics of academics tried to squelch my enthusiasm.

Finally, I wish to thank a few special friends for their support, which allowed me to survive the U of I Graduate Program: William Manzo, Sandy Sobkowiak, Karen Crawford, Ralph Swarr, Dr. William Fenno, Dr. Hulon Creighton, Dr. Bruce Wheeler, Dennis Kucik, Dr. Terri Bert (for making the goal realizable) my mother, father, brother and 3 other sisters. A special thanks to Dr. Nancy-Colter Lathrop, who was instrumental in my career change and Dr. Nadine Kaslow, who helped me pick up the pieces after the death of my friend, Rev. Hopkins.

Finally, thanks to NIH for supporting this work with grant NIHEY004364.

## TABLE OF CONTENTS

	<i>page</i>
LIST OF TABLES.....	x
LIST OF FIGURES.....	xi
LIST OF ILLUSTRATIONS.....	xiv
CHAPTER 1: BACKGROUND.....	1
Section 1.0: Introduction.....	1
Section 1.1: The identity of $g_{hv}$ .....	13
Section 1.2: $Na^+/K^+/Ca^{2+}$ exchange in rod outer segments.....	30
Section 1.3: Calcium regulation in rods.....	31
Section 1.4: Pharmacology of colchicine and other selected tubulin-binding agents.....	37
Section 1.5: Electrophysiological effects of colchicine.....	42
Section 1.6: Ionic currents in the rod inner segment.....	45
CHAPTER 2: METHODS.....	50
Section 2.1: Animal Procurement, Care and Dissection.....	50
Section 2.2: Experimental Setup.....	51
Section 2.3: Solutions.....	57
Section 2.4: Microelectrode Preparation.....	58
Section 2.5: Pressure Delivery System.....	67
Section 2.6: Electrode Placement and Rod Cell Impalement.....	67
Section 2.7: Data Recording Apparatus.....	69
CHAPTER 3: RESULTS.....	71
Section 3.1: Effects of colchicine on $g_{hv}$ .....	71
Section 3.2: Some of colchicine's effects are mimicked by increased $[Ca^{2+}]_i$ .....	83
Section 3.3: Colchicine increases $[Ca^{2+}]_o$ , and probably releases $Ca^{2+}$ from internal stores.....	89

Section 3.4: Effects of colchicine during alteration of $[Ca^{2+}]_o$ .....	125
Section 3.5: Colchicine reverses many effects of low $[Ca^{2+}]_o$ .....	144
Section 3.6: Effects of colchicine on $V_m$ and $V_m$ photoresponses during increased $[Ca^{2+}]_i$ .....	152
Section 3.7: Injections of cGMP during colchicine and high $[Ca^{2+}]_o$ superfusions.....	157
Section 3.8: Tests for possible tubulin or microtubule mediation of colchicine's effects.....	158
CHAPTER 4: DISCUSSION.....	175
Section 4.0: Colchicine blocks $g_{hv}$ .....	175
Section 4.1: Colchicine probably is not a competitive or allosteric inhibitor of cGMP-channel binding.....	177
Section 4.2: Colchicine releases $Ca^{2+}$ from intracellular stores.....	182
Section 4.3: Effects of colchicine not attributable to increased $[Ca^{2+}]_i$ : colchicine may increase GTPase activity of transducin and inhibit the light-evoked enzymatic cascade.....	207
Section 4.4: Tubulin remains a plausible protein-mediator of colchicine's effects on rods.....	209
Section 4.5: Future research concerning colchicine's effects: unanswered questions and plausible experiments.....	214
Section 4.6: Speculations regarding the consequences that these thesis results may have for other systems.....	214
APPENDIX.....	216
BIBLIOGRAPHY.....	223
VITA.....	256

**LIST OF TABLES**

	<i>page</i>
Table 1: Pharmacology and action of proteins regulating $[cGMP]_i$ .....	27
Table 2: Physical and pharmacological properties of rod transmembrane currents.....	47
Table 3: Composition of superfusion solutions in millimolarity.....	53
Table 4: Composition of intracellular injection solutions in millimolarity.....	60

## LIST OF FIGURES

	<i>page</i>
Figure 1: Voltage responses to light flashes ( $V_m$ photoresponses) of varying intensity.....	9
Figure 2: $Ca^{2+}$ ion-selective electrode calibration.....	66
Figure 3: The effects of colchicine on dark-adapted $V_m$ and $V_m$ photoresponses....	73
Figure 4: Measurement of $R_i$ during colchicine superfusion.....	76
Figure 5: The effects of colchicine on $V_m$ and $V_m$ photoresponses in the presence of a cocktail blocking the inner segment conductances.....	79
Figure 6: The effects of 20 mM colchicine on light-stimulated rods.....	82
Figure 7: The effects on rod voltage of treatments raising $[Ca^{2+}]_i$ and altering $[Ca^{2+}]_i$ regulation.....	86
Figure 8: Effects of treatments increasing $[Ca^{2+}]_i$ and altering $[Ca^{2+}]_i$ regulation on $V_m$ photoresponse kinetics.....	88
Figure 9: Light-evoked changes in $V_{Ca^{2+}}$ .....	94
Figure 10: Changes in $V_{Ca^{2+}}$ during constant illumination.....	97
Figure 11: Changes in $V_{Ca^{2+}}$ during steps of illumination of varying lengths and irradiances.....	100
Figure 12: The effects of IBMX on photoreceptor $V_{Ca^{2+}}$ and $V_m$ .....	103
Figure 13: Effect of stimulus interval on light-evoked $V_{Ca^{2+}}$ responses in IBMX.....	105
Figure 14: The effect of $Li^+$ replacement of $Na^+$ on $V_{Ca^{2+}}$ and $V_{Ca^{2+}}$ photoresponses.....	108
Figure 15: Effects of replacing $Na^+$ with $Li^+$ and subsequent addition of IBMX on $V_m$ and $V_m$ photoresponses.....	111
Figure 16: Changes in $V_{Ca^{2+}}$ evoked by $Li^+$ replacement of $Na^+$ and vis a' vis in the presence of IBMX.....	113



	<i>page</i>
Figure 17: Effects of colchicine and colchicine + IBMX on $V_{Ca^{2+}}$ and $V_m$ .....	116
Figure 18: Effects of colchicine on $V_{Ca^{2+}}$ photoresponses.....	118
Figure 19: Effects of colchicine on $V_{Ca^{2+}}$ and $V_{Ca^{2+}}$ photoresponses in the presence of IBMX.....	121
Figure 20: Effects of colchicine on $V_{Ca^{2+}}$ during constant illumination.....	124
Figure 21: The effects of lowering $[Ca^{2+}]_o$ in the presence of colchicine.....	128
Figure 22: The adaptation-like effects of lowering $[Ca^{2+}]_o$ in the presence of colchicine.....	130
Figure 23: The effects of EGTA injections on $V_m$ and $V_m$ photoresponses during superfusion with increased $[Ca^{2+}]_o$ .....	133
Figure 24: The effects of EGTA injections on $V_m$ and $V_m$ photoresponses during superfusion with colchicine.....	136
Figure 25: The effects of increased $[Ca^{2+}]_o$ on the kinetics of EGTA-evoked depolarizations.....	138
Figure 26: The effects of colchicine on the kinetics of EGTA-evoked depolarizations.....	141
Figure 27: Further effects of colchicine on the kinetics of EGTA-evoked depolarizations.....	143
Figure 28: Effects of lowering $[Ca^{2+}]_o$ below $10^{-7}$ M on $V_m$ and $V_m$ photoresponses.....	146
Figure 29: Effects of colchicine on low- $Ca^{2+}$ evoked desensitization.....	149
Figure 30: Effects of colchicine on rods desensitized with low $Ca^{2+}$ .....	151
Figure 31: The effects of colchicine during superfusion with non-desensitizing low- $Ca^{2+}$ concentrations.....	154
Figure 32: Effects of colchicine on $V_m$ and $V_m$ photoresponses during superfusion with increased $[Ca^{2+}]_o$ .....	156

	<i>page</i>
Figure 33: Effects of colchicine and Na <sup>+</sup> replacement by Li <sup>+</sup> on V <sub>m</sub> recovery kinetics from pressure-injected cGMP.....	160
Figure 34: The concentration-dependency of the effects of superfused colchicine on V <sub>m</sub> .....	163
Figure 35: The concentration-dependency of the effects of superfused colchicine on V <sub>m</sub> photoresponses.....	165
Figure 36: The effects of β-lumicolchicine on V <sub>m</sub> and V <sub>m</sub> photoresponses.....	169
Figure 37: Comparative effects of β-lumicolchicine and colchicine on V <sub>m</sub> and V <sub>m</sub> photoresponses in the same rod.....	171
Figure 38: The effects of vincristine on V <sub>m</sub> , V <sub>m</sub> photoresponses and cGMP-evoked depolarizations.....	174

**LIST OF ILLUSTRATIONS**

	<i>page</i>
Illustration 1: Histology of rod photoreceptors.....	4
Illustration 2: Characterized ionic currents in rod photoreceptors.....	6
Illustration 3: Light-evoked activation and the deactivation of the cGMP enzyme cascade .....	24
Illustration 4: Negative feedback regulation of Ca <sup>2+</sup> on the light-sensitive conductance.....	34
Illustration 5: Molecular structures of selected tubulin-binding drugs.....	40
Illustration 6: Superfusion apparatus and retinal mounting chamber.....	56
Illustration 7: Rate plots of the equation governing cGMP formation by guanylate cyclase and degradation by phosphodiesterase.....	199

## CHAPTER 1

### BACKGROUND

#### **Section 1.0: *Introduction***

The process by which the vertebrate nervous system codes information about the external world begins by transducing important physical parameters into graded changes in the membrane voltage,  $V_m$ , of specialized cells. These cells, called receptors, are commonly grouped according to the type of energy to which they preferentially respond. Typical groupings include mechanoreceptors, chemoreceptors, thermoreceptors, electroreceptors and photoreceptors. The mechanisms responsible for transduction in these cells occur at the molecular level, and are currently under intense investigation. Although each group of receptors is highly specialized in structure and function, there are similarities in their mechanisms of action. It is hoped that elucidating the mechanisms involved in transduction in one type of receptor will also give clues to the mechanisms of action in the others.

Many receptors also share a common property known as adaptation. The phenomena of adaptation allows a receptor to remain sensitive to small changes in stimulus intensity despite relatively intense background stimulation. Without adaptation, the range of intensities over which a receptor responds must be balanced against sensitivity to small changes in the environment, i.e., the organism would sacrifice sensitivity to small stimulus changes in order to increase the response range. It is often changes in external stimuli, and not the absolute stimulus strength, that contains the information that is important for the survival of an organism. Therefore, receptors have evolved the property of adapting to non-changing external stimuli in order to increase sensitivity, yet maintain a wide response range. In receptors that demonstrate adaptation, the mechanism causing the cell to adapt to background stimulation must be linked to the mechanism of transduction.

Photoreceptors exhibit this property of adaptation, which can be studied in conjunction with transduction.

### *1.0.1: Phototransduction*

Transduction in vertebrate rod photoreceptors has been particularly well-studied for the past fifteen years. Currently, studies are trying to correlate the biochemistry of phototransduction with electrophysiological events, although the biochemical and electrophysiological studies have usually been conducted in different animal genera. Electrophysiological studies of rods have traditionally used amphibian photoreceptors, because they are large and can be easily penetrated with microelectrodes, which eases the technical difficulties of recording voltages from these cells. Biochemical studies of transduction, however, have mainly used bovine photoreceptors, since slaughterhouses can provide the relatively cheap supply of large numbers of retinas needed for enzyme purification. Cross studies indicate that the functional mechanisms of the different vertebrate genera are very similar. It has been possible, then, to correlate most of the biochemical findings in bovine receptors with the electrophysiological studies in amphibians, which has allowed the molecular biology and biochemistry leading to the electrophysiological events of transduction to be elucidated. Since the experiments of this thesis are electrophysiological in nature, toad rods were used for the investigations.

Rods are highly specialized, both structurally and functionally, and provide an excellent model system for studying transduction. Most, if not all, of the current-carrying transport mechanisms in rods have been classified and characterized by their ion specificities, voltage sensitivities and pharmacology. The transmembrane currents of rods are compartmentalized into two anatomical subdivisions of the cell. A light-sensitive current (Hagins et al, 1970; Korenbrot & Cone, 1972; Baylor et al, 1979) and a sodium-calcium exchange current (Yau & Nakatani, 1984a) are located in the rod outer segment (see Illus. 1 & 2), which also contains the overwhelming majority of the photo-sensitive pigment, rhodopsin (for a review, see Dratz & Hargrave, 1983). Most other voltage-sensitive and

**Illustration 1. *Histology of rod photoreceptors.***

The anatomical regions of the retina are indicated by the labeled vertical line on the far left. The anatomical subregions of the rod are labeled by the adjacent vertical lines. Important organelles are labeled by the arrows.

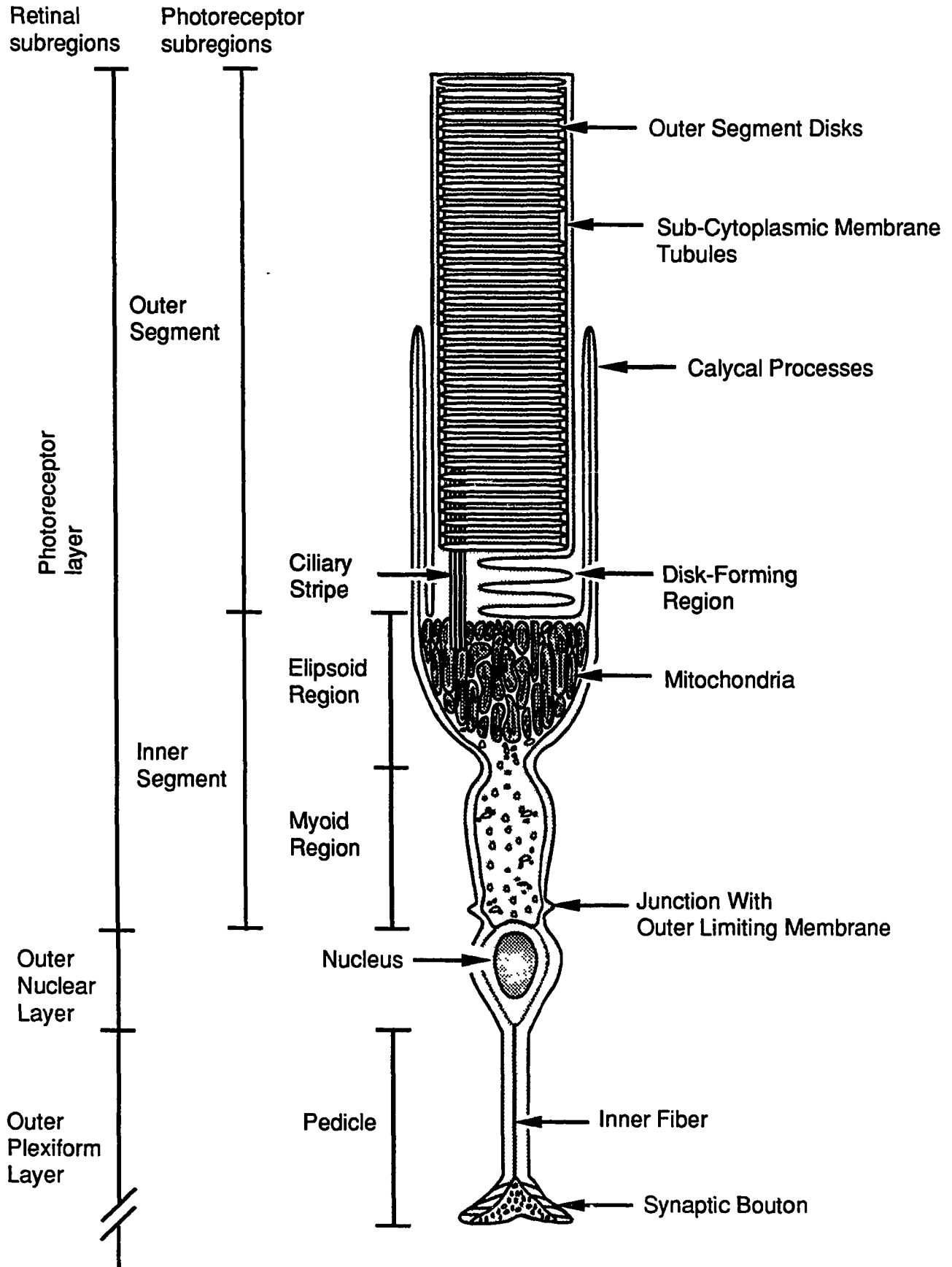


Illustration 1: Histology of rod photoreceptors

**Illustration 2. *Characterized ionic currents in rod photoreceptors.***

Rod photoreceptor currents are notably specialized. They occur on the cells in an asymmetric fashion (Baylor et al, 1984), such that the ionic fluxes across the cell membrane are very different in the rod outer segment and the rod inner segment. The differences produce an intracellular current along the long axis of the rod, which sets up an extracellular current, known as the dark current,  $I_D$ , (Yoshikami & Hagins, 1973). This dark current is shown in the inset. Individual transmembrane currents, characterized or suspected, are shown in the main diagram. Characteristics of the currents are listed in Table 2.



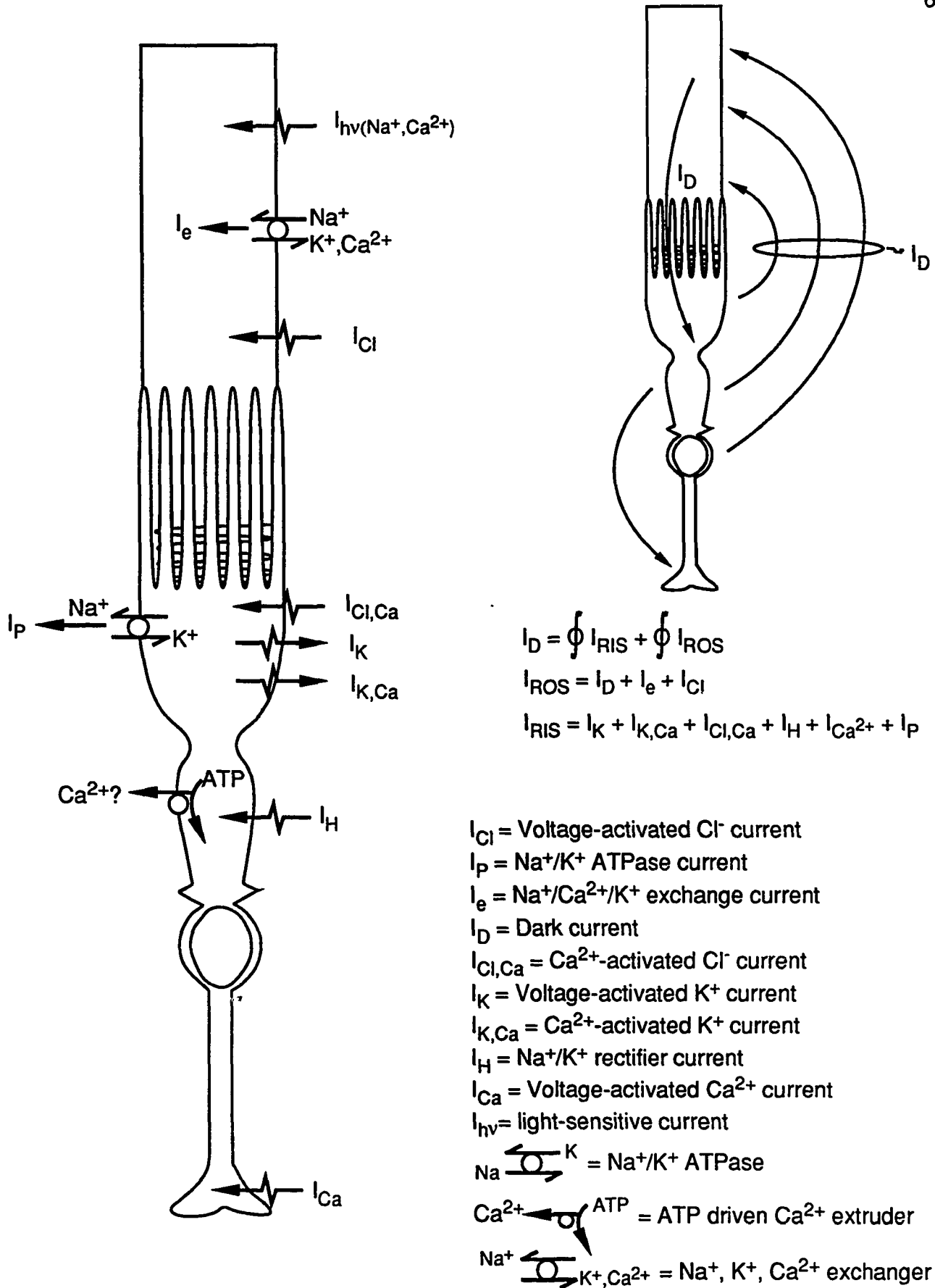


Illustration 2: Characterized ionic currents in rod photoreceptors

calcium-sensitive currents are thought to be located in various regions of the anatomical subdivision known as the rod inner segment (Bader et al, 1982; Baylor et al, 1984).

When the photoresponsive outer segment is exposed to a flash of light, the rod  $V_m$  undergoes a transient hyperpolarization ( $V_m$  photoresponse) for several seconds (Barloff & Norton, 1965; Toyoda et al, 1970; Swartz, 1973). The amplitude, duration and shape of the resulting voltage change is related to the intensity and duration of the flash (Sillman & Tomita, 1969; Brown & Pinto, 1974; Capovilla et al, 1981; Korenbrot & Cone, 1972; Yoshikami & Hagins, 1973; Woodruff et al, 1982; see also Fig. 1). Rod hyperpolarization begins with the decrement of a unique inward current present in dark-adapted cells. This current is referred to as the light-sensitive current. The light-sensitive current results from the net inward movement of cations through a special type of protein channel that also binds 3'-5' cyclic guanosine monophosphate, cGMP (Fesenko et al, 1985; Yau & Nakatani, 1985b; Matthews, 1986; Matesic & Liebman, 1987). The dominant cations traversing the channels in the inward direction under physiological conditions are  $\text{Na}^+$  and  $\text{Ca}^{2+}$  (Yau & Nakatani, 1984b), and the binding of cGMP to the channel protein increases the proportion of time the channels are open (Matthews & Watanabe, 1988).

When photons of light strike a rod cell, the free cGMP level in the cell,  $[\text{cGMP}]_i$ , decreases as the activity of the enzymes regulating  $[\text{cGMP}]_i$  change (Cote et al, 1984). This results in a net decrease in the number of cGMP-bound channels (Matthews, 1986; Matthews & Watanabe, 1987, 1988). Macroscopically, this can be measured as a decrease in conductance (Bader et al, 1979). This cGMP-sensitive conductance of the rod outer segment is now known to be synonymous with the light-sensitive conductance,  $g_{hv}$  (Matthews, 1986; Matthews & Watanabe, 1987, 1988). Thus cGMP controls  $g_{hv}$ .

Experiments have elucidated the major biochemical pathways regulating  $[\text{cGMP}]_i$ . The enzymatic pathways regulating  $[\text{cGMP}]_i$  are sensitive to both light and intracellular free  $\text{Ca}^{2+}$ ,  $[\text{Ca}^{2+}]_i$  (for a review, see Fung, 1989). Intracellular cGMP, in turn, helps to regulate  $[\text{Ca}^{2+}]_i$  in the rod outer segment, since the major  $\text{Ca}^{2+}$  influx into the rod outer segment is

**Figure 1.** Voltage responses to light flashes ( $V_m$  photoresponses) of varying intensity.

**A.** The record labeled  $V_m$  shows the intracellular voltage of a rod recorded with a single-barrel, micropipette electrode during stimulation with flashes of light (100 ms). The pulses in the record labeled LM mark the times of stimulation. The heights of the pulses indicate the log of the relative intensity of the flashes (C1 & B1: 0.98 quanta/rod/flash; C2 & B2: 9.8 rod/quanta/flash; C3 & B3: 98 quanta/rod/flash; C4 & B4: 980 quanta/rod/flash; B5: 9800 quanta/rod/flash).

**B.** The photoresponses B1-B5 are replotted on expanded time and voltage scales.

**C.** The photoresponses C1-C4 are replotted on expanded time and voltage scales.

The responses in B and C are compared to show that the amplitudes and durations of the responses were not affected by the intensity of the previous flash.

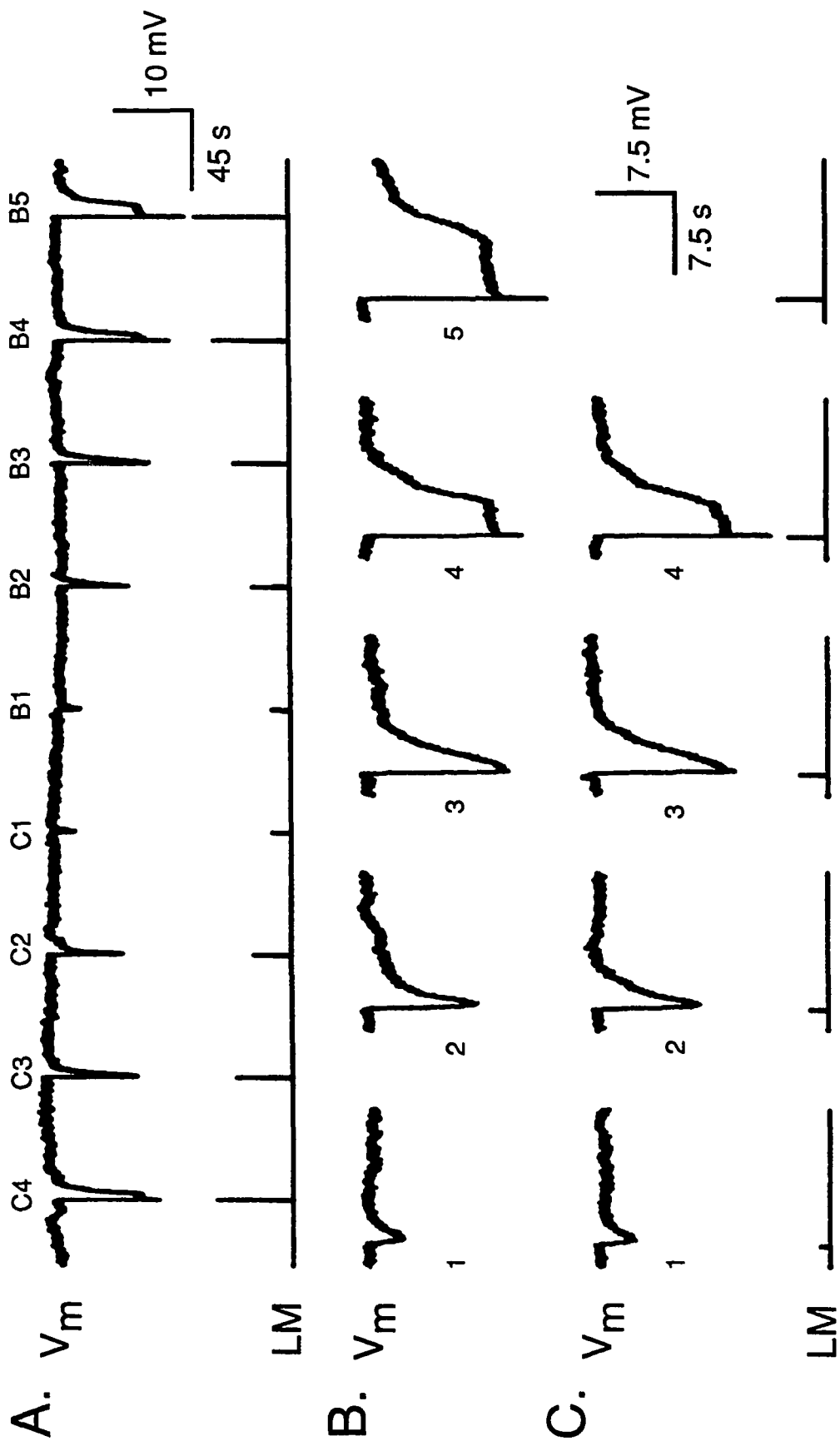


Fig. 1. Voltage responses to light flashes of varying intensity.

through the cGMP-regulated conductance (Yau & Nakatani, 1984b; Miller & Korenbrot, 1987). Thus  $\text{Ca}^{2+}$  and cGMP have mutual regulatory effects, which will be further discussed in following sections.

Finally, the voltage waveform resulting from photostimulation is not only influenced by the light-sensitive current, but also by changes in the voltage-sensitive and  $\text{Ca}^{2+}$ -sensitive currents of the inner segment (Bader et al, 1978, 1982; Fain et al, 1980; Baylor et al, 1984). When studying rod  $V_m$  and rod  $V_m$  photoresponses, these currents must be taken into account. Therefore, their characteristics will be discussed further in Section 1.7 in order to aid data interpretation.

### *1.0.2: Adaptation*

Toad rods have the ability to partially restore their photoresponsiveness to light flashes in the presence of dim background light (Fain, 1976; Bastian & Fain, 1979). This process is known as cellular light adaptation, which is generally found in vertebrate cones but is found in the rods of only some animals (Baylor & Hodgkin, 1974; Norman & Periman, 1979; Valeton & van Noren, 1983). This process of adaptation to dim light involves regulation of steady-state levels of cGMP and  $\text{Ca}^{2+}$  (Matthews et al, 1988; Nakatani & Yau, 1988). Much less is known about adaptation to long-term, bright illumination, which bleaches the majority of, rhodopsin molecules. Adaptation to this extensive bleaching, however, involves other complex biochemical and physiological effects, including a decrease in quantal catch (Dowling, 1963; Rushton, 1965, 1981), and rhodopsin regeneration. The complete mechanism of rhodopsin regeneration has not yet been elucidated.

There are generic differences in adaptation mechanisms. In Teleosts, rods do not undergo cellular adaptation (Witkovski et al, 1973, 1975; Malchow & Yazulla, 1986). Instead, rods elongate and cones contract in a process known as retinomotor movements (for a review, see Burnside and Nagle, 1983). When Teleost rod cells elongate, they become buried in the pigment epithelium and leave the cones, which do undergo cellular adaptation, to become the main phototransducing cells. Primate rods also do not undergo

cellular adaptation, yet rod elongation is minimal. Primates, instead, rely on functional / anatomical separation of rods & cones.

*1.0.3: The hypothesis that colchicine reduces the  $g_{hv}$ .*

Prior to the discovery that cGMP opens the light-sensitive conductance channels (Fesenko et al, 1985) and that  $Ca^{2+}$  regulation of cGMP mediates cellular light adaptation (Nakatani & Yau, 1988; Matthews et al, 1988), two groups of investigators had hypothesized that the  $g_{hv}$  might also be affected by cytoskeletal elements in the rod outer segment (Bert and Oakley, 1984, 1985; Del Priore et al, 1985a). Both groups of investigators based this hypothesis on several important results known at the time:

1. Regulation of  $g_{hv}$  involved cGMP,  $Ca^{2+}$  and guanosine triphosphate (GTP). This regulatory combination was very similar to the cAMP,  $Ca^{2+}$  and adenosine triphosphate (ATP) regulatory system controlling actomyosin contraction in smooth muscle.
2. Calcium, cGMP and GTP also regulate microtubule polymerization, and microtubule-like structures exist in two distinct locations in the rod outer segments (Steinberg and Wood, 1975).
3. Cytoskeletal proteins had been found which connected the rhodopsin-containing disks in the rod outer segment to the plasma membrane ( Usukura & Yamada, 1981; Roof and Heuser, 1982). These proteins resemble fodrin and  $\alpha$ -spectrin, which are actin cross-linking proteins found in brain neurons (Nagle & Burnside, 1984). Actin and myosin had also been located at other sites in the rod outer segments (Chaitin et al, 1984; Chaitin & Bok, 1985).
4. The drug colchicine, known to disrupt microtubules by binding to tubulin monomers, affected infrared light scattering linked to GTP-binding proteins in rod disk preparations (Peter Stein, personal communication, later published in Caretta & Stein, 1986).

In order to test this hypothesis, experimentation with drugs which disrupt microtubules

and microfilaments began. Several drugs which disrupt these cytoskeletal elements affected rod  $V_m$  and  $V_m$  photoresponses (Bert & Oakley, 1984, 1985; Bert et al, 1986). These drugs included colchicine, vincristine and cytochalasin B. The effects on  $V_m$  of the two microtubule disrupting drugs differed in polarity, however, so these drug effects were not attributed to microtubule disruption, *per se*.

In 1985 and 1986, patch clamping experiments conducted on the rod outer segment membrane revealed that  $g_{hv}$  was directly affected by cGMP (Fesenko et al, 1985; Yau & Nakatani 1985; Matthews, 1986). Since then, the channel protein has been isolated, purified and reconstituted into membranes, where it maintains its cGMP sensitivity (Matesic & Liebman, 1987). Thus the cGMP-dependence of  $g_{hv}$  results from direct binding of cGMP to a channel protein, and not from the cGMP regulation of cytoskeletal contraction. These results, then, leave the effects of the cytoskeletal drugs unexplained.

Of the cytoskeletal drugs that affect photoreceptor electrophysiology, colchicine is the most interesting for the following reasons:

1. Colchicine's effects resemble adaptation to dim background light (see Chapter 3).
2. Colchicine affects enzymes involved in transduction (Caretta & Stein, 1986).
3. Colchicine also has light-like effects on the light-regulated processes of disk morphogenesis and retinomotor movements, and these effects are probably not microtubule-mediated either (O'Connor & Burnside, 1981, 1982; Besharse & Dunis, 1982).
4. Colchicine affects conductances in a wide variety of neural tissue, including the related  $\beta$ -adrenergic system (see Section 1.4).

Because many of colchicine's effects on rods resembled illumination, it was hypothesized that colchicine blocks  $g_{hv}$ . This thesis, then, first focuses on testing this hypothesis, which is supported by the results. The focus of the research then shifts to elucidating the mechanism by which colchicine blocks the conductance. Specifically, the experiments presented test the hypotheses that colchicine's effects are mediated by increased  $[Ca^{2+}]_i$ ,

and that colchicine's effects are tubulin mediated.

The other sections of this chapter review the literature regarding: the regulation and control of  $g_{hv}$  and of  $Na^+/K^+/Ca^{2+}$  exchange in the rod outer segment, emphasizing the inter-regulation of  $Ca^{2+}$  and cGMP; the characteristics of colchicine-tubulin binding, and other selected aspects of tubulin pharmacology referred to in this thesis; the effects of colchicine on the electrophysiology of other types of neurons; the voltage-sensitive and  $Ca^{2+}$  sensitive currents of the rod inner segments. Chapter 2 contains the experimental methods. Chapter 3 contains results supporting the hypothesis that colchicine closes  $g_{hv}$  by releasing  $Ca^{2+}$  from intracellular stores. Results presented in this chapter also demonstrate, however, that colchicine's attenuation and recovery enhancement of  $V_m$  photoresponses are not  $Ca^{2+}$  mediated. Results are also presented in this chapter which attempted to test the hypothesis that colchicine's effects are tubulin mediated. Chapter 4 contains a discussion of the results and possible directions for future research.

### **Section 1.1: *The identity of $g_{hv}$ .***

The predominant transmembrane current in the rod outer segment is a voltage-insensitive cation current, thought to be of a single channel type, that is blocked upon illumination. The light-sensitive current has been well-characterized recently using several techniques. It has been shown to be an inward current (Yoshikami & Hagins, 1973; Bader et al, 1979; Capovilla et al, 1981, 1983), resulting from cations passing through a transmembrane pore (Zimmerman and Baylor, 1986; Matthews, 1986; Matthews & Watanabe, 1987, 1988). The pore is thought to be formed by a transmembrane protein that binds cGMP (Tanaka et al, 1987; Cook et al, 1987; Matesic & Liebman, 1987; Clack & Stein, 1988). Although there is some dispute over the identity of this protein (Cook et al, 1987; Matesic & Liebman, 1987; Clack & Stein, 1988), it may, in fact, be rhodopsin (Clack & Stein, 1988) or a modified form of rhodopsin (Matesic & Liebman, 1989). Another protein which co-purifies with the rhodopsin-like channel protein, formerly thought to be the cGMP-sensitive channel (Cook et al, 1987), appears to be a membrane form of tubulin (Matesic &



Liebman, 1989; Peter Stein, personal communication).

Pharmacological evidence has been presented indicating that there are possibly two different cGMP-dependent channels (Schnetkamp, 1987; Nicol et al, 1987; Koch et al, 1987; Pierce et al, 1988). It has not yet been determined, however, whether there are indeed two cGMP-sensitive channels or whether the pharmacological differences result from the different conductance states of the channel (Lipton, 1985; Haynes et al, 1986; Zimmerman & Baylor, 1986; Nicol et al, 1987).

### 1.1.1: Ionic permeability of $g_{hv}$ .

Ion substitution experiments have shown this conductance to be permeable to many cations, including  $\text{Li}^+$ ,  $\text{Na}^+$ ,  $\text{Rb}^+$ ,  $\text{K}^+$ ,  $\text{Cs}^+$ ,  $\text{Mn}^{2+}$ ,  $\text{Ba}^{2+}$ ,  $\text{Ca}^{2+}$ ,  $\text{Co}^{2+}$ ,  $\text{Mg}^{2+}$  and  $\text{Sr}^{2+}$  (Capovilla et al, 1983). The relative permeabilities for some of these ions were found to be:

1.0 : 1.00	$\text{Na}^+ : \text{Li}^+$
1.0 : 0.70	$\text{Na}^+ : \text{K}^+$
1.0 : 0.45	$\text{Na}^+ : \text{Rb}^+$
1.0 : 0.25	$\text{Na}^+ : \text{Cs}^+$
1.0 : 0.20	$\text{Na}^+ : \text{Ca}^{2+}$

(Yau and Nakatani, 1984b). Of particular interest for this thesis is the near-unity permeability ratios of  $\text{Li}^+$  and  $\text{Na}^+$ . This permeability ratio means that  $\text{Li}^+$  can support the dark current when it replaces  $\text{Na}^+$  as the dominant external cation, although  $\text{Li}^+$  does not support  $\text{Na}^+/\text{K}^+/\text{Ca}^{2+}$  exchange in the rod outer segment (Yau & Nakatani, 1984a).

### 1.1.2: The known pharmacology of $g_{hv}$ .

The cGMP sensitivity of the channel can be approximated by the Hill equation, but several different Hill coefficients have been reported, ranging from 2.0-3.0 (Fesenko et al, 1985; Yau and Nakatani, 1985b; Matthews, 1986; Stern et al, 1986). Coefficients greater than one have been assumed to imply cooperative binding (Hill, 1910). The variations in measurements of the Hill coefficient reported by the various observers may be due to

differences in the ionic makeup of the solutions in the patch electrodes. Haynes et al (1986) measured a Hill coefficient of 2.9 under low- $\text{Ca}^{2+}$  conditions, while Fesenko et al, (1985) measured a Hill coefficient of 1.8 under standard extracellular  $\text{Ca}^{2+}$  conditions. Similarly, the cGMP half-saturation parameter of the channel also varied in the reports, and was reported to be between 14-45  $\mu\text{M}$  (Fesenko et al, 1985; Haynes et al, 1986). Furthermore, patch-clamp studies of  $g_{\text{hV}}$  have shown that divalent cations tend to block this conductance in the direction of their flux (Zimmerman and Baylor, 1986; Matthews, 1986; Stern et al, 1986). Further studies have also shown that  $\text{Ca}^{2+}$  and  $\text{Mg}^{2+}$ , when applied to the intracellular face of patches, inhibit the channel conductance in the absence of cGMP, i.e., they further reduce the conductance of closed channels (Stern et al, 1987; Zimmerman & Baylor, 1988). The concentrations of ions required to produce these effects are 0.1 - 1.0 mM, thus  $\text{Mg}^{2+}$  is likely to be the only ion of physiological significance concerning this effect (Stern et al, 1987).

The vasodilator, l-cis-diltiazem (see Fig. 3) and the amiloride derivative 3', 4'-dichlorobenzamid, DCPA, block  $g_{\text{hV}}$  in excised patches when applied to the cytoplasmic surface of the patch in 10  $\mu\text{M}$  concentrations (Stern et al, 1986; Nicol et al, 1987; Rispoli & Menini, 1988). However, superfusion of 1 mM l-cis-diltiazem only partially decreased the light-sensitive current of intact rods, and, surprisingly, intracellular dialysis of the drug at 2.3 mM concentration had no effects on  $g_{\text{hV}}$  (Stern et al, 1986). The drug DCPA, however, suppressed the dark current almost completely when superfused onto isolated rods at 25  $\mu\text{M}$  concentrations (Nicol et al, 1987). Furthermore, the conductance blocking ability of DCPA, but not l-cis diltiazem, is  $\text{Ca}^{2+}$ -sensitive (Nicol et al, 1987). Superfusion of DCPA in low- $\text{Ca}^{2+}$  solutions can reverse the direction of photo-induced currents in isolated rods. This phenomena has been interpreted as indicating that DCPA either alters the conductance characteristics of the cGMP-sensitive channel; or that multiple cGMP-sensitive channels exist (Nicol et al, 1987).

### *1.1.3: Conductance characteristics of $g_{hv}$ .*

The open cGMP-sensitive channel has been shown to exist in two conductance states (Haynes et al, 1986; Zimmerman & Baylor, 1986). The channels exhibit a bursting pattern of opening. Binding cGMP does not increase the mean open time of the channel or duration of bursts, but instead, increases the frequency of bursts (Matthews & Watanabe, 1988).

### *1.1.4: Biochemical regulation of $g_{hv}$ .*

The biochemical control of cGMP levels is, the photoreceptor's primary method of reducing of  $g_{hv}$  (for a review, see Fung, 1989). Much of the biochemistry involved in changing cGMP levels in response to a photostimulus has been worked out over the last 10 years. Rhodopsin plays at least a dual role: it captures a photon and starts the activation of an enzymatic cascade which degrades cGMP. Less is known about the cGMP synthetic pathway, but it is apparently activated by the fall in  $[Ca^{2+}]_i$  which follows photostimulation (Pepe et al, 1986; Koch & Stryer, 1988).

Prior to the discovery that cGMP directly controlled plasma membrane channels,  $Ca^{2+}$  was thought to have this effect. The evidence now clearly indicates that calcium effects are mediated by regulating the enzymes controlling  $[cGMP]_i$  (for a review, see Pugh, 1987). Current investigations are examining the specific proteins inhibited by  $Ca^{2+}$ . It appears that  $[Ca^{2+}]_i$  may regulate enzymes in both the synthetic and degradative pathways (for a review, see Stryer, 1986; see Kawamura & Bownds, 1981; Hodgkin & Nunn, 1988; Detwiler et al, 1989). In the following subsections the synthetic and degradative enzymatic pathways of cGMP are reviewed. Special attention is given to the  $Ca^{2+}$  sensitivities of various proteins in these pathways.

### *1.1.5: Synthesis of cGMP*

Cyclic guanosine monophosphate is synthesized directly from GTP in a reaction catalyzed by the enzyme guanylate cyclase [GTP pyrophosphate-lyase; (cyclising), EC

4.6.1.2]. This enzyme has been partially characterized in preparations from several animals, including: light-adapted bovine rods (Krishnan et al, 1978; Koch & Stryer, 1988), mouse rods (Troyer et al, 1978) and toad rods (Pepe et al, 1986). Furthermore, using an immunolocalization technique, guanylate cyclase activity has been localized in light-adapted, dark-adapted and dimly lit retinas from brook trout (Athanasios et al, 1984).

There are some apparent contradictions concerning light activation of guanylate cyclase activity in the literature. Purified guanylate cyclase activity has been reported to be light-inhibited (Krishna et al, 1976), light-activated (Pepe et al, 1986) and unaffected by illumination (Koch & Stryer, 1988), while ultracytochemical techniques indicated that guanylate cyclase activity increased with partial light-adaptation, but decreased with full light adaptation (Athanasios et al, 1984). This phenomena is interesting considering that rods function primarily in dim light, where changes in phosphodiesterase activity are also maximal.

Reports on the location of guanylate cyclase have also been contradictory. Krishnan et al (1978) reported that guanylate cyclase activity appeared almost entirely in particulate (membrane bound) cell fractions. Troyer et al (1978), identified both soluble and membrane-bound forms of guanylate cyclase in the mouse retina, which have very different properties. A particular membrane-bound form of guanylate cyclase was localized only in photoreceptors. This membrane-bound guanylate cyclase had a high affinity for GTP ( $K_m = 42 \mu\text{M}$ ), was unaffected by compounds that activate guanylate cyclase in other neurons and was inhibited by  $\text{Ca}^{2+}$ . A ubiquitous soluble guanylate cyclase was also found in photoreceptors. This soluble enzyme was stimulated by  $\text{Ca}^{2+}$  in the absence of  $\text{Mn}^{2+}$ . Ultracytochemical techniques have been used to localize guanylate cyclase activity *in situ* (Athanasios et al, 1984). These results showed that the location of guanylate cyclase activity depended on the state of illumination. Membrane bound guanylate cyclase activity was highest in the partially light-adapted state and was localized mostly on the inner membrane surface of the rod outer segment disks (intradiskally, see Illus. 1). A small

degree of guanylate cyclase activity was found in the calycal processes and along the axoneme. Under fully light-adapted conditions, however, cytoplasmic guanylate cyclase activity increased, while particulate guanylate cyclase activity diminished and changed location to the outer disk membrane surface (interdiskally). When rods were transferred to darkness, guanylate cyclase activity stopped transiently, but traces of activity reappeared on the outer surfaces of the disk membranes.

The light-dependent localization of guanylate cyclase activity is interesting, since physiological evidence using the patch clamp technique also provided data that supports light-activation of localized submembranous populations of guanylate cyclase (Detwiler et al, 1989). These researchers showed that in patches taken from dark adapted rods, GTP alone can increase  $g_{hv}$ , indicative of localized submembranous guanylate cyclase activity.

There are discrepancies reported in the turnover number and Michaelis constant for the enzyme as well. These discrepancies may, however, result from generic differences. Pepe et al (1986) assayed cyclase activity in dark-adapted toads, and reported 3 nmole cGMP formed/min per mg protein. This compares to 10 nmole/min per mg protein found by Krishnan et al (1978) in light-adapted bovine rods, under optimum Mn : GTP (1 : 1) conditions.

Likewise, discrepancies have been measured in the Michaelis constant of the enzyme. Krishnan et al reported that the substrate-enzyme relationship of guanylate cyclase was Michaelian ( $K_m = 800 \mu\text{M}$ ) in equimolar  $\text{Mn}^{2+}$  and GTP, but exhibited negative cooperativity in the presence of free  $\text{Mn}^{2+}$ . These researchers suggested, then, that there is possibly more than one enzyme subtype. The Michaelis constant of membrane bound guanylate cyclase in mouse photoreceptors was  $38 \mu\text{M}$  (Troyer et al, 1978), which varied from the Michaelis constant ( $237 \mu\text{M}$ ) of membrane bound guanylate cyclase from mouse brain extracts.

Finally, although all purified and partially purified preparations exhibited divalent cation sensitivity, the effects of divalent cations varied between the preparations. Krishnan et al

(1978), report that  $Mn^{2+}$  is a required cofactor for guanylate cyclase activity, and the maximal enzyme activity occurs when  $Mn^{2+}$  and GTP are present in equimolar amounts. Concentrations of  $Mn^{2+}$  that exceed GTP concentrations, however, became inhibitory. The only other divalent cation found to activate guanylate cyclase was  $Mg^{2+}$ , which was reported to be about 10% as effective as  $Mn^{2+}$  in activating guanylate cyclase. Finally, these researchers also reported that  $Ca^{2+}$  inhibits guanylate cyclase activity by up to 32% when present at 0.5 mM concentration. They noted, however, that  $Ca^{2+}$  had little effect on guanylate cyclase activity at concentrations closer to the physiological range ( $10^{-4}$ - $10^{-6}$  M). The divalent sensitivity of mouse guanylate cyclase (Troyer et al, 1978) was in agreement with the bovine results except for  $Mg^{2+}$  sensitivity. Troyer et al reported that 5 mM  $Mg^{2+}$ , in the absence of  $Mn^{2+}$ , supports 2 / 3 the guanylate cyclase activity observed when 5 mM  $Mn^{2+}$  was used as the essential cofactor. They noted, however, that 5 mM concentrations of  $Mg^{2+}$  and other divalent cations became inhibitory in the presence of 0.5 mM  $Mn^{2+}$ . Pepe et al (1986) reported that varying  $Ca^{2+}$  concentrations from  $10^{-9}$ - $10^{-4}$  M in dark adapted toad rods did not affect guanylate cyclase activity in the dark. These researchers, however, reported that  $Ca^{2+}$  had a dramatic inhibitory effect on guanylate cyclase activity in rod suspensions activated with flashes of light. The inhibitory effects occurred over physiological  $Ca^{2+}$  concentrations ( $<10^{-8}$ - $10^{-5}$  M), and varied with the intensity of the stimulus. Furthermore, during low- $Ca^{2+}$  conditions ( $10^{-8}$  M), a moderate light flash (0.07% rhodopsin bleached) increased guanylate cyclase activity more than 30-fold. Increasing the  $Ca^{2+}$  concentration to  $10^{-4}$  M, however, inhibited this guanylate cyclase activity, and the enzyme activity returned to 80 % of its dark value. The results of Pepe et al cannot be directly compared with those of other previous researchers, however, since the earlier workers measured enzyme activity in the completely light-adapted state.

Recently, a new study of bovine guanylate cyclase has shown the enzyme to be very sensitive to  $Ca^{2+}$  changes in the range of 50  $\mu$ M - 200  $\mu$ M in the dark (Koch & Stryer, 1988). These researchers found that the  $Ca^{2+}$  inhibition of guanylate cyclase was highly

cooperative, with a Hill coefficient of 3.9, and that the  $\text{Ca}^{2+}$  inhibition of guanylate cyclase depended on a loosely bound membrane protein, which activates guanylate cyclase in the absence of  $\text{Ca}^{2+}$ . They also found  $\text{Ca}^{2+}$  inhibition of guanylate cyclase to be independent of light stimulation.

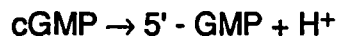
At least one group of researchers has reported that GTP may have a regulatory as well as a substrate role, and that ATP regulates guanylate cyclase (Krishnan et al, 1978). High concentrations of ATP (1 mM) produced 30% inhibition of the enzyme, whereas lower concentrations (0.1 mM) increased activity up to 40%.

In summary, the molecules ATP and GTP, and the divalent cations  $\text{Mg}^{2+}$ ,  $\text{Mn}^{2+}$  and  $\text{Ca}^{2+}$  have been shown to affect guanylate cyclase activity *in vitro*. Yet, when these substances were controlled in experiments using toad photoreceptors (Pepe et al, 1986), light still activated guanylate cyclase. This result was not found, however, in bovine photoreceptors (Koch & Stryer, 1988). Thus it is not clear whether or not there is light-activated protein modulation of guanylate cyclase. It seems more likely that changes in the concentrations of  $\text{Ca}^{2+}$ ,  $\text{Mg}^{2+}$ , ATP and / or GTP ( $\text{Mn}^{2+}$  probably is not physiologically significant) account for the light-dependent changes in guanylate cyclase activity proposed *in vivo* (Hodgkin & Nunn, 1988). Variations in  $\text{Mg}^{2+}$  concentrations could be of significant importance, but all of the transport processes that regulate this ion have not yet been elucidated. It has been shown, however, that  $\text{Mg}^{2+}$  permeates the rod outer segment conductance (Nakatani & Yau, 1988a). Guanosine triphosphate supposedly plays both a regulatory and substrate role in cGMP synthesis (Krishnan et al, 1978). It is present in rod outer segments in large concentrations (>1.0 mM), and occurs mostly in the free state (T.G. Ebrey, personal communication). During illumination, however, GTP levels vary only over the 0.5 - 1.0 mM range, and these concentrations are sufficient to saturate guanylate cyclase ( $K_m \sim 30 \mu\text{M}$ ). Thus, the small changes in GTP concentrations during light exposure make GTP an unlikely physiological regulator of guanylate cyclase. The ATP in rod outer segments is also mostly in the free state (T.G. Ebrey, personal communication).

Only small changes in ATP levels occur during illumination (Robinson & Hagins, 1979), making it, too, an unlikely physiological regulator of guanylate cyclase activity, despite its activating and inhibiting effects at near physiological concentrations (Krishnan et al, 1978). Large, light-induced changes in  $[Ca^{2+}]_i$  ( $\sim 10^{-6}$  M -  $\sim 10^{-9}$  M) are known to occur during illumination (McNaughton et al, 1987; Ratto et al, 1988), and these changes seem to influence guanylate cyclase activity significantly *in vivo* (Hodgkin & Nunn, 1988; Detwiler et al, 1989). Thus  $Ca^{2+}$  is probably the most important physiological regulator of guanylate cyclase in rod outer segments. This regulatory effect of  $[Ca^{2+}]_i$  has important consequences in interpreting the effects of colchicine on rod electrophysiology.

#### 1.1.6: Light-activated degradation of cGMP

Stimulating photoreceptors with light begins an enzymatic cascade that culminates in a dramatic increase in the activity of a cGMP phosphodiesterase that catalyzes the reaction:



(see Illus. 3A). The reverse reaction, converting 5'-GMP to cGMP, is unlikely to occur to any significant extent because the thermodynamics are unfavorable at cellular conditions.

Endogenous 5'nucleosidase activity in the rod outer segments (Ueno et al, 1984a) hydrolyzes 5'-GMP and keeps local concentrations of this compound low enough to prevent mass action from driving the reverse reaction.

It is believed that the local light-activation of a cGMP phosphodiesterase decreases  $[cGMP]_i$ , which results in a reduction of the cGMP-sensitive conductance (for a review, see Fung, 1989; see also Baylor & Lamb, 1982). The enzymatic cascade leading to phosphodiesterase activation is initiated by the absorbance of a photon by the molecule, rhodopsin. After absorbing a photon, rhodopsin passes through several conformational states (for reviews, see Ebrey and Honig, 1975; Zurer, 1983) eventually reaching the active metarhodopsin II ( $\rho^*$ ) state. In this state,  $\rho^*$  activates a GTP-binding protein now called transducin (Fung & Stryer, 1980; Bennett et al, 1982). Transducin is an oligomer, consisting of three subunits, alpha, beta and gamma (Kuhn, 1981, Stryer et al, 1981). Upon



stimulation by  $\rho^*$ , GTP is exchanged for GDP, and the subunits dissociate into soluble ( $\alpha$ ) and ( $\beta$ - $\gamma$ ) forms (Fung, 1983). The GTP-bound  $\alpha$  subunit activates the phosphodiesterase (Fung, 1983), apparently by removing an inhibitory subunit of the phosphodiesterase. The GTP-bound  $\alpha$  subunit stays bound to phosphodiesterase in its light-activated form (Sitaramayya et al, 1986). Phosphodiesterase is a heterotrimer (Baehr et al, 1979) that becomes loosely bound to the rod outer segment disk membranes via transducin (Sitaramayya et al, 1986; Yamazaki et al, 1983). In the dark, the three subunits,  $\alpha$ ,  $\beta$ , and  $\gamma$  oligomerize (Baehr et al, 1979). The binding of the  $\gamma$  subunit to the  $\alpha$  and  $\beta$  subunits inactivates the oligomer (Hurley and Stryer, 1982). The  $\gamma$  subunit is most likely displaced or replaced during light-activation of phosphodiesterase (Parkes et al, 1985). Recently, evidence has been given that the inhibitory subunit is, in actuality, two subunits that are removed sequentially (Deterre et al, 1988).

Once the enzymatic cascade is initiated, a second series of reactions begin which ultimately stop the process (Illus. 3B). This quenching mechanism begins with the phosphorylation of  $\rho^*$  by ATP in a reaction catalyzed by the enzyme rhodopsin kinase, a 68 kilodalton protein (Kuhn & Dreyer, 1972; Bownds, et al, 1972). Once phosphorylated, metarhodopsin II eventually becomes unable to activate transducin (Arshavsky et al, 1985). The phosphorylation of activated rhodopsin enhances its binding to a soluble 48 kilodalton protein, arrestin (Kuhn et al, 1984). The binding of arrestin effectively stops G-protein activation by  $\rho^*$ , and completes the quenching sequence (Zuckerman et al, 1985; Wilden et al, 1986).

Calcium may play a role in quenching phosphodiesterase activity. It is believed that decreasing  $[Ca^{2+}]_i$  *in vivo* leads to a reduction of phosphodiesterase activity (Detwiler, 1989). The only discernible effect of  $[Ca^{2+}]_i$  on the enzyme cascade *in vitro* has been inhibition of ATP-dependent phosphodiesterase quenching (Kawamura & Bownds, 1981; Del Priore & Lewis, 1983; Barkdoll et al, 1989). The  $Ca^{2+}$  concentrations required for this effect ( $K_d$  1.0 - 1.5 mM) are above the physiological range of cytoplasmic free  $Ca^{2+}$

**Illustration 3. Light-evoked activation and the deactivation of the cGMP enzyme cascade.**

**A.** The relationships between the proteins leading to the hydrolysis of cGMP are shown. Arrows indicate normal direction of enzyme activation. Inhibitory effects by proteins or small molecules are indicated by a filled ball at the site of inhibition. Active forms of the enzymes are indicated by a \*. Symbols are as follows:

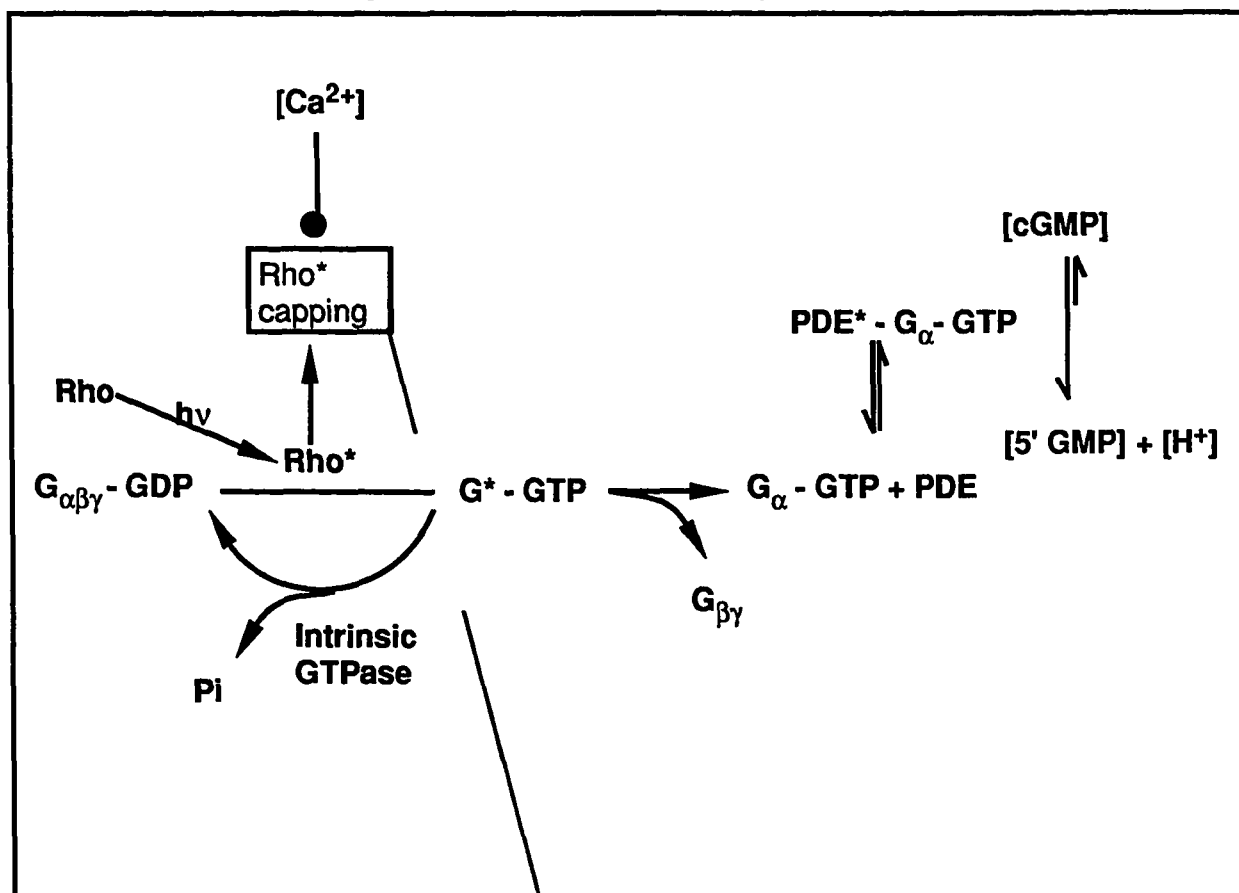
- Rho: rhodopsin
- G: the GTP-binding protein, transducin
- hv: a photon of light (~500 nm)
- PDE: cGMP phosphodiesterase
- cGMP: 3',5'-cyclic guanosine monophosphate
- 5'GMP: 5' guanosine monophosphate
- Pi: inorganic phosphate
- GDP: 5' guanosine diphosphate
- GTP: 5' guanosine triphosphate
- Ca<sup>2+</sup>: free ionized intracellular calcium

**B.** The relationship of proteins and small molecules participating in the deactivation of activated rhodopsin. Symbols besides those described in A are:

- nATP: a number of molecules of 5' adenosine triphosphate
  - nP: a number of molecules of inorganic phosphate
  - Arrestin: a 48 kilodalton protein which binds to phosphorylated rhodopsin
  - R kinase: rhodopsin kinase
- See text for description of proteins.

A

## Light-activated [cGMP] Degradation



B

Rho\* Capping (see text)

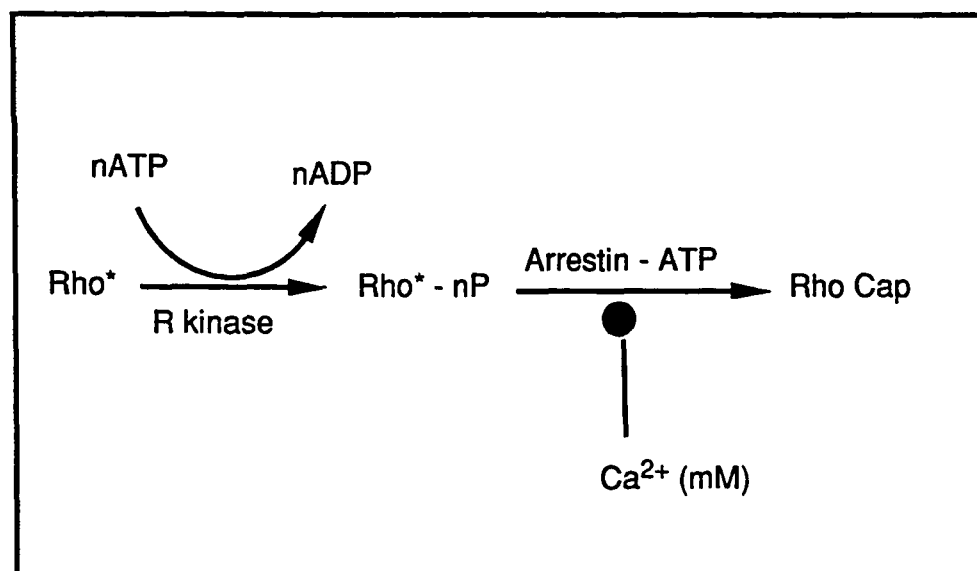


Illustration 3. Light-evoked activation and the deactivation of the cGMP enzyme cascade

normally found in rods. The pharmacology and divalent ion sensitivity of the major proteins involved in the transduction cascade are listed in Table 1. Relevant aspects of the enzyme activity, pharmacology, and divalent ion sensitivity that will be referred to later in this thesis are discussed below.

**Phosphodiesterase.** A portion of the rod outer segment phosphodiesterase exists in the active state in the dark, i.e. it has intrinsic thermal activity (Yee & Liebman, 1978). This activity increases dramatically when the rod outer segment is stimulated with light (Yee and Liebman, 1978). Phosphodiesterase activity has been localized in rod cells (Ueno et al, 1984a, b) and was found primarily on the disk and plasma membranes of the rod outer segment. The proteins involved in light-evoked activation of phosphodiesterase were discussed above.

*Pharmacology.* Rod outer segment PDE can be directly inhibited by several drugs, but the extent of inhibition has not been entirely characterized. The most common inhibitor is isobutylmethylxanthine, (IBMX), which causes a two-fold inhibition of phosphodiesterase at 0.5 mM concentrations both in the dark and after light stimulation (Kawamura and Bownds, 1981). Other phosphodiesterase inhibitors are given in Table 2. The nucleotide triphosphates ATP and GTP have indirect effects on phosphodiesterase activity. The nucleotide triphosphate ATP decreases the light-sensitivity of phosphodiesterase, and increases its deactivation rate in reconstituted membrane suspensions in a  $\text{Ca}^{2+}$ -dependent manner (Kawamura and Bownds, 1981; Barkdoll et al, 1989). This effect is mediated by rho\* phosphorylation and the 48 kilodalton protein, arrestin (Zuckerman et al, 1982, 1985).

Light-sensitive activation of phosphodiesterase requires GTP (Miki et al, 1973; Bitenski et al, 1973; Wheeler and Bitenski, 1977), and the GTP-binding protein, transducin, as described above. In the inactive state, phosphodiesterase binds cGMP at two non-active sites, which decrease in binding activity once the enzyme becomes activated (Yamazaki & Bitenski, 1980; Yamazaki et al, 1982).

**Table 1. Pharmacology and action of proteins regulating [cGMP]<sub>i</sub>**

The data in this table was compiled from references cited in the text, or given in the Bibliography. Abbreviations are:

T or G:	the GTP-binding protein, transducin
PDE:	cGMP phosphodiesterase
GC:	guanylate cyclase
ATP:	5' adenosine triphosphate cGMP: 5' guanosine triphosphate
GPPNP:	the nonhydrolyzable analog of GTP, guanosine 5'diphosphoramidate
GDP:	5' guanosine diphosphate
cGMP:	3',5'-cyclic guanosine monophosphate
IBMX:	isobutylmethylxanthine
R*:	activated rhodopsin
B.P.:	Bordetella Pertussis
nP:	a number of molecules of inorganic phosphate
Arrestin:	a 48 kilodalton protein which binds to phosphorylated rhodopsin
R kinase:	rhodopsin kinase
K <sub>m</sub> :	Michaelis Constant

Enzyme	Pharm. Agent	Optimal	Concentration Effective Range	Action
Degradative Pathway PDE	T-GDP	1:1 T:PDE	1:10-10:1 T:PDE	inhibits (dir.) PDE in GDP bound form. G-GTP activates PDE.
	ATP	10-5 M	10-7-10-5 M	inhibits (dir.), requires rhodopsin kinase, arrestin. activates (indir.), requires activated Transducin.
	GTP			inhibits (dir.), 2-fold decrease in activity (at optimal conc.).
	IBMX		0.5-2.0 mM	inhibits (dir.), 2-fold decrease in activity (at optimal conc.).
	Theophylline		0.5-2.0 mM	inhibits (dir.), 2-fold decrease in activity (at optimal conc.).
	Vanadate	Km=0.1 mM	10.0 mM (typ.)	activates (dir.) in the dark, even at 10-9 M Ca2+ (not reported)
	Molybdate	Km=3.0 mM	10.0 mM (typ.)	activates (dir.) in the dark, even at 10-9 M Ca2+ (not reported)
	Tungstate	Km=1.0 mM	10.0 mM (typ.)	activates (dir.) in the dark, even at 10-9 M Ca2+ (not reported)
	Fl-	4.0*10-6 M	0.1-20.0 mM	activates (indir.): disinhibits via binding to transducin (T)
	Ca2+	20.0 mM	1.0-20.0 mM	inhibits (dir.) in absence of T (indirect effects dominate).
		2.0-8.0 mM	0.1-10.0 mM	inhibits (dir.) PDE in absence of soluble enzymes.
		3.0 mM	10-9-10-6 M	increases (indir.) activity by inhibiting ATP-dep. deactivation.
	Mg2+	0.1-1.0 mM	0.1-10 mM	at zero Ca2+ levels. Activates PDE in a Ca2+-sensitive manner.
				at 1 mM Ca2+.
Transducin (T)	R* + GTP	K=0.3-0.5 * 10-6 M	10-6 M for GTP+T	activates (dir.) T by inducing dissociation of alpha subunit.
	G subunit		1:01	causes oligomerization of alpha-beta-gamma subunits.
	B.P. toxin	0.05 mg/ml		light-independent inhibition of GTPase. Transfers ADP-ribose from NAD
	Choleragen	0.25 mg/ml		light- and GPPNP-dependent ribosylation of Galph. Stops GTPase
	GMPNP	1:01		cannot be hydrolyzed, deepens T activated once active complex is formed.
	Fl-	10 mM		activates (dir.) T, releases Galpha from the membrane.
	Ca2+, Mg2+	>2 mM		divalent cations increase membrane binding of transducin.
Rhodopsin	Hydroxylamine	5 mM typ.		inhibits activated rhodopsin (rho*) action; shortens life of Met.II.
	pH			yields increase rho*-T binding; Met.II form. is pH, GTP-sensitive.
Rhodop. Kinase	T	1.0 mM		competitively inhibits RK phosphorylation of rho*.
	GTP			activates (indir.) by removing T from T-rho* complex.
	ATP	Km=4.0*10-6 M		needed for rhodopsin phosphorylation ATP--ADP.
	cGMP			inhibits rhodopsin phosphorylation.
	Mg2+			necessary for rhodopsin phosphorylation.
	Ca2+			activates in the absence of Mg2+, inhibits in the presence of Mg2
Arrestin	not characterized			
5' Nucleosidase	not covered in text			

Table 1: Pharmacology and Action of Proteins Regulating [cGMP]i

**Ionic effects.** Calcium has a direct inhibitory action on partially purified phosphodiesterase (Cook et al, 1986), and lowers the sensitivity of this enzyme to  $Mg^{2+}$  activation. The range over which this occurs ( $\sim 0.1 - 5.0$  mM) is probably not physiological ( $\sim 10^{-6} - 10^{-9}$ , Ratto et al, 1988). This is opposite to the effects of this ion seen in intact rod outer segment suspensions, where  $Ca^{2+}$  mildly stimulates phosphodiesterase in the dark, and increases the light-sensitive activation of this enzyme (Kawamura and Bownds, 1981; Del Priore and Lewis, 1983; Barkdoll et al, 1989). *In Vivo*,  $Ca^{2+}$  acts by inhibiting the ATP-dependent deactivation of phosphodiesterase as previously discussed (Kawamura and Bownds, 1981; Del Priore & Lewis, 1983). It has been suggested that the  $Ca^{2+}$ -induced activation of phosphodiesterase which dominates *in vivo* is mediated by a direct inhibitory action on the 48 kilodalton protein, arrestin (Zuckerman et al, 1982, 1985). Recent evidence has not supported this hypothesis (Sitaramayya et al, 1988; Barkdoll et al, 1989)

Manganese and  $Mg^{2+}$  appear to be essential cofactors for phosphodiesterase activation (Chader et al, 1974a, b; Yee and Liebman, 1978), where  $Mg^{2+}$  is likely to be the most important ion physiologically (Yee and Liebman, 1978). The direct influence of  $Mg^{2+}$  on phosphodiesterase activity has recently been characterized using partially purified phosphodiesterase, and the optimal range is given in Table 2 (Cook et al, 1986). The range over which  $Mg^{2+}$  maximally effects phosphodiesterase is likely to be within the  $Mg^{2+}$  concentrations found physiologically (Farber and Lolley, 1976).

**Transducin.** Factors that regulate transducin are presented in Table 2 and are discussed here. The gamma subunit of transducin is required for oligomerization of the protein, and for membrane binding (Shichi and Somers, 1984). Post stimulus subunit reassociation requires GTPase activity (Fung, 1983). The 48 KD protein, arrestin, competitively inhibits the interaction of phosphorylated rhodopsin with transducin (Kuhn et al, 1984).

**Pharmacology.** Pharmacological agents that affect transducin are given in Table 2.

*Ionic effects.* Calcium and  $Mg^{2+}$  have been reported to increase the membrane-binding nature of transducin (Kuhn, 1981). The physiological significance of these effects cannot be ascertained, however, since divalent ion effects on transducin-membrane binding began at 0.2 mM, which is above the upper physiological limit of free cytoplasmic  $Ca^{2+}$ . Studies of direct effects of  $[Ca^{2+}]_i$  and  $[Mg^{2+}]_i$  on purified transducin activity were not found in the literature.

**Rhodopsin.** Rhodopsin is a 41 KD, transmembrane protein found in the plasma membrane and densely concentrated in the membranous disks of the rod outer segment. Its carboxy terminal is located toward the cytoplasmic surfaces, whereas its polysaccharide-bound amino terminal is located intradiskally and extracellularly (for a review, see Dratz & Hargrave, 1983). Upon illumination, rhodopsin undergoes conformation changes (Hubbard & Kropf, 1958; Rosenfield et al, 1976; Honig et al, 1979; Milder & Kliger, 1986) that expose sites of activity at the cytoplasmic surface (Aton & Litman, 1984; Pellicone et al, 1985a, b). The biochemically-active transition state, metarhodopsin II, (Met II) preferentially binds transducin and initiates the enzymatic cascade that results in cGMP degradation (Bennett et al, 1982). The binding of transducin to Met II has been reported to stabilize the Met II transition state (Pfister et al, 1983). It has been reported that rhodopsin is capable of activating transducin in states subsequent to Met II (Knowles, 1984). In addition to thermal degradation, the Met II intermediate state is deactivated by phosphorylation as discussed above.

**Rhodopsin Kinase.** The amount of this kinase in the rod outer segment is small (1:1000, kinase:rhodopsin) (Kuhn, 1978). It becomes membrane bound after light stimulation due to its preferential binding to  $\rho^*$  (Pfister et al, 1983). Rhodopsin kinase phosphorylates up to 9 sites on  $\rho^*$  (Wilden & Kuhn, 1982).

*Pharmacology and ionic effects.* Phosphorylation of  $\rho^*$  requires the presence of  $Mg^{2+}$  (Kuhn & Dreyer, 1972), and is competitively inhibited by transducin (Pfister et al, 1983). Rhodopsin kinase is disinhibited indirectly by GTP, which induces the removal of



transducin from  $\rho^*$ . Cyclic GMP has been reported to have an undefined inhibitory effect on phosphorylation of rhodopsin (Szuts, 1985).

**Arrestin.** Arrestin is an approximately 48 KD (42-50.5 KD reported in various measurement techniques) soluble protein that is found in photoreceptor cells at approximately 1:1 molar ratio with rhodopsin (Broekhuysse et al, 1985). Arrestin undergoes light-induced binding to rod outer segment disks (Kuhn, 1978), enhanced by phosphorylation of rhodopsin (Kuhn et al, 1984). This binding produces a redistribution of arrestin from the entire intracellular space of the rod to just the rod outer segment (Broekhuysse et al, 1985).

*Pharmacology and Ionic effects.* Most importantly, the ATP-dependent quench of activated phosphodiesterase is inhibited by  $\text{Ca}^{2+}$  (Bownds et al, 1981; Del Priore & Lewis, 1983). This inhibitory effect of  $\text{Ca}^{2+}$  on phosphodiesterase quenching is kinase dependent (Paul Liebman, personal communication).

### **Section 1.2. $\text{Na}^+/\text{K}^+/\text{Ca}^{2+}$ exchange in rod outer segments.**

The first evidence for a  $\text{Ca}^{2+}$  extrusion mechanism in the rod outer segment came from measuring increases in the concentration of extracellular  $\text{Ca}^{2+}$ ,  $[\text{Ca}^{2+}]_o$ , in the interphotoreceptor space during light flashes (Yoshikami et al, 1980; Gold & Korenbrot, 1980). These observations demonstrated that some mechanism of  $\text{Ca}^{2+}$  transport must be present in rod plasma membranes to extrude  $\text{Ca}^{2+}$  from rods during illumination. Another early study which supported a  $\text{Na}^+/\text{Ca}^{2+}$  antiport mechanism included electrophysiological evidence that  $\text{Li}^+$  ( which does not support  $\text{Na}^+/\text{Ca}^{2+}$  exchange) substitution for  $\text{Na}^+$  in retinal bathing solutions increased  $[\text{Ca}^{2+}]_i$  in rods (Bastian & Fain, 1982b). More recently, experiments using suction-pipette electrodes to measure  $\text{Ca}^{2+}$  currents in isolated rods have indicated that an electrogenic  $\text{Na}^+/\text{Ca}^{2+}$  antiport mechanism exists in rod outer segments (Yau and Nakatani, 1984a; Hodgkin et al, 1987; Hodgkin & Nunn, 1987; Cervetto et al, 1989). First reports indicated that the antiporter moved one  $\text{Ca}^{2+}$  ion out of the photoreceptor in response to the movement of three  $\text{Na}^+$  ions into the cell (Yau and

Nakatani, 1984a). More recently, this antiporter has been found to transport both a  $K^+$  ion and a  $Ca^{2+}$  ion out of the photoreceptor in exchange for the movement of 4  $Na^+$  ions into the cell (Cervetto et al, 1989), and this antiporter is now referred to as a  $Na^+/K^+/Ca^{2+}$  exchanger. Thus  $Ca^{2+}$  extrusion from photoreceptors is affected by gradients of all three ions (Cervetto et al, 1989), as well as voltage (Lagnado et al, 1988). The exchanger is now known to be a 220 KD protein that has been purified and reconstituted with artificial membrane (Cook & Kaup, 1988).

The extrusion of  $Ca^{2+}$  by the  $Na^+/K^+/Ca^{2+}$  exchanger balances  $Ca^{2+}$  influx through  $g_{hv}$  in the dark. It produces an inward current of ~5.5 pA in the salamander and should produce an inward current of about 2 pA in the toad.

### **Section 1.3. Calcium regulation in rods.**

Rod photoreceptors have a total  $Ca^{2+}$  concentration of 3 - 9 mM (Hagins & Yoshikami, 1975; Farber & Lolley, 1976; Schnetkamp, 1979; Fain & Schroeder, 1985), yet the free cytoplasmic  $Ca^{2+}$ , capable of interacting with enzymes, is only about 0.1 - 1.0  $\mu$ M (Wormington & Cone, 1978; McNaughton et al, 1986; Ratto et al, 1988). Most of the  $Ca^{2+}$  in rods exists in buffer sites, bound to the intradiskal surfaces of the disk membranes (Schnetkamp, 1985; Schnetkamp & Kaup, 1988). Measurement of intradiskal  $Ca^{2+}$  exchange, using radioactive  $Ca^{2+}$  isotopes and laser-active micro mass analysis, have shown that this intradiskal  $Ca^{2+}$  exchanges with cytoplasmic  $Ca^{2+}$  only very slowly (only 10 % exchange of total  $Ca^{2+}$ / Hr.: Fain & Schroeder, 1985). Furthermore, measurements of  $Ca^{2+}$  fluxes across the plasma membrane, using  $Ca^{2+}$  ionselective microelectrodes, have shown that the plasma membrane fluxes control cytosolic free  $Ca^{2+}$  during short periods (minutes) of illumination (Miller & Korenbrot, 1987).

In the dark,  $[Ca^{2+}]_i$  remains constant, but there is a continual turnover of intracellular  $Ca^{2+}$  ( Fain & Schroeder, 1985) resulting from the influx of  $Ca^{2+}$  through  $g_{hv}$  and the efflux of  $Ca^{2+}$  via  $Na^+/K^+/Ca^{2+}$  exchange (Yau & Nakatani, 1984a, b; Gold, 1986; Miller &

Korenbrot, 1987). The rate of  $\text{Ca}^{2+}$  efflux via the  $\text{Na}^+/\text{K}^+/\text{Ca}^{2+}$  exchanger increases with  $[\text{Na}^+]_o$ ,  $[\text{Ca}^{2+}]_i$  and  $[\text{K}^+]_i$ , but decreases with increasing  $[\text{K}^+]_o$ ,  $[\text{H}^+]_o$ ,  $[\text{Ca}^{2+}]_o$ ,  $V_m$ , and  $[\text{Mg}^{2+}]_i$  (Yau & Nakatani, 1984a, 1985a; Hodgkin & Nunn, 1987; Cervetto et al, 1989). The rate of  $\text{Ca}^{2+}$  influx increases with  $g_{hv}$  and  $[\text{Ca}^{2+}]_o$ , but decreases with increasing  $[\text{Ca}^{2+}]_i$  and  $V_m$ .

After a step of illumination, then,  $\text{Ca}^{2+}$  extrusion should initially speed up as the rod hyperpolarizes. As  $[\text{Ca}^{2+}]_i$  decreases, however,  $\text{Ca}^{2+}$  efflux begins to slow (Miller & Korenbrot, 1987). Calcium influx, however, initially decreases as a result of the dominant effect of reducing  $g_{hv}$ . Most importantly,  $[\text{Ca}^{2+}]_i$  exerts an inhibitory action on  $g_{hv}$ , by lowering  $[\text{cGMP}]_i$  through inhibition of guanylate cyclase (Hodgkin & Nunn, 1988; Barkdoll et al, 1989; Koch & Stryer, 1988) and, possibly, through stabilization of PDE activation (Detwiler, 1989). After the initial decrease in  $\text{Ca}^{2+}$  influx during a step of illumination,  $g_{hv}$  begins to increase as the inhibitory action of  $[\text{Ca}^{2+}]_i$  is removed, which leads to increased  $\text{Ca}^{2+}$  influx. Illustration 4 shows a model of the  $[\text{Ca}^{2+}]_i$  negative feedback regulation of  $g_{hv}$ .

Thus a step of light results in a rapid decrease in  $[\text{Ca}^{2+}]_i$ , which has been measured using photosensitive dyes under nonphysiological conditions (McNaughton et al, 1985; Ratto et al, 1988), and which has been modeled mathematically, ignoring contributions from  $\text{Ca}^{2+}$  buffering (Miller & Korenbrot, 1987). A step of illumination also leads to a net efflux of  $\text{Ca}^{2+}$  from rods, which has likewise been measured (Hagins & Yoshikami, 1980; Gold & Korenbrot, 1980; Gold, 1986; Miller & Korenbrot, 1987). Free intracellular  $\text{Ca}^{2+}$  should eventually approach a steady state during light steps as the decreasing  $\text{Ca}^{2+}$  efflux eventually equals the increasing  $\text{Ca}^{2+}$ .

The intracellular  $\text{Ca}^{2+}$  regulation of rods, then, serves two important purposes. The first is that it creates a great stability with regard to  $[\text{Ca}^{2+}]_i$ . Any perturbation in  $[\text{Ca}^{2+}]_i$  leads to compensation by the regulatory mechanisms. For instance a sudden increase in  $[\text{Ca}^{2+}]_i$  decreases  $g_{hv}$ , which reduces  $\text{Ca}^{2+}$  influx. The resulting hyperpolarization helps contribute to the increase in  $\text{Ca}^{2+}$  efflux, which is also sensitive to the increase in  $[\text{Ca}^{2+}]_i$ . This point is important to remember when considering the physiological significance of buffered

**Illustration 4. Negative feedback regulation of  $Ca^{2+}$  on the light-sensitive conductance.**

The relationships between the proteins and small molecules are shown by the various lines. Lines with arrows indicate chemical reactions. Lines with filled balls indicate points of inhibition, while lines with open triangles indicate points of stimulation. The proteins and enzymes catalyzing the reactions are described in the text. See also Illus. 3.

The inset shows the overall relationship between  $[Ca^{2+}]_i$ , cGMP and the light-sensitive conductance,  $g_{hv}$ .

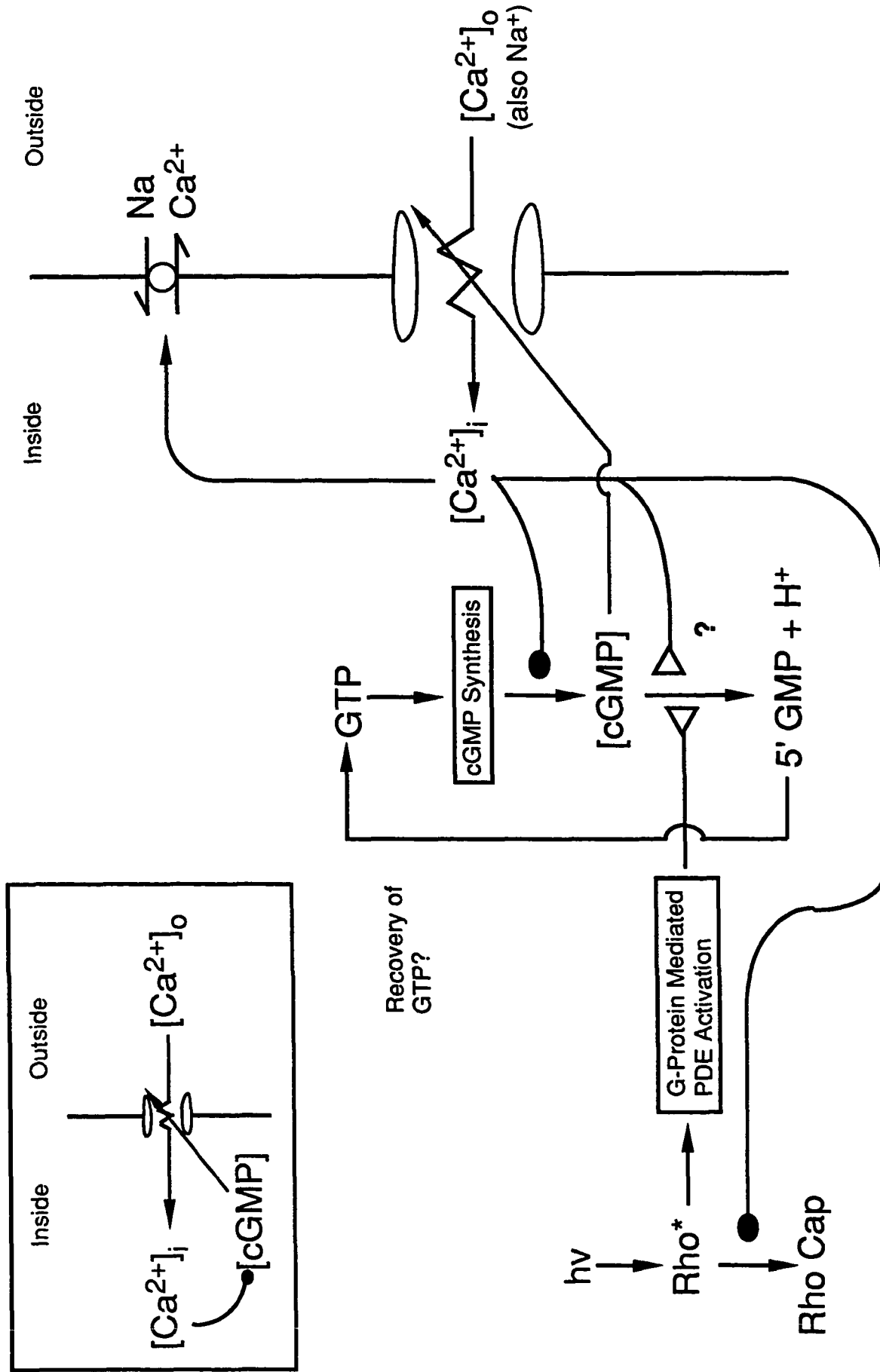


Illustration 4. Negative feedback regulation of  $\text{Ca}^{2+}$  on the light-sensitive conductance.

intracellular  $\text{Ca}^{2+}$ . The second point is that  $[\text{Ca}^{2+}]_i$  provides an important means of regulating  $g_{\text{HV}}$ . This regulation has been proposed to be solely responsible for the short term adaptation described in Section 1.0.2 (Nakatani & Yau, 1988; Matthews et al, 1988).

Whether or not buffered intracellular  $\text{Ca}^{2+}$  contributes to  $[\text{Ca}^{2+}]_i$  regulation during photoexcitation remains controversial. Investigations concerning the exchangeability of intracellular buffered  $\text{Ca}^{2+}$  with  $[\text{Ca}^{2+}]_i$  will be briefly reviewed.

Over 85 % of calcium buffering in the rods is intradiskal (Schnetkamp, 1985b). Intradiskal  $\text{Ca}^{2+}$  is reportedly tightly bound to the negative charges of phosphatidyl serine, and act as counter ions to offset the repulsive forces between the two opposing phospholipid surfaces of the disks (Schnetkamp, 1985b). This investigator reported earlier that at least some of the  $\text{Ca}^{2+}$  buffer sites are in equilibrium with  $[\text{Ca}^{2+}]_i$ , and that the binding affinity of the buffer sites is similar to that of the  $\text{Ca}^{2+}$  chelator, EGTA (Schnetkamp, 1979). Protons and alkali cations can reportedly replace  $\text{Ca}^{2+}$  as bound counterions, and release  $\text{Ca}^{2+}$  from the buffer sites when disk membranes were permeabilized.

Other reports about  $\text{Ca}^{2+}$  release from the intradiskal pool have been contradictory. Some of the differences in the results appear to come from the techniques used to study release of intradiskal  $\text{Ca}^{2+}$ , which in most cases has been membrane suspensions of "purified" rod outer segment disks. Apparently the  $\text{Ca}^{2+} / \text{H}^+$  ionophore, A23187, is capable of releasing all of the  $\text{Ca}^{2+}$  from intradiskal stores (Schnetkamp, 1986). There have also been reports suggesting that there are two separate intradiskal pools of bound  $\text{Ca}^{2+}$ , one that releases  $\text{Ca}^{2+}$  rapidly upon activation of a  $\text{Na}^+/\text{K}^+/\text{Ca}^{2+}$  exchanger or addition of cGMP (Kaup & Koch, 1984; Schnetkamp & Kaup, 1985; Schnetkamp, 1986, 1987; Volotovski & Khovratovik, 1986). Cyclic GMP or  $\text{Na}^+/\text{K}^+/\text{Ca}^{2+}$  exchange-mediated release of  $\text{Ca}^{2+}$  from disks has, however, been disputed (Smith & Capalbo, 1985; Schnetkamp & Bownds, 1987; Baur, 1988). Experimenters using sonicated disk preparations have not found cGMP or  $\text{Na}^+/\text{K}^+/\text{Ca}^{2+}$  exchange increases in  $\text{Ca}^{2+}$  released from disk membrane suspensions (Smith & Capalbo, 1985; Baur 1988). It has been

proposed that the cGMP sensitive and the  $\text{Na}^+/\text{K}^+/\text{Ca}^{2+}$  exchange sensitive release of  $\text{Ca}^{2+}$  from the disks results from plasma membrane contamination of the disk preparations, and that this contaminating fraction destroyed by sonication (Baur, 1988). These results are consistent with recent reports that proteins extracted from purified disk membranes do not contain the proteins thought to be the cGMP channels and  $\text{Na}^+/\text{K}^+/\text{Ca}^{2+}$  exchanger in the plasma membrane (Molday, 1989; Cook et al, 1987; Matèsic & Liebman, 1987; Cook & Kaup, 1988), and with results that the  $\text{Ca}^{2+}$  permeability of disks is as much as  $10^3$  smaller than the plasma membrane (Fain & Schroeder, 1985; Schnetkamp & Bownds, 1987).

Others have reported ATP-dependent uptake of  $\text{Ca}^{2+}$  by disk membranes (George & Hagins, 1983; Puckett et al, 1985) and light dependent release of  $\text{Ca}^{2+}$  from rod outer segment disk preparations (George & Hagins, 1983; Smith & Capalbo, 1985). These results, as well as pH-sensitive release of  $\text{Ca}^{2+}$  from disks described earlier, have also been proposed to be artifacts, resulting from  $\text{Ca}^{2+}$  chelation by ATP and pH sensitive release of  $\text{Ca}^{2+}$  from the EGTA buffers used in the suspension medium when pH was lowered directly or by light-evoked hydrolysis of cGMP. These observations were based on the fact that replacement of cGMP in the suspension media with 8-Bromo-cGMP, which is non-hydrolyzable but activates cGMP channels, did not produce a light-evoked  $\text{Ca}^{2+}$  release (Schnetkamp & Bownds, 1987).

Thus  $\text{Ca}^{2+}$  release from disks appears to occur slowly, if at all, under normal physiological conditions during illumination (Fain & Schroeder, 1985), and may play only a minimal role in buffering  $[\text{Ca}^{2+}]_i$  changes during brief photostimulation (Schnetkamp & Bownds, 1987; Miller & Korenbrot, 1987). The actual contribution of intracellular  $\text{Ca}^{2+}$  buffering to damping  $[\text{Ca}^{2+}]_i$  changes during illumination, then, have yet to be quantitated. It seems reasonable to assume that  $\text{Ca}^{2+}$  buffering plays a minimal role during normal photostimulation, but may act as a set point controller to assure that  $[\text{Ca}^{2+}]_i$  stays above some finite level, defined by the affinity of the buffer site ( $\sim 10^{-9}$  M).

#### **Section 1.4. *Pharmacology of colchicine and other selected tubulin-binding agents.***

The drug, colchicine, is one of oldest medicinal drugs. The drug is purified from the autumn lily, *colchicinum autumnale*, and has been used to treat gout for centuries. The best-characterized pharmacological effect of colchicine is its binding to the cytoskeletal protein, tubulin. Colchicine binds free dimeric tubulin and changes the protein's conformation, thus preventing tubulin polymerization into microtubules (Borisy & Taylor, 1967; for a review of microtubule assembly, see Hyams & Roberts, 1980). Since microtubules are often in a dynamic equilibrium with free tubulin, treatment with colchicine often leads to disassembly of microtubules in a specific way. Microtubules are structurally polar, with assembly occurring at one end, while disassembly occurs at the opposite end. Drugs such as colchicine affect these structures by inhibiting polymerization at the + end, while disassembly continues at the other end (see Scheele & Borisy 1979).

##### **1.4.1. *Effects of colchicine on membranes.***

Anatomical and physiological effects of colchicine, then, are often attributed to a disruption of microtubules. It is unlikely that colchicine's effects on rod photoreceptors result from microtubule disruption for reasons given in Section 1.0.3, and because microtubules in the rod outer segment appear to be resistant to disruption by colchicine (Kaplan et al, 1985; Sale et al, 1988). Other effects of colchicine have been reported, however, that are not likely to involve microtubules. These include: the binding of colchicine to liver microsomal and nuclear membranes (Hotta & Shepard, 1973; Stadler & Franke, 1972, 1974), the induction of membrane particle aggregation in SV 3T3 cells (Furcht & Scott, 1975), the inhibition of nucleoside transport (Loike & Horwitz, 1976), the inhibition of biopterin uptake (Rembold & Langenbach, 1978) and the inhibition of galactosyl- and sialyl-transferases (Mitranic et al, 1981). The mechanisms by which colchicine affects these systems have not been determined, but they apparently involve proteins with some binding similarities to tubulin (for a summary, see Ludueña, 1979). Colchicine does not, however, have non-specific effects on lipid bilayers (Alstiel &



Landsberger, 1977).

These membrane effects of colchicine might be explained by colchicine's binding to a tubulin epitope. A specific subpopulation of tubulin exists as an integral membrane protein, and this membrane tubulin has a significantly greater dissociation rate than soluble tubulin (Garland, 1975; Blitz & Fine, 1974; Kornguth & Sutherland, 1975; Feit et al, 1977; Rodriguez & Barra, 1983; Regula et al, 1986). Recently, this form of tubulin has begun to attract attention, as it has been associated with  $\beta$ -adrenergic receptors in cardiac muscle (Lampedis et al, 1986) and brain neurons (Rasenick et al, 1981, 1986, 1988). The  $\beta$ -adrenergic system is of particular interest, since noradrenergic binding to these receptors alters adenylate cyclase activity, and this action is mediated by a family of G-proteins with marked homologies to transducin (see Yamazaki et al, 1985). The membrane tubulin in both the cardiac muscle and brain neuron systems was affected by colchicine (Lampedis, 1986; Rasenick et al, 1981, 1986, 1988). Similarly, in light-scattering studies on rod outer segment disk membranes, colchicine has been found to block the GTP- and G-protein-dependent binding of PDE to membrane vesicles, although the concentration-dependency of these effects (mM) was quite high (Carreta & Stein, 1986).

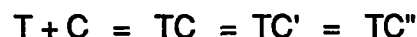
#### *1.4.2. Tubulin in rod outer segments.*

Membrane tubulin has recently been found to exist in photoreceptor plasma membranes, and it copurifies with the cGMP-sensitive channel proteins in some preparations (Matesic & Liebman, 1989). The concentration of total tubulin in the outer segment is roughly equal to the concentration of G-Protein (Robinson & Hagins, 1979), and much of the tubulin in the outer segment is acetylated (Sale et al, 1988). Acetylation is a post-translational modification of tubulin which has unknown consequences (Joe Besharse, personal communication), and it is not known whether the rod outer segment membrane tubulin subpopulation is also acetylated (Paul Liebman, personal communication). Thus determining if colchicine's effects are mediated by membrane tubulin becomes a central question, and it is of interest to review the tubulin-binding characteristics of colchicine.

Other aspects of tubulin pharmacology for interpreting the experiments presented in this thesis are also reviewed below.

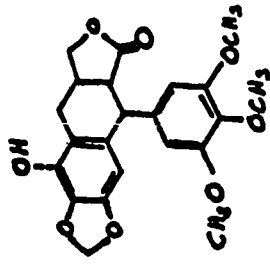
#### 1.4.3. *Tubulin-colchicine binding.*

A proposed mechanism for the tubulin-dimer binding action of colchicine is:

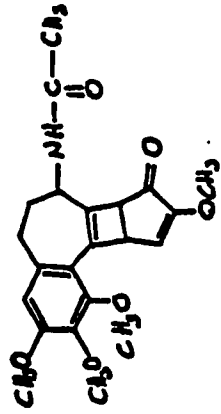


The first two reactions are fast, and the last one is slow (Garland, 1977), making tubulin-colchicine binding time-dependent (Borisy & Taylor, 1967). Tubulin binding by colchicine is also temperature-dependent, with nearly zero binding occurring at 0° C (Wilson, 1975). The dissociation constant for binding has been measured by both equilibrium methods and kinetic methods with results varying from about  $5.0 \times 10^{-8}$  to  $9.1 \times 10^{-7}$  M (Borisy & Taylor, 1967; McClure & Paulson, 1977; Owellen et al, 1974; Sherline et al, 1975; Bhattacharyya & Wolf, 1976).

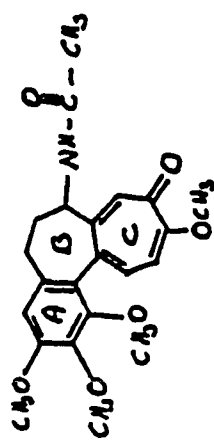
The binding of colchicine to tubulin is a two-step process, where two functional groups on colchicine act as individual binding ligands. The functional groups are the trimethoxyphenol, or "A" ring and the tropolone, or "C" ring (Andreau & Timasheff, 1986; see Illus. 5). The tubulin-colchicine interaction begins with the binding of the tropolone ring, which probably involves hydrogen bonding to the carbonyl group, followed by a tubulin conformational change and the binding of the trimethoxyphenol ring. The great affinity of colchicine for tubulin depends on this double-ligand binding, which creates the favorable thermodynamics (Andreau & Timasheff, 1986). This is exemplified by the much weaker binding of the colchicine analogs,  $\beta$ -lumicolchicine and N-acetyl mescaline (see Illus. 5), which contain normal trimethoxyphenol rings but not tropolone rings (Wilson et al, 1974; Andreau & Timasheff, 1986). The binding affinity of tubulin matches the combined affinities of  $\beta$ -lumicolchicine or N-acetyl mescaline and tropolone, plus the cractic free energy associated with the binding of a double ligand drug (Andreau & Timasheff, 1986). The time



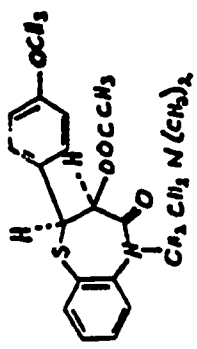
Podophyllotoxin



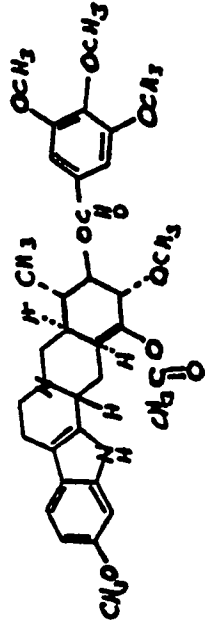
$\beta$ -lumicolchicine



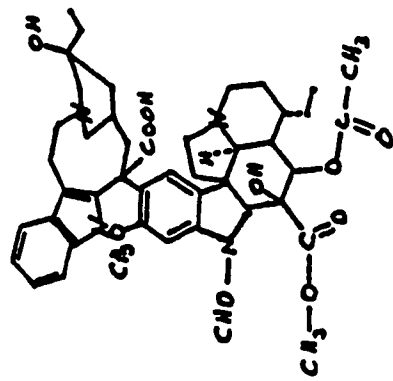
Colchicine



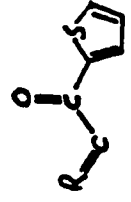
l-cis diltiazem



Reserpine



Vincristine



Nocodazole

Illustration 5: Molecular structures of selected tubulin-binding drugs

and temperature dependency of binding result from the conformational change required after binding the tropolone ring prior to the trimethoxyphenol ring's binding.

#### 1.4.4: Pharmacology of tubulin-colchicine binding.

The binding of colchicine to tubulin is affected by GTP, which stabilizes tubulin-colchicine binding and *vis versa*. There are two binding sites for GTP on tubulin: one exchangeable and one non-exchangeable (Bryan, 1972). It is the exchangeable site that stabilizes colchicine binding and *vis versa* (Bhattacharyya & Wolf, 1976; Hadjian et al, 1977). It is not certain, however, which of the binding ligands of colchicine confers the stability to the exchangeable GTP-binding site, but thus far evidence favors tropolone (Andreau & Timasheff, 1986). The GTP-binding of tubulin to the exchangeable site requires  $Mg^{2+}$ . It is also the exchangeable site that stabilizes microtubule polymerization, while it inhibits non-specific aggregation of tubulin. The exchangeable site becomes non-exchangeable in intact microtubules (Arai & Kaziro, 1977). The exchangeable GTP binding site is also the site of a known GTPase activity of tubulin, which is induced by mobilization for subunit assembly or by the drug colchicine (for a review, see Jacobs, 1979). Binding of both ligands is required to confer GTPase activity by colchicine (Andreau & Timasheff, 1986). The function of the non-exchangeable site has not been elucidated.

Calcium also binds to tubulin at multiple sites: one with a high affinity ( $K_m \sim 3 \times 10^{-6}$  M) and about 16 with low affinity ( $K_m \sim 2.5 \times 10^{-4}$  M). Low levels of  $Mg^{2+}$  ( $10^{-7}$  -  $10^{-6}$  M) increase the affinity of the low-affinity  $Ca^{2+}$  binding sites, but higher concentrations of  $Mg^{2+}$  inhibit both low and high affinity  $Ca^{2+}$  binding (Solomon, 1977). High concentrations of KCl (100 mM) also inhibits tubulin's  $Ca^{2+}$  binding, whereas GTP, colchicine and vinca alkaloids do not affect tubulin's binding to  $Ca^{2+}$  *in vitro* (Solomon, 1977). Given the intracellular conditions of rod outer segments ( $\sim 1$  mM  $Mg^{2+}$ ,  $\sim 100$  mM  $K^+$ ,  $>10^{-6}$  M  $Ca^{2+}$ ), it seems unlikely that cytoplasmic tubulin there has any significant bound  $Ca^{2+}$ .

Other pharmacological agents can affect colchicine's binding to tubulin. Some anions, such as sulfate, appear to increase tubulin-binding by colchicine (Bhattacharyya & Wolf,

1976c). Colchicine shares at least part of its binding site, the trimethoxyphenyl ring, with other tubulin-binding drugs, notably podophyllotoxin and reserpine (Cortese et al, 1977; Wilson, 1970; Poffenbarger & Fuller, 1977). Other drugs that compete with the binding site of colchicine include: yohimbine; rotenone; chlorpromazine and nocodazole, although nocodazole does not share any binding sites with colchicine (Tan & Lagnado, 1975; Barham & Brinkley, 1976; Hinman & Cann, 1976; Davidse & Flach, 1977). The antitumor drugs known as the vinca alkaloids, which include the chemotherapy drugs vinblastine and vincristine, stabilize colchicine binding, although these drugs bind tubulin at sites distant from colchicine (Wilson, 1970; Mandelbaum-Shavit et al, 1976; Owellen et al, 1974; Wilson et al, 1974; Wilson, 1975).

Some of these drugs have been tested for their effects on rods in experiments described in this thesis. The drug, vincristine, was found to affect rod electrophysiology quite differently than colchicine, and is therefore briefly discussed.

Tubulin-vincristine binding is temperature-,  $\text{Ca}^{2+}$  - and GTP-independent (Bhattacharyya & Wolf, 1976c). Vincristine induces crystallization of tubulin when the drug is present at concentrations greater than  $10^{-4}$  M, and is often used in tubulin-purification processes (Bensch et al, 1969; Marantz et al, 1969). It stabilizes colchicine and GTP binding to tubulin, and increases the rate constant for colchicine-binding (Garland & Teller, 1975; Tan & Lagnado, 1975; Wilson, 1970).

### **Section 1.5. *Electrophysiological effects of colchicine.***

Many researchers have hypothesized that the cytoskeleton of neurons and other excitable tissues may play a role in the regulation of membrane conductances (Moran & Varela, 1971; Terakawa & Watanabe, 1976; Matsumoto & Sakai, 1979; Matsumoto et al, 1980; Fukuda et al, 1981; Baux et al, 1981; Ozaki et al, 1986). In testing this hypothesis, these groups of researchers measured the effects of colchicine on membrane conductance with positive results. Many of the researchers assumed that the effects of colchicine resulted from a disruption of membranous microtubules. Because of the high

concentrations and short time-course of colchicine application used in these experiments, however, this assumption may have been erroneous in some cases. For instance, in squid giant axons, colchicine was found to affect membrane excitability (Matsumoto & Sakai, 1979), but the effects of colchicine were later shown to occur without the destruction of submembranous microtubules (Terakawa & Nakayami, 1985). At this time, then, the mechanism of colchicine's effects on these tissues remains obscure. Nevertheless, the effects of colchicine on these neuronal tissues may have important implications for the work presented in this thesis, and are therefore briefly reviewed.

Colchicine affects the neuromuscular junctions of frogs and rats by reducing both the quanta released per action potential and the amplitude of the miniature end-plate potentials (Katz, 1975). It has been proposed that these effects result from a colchicine-induced reduction in the voltage-dependent  $\text{Ca}^{2+}$  currents in presynaptic terminals and in the postsynaptic acetylcholine-sensitive  $\text{Cl}^-$  currents, since it effects both of these types of currents in the somatic cells of *Aplysia* (Baux et al, 1981).

In fact, several neuronal conductances in *Aplysia* L<sub>1</sub>-L<sub>6</sub> neurons are affected by colchicine. Adding 0.1 - 5.0 mM colchicine to superfusates depressed both cholinergic and non-cholinergic synaptic transmission in these cells. Furthermore, superfusion with colchicine in the 0.1 - 5.0 mM range or intracellularly injecting colchicine to lesser concentrations blocked  $\text{Ca}^{2+}$  spikes (attributed to voltage activated  $\text{Ca}^{2+}$  channels) after a 20 min. exposure period. These  $\text{Ca}^{2+}$  channels were also blocked by  $\text{La}^{3+}$ , but not  $\text{Co}^{2+}$ . Additionally, colchicine also shifted the reversal potential of acetylcholine-activated  $\text{Cl}^-$  channels, and reduced acetylcholine induced channel openings. Finally, colchicine moderately reduced voltage-dependent  $\text{Na}^+$  and  $\text{K}^+$  entry into these cells (Baux et al, 1981).

Colchicine also affects cultured mammalian neurons. Colchicine, but not  $\beta$ -lumicolchicine, selectively reduced the  $V_{\text{max}}$  and the duration of  $\text{Ca}^{2+}$  spikes, but not  $\text{Na}^+$  spikes, in cultured guinea pig neurons. In these experiments, the cells had been exposed

to  $\mu\text{M}$  colchicine for two days prior to the electrophysiological recordings (Fukuda et al, 1981). The effects of colchicine in this case can probably be attributed to tubulin involvement.

As previously mentioned, early reports showed that colchicine can also affect axonal conductances. Colchicine altered the conductance of a type of  $\text{K}^+$  channel in crayfish axons (Terakawa & Watanabe, 1976), and altered the fast  $\text{Na}^+$  conductance in squid giant axon (Matsumoto & Sakai, 1979; Matsumoto et al, 1980, 1984) when added to intracellular perfusion solutions. More recently, however, colchicine's effects on squid giant axon excitability have been shown to be pressure sensitive (Terakawa & Nakayami, 1985). In their report, the researchers showed that 5 mM colchicine only affected axonal excitability when the intracellular perfusion pressure exceeded 15 cm  $\text{H}_2\text{O}$ . Thus colchicine reduced the resistance of excitability to mechanical stress in this system. Lumicolchicine had similar effects at these concentrations, as did perfusion with solutions containing the chaotropic anions,  $\text{Cl}^-$  and  $\text{Br}^-$ , rather than the usual  $\text{F}^-$ . Perfusion with these chaotropic anions removed submembranous microtubules, but colchicine did not.

There have also been reports of colchicine affecting other types of neuronal transducers. Colchicine and vinblastine disrupted microtubules and abolished the mechanotransducing ability of the campaniform sensilla, a modified cilia on the legs of cockroaches (Moran & Varela, 1971). In these experiments, the cockroach sensilla had been exposed to 50 mM colchicine or 10 mM vinblastine for two hours. Although these drug concentrations were unusually high, electron microscopy revealed that disruption of the extensive microtubule arrays in these cilia accompanied functional loss of mechanotransduction. In chemoreceptors, pretreatment with colchicine (25 mM for 2 min.), prior to destroying the distal processes of the labellar chemosensilla of the blowfly with sodium deoxycholate, prevented regeneration of the distal processes and of the functional responsiveness of sugar receptors (Ozaki et al, 1986).

## **Section 1.6. *Ionic currents in the rod inner segment.***

At least five distinguishable voltage-sensitive currents have been partially characterized in the rod inner segment, cell body and pedicle (Bader et al, 1982; Kolesnikov et al, 1984). These voltage-sensitive currents have been classified by their distinctive pharmacology. The voltage / current relationships for these currents have been partially characterized in the salamander (Bader et al, 1982). These currents, along with rod outer segment currents, are listed in Table 2, which contains: lists of drugs that block these currents; mathematical current-voltage relationships for these channels; and other important parameters, such as the main ions carrying the currents and the reversal potentials of the currents. The results are tabulated from Bader et al (1982) and others. A schematic representation of these current and the roles they play in the dark current are shown in Illus. 2. The steady-state rod cell membrane voltage in the dark-adapted rods is about -40 mV, such that several of the voltage-sensitive currents are at least partially activated in the dark-adapted state. Electrogenic Na<sup>+</sup>/K<sup>+</sup>-ATPase activity also exists in the rod inner segment. As in most cells, this exchanger regulates intracellular Na<sup>+</sup> and K<sup>+</sup>. In rods, maintaining proper intracellular ion concentrations is also necessary for maintaining the dark current. The ion concentration dependency of this exchanger has been partially characterized in toads (Oakley, 1983; Shimazaki and Oakley, 1984, 1986). To maintain a steady-state voltage in the toad rods, this exchanger must produce an outward current of approximately 6.7 pA. Other aspects of this exchanger are listed in Table 2.

The cGMP-sensitive current of the outer segment has recently been patched from inner segments as well (Matthew & Watanabe, 1988), although the density of the channels in the inner segment is much lower.

### *1.6.1: A disputed current of both the rod inner and outer segments.*

Using the excised patch-clamp technique, voltage-sensitive chloride channels have been found in both the rod inner segment and the rod outer segment (Kolesnikov et al, 1984). It has not been determined if this is the same anion channel reported by Bader et al;



**Table 2. Physical and pharmacological properties of rod transmembrane currents.**

Currents in rod photoreceptors (see illus. 2) have been studied extensively since 1971. Using both standard and novel electrophysiological techniques, the ionic specificity, equilibrium voltage and  $\text{Ca}^{2+}$  or voltage sensitivities of these component currents have been characterized. . The pharmacology of these currents have also been studied, and mathematical relationships have, in some cases, been developed for important physical and biochemical parameters These properties are shown under the appropriate heading. Data was compiled from the following: Yoshikami & Haggins, 1971, 1973; Bastian & Fain, 1979, 1982b; Baylor et al, 1979; Capovilla et al, 1980, 1981; Corey et al, 1984; Bader et al, 1982; Shimazaki & Oakley, 1984; Yau & Nakatani, 1984a, b; Yau & Nakatani, 1985b; Stern et al, 1986; Nicol et al, 1987; Fesenko et al, 1985; Zimmerman and Baylor, 1986, 1987.

Current	Physio.	Pharm.	Magnitude*	Potential par.**	Ionic	Mathematical	
	Direction	Inhibitors	Resting Max	VT	VR	Permiability relationships	
ROS	LSC	inward	1-cis- 55.0	>800*	none	0-10	Li+:Na+:Rb+:K+:Cs I = f(cGMP)
		diltiazem,					1.0:1.0 : 0.7 :0.5:0.3
		extracellular divalent cations					Na+:Ca+:Mg+ cGMP = f(Lt ,Cs ,t)
IE,Ca	inward	Colchicine*	5.5	40.0	none	***	1.0: 0.2: 0.2 3Na+:1Ca2+
		Li+-Na+					
		replacement, La3+, K+, Podophytotoxin* Amiloride*					

Table 2: Physical and Pharmacological Properties of Rod Transmembrane Currents

RIS

ICl	inward*	unknown	<1.0	<3.0	< -50	undet.	Cl <sup>-</sup> : F <sup>-</sup> : NO <sub>3</sub> <sup>-</sup>	I = f(V,t)
							1.0: 0.2: 0.4	
IK	outward	extracellular	undet.	-70	-72			I = f(V,t)
		TEA, 4-AP						
			IK+IK,Ca=36					
IK,Ca	outward	intracellular	undet.	--	-72			I = f(V,t)
		Cs <sup>+</sup>						
		Low [Ca <sup>2+</sup> ] <sub>if</sub>						
Ih	inward	extracellular	0.0	25-70	-40	-32		I = f(V,t)
		Cs <sup>+</sup>						

Table 2: Physical and Pharmacological Properties of Rod Transmembrane Currents

(1982). If they are the same, then some discrepancies exist. Bader et al found little voltage-sensitivity in their measurements of the inner segment current, yet Kolesnikov et al found that the channels they measured using the patch clamp technique were voltage sensitive.

The voltage-sensitive anion conductance studied by Kolesnikov et al was also found in rod outer segments. This result supported earlier experimental evidence for such a conductance (Korenbrod and Cone, 1972; Zuckerman, 1973), which has more recently been challenged (Baylor and Lamb, 1982). The current passing through the voltage-sensitive chloride channels is expected to be very small, but may contribute to repolarization kinetics from experimentally-induced depolarizations (Kolesnikov et al, 1984). The channels are mostly closed under dark-adapted conditions. An estimated upper limit for the total conductance occurring in a rod is ~2 nS at -40 mV, and 50 - 100 nS near 0 mV. The estimated current produced at dark resting voltages is less than 1 pA (~ -40 mV), but at 0 mV it should increase up to 2 pA . These channels were not tested for cGMP sensitivity.

## CHAPTER 2

### METHODS

The experimental techniques are described in this chapter, which is divided into six sections: Section 1: *Animal Procurement, Care and Dissection*; Section 2: *Experimental Setup*; Section 3: *Solutions*; Section 4: *Microelectrode Preparation and Characterization*; Section 5: *Pressure Injection System*; Section 6: *Rod Cell Impalement* and Section 7: *Data Recording Apparatus*.

#### **Section 2.1: *Animal Procurement, Care and Dissection***

Toads, *Bufo marinus*, were purchased from a supplier in the southern United States during the years 1983 through 1987. During most of 1988, the toads were purchased from a supplier based in Connecticut. From 1984 through 1987, toads came from Mexico, except during the months of June through August in 1984 and 1985, when they came from Florida. The supplier used in 1988 obtained toads from the Caribbean islands. No seasonal or supplier variations in light responsiveness of the retinas were ever observed; however, the membrane voltage had a greater tendency to oscillate during membrane voltage recovery in toads purchased in mid-to-late summer.

Upon arrival, the toads were placed in a controlled environment under artificial light with 12-hour cycles of light and darkness. They were kept from one to three weeks and were fed live crickets two to three times weekly. Toads were dark adapted at room temperature for at least 12 hours prior to dissection. Dissection proceeded under dim red light. The toads were pithed both rostrally and caudally and an eye was enucleated. Microdissection then proceeded under infrared illumination using a dissecting microscope fitted with image converters similar to the system described below under Experimental Setup. A small, approximately 5 mm diameter, posterior portion of the eye adjacent to the optic disk was transected with a razor blade and placed into a 0.3 ml chamber filled with

oxygenated control superfusion solution (either solution A1 or B1, Table 3). The retina was then peeled away from the pigment epithelium and pinned down, leaving the photoreceptor outer segments face up (see Illustration 6). The chamber was then transferred to the microscope in the experimental cage (described below).

## **Section 2.2: *Experimental Setup***

**Experimental Cage.** A monocular compound microscope fitted with an infrared optical viewing system was mounted on an air table in a darkened, three-sided, shielded cage that opened to the front. The front of the cage was covered with a black curtain lined with wire mesh to prevent accidental illumination of the retina and to provide electrical shielding.

**Infrared viewing system.** The infrared viewing system was comprised of an infrared image converter (model 6914, Varo Instr., Garland, TX) mounted on one end of a custom-made chassis, with a 6x, non-inverting triplet lens system (Edmond Scientific, Barrington, NJ) mounted on the other end. Non-inverting optics were used to aid the experimenter in electrode placement. This system was then mounted on the monocular inclined tube of the compound microscope in the experimental cage. A similar system was mounted on each of the oculars of the binocular dissecting microscope described in Section 1. Both microscopes used visible light sources fitted with infrared filters to provide infrared illumination (>850 nm).

**Solution Control System.** The superfusion apparatus supplied fresh, oxygenated salt solution to the retinal chamber at a rate of about 1 ml/min. The composition of the various superfusion solutions used in the experiments are listed in Table 3. Glass bottles filled with solutions were placed on a shelf inside the experimental cage and were connected to a 4-way valve also mounted inside the cage and equipped with an external switch. This setup allowed the solutions to be switched rapidly without illuminating the retina during experimental recordings. It also allowed the valve to be located near the retinal chamber, in order to reduce dead space and the resulting lag time between solution

**Table 3. Composition of Superfusion Solutions in Millimolarity.**

All five types of solution had 2.4 mM KCl, 5.55 mM glucose, 0.014 mM phenol red for pH indication, 2.8 mM HEPES buffer and 0.01 mM EDTA. All had their pH adjusted to ~7.8 by addition of 1.0 N NaOH. The pH endpoint was determined by comparing the color to a standard calibrated with a pH meter. All solutions were equilibrated with 100% O<sub>2</sub> prior to experimentation.

Unsubstituted solutions of types A, B and C also contained 108 mM NaCl and 1.3 mM MgSO<sub>4</sub>. When drugs or ions were added to these solutions, NaCl was decreased as needed to maintain constant osmolarity. The salt MgSO<sub>4</sub> was decreased in solution A6 to reduce Mg<sup>2+</sup> influx into rods via the ionophore A23187. Calcium ion concentrations in EGTA buffered solutions were calculated using the formula given in the Appendix under Derivation 1, modified from Caldwell, 1976. The equilibrium constants were adjusted for pH 7.8 according to the formula given in Caldwell, 1976. EGTA and CaCl<sub>2</sub> were added by serial dilution to ascertain the accuracy given in the table in solutions D9-D11, which were used for ion electrode calibration.

Abbreviations are as follows:

1. Mix Ch Blk: combination of channel blockers added to normal ringers solution
2. Colch: colchicine added to normal ringers solution
3. Lumicolch: beta-lumicolchicine
4. HEPES: N-2-hydroxyethylpiperazine-n'-2-ethanesulphonic acid
5. EDTA: Ethylenediaminetetraacetic acid
6. 4-AP: 4-aminopyridine
7. TEA-Cl: Tetraethylammonium chloride
8. low Ca: low-calcium solutions, with or without colchicine where indicated
9. Not shown is the solution for the vincristine experiment. The solution was made by adding 0.15 mM vincristine sulphate to solution A1.
10. IBMX: 3-isobutyl-1-methylxanthine

**COMPOSITION OF SUPERFUSION SOLUTIONS IN MILLIMOLARITY**

<b>Type A Solutions</b>		NaCl	KCl	CaCl <sub>2</sub>	MgSO <sub>4</sub>	CoCl <sub>2</sub>	TEA-Cl	CsCl	4-AP	colch
Solutions										
A1. Standard solution		108.0	2.40	0.90	1.30	—	—	—	—	—
A2. 10 mM colchicine		103.0	2.40	0.90	1.30	—	—	—	—	10.0
A2a. 20 μM colchicine		98.0	2.40	0.90	1.30	—	—	—	—	20.0
A3. 5 mM colchicine		105.5	2.40	0.90	1.30	—	—	—	—	05.0
A4. 1 mM colchicine		108.0	2.40	0.90	1.30	—	—	—	—	01.0
A5. 0.5 mM colchicine		108.0	2.40	0.90	1.30	—	—	—	—	00.5
A6. 0.5 mM β-Lumi colchicine		108.0	2.40	0.90	1.30	—	—	—	—	00.5
A7. 6.67 mM cobalt		98.0	2.40	0.90	1.30	6.67	—	—	—	—
A8. 6.67 mM cobalt and 10 mM colchicine		93.0	2.40	0.90	1.30	6.67	—	—	—	10.0
A9. cocktail		86.75	2.40	0.90	1.30	0.50	10.0	10.0	1.0	—
A10. cocktail + 10 mM colchicine		81.75	2.40	0.90	1.30	0.50	10.0	10.0	1.0	10.0
A11. 5X Ca <sup>2+</sup>		102.6	2.40	4.50	1.30	—	—	—	—	—
<b>Type B Solutions</b>		NaCl	KCl	CaCl <sub>2</sub>	MgSO <sub>4</sub>	IBMX	Diltiazem	Colchicine	NaAspartate	LaNO <sub>3</sub>
Solutions										
B1. Standard solution		98.0	2.40	0.10	1.30	—	—	—	10.0	—
B2. 10 mM colchicine		98.0	2.40	0.10	1.30	—	—	10.0	10.0	—
B3. 10 mM colchicine + IBMX		98.0	2.40	0.10	1.30	0.50	—	10.0	10.0	—
B4. 500 μM IBMX		98.0	2.40	0.10	1.30	0.50	—	—	10.0	—
B6. 1.0 mM diltiazem		98.0	2.40	0.10	1.30	—	1.00	—	10.0	—
B7. 1.0 mM diltiazem + IBMX		98.0	2.40	0.10	1.30	0.50	1.00	—	10.0	—
B8. 0.1 mM La <sup>3+</sup>		98.0	2.40	0.10	1.30	—	—	—	10.0	0.10
B9. 0.1 mM La <sup>3+</sup> + IBMX		98.0	2.40	0.10	1.30	0.50	—	—	10.0	0.10

Table 3: Composition of superfusion solutions in millimolarity.



<b>Type C Solutions</b>									
Solutions	NaCl	KCl	CaCl <sub>2</sub>	MgSO <sub>4</sub>	Colchicine				
C1. 5X Ca <sup>2+</sup>	102.6	2.40	4.50	1.30	—				
C2. 6X Ca <sup>2+</sup>	93.6	2.40	5.40	1.30	10.0				
C3. 10 mM colchicine									
+ 5X Ca <sup>2+</sup>	98.0	2.40	—	1.30	10.0				
C4. 10X Ca <sup>2+</sup>	98.0	2.40	—	1.30	—				
<b>Type D Solutions</b>									
Solutions	NaOH	KCl	CaCl <sub>2</sub>	MgSO <sub>4</sub>	HCH <sub>3</sub> SO <sub>3</sub>	EGTA	colchicine		
D1. 10 <sup>-5.6</sup> M Ca <sup>2+</sup>	108	2.40	0.90	1.30	108	0.90	—		
D2. 10 <sup>-5.6</sup> M Ca <sup>2+</sup>	108	2.40	0.90	1.30	108	0.90	10.0		
D3. 10 <sup>-6.4</sup> M Ca <sup>2+</sup>	108	2.40	0.90	1.30	108	0.92	—		
D4. 10 <sup>-6.4</sup> M Ca <sup>2+</sup>	108	2.40	0.90	1.30	108	0.92	10.0		
D4a. 10 <sup>-6.4</sup> M Ca <sup>2+</sup>									
+ 20 μM colchicine	108	2.40	0.90	1.30	108	0.92	20		
D5. 10 <sup>-6.9</sup> M Ca <sup>2+</sup>	108	2.40	0.90	1.30	108	0.96	—		
D6. 10 <sup>-6.9</sup> M Ca <sup>2+</sup>	108	2.40	0.90	1.30	108	0.96	10.0		
D7. 10 <sup>-7.1</sup> M Ca <sup>2+</sup>	108	2.40	0.90	1.30	108	1.00	—		
D8. 10 <sup>-7.1</sup> M Ca <sup>2+</sup>	108	2.40	0.90	1.30	108	1.00	10.0		
+ colchicine									
D9. 10 <sup>-6</sup> M Ca <sup>2+</sup>	108	2.40	1.800	1.30	—	1.815	—		
D10. 10 <sup>-8</sup> M Ca <sup>2+</sup>	108	2.40	1.800	1.30	—	3.180	—		
D11. 10 <sup>-8</sup> M Ca <sup>2+</sup> + colchicine	98	2.40	1.800	1.30	—	3.180	20.0		

Table 3: Composition of superfusion solutions in millimolarity.

Type E Solutions	LiCl	KCl	CaCl <sub>2</sub>	MgSO <sub>4</sub>	IBMX	LiOH	HCH <sub>3</sub> SO <sub>3</sub>	EGTA	NaCl	NaAsp
Solutions										
E1. Standard 100% Li	108	2.40	0.90	1.30	—	—	—	—	—	—
E2. 90% Li, 10% Na	97.2	2.40	0.90	1.30	—	—	—	—	10.8	—
E3. 65% Li, 35% Na	70.2	2.40	0.90	1.30	—	—	—	—	38.8	—
E4. 50% Li, 50% Na	54.0	2.40	0.90	1.30	—	—	—	—	54.0	—
E5. 10% Li, 90% Na	10.8	2.40	0.90	1.30	—	—	—	—	97.2	—
E6. 100% Li + colchicine	108	2.40	0.90	1.30	—	—	10.0	—	—	—
E7. Li, 10 <sup>-5.6</sup> Ca <sup>2+</sup>	—	2.40	0.90	1.30	—	108	—	0.90	—	—
E8. Li, 10 <sup>-6.4</sup> Ca <sup>2+</sup>	—	2.40	0.90	1.30	—	108	—	0.92	—	—
E9. Li, 10 <sup>-6.9</sup> Ca <sup>2+</sup>	—	2.40	0.90	1.30	—	108	—	0.96	—	—
E10. Li, 10 <sup>-4.0</sup> Ca <sup>2+</sup>	98.0	2.40	0.10	1.30	—	—	—	—	—	10
E11. Li, 10 <sup>-4.0</sup> Ca <sup>2+</sup> + IBMX	98.0	2.40	0.10	1.30	0.50	—	—	—	—	10

Table 3: Composition of superfusion solutions in millimolarity.

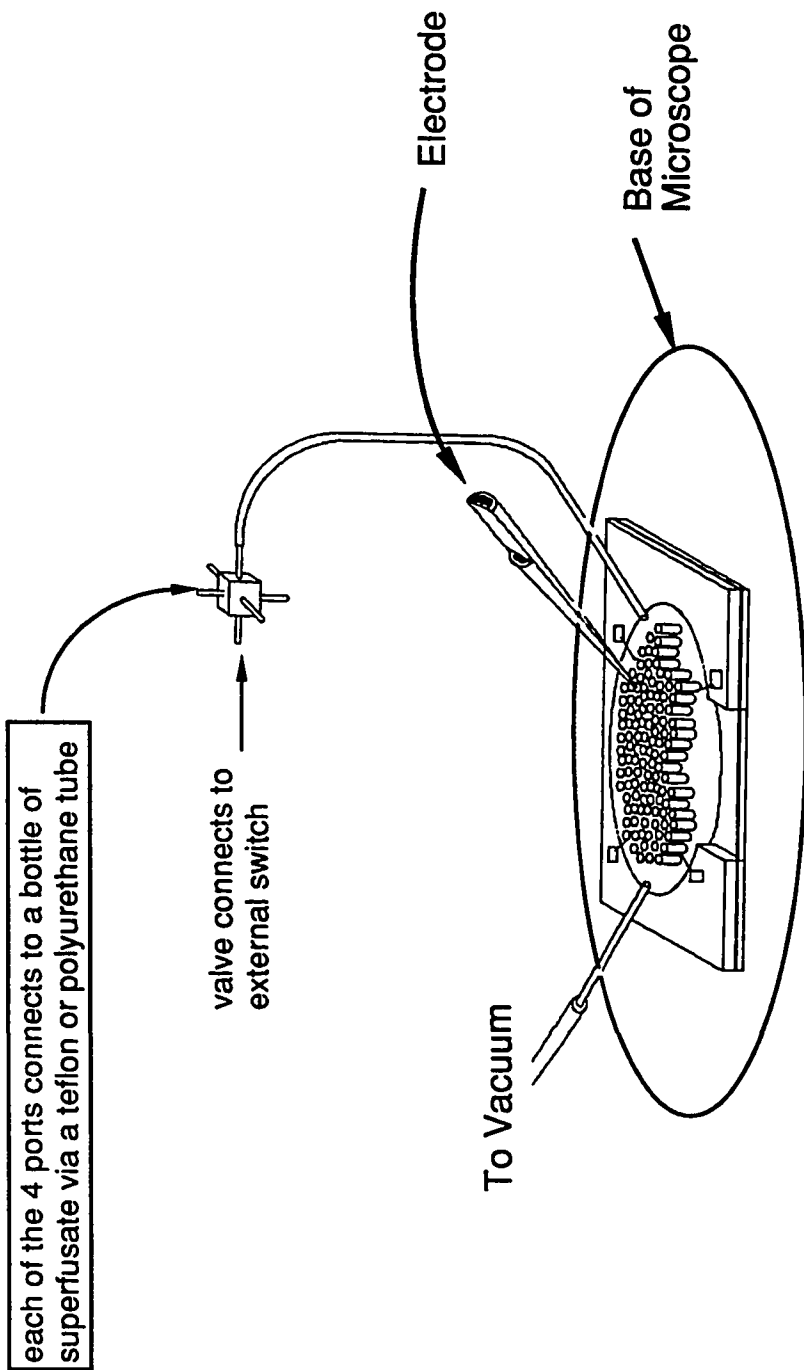


Illustration 6: Superfusion apparatus and retinal mounting chamber.

changes. Still, the lag time was typically about 30 s. Lag time was measured by switching between two solutions containing different concentrations of a single ion. The appearance of changes in ionic concentrations using ion-selective electrodes marked the appearance of the new solution in the dish.

**Optical Stimulation System.** Light stimuli were delivered to the retina from a white light source mounted on an optical bench located next to the experimental cage. A light beam from this source was directed through a series of lenses, a narrow band interference filter with a center wavelength of 500 nm, a variable series of neutral density filters, an electromagnetic shutter (model 275, Vincent Assoc., Rochester, N.Y.), a hole in the light-control cage and a beam-splitting prism mounted above the light source of the microscope. The prism was placed to allow both the stimulus beam and the microscope's light source to pass through the microscope optics and the retina. The stimulus lenses and the microscope condenser were adjusted so that the retina received a diffuse, 0.5 mm diameter beam of light with uniform intensity. The diameter of the light stimulus met the requirements for full-field illumination of rods (Leeper et al., 1978; Griff and Pinto, 1981). The irradiance of the unattenuated stimulus in the plane of the retina was  $9.2 \times 10^3$  quanta  $\text{sec}^{-1} \mu\text{m}^{-2}$  as measured with a calibrated photodiode (United Detector Technology, model 40X). When periodic flashes of light were presented to the retina, the pulse width and duty cycle were controlled by a programmable digital control system connected to the electromagnetic shutter (shutter pulse range = 100 ms - 999 s).

### **Section 2.3: Solutions**

**Superfusion solutions.** Superfusion solutions were made based on a standard salt solution resembling the extracellular fluid of the toad's eye (Oakley and Pinto, 1983). Their compositions are shown in Table 3. Five standard types of superfusion solutions were used: A, B, C, D and E. Except for  $\text{Ca}^{2+}$  concentration, types A, B and C were essentially the same. Type A solutions contained 0.9 mM  $\text{Ca}^{2+}$ , type B contained 0.1 mM  $\text{Ca}^{2+}$  and type C contained no added  $\text{Ca}^{2+}$ . Type D solutions contained the  $\text{Ca}^{2+}$  buffer, EGTA, to

buffer  $\text{Ca}^{2+}$  to very low levels. These solutions used  $\text{NaCH}_3\text{SO}_3$  rather than  $\text{NaCl}$  to help stabilize the photoreceptor voltages (Bastian & Fain, 1979). Type E solutions contained  $\text{Li}^+$  substituted for  $\text{Na}^+$  in the percentages shown.

**Injection Solutions:** When drugs or ions were injected intracellularly, they were mixed with a standard solution consisting of 100 mM potassium acetate, 25 mM MOPS (3-(N-morpholino)propane sulfonic acid) and 10 mM KOH to bring the pH to about 7.2. The specific compositions of the injection solutions are given in Table 4.

#### **Section 2.4: *Microelectrode Preparation***

**Single-barrel micropipette electrodes.** Single barrel micropipette electrodes were pulled from borosilicate glass tubing (style 1011, omega-dot, 1.0 mm o.d., 0.5 mm i.d., Glass Co. of America, Bargaingtown, NJ) on a horizontal-mount electrode puller (either Model P77 or P80, Sutter Instrument Co., San Rafael, CA). These electrodes were used for intracellular recording of the rod outer segment membrane voltage,  $V_m$ . The resistance of these electrodes were measured in the superfusion solution prior to intracellular recording (approximately 220 mM charge carriers). This measurement was made by passing a 1 nA current through the electrode, bath and salt bridge to ground, while recording the electrode potential. Electrode resistances used were typically 400 - 600 M $\Omega$ .

This impedance range was found to be optimal for holding cells during the experiments.

**Double-barrel micropipette electrodes.** Double-barrel micropipette electrodes, made from glass 'theta' tubing (1.5 mm o.d., 1.3:1.0 septum: wall ratio; style 1A, R & D Optical Co., New Windsor, MD) were used either to measure rod photoreceptor network input resistance ( $R_i$ ) or to inject drugs intracellularly. Each barrel was used independently: one for voltage-recording, the other for either current injection or pressure injection of drugs (Meech, 1972). The resistance of each barrel was comparable with the single-barrel electrodes described above. At the back end of the micropipette, one of the barrels was cut away for a distance of about 1.0 cm using a diamond abrasive tool (Brown

**Table 4. Composition of intracellular injection solutions in millimolarity.**

Solution compositions were as shown. Abbreviations:

1. KAc: Potassium acetate
2. Colch: colchicine
3. Lumicolch: beta-lumicolchicine
4. MOPS: Morpholinopropane Sulfonic Acid
5. EGTA: Ethyleneglycol-bis-(beta-aminoethyl ether)N,N'-tetra-acetic acid
6. KOH: Potassium hydroxide
7. cGMP: Sodium (or Potassium) Guanosine 3',5' cyclic monophosphate
8. GTP: Guanosine triphosphate
9. GTP $\gamma$ S: Guanosine - 5'-O-(3-thiotriphosphate)

## COMPOSITION OF INTRACELLULAR INJECTION SOLUTIONS IN MILLIMOLARITY

Solutions	KAc	MOPS	KOH	EGTA	cGMP	Colch	GTP	GTP $\gamma$ S
A	100	25	10	--	30	--	--	--
B	100	25	10	100	--	--	--	--
C	100	25	10	--	--	10	--	--
D	100	25	10	--	--	--	1000	--
E	100	25	10	--	--	--	--	1000

Table 4: Composition of intracellular injection solutions in millimolarity

& Flaming, 1977) to facilitate connecting the electrodes to the pressure injection system and to prevent electrical coupling between the barrels. These electrodes were also pulled on a horizontal-mount electrode puller (Model 77 or P80, Sutter Instrument Co., San Rafael, CA). The barrel used for recording membrane voltage was always filled with 1.0 mM potassium acetate, buffered to pH 7.1 with 10.0 mM MOPS. A chlorided silver wire was placed in the back of the barrel to make electrical contact with the solution and was connected to the voltage amplifier system described in Section 7. The other barrel, when used to measure  $R_i$ , was prepared in a manner identical to the voltage barrel. The external surfaces of both barrels were kept dry and their back ends were coated with mineral oil to improve electrical isolation. Before impalement of a rod outer segment, the electrode coupling resistance was measured by passing a 1 nA current through one barrel to ground, while recording the voltage of the other barrel (Oakley and Pinto, 1983). Therefore, the coupling resistance included the resistance of the bath and agar bridge. Only electrodes whose coupling resistances were less than 5 M $\Omega$  were used. Upon impalement of a rod cell, a periodic current pulse between 0.01 nA - 0.15 nA was driven through one barrel of the electrode as before. The other barrel then measured the potential created by this current as it passed through the coupling resistance and the photoreceptor network to ground. This gives the input resistance,  $R_i$ , calculated by the formula  $R = V/I$ . Input resistance typically ranged from 200 to 800 M $\Omega$  in the photoreceptor network. Thus the coupling resistance caused an over-estimation of the rod network resistance of approximately 0.6 - 2.5 % (maximum).

For pressure injection of drugs, one barrel was partially filled with a small amount of injection solution (compositions are shown in Table 4). A two-inch, 30-gauge needle was then sealed into the barrel with a low-heat dental impression compound (Mizzy Inc., Clifton Forge, VA). The hypodermic needle was then connected to the pressure delivery system described below by number 260 polyethylene tubing. Before each pressure injection, the resistance of the voltage barrel was measured as previously described. Electrode



resistance was typically 400 - 700 M $\Omega$ . Electrodes were tested for mechano-electrical coupling by applying a test pressure pulse to the injection barrel while measuring voltage in the other barrel; electrodes that exhibited a potential change when the pressure pulse was applied were discarded.

**Ion-selective microelectrodes.** The interphotoreceptor calcium concentration,  $[Ca^{2+}]_o$ , was measured with  $Ca^{2+}$ -ion selective microelectrodes. Calcium ion-selective microelectrodes were made using figure 8 glass tubing (two glass barrels side-by-side, style 1021, omega-dot; each barrel 1.0 mm o.d., 0.5 mm i.d., Glass Co. of America, Bargaintown, NJ ). The back of one barrel was cut away for about 1 cm as described above for theta tubing. The glass tubing was then pulled into an electrode having a single tip using a horizontal-mount electrode puller (model P80, Sutter instruments, San Rafael, CA). The longer barrels of the electrodes were then vapor silanized in the following manner (Oakley, 1987): they were inserted into a custom-made teflon plate with holes drilled through it that snugly fit them. The plate had been made to fit tightly onto a 100-ml glass beaker. About 15  $\mu$ l of N,N-dimethyltrimethylsilylamine (catalog # 41720, Fluka Chemical Co., Ronkonkoma, NY) was transferred to the beaker using a glass syringe and needle. The ends of the shorter barrels rested against the outside surface of the plate. This helped to occlude the shorter barrels and kept them outside the high silane vapor pressure chamber formed by the beaker and teflon plate. The entire unit was then baked in an oven, set at 255 $^{\circ}$  C for one hour. The oven was then turned off and the electrodes allowed to cool with the door open. Once cooled, calcium ion-selective cocktail {(Fluka 21048 calcium ionophore I-cocktail A, containing the ion carrier (-1-(R,R)-N,N'-bis-[11- (ethoxycarbonyl)-undecyl] N,N',4,-5 tetramethyl-dioxaoctane diamide))} was placed into the longer barrel as close to its neck as possible. The tip of the electrode was then allowed to fill overnight. The following day, the electrode reference barrels were backfilled with 1 M LiCl to prevent salt crystallization at the electrode tip. Typically, 100 mM  $CaCl_2$  was used to backfill the barrel containing the cocktail. This high concentration of  $Ca^{2+}$  in the reference barrel was used to

help stabilize the electrode. The interface between the backfilling solution and the ion-selective cocktail was observed under a light microscope to determine the adequacy of the silanization process. Electrodes were judged to be adequately silanized if a hemispherical meniscus of ion exchanger "wetting" the walls of the electrode was seen (Munoz et al., 1983; Tripathi et al., 1985; Oakley 1987). The electrodes were then beveled with a diamond dust-coated plate (Brown and Flaming, 1979) until the reference barrel had an impedance of 20-50 M $\Omega$ . The tip diameters were typically 3-8  $\mu\text{m}$ .

The tips of the electrodes were painted with Dow Corning 1107 fluid (Dow Corning Inc., Midland, MI) and allowed to dry prior to characterizing the responses. It was found that this coating improved the performance characteristics of the electrode (i.e., it reduced noise and lowered the response time).

The response times of the electrodes were fast compared to the  $\text{Ca}^{2+}$  changes occurring during experimentation. Typical  $\text{Ca}^{2+}$  photoresponses had durations  $>20$  s, while ETH1001 - based electrodes similar to those used in this thesis typically have response times of 40 - 150 ms (Ammann, 1986) when calcium is ionophoresed near the electrode tip. A standard calibration curve for the electrodes was constructed and is shown in Fig. 2. Data points were taken at  $10^{-2}$ ,  $10^{-3}$ ,  $10^{-4}$ ,  $10^{-6}$  and  $10^{-8}$  M  $\text{Ca}^{2+}$ , and the solutions all contained concentrations of the other ions found in normal control solution (solution A1, Table 3). Individual electrodes used in each experiment were then calibrated using 10 mM, 1 mM and 0.1 mM  $\text{Ca}^{2+}$ , and compared to the standard curve. The electrodes used in the experiments all had  $28 \pm 1$  mV/decade responses when measured in this fashion.

The dc level of the electrode voltage was typically set to zero in the control bath solution at the start of each experiment. The stimuli being studied typically caused micromolar changes in  $[\text{Ca}^{2+}]_o$ , which resulted in relative changes in the voltage output,  $V_{\text{Ca}^{2+}}$ , of the  $\text{Ca}^{2+}$ -selective microelectrode from tenths of a mV to a few mV.

When measuring the effects of drugs or of solutions containing non-standard ion

compositions on  $\text{Ca}^{2+}$  fluxes in rods, it was necessary to ascertain that none of the solutions being used contained measurable differences in  $[\text{Ca}^{2+}]$ . Therefore, all of the solutions used in a given experiment were made from split samples of a 0.1 mM calcium starter solution. Typically, a two liter, pH-buffered starter solution was made which contained  $\text{Ca}^{2+}$  and the other common ions. This starter solution was then split into samples, and the drugs or special ions were then added as required to make the test solutions. Furthermore,  $V_{\text{Ca}^{2+}}$  was measured during trial bath solution changes both before and after each experiment. In the data reported in this thesis, no differences in  $V_{\text{Ca}^{2+}}$  between the control and the test solutions were measured either before or after the experiments.

Figure 2 also shows a partial calibration curve ( $10^{-2}$  -  $10^{-4}$  M  $\text{Ca}^{2+}$ ) for solutions containing 10 mM colchicine in addition to the other standard ions and small molecules (solid line). The presence of colchicine can be seen to have negligible effects on the calibration curve.

When the trivalent ion,  $\text{La}^{3+}$ , or the drug amiloride (which are typically used to block  $\text{Na}^+/\text{K}^+/\text{Ca}^{2+}$  exchange) was added to control solutions, the  $\text{Ca}^{2+}$ -microelectrodes responded to solution changes between the control superfusate and these drug-containing superfusates. These drugs, then, could not be used to measure  $V_{\text{Ca}^{2+}}$  changes caused by blocking  $\text{Na}^+/\text{K}^+/\text{Ca}^{2+}$  exchange. Instead, in experiments measuring  $V_{\text{Ca}^{2+}}$  changes evoked by blocking  $\text{Na}^+/\text{K}^+/\text{Ca}^{2+}$  exchange, superfusates were used in which  $\text{Li}^+$  replaced  $\text{Na}^+$  (Badian & Fain, 1982b; Yau & Nakatani, 1984a; Hodgkin & Nunn, 1987). Lithium substitution for  $\text{Na}^+$  neither produced extrinsic responses in the  $\text{Ca}^{2+}$  microelectrodes nor changed the calibration characteristics of the electrodes. The electrodes still had  $28 \pm 1$  mV/decade responses in the  $\text{Li}^+$ -based solutions. Since the  $\text{Li}^+$  selectivity coefficient ( $-3.3 = \log K^{\text{pot}/\text{CaM}}$ ) is less than that of  $\text{Na}^+$  ( $-5.5 = \log K^{\text{pot}/\text{CaM}}$ ), it might be expected that  $\text{Li}^+$  would cause a greater amount of interference with  $\text{Ca}^{2+}$  than would  $\text{Na}^+$ . Therefore, the  $[\text{Ca}^{2+}]$  response curve should be slightly steeper in  $\text{Li}^+$ -based solutions. The failure to

**Figure 2.  $\text{Ca}^{2+}$  ion-selective electrode calibration.**

Calibration of the electrodes over the range  $10^{-2}$  M -  $10^{-4}$  M [ $\text{Ca}^{2+}$ ] used solutions whose compositions, except for [ $\text{Ca}^{2+}$ ], were the same as Solution 1A, Table 3. Calibration over the range  $10^{-6}$  M -  $10^{-8}$  M used solutions D1 and D10, Table 3.

The average from a series of mV readings at each concentration provided data points for the electrode. The total number of measurements taken at each data point is indicated. The error bars show the standard deviations for the series of readings taken at each concentration. The data from two electrodes was grouped together for the  $10^{-2}$  M -  $10^{-4}$  M [ $\text{Ca}^{2+}$ ] range.

Because the solution apparatus could measure only four solutions at a time, the total range was measured in two shifts, first over the range  $10^{-2}$  -  $10^{-4}$ , then over the range  $10^{-4}$  -  $10^{-8}$ . When measuring the lower  $\text{Ca}^{2+}$  range, the voltage of the electrode was set to the average voltage recorded at  $10^{-4}$  M [ $\text{Ca}^{2+}$ ] when the higher range was measured. Thus all measurements were relative to each other.

The slope of the data curve over the  $10^{-2}$  -  $10^{-4}$  range was 28 mV/decade. The dashed line shows the theoretical Nernst curve ( $2.3 \text{ RT/ZF}$ ), with a slope of 29.4 mV/decade (Amman, 1986).

The error bars indicated greater variability in the measurements as the [ $\text{Ca}^{2+}$ ] decreased. The primary source of the variability resulted from measured hysteresis when changing from one [ $\text{Ca}^{2+}$ ] to another and back (for a discussion of hysteresis, see Amman, 1986). The decreased slope of the curve with respect to the  $\text{Ca}^{2+}$  Nernst curve most likely resulted from  $\text{Na}^+$  interference in the solutions (Amman, 1986), since  $\text{Na}^+$  was present in concentrations 100 times greater than other ions, and since most ions other than  $\text{Ca}^{2+}$  have selectivity coefficients similar to  $\text{Na}^+$  (Amman, 1986).

Painting the tips of the electrodes with Dow-Corning 1107 fluid helped reduce the hysteresis of the electrodes used in later experiments.

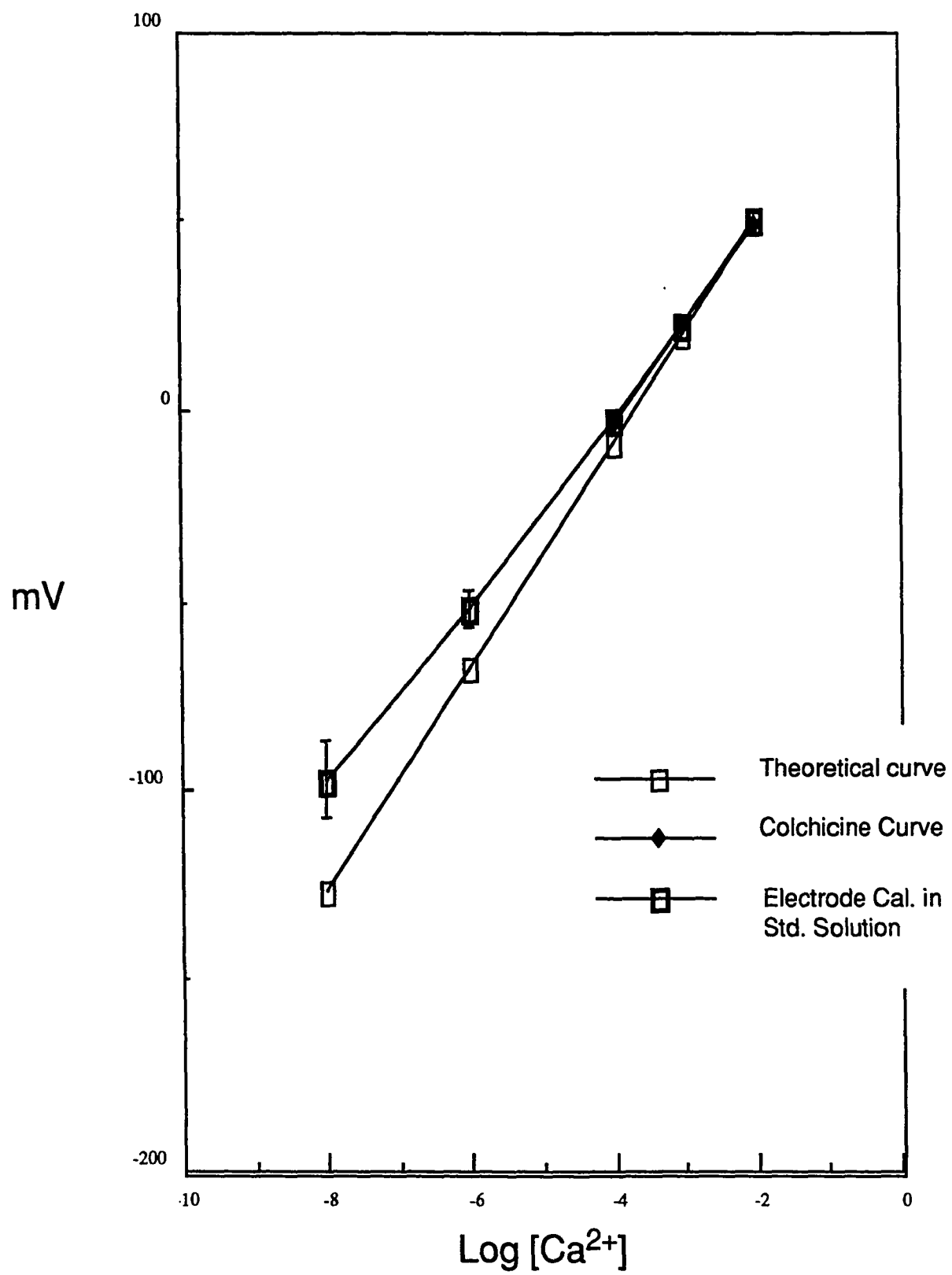


Fig. 2.  $\text{Ca}^{2+}$  ion-selective electrode calibration

detect a difference in the response curves over the range tested ( $10^{-2}$  M -  $10^{-4}$  M) was most likely resulted from the small variation in the response curve slope that  $\text{Li}^+$  substitution for  $\text{Na}^+$  would create and the large tolerances ( $\pm 1$  mV) typically occurring in the measurement. The expected slope in  $\text{Li}^+$  solutions would be between 28 mV/decade and 29 mV/decade.

**Microelectrode mounting.** Microelectrodes for intracellular recording were attached to a remotely controlled, electromechanical microdriver (Burleigh Instruments, Model PZ-550, Fishers, NY). The driver arm was mounted at an angle  $30^\circ$  from horizontal, on a brass arm connecting it to an x,y,z micromanipulator. The micromanipulator was used for adjusting the electrode tip to a position just above the retina.

When simultaneously measuring  $V_{\text{Ca}^{2+}}$  and  $V_m$ ,  $\text{Ca}^{2+}$ -selective microelectrodes were mounted on a Huxley-type micromanipulator  $15^\circ$  from the horizontal with a custom-made plexiglass holder. Electrodes were lowered into the interphotoreceptor space manually. During measurements of  $\text{Ca}^{2+}$  gradients, the  $\text{Ca}^{2+}$ -selective microelectrodes were mounted on the Burleigh microdriver as described above.

### **Section 2.5: *Pressure Delivery System***

The pressure delivery system for intracellular injections consisted of compressed nitrogen gas directed through a variable-regulator (0-14 bar) and a remote-control valve. The control valve was operated by the digital pulse generator described above (used in producing the current pulses). The applied pressure was monitored using a semiconductor pressure transducer (LX 1730G, National Semiconductor).

### **Section 2.6: *Electrode Placement and Rod Cell Impalement***

**Placement of intracellular electrodes.** The electrodes were positioned using the x,y,z micromanipulator under the visual control of the infrared-equipped microscope. When the tip of the electrode was within the depth of field of the tip of the rod outer segments, the experimental cage curtain was closed. Electrode advancement was continued in 2- $\mu\text{m}$  steps with the microdriver. The electrode potential was monitored on an oscilloscope and

on an audio monitor. Contact with the retina was determined by small, sudden shifts in electrode potential during advancement. Sometimes advancement alone was sufficient for impaling a rod. More often, however, cell impalement was achieved by "buzzing" the electrode with an electrical-current oscillator built into the recording system. Cell impalement could be detected by a sudden hyperpolarization of more than 15 mV. Data was collected only from cells that had stable resting potentials and that, demonstrated a hyperpolarizing transient followed by a plateau response greater than 10 mV (see Figure 1) when stimulated by a 100-ms light flash at high intensities (9,800 quanta per rod per flash).

Recordings were judged to be from the outer segment when a cell was penetrated between initial electrode contact with the retina and when vertical advancement was still less than 50  $\mu\text{m}$ . A check that the data had been taken from a rod outer segment was verified by observing that the outer limiting membrane of the retina, which lies distal to most of the inner segment, could be penetrated only after a further advancement of at least 10  $\mu\text{m}$  upon finishing data collection. Outer limiting membrane penetration was judged by a sudden 80 - 90 mV hyperpolarization, indicating penetration of Müller cells, whose distal processes join the outer limiting membrane of the retina (for a review, see Rodieck, 1973).

**Placement of  $\text{Ca}^{2+}$ -selective microelectrodes.** In the first few experiments measuring interphotoreceptor  $[\text{Ca}^{2+}]_o$ , the retinas were first superfused with 0.9 mM  $\text{Ca}^{2+}$  control solution, and the  $\text{Ca}^{2+}$ -selective microelectrode was placed into the interphotoreceptor space at this time. The superfusion solution was then switched to the 0.1 mM  $\text{Ca}^{2+}$  control solution and allowed to stand 10 to 12 minutes, until the voltage of the  $\text{Ca}^{2+}$ -selective microelectrode stopped decreasing. The voltage of the  $\text{Ca}^{2+}$ -selective microelectrode typically decreased about 28 mV while switching to the 0.1 mM  $\text{Ca}^{2+}$  solution, giving good agreement with the theoretical prediction of 29 mV and indicating that the interphotoreceptor  $[\text{Ca}^{2+}]_o$  closely approached that of the bath.

When  $V_m$  was measured simultaneously with  $V_{\text{Ca}^{2+}}$ , a second, single-barrel

microelectrode for measuring intracellular voltage was mounted in the Burleigh microdriver and placed at the distal edge of the retina within 1 mm of the calcium-selective electrode, under visual control. Using the Burleigh microdriver, the intracellular electrode was advanced until a cell was penetrated.

### **Section 2.7: Data Recording Apparatus**

A chlorided silver wire inserted into the backfilled microelectrodes provided the electrical connection to a voltage preamplifier, which was designed to follow the electrode voltage with a gain increase of ten. Two different types of preamplifiers were used: either a custom-built model or an Axoprobe 1 (Axon Inst., Inc., Burlingame, CA). No differences other than noise levels were noted in data recorded with the two different preamplifiers (lower noise was noted when the Axoprobe 1 was used). Either type of preamplifier had a high impedance headstage capable of driving a current up to 100 nA across a 100 M $\Omega$  resistance without affecting the voltage output. The headstage was connected to a voltage-to-current conversion circuit, which could be driven by an external voltage signal.

For measuring  $R_i$ , the attenuated output voltage of a programmable digital control system was used to supply the input voltage signals used to inject the current pulses. The Axoprobe amplifier had two independent channels, so one channel was used for voltage recording while the other channel was dedicated to driving current pulses. When custom-built amplifiers were used to measure  $R_i$ , an independent amplifier was used for each of these functions.

A custom-built, two-channel differential preamplifier with high input impedance headstages was used for recording signals from ion-selective microelectrodes. The voltage of the reference barrel was subtracted from the voltage of the ion-selective barrel to produce an output signal ( $V_{Ca^{2+}}$ ) depending only on ion concentration. The amplifiers contained a capacitance feedback circuit, which acted as "negative capacitance", and which could be adjusted to decrease the response time of the electrodes. The headstages were connected to the microelectrodes as described for voltage recording above.



A silver-silver chloride reference electrode connected the ground of the preamplifier(s) in use to one end of a salt-agar bridge (4 % agar in 2 M KCl). The other end of the bridge was inserted into the solution bath. The preamplifier outputs were amplified using a custom-made, variable-gain DC amplifier. When  $R_i$  was being measured, the voltage signal used to drive the current source was also recorded and amplified. The amplified signals were displayed on an oscilloscope (model 5111A, Tektronix) and a chart recorder (model 1210, MFE Corp., Salem, NH) for observation during experimentation. The chart recorder contained a built-in event marker which was used to mark solution changes, etc. Data were also output to a four-channel FM tape recorder (Store 4DS, Racal Corp., Sarasota, FL) for permanent storage and off-line analysis. One channel was used for recording the 5 V command pulse to the shutter, thus recording periods of light stimulation, and a second channel was used for recording narration (e.g. solution changes, stimulus intensity). The remaining two channels were used to record membrane voltage, current pulses, pressure pulses or ion-selective electrode output as needed for the particular experiment. The tape-recorded signals from the three data channels could be digitized by a computer (model LSI 11-23, Digital Equipment Corp.) and figures made using a digital plotter (model DMP-4, Houston Inst. Co., Austin, TX).

## CHAPTER 3

### RESULTS

#### **Section 3.1: *Effects of colchicine on $g_{hv}$ .***

As discussed in Chapter 1, colchicine affects both dark-adapted  $V_m$  and  $V_m$  photoresponses of rods. Figure 3 shows the typical effects of superfusion with 10 mM colchicine on  $V_m$  and  $V_m$  photoresponses. During colchicine superfusion, the dark-adapted rod hyperpolarized by ~8 mV, and the waveforms of the  $V_m$  photoresponses changed. The colchicine-induced hyperpolarization is seen best in Fig. 3A, while the colchicine-induced waveform changes are seen best in Fig. 3B. Colchicine reduced the amplitudes of the waveforms and noticeably affected the waveform kinetics. These kinetic effects are further illustrated in Fig. 3C and Fig. 3D. Colchicine substantially shortened the duration of the  $V_m$  photoresponses, seen best in Fig. 3C, and slightly increased the response time-to-peak, seen best in Fig. 3D.

These effects of colchicine have some similarities with both the effects of dim background illumination and the effects of increased  $[Ca^{2+}]_i$  on rods (compare colchicine's effects to the effects of increased  $[Ca^{2+}]_i$  reported by Bastian & Fain, 1979). The latter two forms of stimulation both hyperpolarize rods by decreasing  $g_{hv}$ , so it was hypothesized that colchicine, too, hyperpolarizes rods by decreasing  $g_{hv}$ . The experiments in this section, described below, tested this hypothesis.

#### ***3.1.1: Colchicine increases $R_i$ during hyperpolarization.***

Although colchicine hyperpolarizes rods and changes  $V_m$  photoresponse kinetics, these effects by themselves are only weak evidence that colchicine blocks the  $g_{hv}$ . It may be possible, for instance, that colchicine's effects result from changes in rod inner segment currents (see Chapter 1 for their description). Because the  $g_{hv}$  passes a positive inward current, blocking it hyperpolarizes rods and increases the rod network input

**Figure 3:** *The effects of colchicine on dark-adapted  $V_m$  and  $V_m$  photoresponses.*

- A.** The waveform record labeled  $V_m$  is the intracellular voltage record from a rod photoreceptor during superfusion changes from a control solution (0.9 mM  $\text{Ca}^{2+}$  solution A1, Table 3) to one containing an additional 10 mM colchicine (solution A2, Table 3), and back. The solution periods are indicated by the horizontal bar above the record. Flashes of light (100-ms, 653 quanta rod<sup>-1</sup> flash<sup>-1</sup>) were used to stimulate the retina every 30 s, where indicated by the pulse records in the light monitor trace labeled LM.
- B.** The  $V_m$  photoresponses numbered in A are plotted on expanded time and voltage scales.
- C.** The voltage responses from B are normalized to the same peak response and superimposed.
- D.** The initial portion of the normalized voltage responses from C is plotted on a further-expanded time scale.

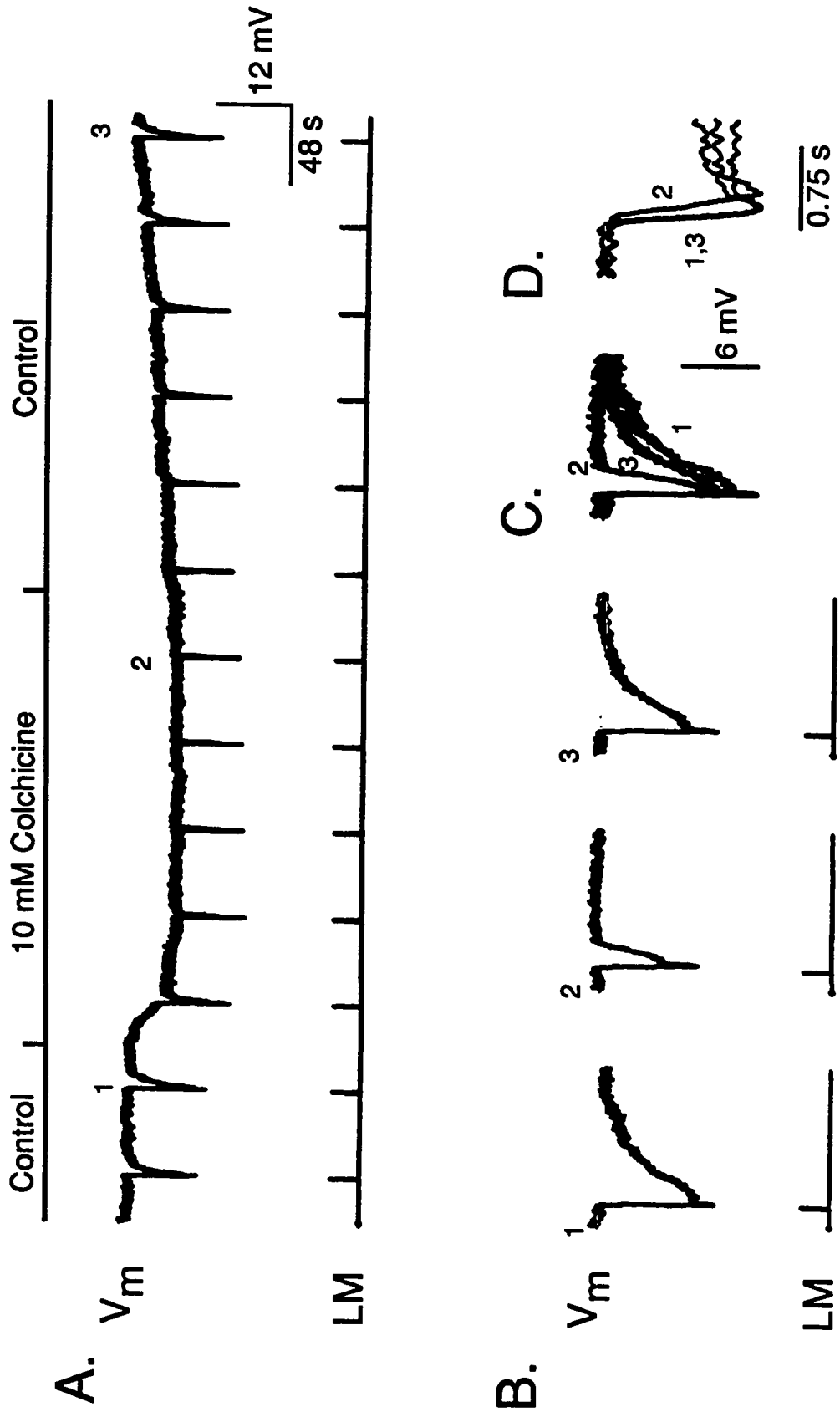


Fig. 3. The effects of colchicine on dark-adapted  $V_m$  and  $V_m$  photoresponses.

resistance,  $R_i$ . By contrast, the largest currents in the rod inner segments are outward currents carried by  $K^+$ , and the conductances associated with these currents would have to increase to hyperpolarize rods. Measuring an increase in the input resistance coincident with a colchicine-induced hyperpolarization, then, would provide stronger evidence that colchicine blocks  $g_{hv}$ .

Colchicine's effect on  $R_i$  is shown in Fig. 4. Cobalt was included with both the control solution and the colchicine-containing test solution during the measurements to block the rod inner segment  $Ca^{2+}$  current (Bader et al, 1984; see Illus. 2). There have been reports of colchicine-induced reductions of voltage-sensitive  $Ca^{2+}$  currents (see Section 1.5). Since the rod inner segment  $Ca^{2+}$  current is also an inward current, it was blocked to allow any colchicine-induced  $R_i$  increase to be more readily attributable to blockage of  $g_{hv}$ . Figures 4A and 4B show that  $R_i$  more than doubled during the colchicine-induced hyperpolarization. This effect of colchicine on  $R_i$  was reversible, although the reversal was incomplete during the time period allowed for drug washout. In general, colchicine's effects on  $R_i$  in the presence of  $Co^{2+}$  are consistent with the hypothesis that colchicine blocks the  $g_{hv}$ .

### *3.1.2: Colchicine's effects persist in the presence of blocked inner segment conductances.*

The facts that colchicine increases  $R_i$  and hyperpolarizes rods supports the hypothesis that colchicine blocks the  $g_{hv}$ , and not the alternative hypothesis that it affects inner segment conductances. This evidence cannot be considered conclusive, however, since other possible explanations for the increase in  $R_i$  exist. For instance, the increase could result from a disruption of network coupling, or some other effect only correlated with the voltage change. Therefore, alternative tests of the hypotheses were performed. The next test consisted of superfusing colchicine during blockade of the measurable currents in the rod inner segment with a cocktail of pharmacological agents. If colchicine blocks  $g_{hv}$ , then blocking the inner segment conductances will not abolish colchicine's effects on  $V_m$  or on  $V_m$  photoresponses as long as a dark current remains. If colchicine acts only on the inner segment conductances, however, their blockade should stop colchicine's effects.

**Figure 4: Measurement of  $R_i$  during colchicine superfusion.**

One barrel of a double-barrel microelectrode was used to record the intracellular voltage in a cell while the other barrel was used to pass current pulses of constant amplitudes (0.01 nA, every 20 s); the changes in voltage during the pulses were proportional to the network input resistance. Cobalt (6.67 mM) was included during colchicine superfusion and for control periods before and after colchicine superfusion (see text; solutions compositions are given in A1, A7 and A8 in Table 3).

**A.** The output from the voltage-recording barrel during the solution changes is plotted in the record labeled  $V_m$ . Light flashes (100-ms, 98 quanta rod<sup>-1</sup> flash<sup>-1</sup>) were presented to the retina at different periods to monitor the effect of colchicine on  $V_m$  photoresponses. The dc level of the voltage output had to be adjusted at one point during the period of colchicine superfusion to prevent saturation of the recording tape. This adjustment was excluded from the record in Fig. 3A for clarity, and is indicated by the break in the record.

**B.** The  $R_i$  measurements numbered above the voltage trace in A are replotted with expanded time scales and with compressed voltage scales.

**C.** The  $V_m$  photoresponses numbered below the voltage trace in A are replotted on expanded time and voltage scales.

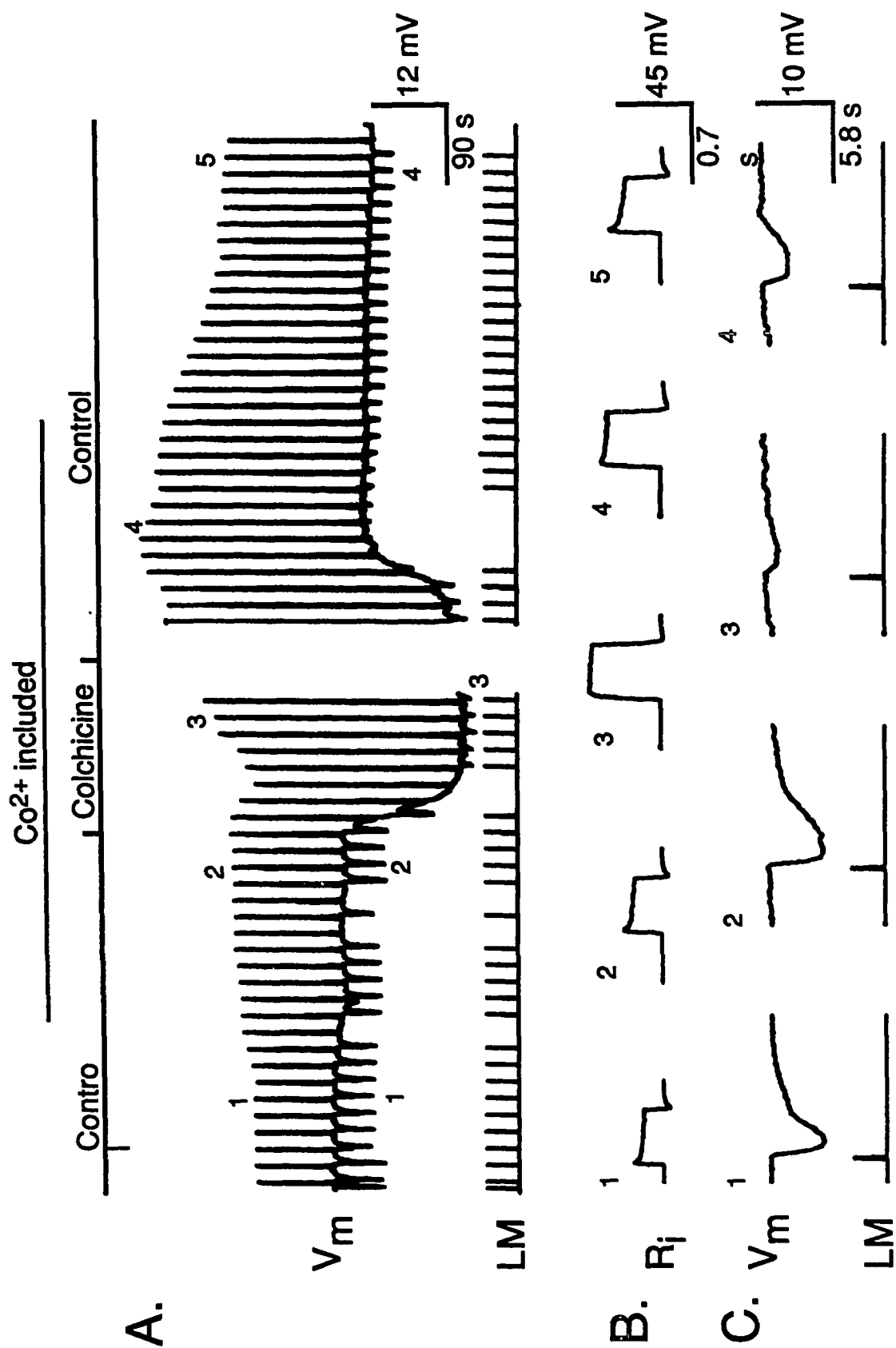


Fig. 4. Measurement of  $R_i$  during colchicine superfusion.

The results from this test are shown in Fig. 5.

Colchicine hyperpolarized the rod, as seen in Fig. 5A, and altered the amplitude and kinetics of the rod's  $V_m$  photoresponses, as seen in Fig. 5B and Fig 5C. Colchicine increased the response time-to-peak and decreased response duration, as it did in previous experiments when the inner segment currents were not blocked. In summary, blockage of the inner segment conductances does not qualitatively change the effects of colchicine on  $V_m$  or  $V_m$  photoresponses, and this result is consistent with the hypothesis that colchicine blocks the  $g_{hv}$ .

### *3.1.3. Colchicine's effects are relative/y specific for $g_{hv}$ .*

The results presented thus far support the hypothesis that colchicine decreases  $g_{hv}$  in rods. They do not, however, address the question of colchicine's specificity, i.e.: does colchicine block only the  $g_{hv}$ , or does it affect multiple rod conductances? Effects of colchicine on rod inner segment conductances could be masked by the loss of the dark current. Furthermore, the pharmacological blockade of the inner segment conductances used in some of the previously described experiments would also have masked any effects of colchicine on these conductances. Effects of colchicine on multiple membrane conductances in *Aplysia* neurons have been reported (Baux et al, 1981), and colchicine has been reported to affect many different conductances in different neuronal systems (see Chapter 1, Section 1.5), so it is plausible that colchicine could block multiple conductances in rods.

A clue that colchicine blocks the rod  $g_{hv}$  specifically comes from the observation that colchicine's effects were enhanced by blocking rod inner segment conductances (compare the effects of 10 mM colchicine seen in Fig. 3, to the effects seen in Fig. 4 and in Fig. 5). If colchicine also blocks inner segment conductances, there is no reason why prior blockade of the these conductances should increase colchicine's effects per se, since the inner segment conductances would also get blocked when only colchicine was applied. If colchicine specifically blocks  $g_{hv}$ , however, then blocking the inner segment conductances



**Figure 5.** *The effects of colchicine on  $V_m$  and  $V_m$  photoresponses in the presence of a cocktail blocking the inner segment conductances.*

The cocktail used to block the inner segment conductances contained 10 mM TEA, 10 mM 4-AP, 1.0 mM Cs<sup>+</sup> and 1.0 mM Co<sup>2+</sup> (solution A9, Table 3).

- A.** The electronic shutter was programmed to provide light flashes of 100-ms duration every 20 s (stimulus irradiance: 980 quanta rod<sup>-1</sup> flash<sup>-1</sup>). The shutter trip mechanism, however, began sticking every other flash; this provided lower-duration flashes every 40 s, with normal, 100-ms flashes intervening. The alternating flash durations appeared to be quite consistent, so the data was recorded. The shutter anomaly provided the advantage of showing the effects of colchicine on  $V_m$  photoresponses to stimuli of different total illumination.
- B.** The  $V_m$  photoresponses numbered in A are replotted on an expanded time scale.
- C.** The waveforms in B are normalized and superimposed.

Inner Segment Channel blockers

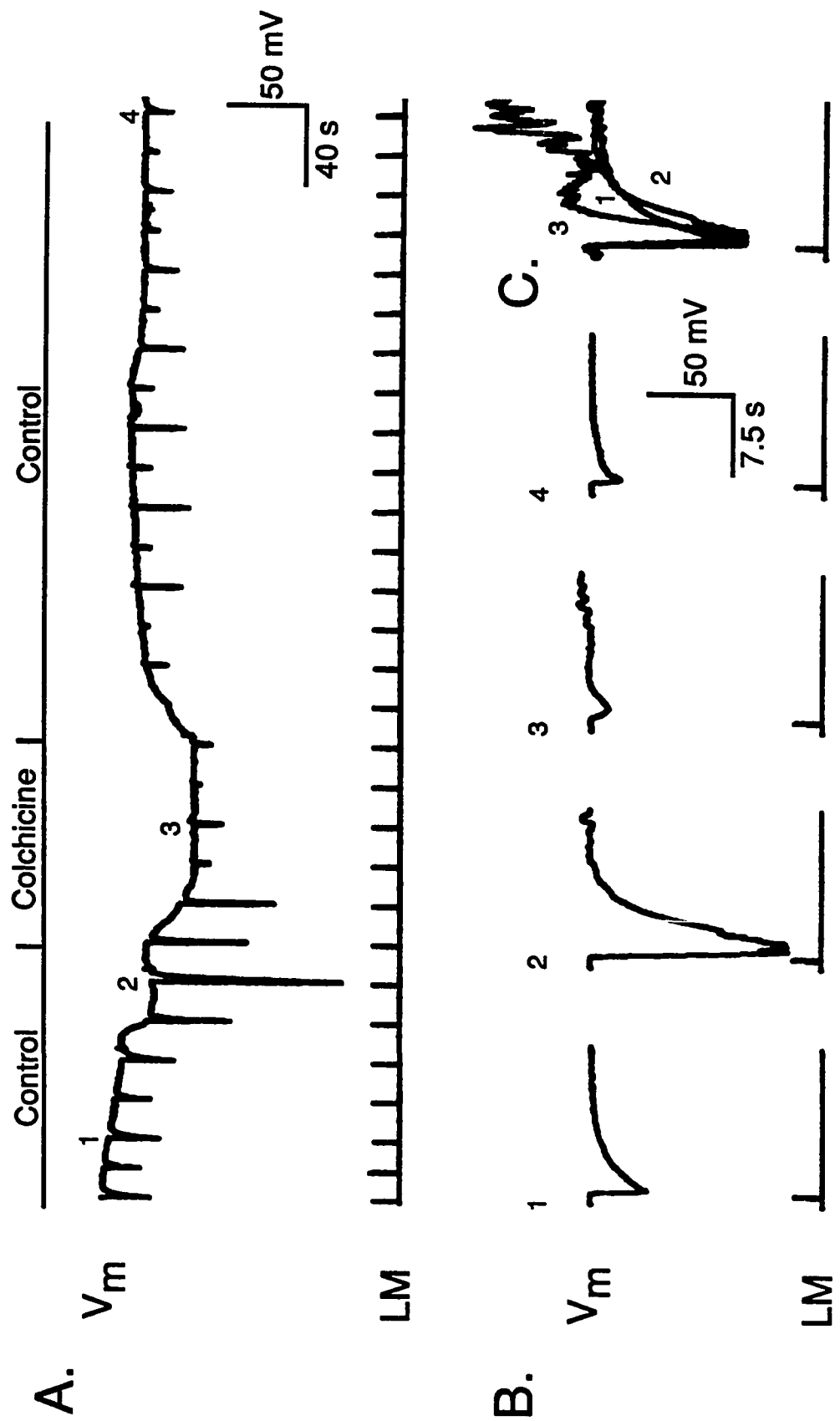


Fig. 5. The effects of colchicine on  $V_m$  and  $V_m$  photoresponses in the presence of a cocktail blocking the inner segment conductances.

should increase colchicine's hyperpolarizing effects, since blocking these channels enhances the hyperpolarizing effect of light (see the light responses #1 & #2 shown in Fig. 5). This clue, then, led to the hypothesis that colchicine affects only  $g_{hv}$  in rods.

The following experiment, shown in Fig. 6, tested the specificity of colchicine more directly. In this experiment, a step of light blocked  $g_{hv}$  prior to colchicine exposure. Figure 5A shows the control response of a photoreceptor during a 2-min. step of light, while Fig. 3B shows the effects of 10 mM colchicine applied during a similar step. Both records are from the same cell; a three-min. recovery period intervened between the two steps of light. The flashes of light (2/min., 100-ms duration,  $260 \text{ quanta rod}^{-1} \text{ flash}^{-1}$ ) given before and after the light steps illustrate the time-course of dark-adaptation following the periods of stimulation, i.e., as the cell dark-adapts, the amplitudes and durations of the  $V_m$  photoresponses increase until the waveforms resemble those seen before stimulation.

Colchicine did not hyperpolarize or depolarize the rod when it was applied during during the period of illumination. This result is consistent with the hypothesis that colchicine specifically blocks  $g_{hv}$ , and it is inconsistent with colchicine affecting conductances other than  $g_{hv}$ , since blockade of other conductances during the period of illumination should have caused changes in rod voltage.

Although colchicine did not hyperpolarize the rod during the period of illumination, it did inhibit light adaptation. During the control step of light, the rod initially hyperpolarized by about 10 mV, then slowly depolarized by about 2 mV during the course of illumination as the cell began to adapt to the light. This slow depolarization appeared to be blocked by colchicine (see Fig. 6B). This result was unexpected, and will be discussed further in Chapter 4.

Another surprising result was that colchicine did not block post-stimulus depolarization (voltage recovery), although it clearly inhibited dark adaptation. Note that after the 2-min. period of stimulation in the control response (Fig. 6A), the rod rapidly depolarized to its pre-stimulus voltage. Despite voltage recovery, the rod exhibited a typical transient reduction in its photoresponsiveness; it took about one minute for the light-evoked waveforms to reach

**Figure 6.** *The effects of 20 mM colchicine on light-stimulated rods.*

**A.** Control: flashes of light (100-ms, 260 quanta rod<sup>-1</sup> flash<sup>-1</sup>, presented every 30 s) stimulated the retina to characterize dark-adapted  $V_m$  photoresponses. A 2-minute control step of light of the same irradiance was then used for sustained stimulation of the retina. After the 2-min. light stimulus, a second pulse of light (10-s) of the same irradiance briefly stimulated the retina to assess the cell's post-stimulus photoresponsiveness. The control light flashes were then resumed.

**B.** After a 3-min. period of darkness to allow the retina to dark adapt, the retina was again exposed to a 2-minute light step. An osmotically-balanced superfusate containing 20 mM colchicine (solution A2a, Table 3) was introduced about 30 s after the initiation of the light step, and continued for nearly 3-min. Light flashes (100-ms) were resumed 30 s after the end of the step of illumination.

**C.** A longer record of the experiment in B is shown to demonstrate the continued effects of colchicine on dark adaptation.

**D.** This record shows results from another similar experiment. The record also shows recovery of normal photoresponsiveness after cessation of colchicine superfusion.

**Note:** The arrow indicates the point at which an artifactual electrode drift began. Notice that  $V_m$  of the recovered cell remains hyperpolarized with respect to the beginning control  $V_m$  by the amount of voltage drift. A similar voltage offset occurred between the bath voltages before and after the experiment, indicative of a change in the electrode ground voltage. Taking this artifact into account, these results are consistent with those shown in A-C.

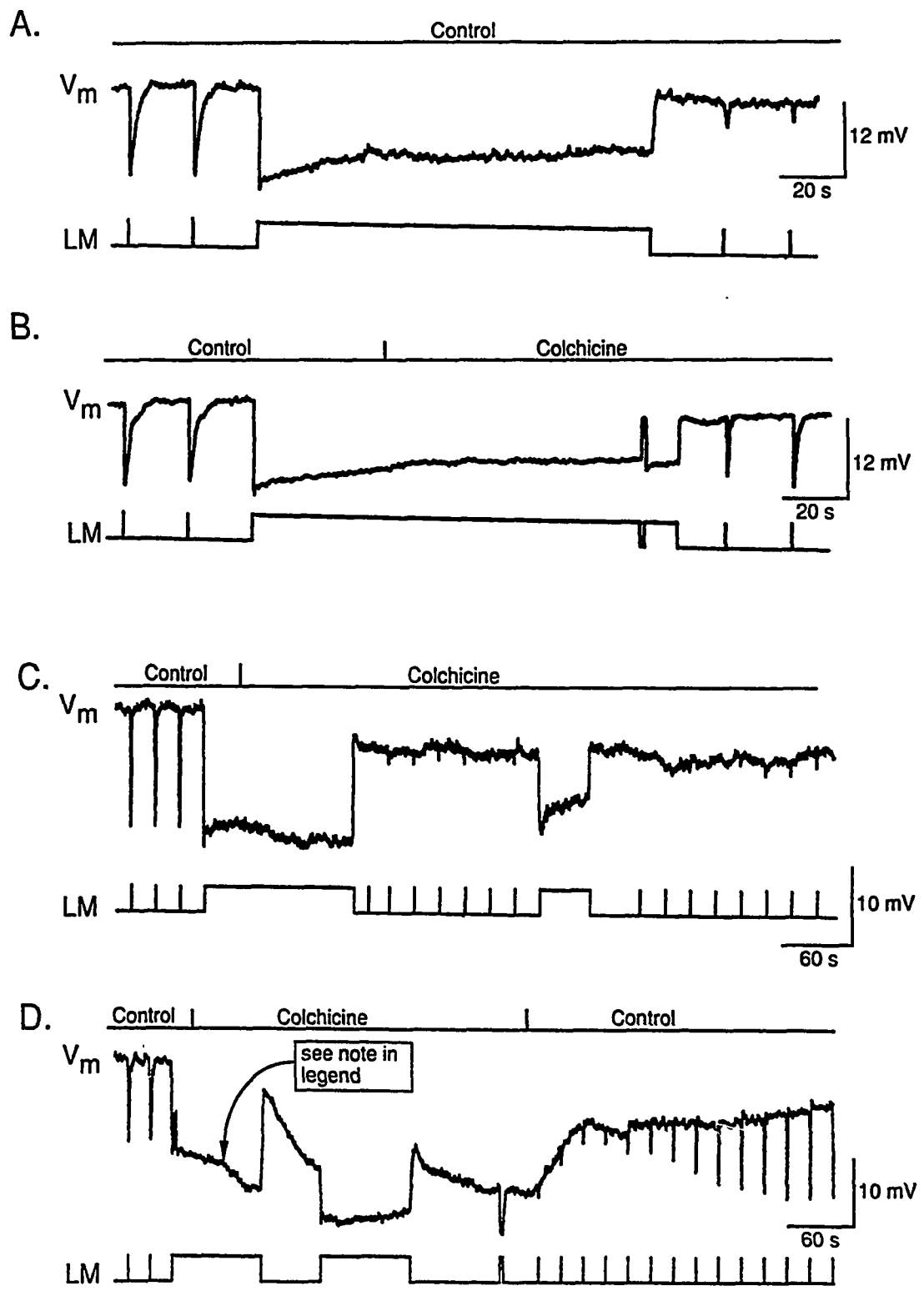


Fig. 6. The effects of 20 mM colchicine on light-stimulated rods.

their pre-stimulus amplitudes and durations. Similarly, after the 2-min. period of stimulation that included colchicine superfusion, the rod also depolarized to its pre-stimulus voltage, but the inhibition of the rod's photoresponsiveness continued several minutes, until colchicine was removed from the superfusate (see Fig. 6C and 6D).

The failure of colchicine to block post-stimulus voltage recovery gives important information about colchicine's effects on  $g_{hv}$ . From this result, it seems unlikely that colchicine has a pharmacological action on the light-sensitive channel proteins themselves. It seems more likely that colchicine indirectly blocks  $g_{hv}$  by lowering  $[cGMP]_i$  levels. A further discussion of this point and the adaptation-inhibiting effects of colchicine is deferred to Chapt. 4.

### **Section 3.2. *Some of Colchicine's effects are mimicked by increased $[Ca^{2+}]_i$ .***

The effects of colchicine on the physiology of rods are complex, as demonstrated in Section 3.1. The results shown in that section led to the hypothesis that colchicine indirectly blocks the  $g_{hv}$  by lowering cGMP levels. If this hypothesis is correct, the mechanism by which colchicine lowers cGMP must explain some complicated findings:

1. Rod voltage can return to dark-adapted values after light-stimulation, despite retinal superfusion with colchicine during the period of stimulation.
2. Colchicine affects the kinetics of rod  $V_m$  photoresponses.
3. Colchicine affects certain aspects of both light and dark adaptation.

It is conceivable that colchicine could cause these effects and also hyperpolarize dark-adapted rods by interfering with  $Ca^{2+}$  regulation. Increasing  $[Ca^{2+}]_i$  is known to lower cGMP levels and hyperpolarize rods (Ebrey et al, 1988), while regulation of  $[Ca^{2+}]_i$  is known to be important in both light and dark adaptation (Matthew, et al, 1987; Nakatani & Yau, 1987). Furthermore, increasing  $[Ca^{2+}]_i$  has been shown to affect the kinetics of rod  $V_m$  photoresponses (Bastian & Fain, 1979) in some ways similar to colchicine. The similarities between the effects of colchicine and increased  $[Ca^{2+}]_i$  led to the hypothesis that colchicine's effects result from increased  $[Ca^{2+}]_i$  (see Chapter 1 for a review of  $Ca^{2+}$

regulation in rods).

Figures 7 and 8 compare the effects of colchicine to the effects caused by increasing  $[Ca^{2+}]_i$  in rods. The techniques used to increase  $[Ca^{2+}]_i$  included reducing  $Ca^{2+}$  extrusion from rods and increasing  $Ca^{2+}$  influx into rods. The results shown using each particular treatment have either been previously reported, or they could have been predicted based on the data of others. The results from each treatment are described below; references are included for similar results that have been previously reported by others:

- A. In Figs. 7A and 8A,  $Li^+$  replaced 50% of the  $Na^+$  in the superfusate during a test period. This treatment hyperpolarized the rods and reduced photoresponse amplitudes (Bastian and Fain, 1982), probably by increasing  $[Ca^{2+}]_i$  as a result of shutting down  $Na^+/K^+/Ca^{2+}$  exchange and trapping  $Ca^{2+}$  in the cell (Yau & Nakatani, 1984; Hodgkin & Nunn, 1986). The substitution of  $Li^+$  for  $Na^+$  also altered the kinetics of  $V_m$  photoresponses. The overall duration of the test response was shorter than the control, but the recovery phase of the waveform began later in the test response than in the control.
- B. In Fig. 7B and 8B,  $La^{3+}$  (100  $\mu M$ ) superfused the retina during a test period. Lanthanum also hyperpolarized the rods and reduced  $V_m$  photoresponse amplitudes, presumably because it blocks  $Na^+/K^+/Ca^{2+}$  exchange (Yau & Nakatani, 1984) and traps  $Ca^{2+}$ , too. The duration of the  $V_m$  photoresponses, however, increased during  $La^{3+}$  superfusion.
- C. In Figs. 7C and 8C, a solution containing increased  $[Ca^{2+}]_o$  superfused the retina during a test period. This test solution also hyperpolarized the rods and reduced  $V_m$  photoresponse amplitudes (Hagins & Yoshikami, 1976; Bastian & Fain, 1979). Increased  $[Ca^{2+}]_i$  presumably caused most of the hyperpolarization, although divalent ion effects on channel conductances are contributory (Detwiler et al, 1989). The resulting change in  $[Ca^{2+}]_i$  caused by a change in  $[Ca^{2+}]_o$  cannot be easily discerned as a result of the feedback regulation discussed in Section 1.3. The duration of the  $V_m$  photoresponses increased during superfusion with

**Figure 7. The effects on rod voltage of treatments raising  $[Ca^{2+}]_i$  and altering  $[Ca^{2+}]$  regulation.**

Test solutions superfused the retina where indicated. Light flashes (100-ms, Fig A and C - 130 quanta rod<sup>-1</sup> flash<sup>-1</sup>, Fig B and D - 1300 quanta rod<sup>-1</sup> flash<sup>-1</sup>) were given periodically (every 30 s in A and B, every 60 s in C and D) to determine the effects of the drugs on the  $V_m$  photoresponses. The treatments included:

- A.** Sodium was partially replaced with Li<sup>+</sup> (50 % replacement: 54 mM Na<sup>+</sup>, 54 mM Li<sup>+</sup>; solution E4, Table 3).
- B.** Lanthanum (100 μM) was added to the superfusate (solution A1, Table 3, but with 500 μM LaNO<sub>3</sub> added).
- C.** Calcium was increased to 5x its control concentration (solution A11, Table 3).
- D.** Colchicine was added to the superfusate (10 mM, solution A2, Table 3).



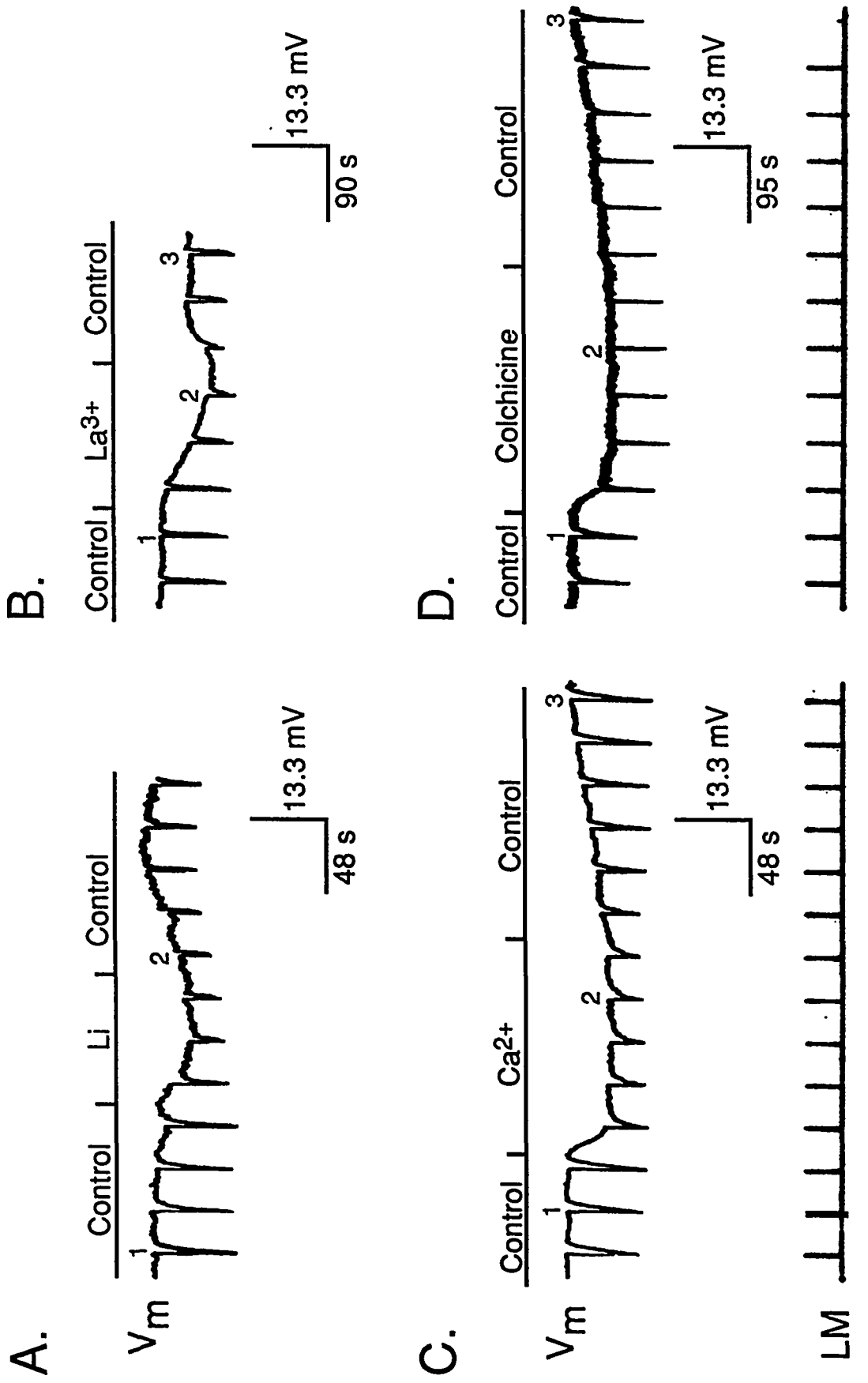


Fig. 7. The effects on rod voltage of treatments raising  $[Ca^{2+}]_i$  and altering  $[Ca^{2+}]$  regulation.

**Figure 8.** *Effects of treatments increasing  $[Ca^{2+}]_j$  and altering  $[Ca^{2+}]_j$  regulation on  $V_m$  photoresponse kinetics.*

The numbered  $V_m$  photoresponses from each treatment and its control(s) are normalized and superimposed to illustrate treatment-induced changes in the response kinetics. The voltage and time scales have been expanded. Treatments included:

- A.** 50% replacement of  $Na^+$  with  $Li^+$  (54 mM  $Na^+$  and 54 mM  $Li^+$ ).
- B.** 100  $\mu M$   $La^{3+}$ .
- C.** 4.5 mM (5x)  $Ca^{2+}$ .
- D.** 10 mM colchicine.

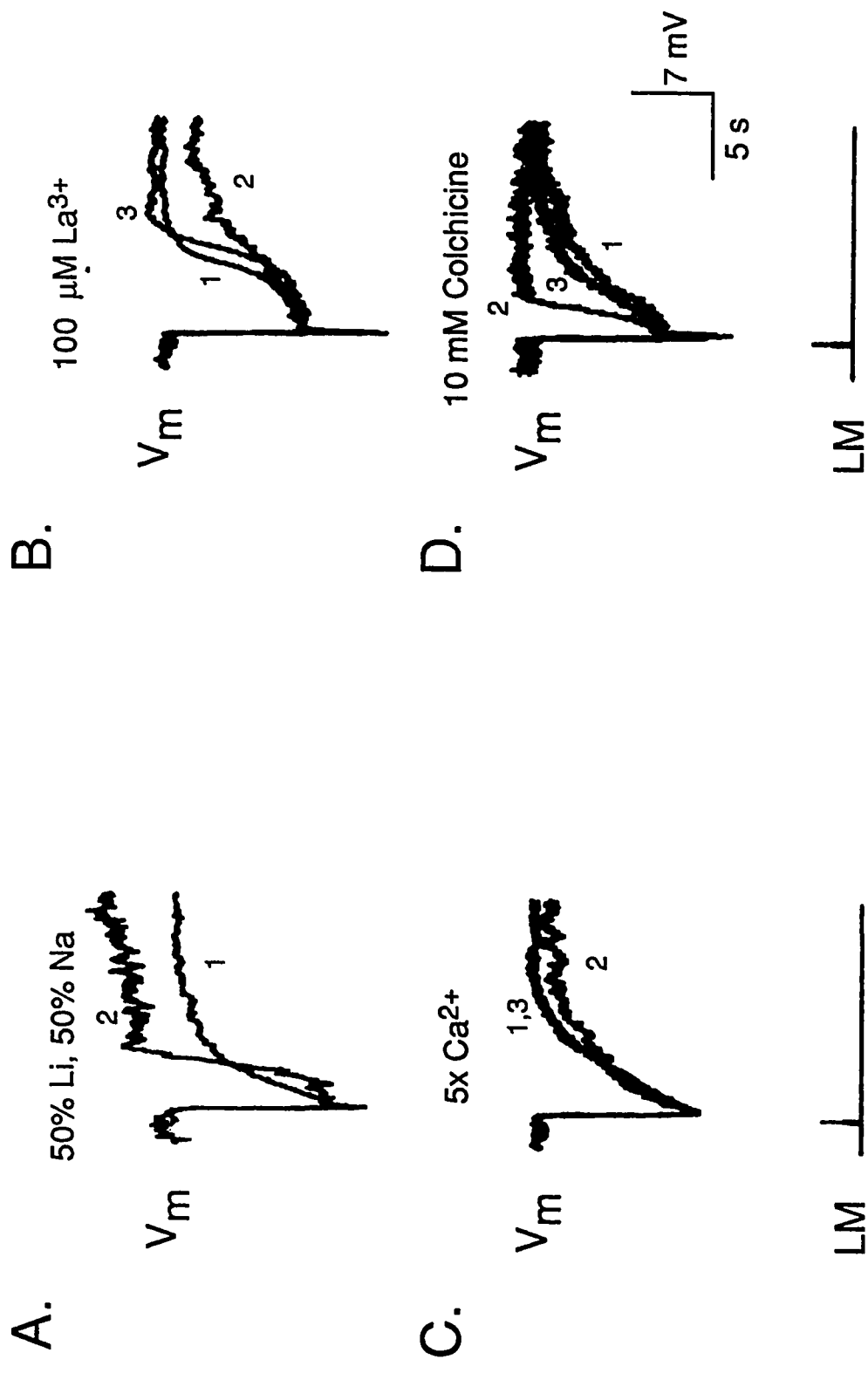


Fig. 8. Effects of treatments increasing  $[\text{Ca}^{2+}]_i$  and altering  $[\text{Ca}^{2+}]_i$  regulation on  $V_m$  photoresponse kinetics.

increased  $[Ca^{2+}]_o$  (Bastian and Fain, 1979) .

D. Figures 7D and 8D show the effects of 10 mM colchicine on rods. Colchicine hyperpolarized the rods and reduced  $V_m$  photoresponse amplitudes, but it dramatically shortened the duration of the  $V_m$  photoresponses.

In summary, each of the treatments, hyperpolarized dark-adapted rods and reduced photoresponse amplitudes, as does colchicine (treatment D). These results, although only correlational, support the hypothesis that colchicine's effects are due to increased  $[Ca^{2+}]_i$ .

There were differences, however, in the effects on  $V_m$  photoresponse kinetics between some of the treatments. The effects of each treatment on  $V_m$  photoresponse kinetics were qualitatively independent of drug concentration (not shown), so the differences seen between treatments cannot be attributed to variations in  $[Ca^{2+}]_i$  between treatments. The degree of change in the  $V_m$  photoresponse kinetics caused by a given drug was, however, dose-dependent (not shown). The different effects on  $V_m$  photoresponse kinetics caused by each of these treatments may reflect differences in the components of  $Ca^{2+}$  regulation affected by the different treatments. If this is the case, then it is interesting that  $La^{3+}$  produced different effects on the  $V_m$  photoresponse kinetics than replacing  $Na^+$  with  $Li^+$ , when the effects of both are thought to increase  $[Ca^{2+}]_i$  by blocking  $Na^+/K^+/Ca^{2+}$  exchange. The results of this section will be discussed further in Chapter 4.

**Section 3.3. Colchicine increases  $[Ca^{2+}]_o$ , and probably releases  $Ca^{2+}$  from internal stores.**

The previous section showed that increasing  $[Ca^{2+}]_i$  by reducing  $Ca^{2+}$  by extrusion or increasing  $Ca^{2+}$  influx produces effects that are similar to the effects of colchicine. Showing that colchicine superfusion increases  $[Ca^{2+}]_i$ , then, would provide strong support for the hypothesis that colchicine's effects are due to increased  $[Ca^{2+}]_i$ .

Methods of directly measuring  $[Ca^{2+}]_i$  in physiologically responsive rods, however, are few. Intracellular  $Ca^{2+}$ -selective microelectrodes small enough to penetrate rods without destroying their physiology have not yet proven reliable due to their very large impedances.

Furthermore, impaling a photoreceptor with a  $\text{Ca}^{2+}$ -selective microelectrode might release  $\text{Ca}^{2+}$  from ruptured lamellar disks, which are  $\text{Ca}^{2+}$ -rich, and might produce artifacts that would make data interpretation difficult.

Photosensitive  $\text{Ca}^{2+}$  chelators have been successfully used to measure  $[\text{Ca}^{2+}]_i$  in some laboratories under non-physiological conditions (McNaughton et al, 1985; Ratto et al, 1988). In one report the experimenters used the drug IBMX to increase  $[\text{Ca}^{2+}]_i$  so that light-evoked changes could be measured (McNaughton et al, 1985). The only other protocol used to date required retinal incubation in a no-added-calcium ringer for one hour (Ratto et al, 1987). It is tenuous to assume that the effects of colchicine on  $[\text{Ca}^{2+}]_i$  measured during such treatments would be indicative of colchicine's effects under standard physiological conditions.

There are even more serious problems in using photosensitive dyes to measure  $[\text{Ca}^{2+}]_i$ . Luminescence from the photosensitive dyes in the visual range stimulates photoreceptors and confounds the results (McNaughton et al, 1985). Perhaps even more problematic would be distinguishing colchicine's effects on the photoreceptors from its effects on more proximal retinal layers.

The problems of directly measuring  $[\text{Ca}^{2+}]_i$  currently seem insurmountable, but the hypothesis that colchicine's effects result from increased  $[\text{Ca}^{2+}]_i$  can be tested with other experimental protocols. These include: measuring changes in  $[\text{Ca}^{2+}]_o$  evoked by colchicine and controls; reducing  $[\text{Ca}^{2+}]_o$  in the presence of colchicine; applying colchicine in the presence of lowered  $[\text{Ca}^{2+}]_o$ ; and injecting EGTA intracellularly during colchicine superfusion. In addition, the results from these experiments would provide information about colchicine's effects on  $\text{Ca}^{2+}$  regulation not obtained by simply measuring  $[\text{Ca}^{2+}]_i$ . The experiments measuring changes in  $[\text{Ca}^{2+}]_o$  evoked by colchicine and controls are described in Subsections 3.3.1-3.3.4, while the results from the other techniques are presented in subsequent subsections.

### 3.3.1. *Measuring and characterizing light-evoked changes in $[Ca^{2+}]_o$ .*

Stimulating photoreceptors with light increases  $[Ca^{2+}]_o$  in receptor-side-up preparations of rat retina to an extent that a voltage change,  $V_{Ca^{2+}}$ , can be measured with  $Ca^{2+}$ -selective microelectrodes (Yoshikami & Hagsins, 1980; Miller & Korenbrot, 1987). The mechanics of this  $V_{Ca^{2+}}$  photoresponse have been the subject of debate in the past, but considerable evidence has shown that these  $V_{Ca^{2+}}$  photoresponses result from a reduction of the  $Ca^{2+}$  influx through  $g_{hv}$ , while  $Ca^{2+}$  efflux into the interphotoreceptor space, via  $Na^+/K^+/Ca^{2+}$  exchange, continues (Yau & Nakatani, 1984a, b; Gold, 1986; McNaughton et al, 1985; Hodgkin & Nunn, 1986; Miller & Korenbrot, 1987; Ratto et al, 1988). Since the mechanics of  $V_{Ca^{2+}}$  photoresponses are now understood,  $V_{Ca^{2+}}$  photoresponses can be helpful in interpreting  $[Ca^{2+}]_o$  changes caused by colchicine, which are described in later subsections. Calcium photoresponses in a receptor-side-up preparation of the toad retina, measured with double-barrel,  $Ca^{2+}$ -selective microelectrodes ( $V_{Ca^{2+}}$  photoresponses), are characterized in Figs. 9 and 10. These figures also show  $V_m$  photoresponses recorded simultaneously from a rod within the same illuminated patch of retina.

Figure 9 shows  $V_{Ca^{2+}}$  photoresponses to 100-ms flashes of light from a range of irradiances ( $26 - 26,000$  quanta  $rod^{-1}$  flash $^{-1}$ ). The  $V_{Ca^{2+}}$  photoresponses had two pronounced components, each with its own rising and falling phases, which correlated with components of the  $V_m$  photoresponses.

In the first  $V_{Ca^{2+}}$  photoresponse component,  $V_{Ca^{2+}}$  began to increase less than a second after the rods began to hyperpolarize. The time-to-peak of the first  $V_{Ca^{2+}}$  photoresponse component did not correlate with the time-to-peak of saturating voltage photoresponses. Instead, the time-to-peak of the first  $V_{Ca^{2+}}$  photoresponse component correlated with the beginning of rod voltage recovery for nonsaturating  $V_{Ca^{2+}}$  photoresponses. For flashes that also saturated the  $V_{Ca^{2+}}$  photoresponse, the time-to-peak of the first  $V_{Ca^{2+}}$  photoresponse component was constant. The declining phase of the first component of the  $V_{Ca^{2+}}$  photoresponse followed the recovery phase of the  $V_m$  photoresponse by 3-4 seconds at all flash irradiances. The peak amplitudes of the first

components increased non-linearly with irradiance over the range studied. Irradiances greater than  $\sim 2600$  quanta  $\text{rod}^{-1}$  flash $^{-1}$  (Fig. 9A.3) caused saturating peak  $V_{\text{Ca}^{2+}}$  changes of about 1 mV (Fig. 9A.3), corresponding to concentration increases of about 8  $\mu\text{M}$ . Only the duration of the peak response increased further with brighter flashes (Fig. 9A.4). The initial rate of the  $V_{\text{Ca}^{2+}}$  changes increased little with flash irradiance over the range studied. Moreover, the rate of  $V_{\text{Ca}^{2+}}$  increase was approximately constant for flash intensities which saturated  $V_m$  photoresponses. Figure 9C plots the initial rate of  $V_{\text{Ca}^{2+}}$  increase against flash irradiance, demonstrating the low correlation of the two variables. The initial rate was estimated from the inverse of the average time to reach a 0.5 mV change in  $V_{\text{Ca}^{2+}}$  for each irradiance. The number of responses averaged for each irradiance are given beside each data point.

The second component of the  $V_{\text{Ca}^{2+}}$  photoresponse was most clearly apparent in responses to flashes that saturated the  $V_m$  photoresponse. In the three flashes, Figs. 9B, 9C and 9D,  $V_{\text{Ca}^{2+}}$  continued to decline for several seconds after  $V_m$  returned to dark-adapted values. The falling phase of this second  $V_{\text{Ca}^{2+}}$  photoresponse component continued until  $V_{\text{Ca}^{2+}}$  undershot its dark-adapted value by up to a few hundred microvolts. This falling phase was followed by a rising phase that returned  $V_{\text{Ca}^{2+}}$  to dark-adapted values. The amplitude of the undershoot increased with the duration of the  $V_m$  photoresponse.

The  $V_{\text{Ca}^{2+}}$  photoresponse apparently resulted from  $\text{Ca}^{2+}$  fluxes only in the photoreceptor layer. Duplicate experiments performed without 10 mM aspartate blocking synaptic transmission to proximal retinal layers gave results that were not noticeably different from those just described. Previously reported experiments with rat retina gave similar results, leading to the suggestion that Müller cells provide a significant diffusion barrier to  $\text{Ca}^{2+}$  (Yoshikami & Hagins, 1980). It seems unlikely, then, that proximal layers of the retina contribute to the  $V_{\text{Ca}^{2+}}$  changes measured in this preparation.

The  $V_{\text{Ca}^{2+}}$  increase seen in the first component of the  $V_{\text{Ca}^{2+}}$  photoresponse apparently resulted from  $\text{Ca}^{2+}$  efflux from the photoreceptors, and not from the loss of any intrinsic  $[\text{Ca}^{2+}]_o$  gradients in the retina, since no clear  $V_{\text{Ca}^{2+}}$  gradients could be measured with

**Figure 9.** *Light-evoked changes in  $V_{Ca^{2+}}$ .*

The record labeled  $V_{Ca^{2+}}$  shows the  $Ca^{2+}$  Nernst voltage measured with a double-barrel,  $Ca^{2+}$ -selective microelectrode in the interphotoreceptor space during 100-ms flashes. The record labeled  $V_m$  shows the  $V_m$  photoresponses from a rod within the same illuminated patch of retina for comparison. Control solution with a reduced  $[Ca^{2+}]$  (100  $\mu M$ ; solution B1, Table 3) was used to superfuse the retina during the recordings to enhance the  $V_{Ca^{2+}}$  signals. The solution included 10 mM aspartate to chemically block light-evoked changes in  $Ca^{2+}$  originating from the proximal retinal layers. The flash irradiances used in each record were:

- A. 1. 26 quanta rod<sup>-1</sup> flash<sup>-1</sup>.
2. 260 quanta rod<sup>-1</sup> flash<sup>-1</sup>.
3. 2,600 quanta rod<sup>-1</sup> flash<sup>-1</sup>.
4. 26,000 quanta rod<sup>-1</sup> flash<sup>-1</sup>.

B. The photoresponses from A are replotted superimposed. The light monitor from A2 is plotted to indicate the relative time of stimulation for all traces.



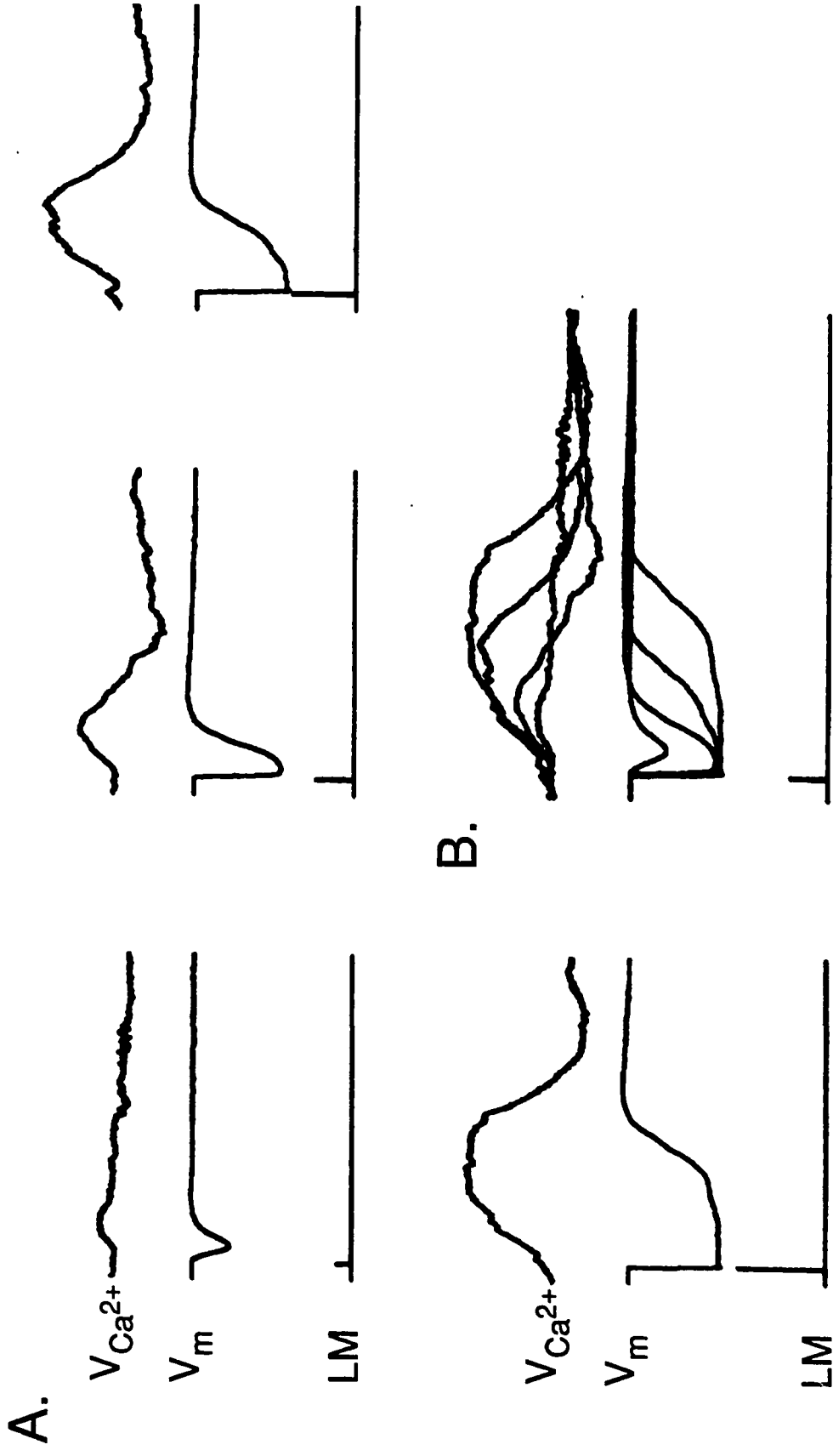


Fig. 9. Light-evoked changes in  $V_{Ca^{2+}}$ .

these electrodes between the interphotoreceptor layer and the surrounding bath during dark adapted periods. Moreover, retraction of the electrode 250  $\mu\text{M}$  into the overlying bath during a  $V_{\text{Ca}^{2+}}$  photoresponse decreased  $V_{\text{Ca}^{2+}}$  to the pre-stimulation level observed in the interphotoreceptor space (see Fig. 10B). This measurement confirmed both that the pre-stimulus interphotoreceptor  $[\text{Ca}^{2+}]$  was the same as the bath  $[\text{Ca}^{2+}]$  and that photostimulation caused the interphotoreceptor  $[\text{Ca}^{2+}]$  to rise above the bath  $[\text{Ca}^{2+}]$ . Thus light stimulation produces a  $[\text{Ca}^{2+}]$  gradient such that  $\text{Ca}^{2+}$  should diffuse from the interphotoreceptor space to the overlying bath.

Tests for  $[\text{Ca}^{2+}]_o$  gradients between the interphotoreceptor space and the bath 250  $\mu\text{m}$  above the tips in non-stimulated retinas only gave negative results when the bath  $[\text{Ca}^{2+}]$  remained constant for at least 10 minutes prior to the measurements. It apparently took many minutes for the interphotoreceptor  $[\text{Ca}^{2+}]$  to equilibrate with the overlying bath, since gradients between the interphotoreceptor  $[\text{Ca}^{2+}]$  and the overlying bath  $[\text{Ca}^{2+}]$  could be measured for several minutes after changing the bath  $[\text{Ca}^{2+}]$  from 0.9 mM to 0.1 mM. This is consistent with the interphotoreceptor space acting as an unstirred layer while  $\text{Ca}^{2+}$  slowly diffused away into the overlying bath. Calcium gradients between the overlying bath and the deeper layers of the retina persisted for an even longer time period, in agreement with the proposition that a  $\text{Ca}^{2+}$  diffusion barrier exists between the photoreceptor layer and the deeper layers of the retina. This result was not studied further.

The lack of a  $\text{Ca}^{2+}$  gradient between the interphotoreceptor space and the overlying bath is consistent with measurements made in the rat retina (Hagins & Yoshikami, 1980) and with measurements made in another lab in toad retina (Chester Kowalski, personal communication).

The  $V_{\text{Ca}^{2+}}$  waveforms produced by steps of light are also of special interest, since they should reflect the emptying of  $\text{Ca}^{2+}$  from rods during the prolonged closure of  $g_{\text{hV}}$ . A typical  $V_{\text{Ca}^{2+}}$  waveform from a 2-min. step of light (2,600 quanta rod<sup>-1</sup> s<sup>-1</sup>) is shown in Fig. 10A, along with a  $V_m$  waveform recorded during this period from the same illuminated patch of retina. For about 20 s after the initiation of the step,  $V_{\text{Ca}^{2+}}$  increased to a peak response

**Figure 10.** *Changes in  $V_{Ca^{2+}}$  during constant illumination.*

**A.** A 2-min. light step ( $2600 \text{ quanta rod}^{-1} \text{ s}^{-1}$ ) illuminated the retina where indicated. A modified control solution, identical to the one used in the experiment described in Fig. 9 ( $0.1 \text{ mM Ca}^{2+}$ , solution B1, Table 3), superfused the retina to enhance the  $V_{Ca^{2+}}$  signal.

**B.** The top record labeled  $V_{Ca^{2+}}$  shows a 3-min. control response similar to the response shown in A. The record labeled  $V_{Ca^{2+}}$  immediately below it shows a subsequent 3-min. response in the same retina at the same position, but at the time indicated by the first arrow, the electrode was withdrawn from the interphotoreceptor space to the overlying bath  $250 \mu\text{m}$  above the tip of the photoreceptors. The second arrow indicates where the electrode was then re-inserted into the interphotoreceptor space back to its original depth,  $\sim 50 \mu\text{m}$  below the tips of the photoreceptors. The lowest record labeled  $V_{Ca^{2+}}$  shows another repetition of this experiment, but the light stimulus was turned off while the electrode remained in the bath above the photoreceptors.

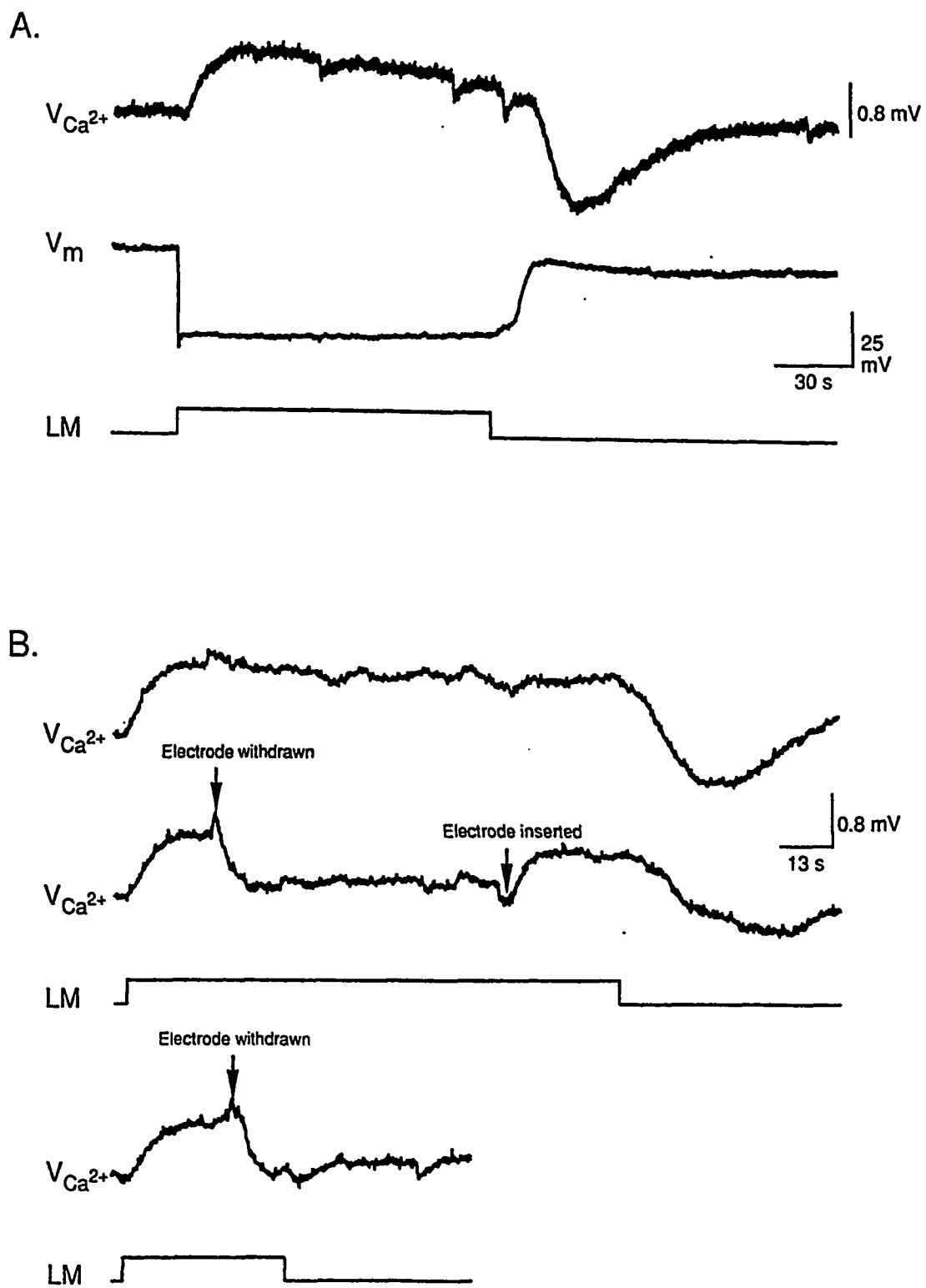


Fig. 10. Changes in  $V_{Ca^{2+}}$  during constant illumination.

before slowly decreasing during the remaining period of illumination. Late in the illuminated period,  $V_{Ca^{2+}}$  had nearly declined to its dark-adapted level. When the light step ended,  $V_{Ca^{2+}}$  rapidly dropped below its dark-adapted level before eventually returning to it about one minute later.

Increasing the stimulus duration changes the  $V_{Ca^{2+}}$  waveforms only slightly. Longer light steps, up to 4-min., allowed  $V_{Ca^{2+}}$  to decline further toward its dark-adapted level during the latter part of stimulation (Fig. 11A). Otherwise, the effects resembled those shown in Fig. 10A.

Increasing the irradiance of light steps had little effect on the  $V_{Ca^{2+}}$  waveform. Increasing the brightness of saturating light steps 10-fold produced similar waveforms, as shown in Fig. 10B. One notable difference seen during very bright steps of light ( $26,000$  quanta  $\text{rod}^{-1} \text{s}^{-1}$ ) was the absence of the post-stimulus undershoot. Instead of undershooting the dark-adapted  $V_{Ca^{2+}}$  level,  $V_{Ca^{2+}}$  gradually declined to its dark-adapted level.

The rods were hyperpolarized during the periods of illumination in each of the cases described above. Light-adaptation during the periods of illumination varied little, and was always considerably less than observed during similar stimuli at higher  $[Ca^{2+}]_o$  (compare Figs. 10A & 6A). Note that in Fig. 10A,  $V_m$  had returned to its dark-adapted level during the post-stimulus undershoot in the  $V_{Ca^{2+}}$  waveform. During brighter illumination ( $26,000$  quanta  $\text{rod}^{-1} \text{s}^{-1}$ ), however,  $V_m$  depolarized much more slowly to its dark-adapted level after the light-stimulation ceased (not shown). The slow depolarization after these brighter light steps coincided with the slow return of  $V_{Ca^{2+}}$  to its baseline level after similar light steps. The results of this section will be discussed in Chapter 4.

### *3.3.2. The effects on $V_{Ca^{2+}}$ caused by increasing rod $Ca^{2+}$ permeability.*

It was previously stated that increasing  $[Ca^{2+}]_i$  has effects on rod voltage which resemble colchicine's. This led to the hypothesis that colchicine's effects result from increased  $[Ca^{2+}]_i$ . One mechanism by which colchicine might increase  $[Ca^{2+}]_i$  would be to

**Figure 11.** *Changes in  $V_{Ca^{2+}}$  during steps of illumination of varying lengths and irradiances.*

**A.** A 2-min. light step ( $2600 \text{ quanta rod}^{-1} \text{ s}^{-1}$ ) illuminating the retina is compared to a 3-min. light step of the same irradiance. A modified control solution, identical to the one used in the experiment described in Fig. 9 ( $0.1 \text{ mM Ca}^{2+}$ , solution B1, Table 3), superfused the retina to enhance the  $V_{Ca^{2+}}$  signal.

**B.** A 2-min. light step ( $2600 \text{ quanta rod}^{-1} \text{ s}^{-1}$ ) illuminating the retina is compared to a 2-min. light step at a brighter irradiance ( $26,000 \text{ quanta rod}^{-1} \text{ s}^{-1}$ ). A modified control solution, identical to the one used in the experiment described in Fig. 8 ( $0.1 \text{ mM Ca}^{2+}$ , solution B1, Table 3), superfused the retina to enhance the  $V_{Ca^{2+}}$  signal.

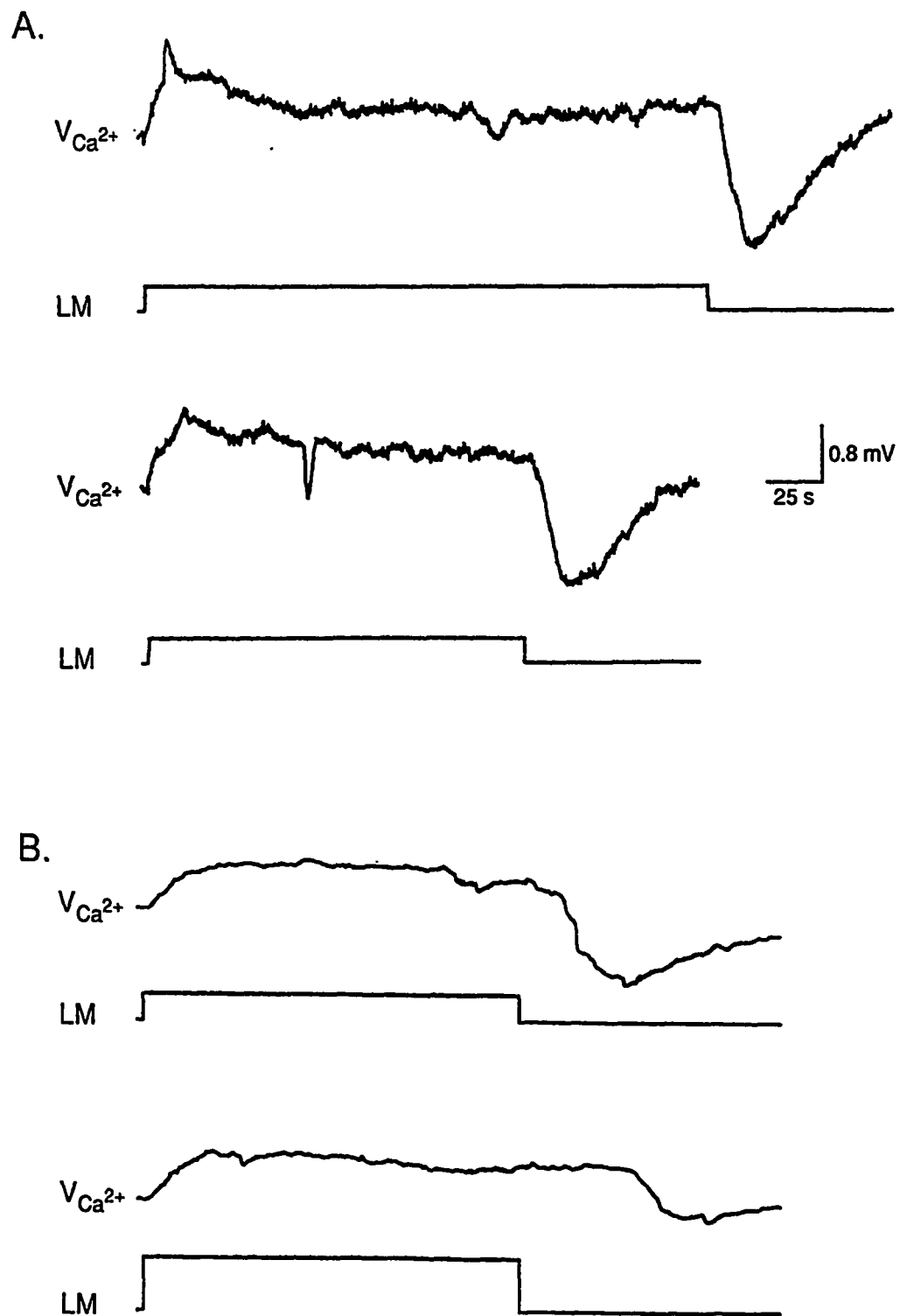


Fig. 11. Changes in  $V_{Ca^{2+}}$  during steps of illumination of varying lengths and irradiances.

increase rod  $\text{Ca}^{2+}$  permeability, perhaps by acting as an ionophore, or simply making the rod leaky to  $\text{Ca}^{2+}$ . The effects of increasing rod  $\text{Ca}^{2+}$  permeability on  $V_{\text{Ca}^{2+}}$ , however, have not been previously established. Therefore, it was necessary to measure  $V_{\text{Ca}^{2+}}$  during an experiment with an established method of increasing rod  $\text{Ca}^{2+}$  permeability to compare to the  $V_{\text{Ca}^{2+}}$  changes caused by colchicine.

Calcium ionophores might have been used to increase  $\text{Ca}^{2+}$  permeability, but their use in photoreceptors requires pretreatment with very low  $\text{Ca}^{2+}$  solutions (Bastian & Fain, 1982). Furthermore, many common  $\text{Ca}^{2+}$  ionophores also transport  $\text{Mg}^{2+}$ , which could have unknown consequences. The phosphodiesterase inhibitor IBMX provided a well-established means of increasing rod  $\text{Ca}^{2+}$  permeability. The drug readily permeates rod plasma membranes, so it can be applied simply by adding it to the superfusate. Furthermore, its mechanism of action is well studied (Waloga et al, 1983; Oakley & Bert, 1985; McNaughton et al, 1985; Hodgkin & Nunn, 1988). It increases the rod's permeability to  $\text{Ca}^{2+}$  by increasing  $g_{\text{hV}}$ , but it does not stop phototransduction.

Figure 12 shows the results of superfusion with 500  $\mu\text{M}$  IBMX on interphotoreceptor  $V_{\text{Ca}^{2+}}$  and on  $V_{\text{m}}$ . The introduction of IBMX produced a sharp transient decrease in the dark-adapted  $V_{\text{Ca}^{2+}}$  level (area enclosed in box 1) while simultaneously depolarizing the rods. After a few minutes in IBMX, however, the dark-adapted  $V_{\text{Ca}^{2+}}$  level eventually increased back toward its pre-drug level (area enclosed by box 2). Although  $V_{\text{Ca}^{2+}}$  appeared to stabilize after about 3 min., it never reached the bath  $V_{\text{Ca}^{2+}}$  level, thus the addition of IBMX created a  $\text{Ca}^{2+}$  gradient between the bath and the interphotoreceptor space. Such a gradient was measured directly by retracting the  $\text{Ca}^{2+}$  microelectrode from the interphotoreceptor space to the overlying bath in other experiments.

Superfusion with IBMX also increased the amplitudes and durations of the  $V_{\text{Ca}^{2+}}$  photoresponses, as well as the duration of the  $V_{\text{m}}$  photoresponses. During the initial period of decreasing  $V_{\text{Ca}^{2+}}$ , the  $V_{\text{Ca}^{2+}}$  photoresponses peaked near the same absolute  $V_{\text{Ca}^{2+}}$  level as control photoresponses (see Fig. 13, box 1). After 4 minutes in IBMX, however, the  $V_{\text{Ca}^{2+}}$  photoresponse reached nearly 3 mV, and peaked at an absolute  $V_{\text{Ca}^{2+}}$



**Figure 12.** *The effects of IBMX on photoreceptor  $V_{Ca^{2+}}$  and  $V_m$*

The phosphodiesterase inhibitor IBMX superfused the retina where indicated (500  $\mu$ M, solution B4, Table 3). Flashes of light (100-ms, 2,600 quanta rod<sup>-1</sup> flash<sup>-1</sup>) stimulated the retina where shown.

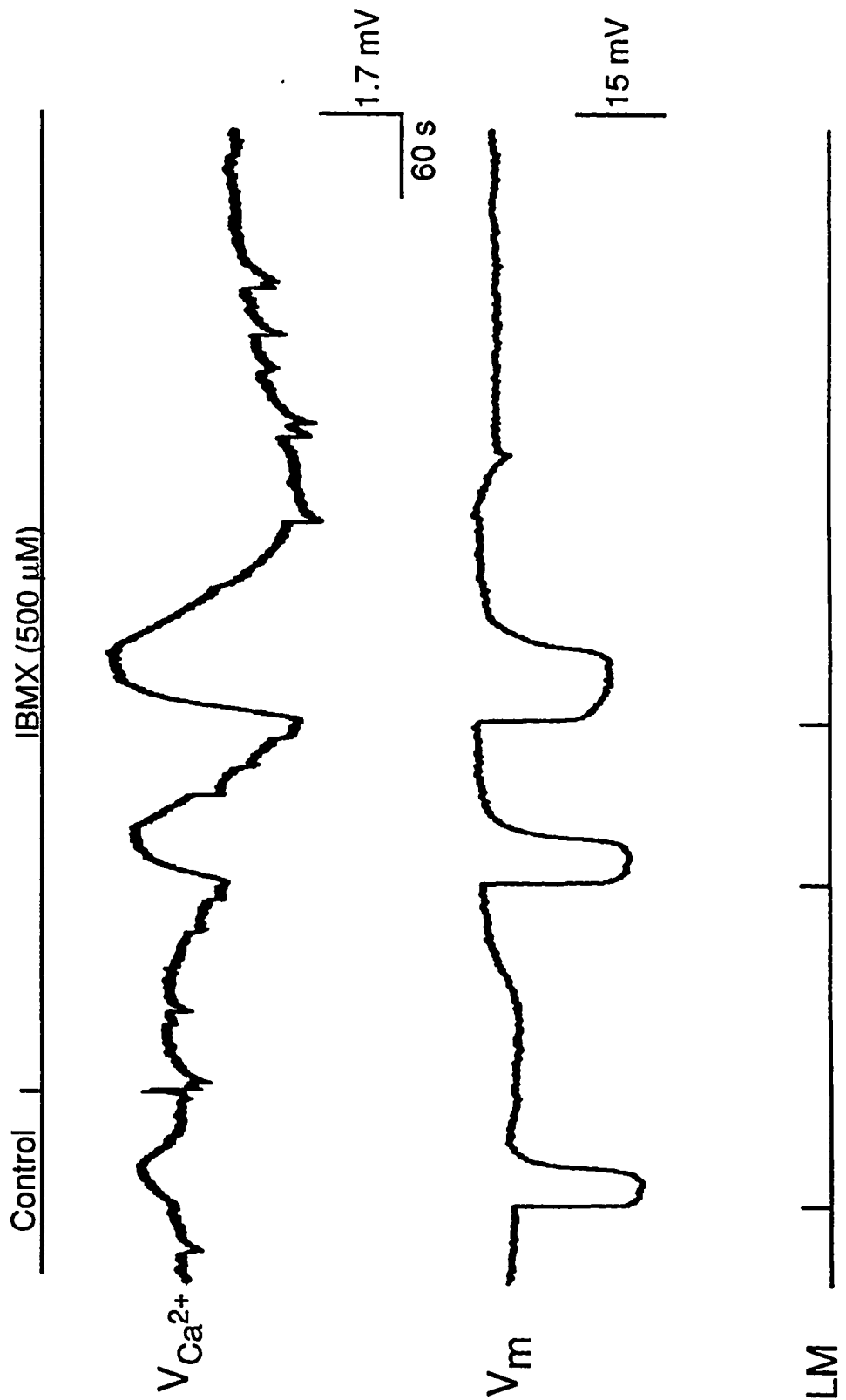


Fig. 12. The effects of IBMX on photoreceptor  $V_{Ca^{2+}}$  and  $V_m$ .

**Figure 13.** *Effect of stimulus interval on light-evoked  $V_{Ca^{2+}}$  responses in IBMX.*

This record shows a longer period of the same experiment shown in Fig. 12. An increased interval between the third and fourth light flashes showed that longer intervals between flashes increased the  $V_{Ca^{2+}}$  photoresponse duration.

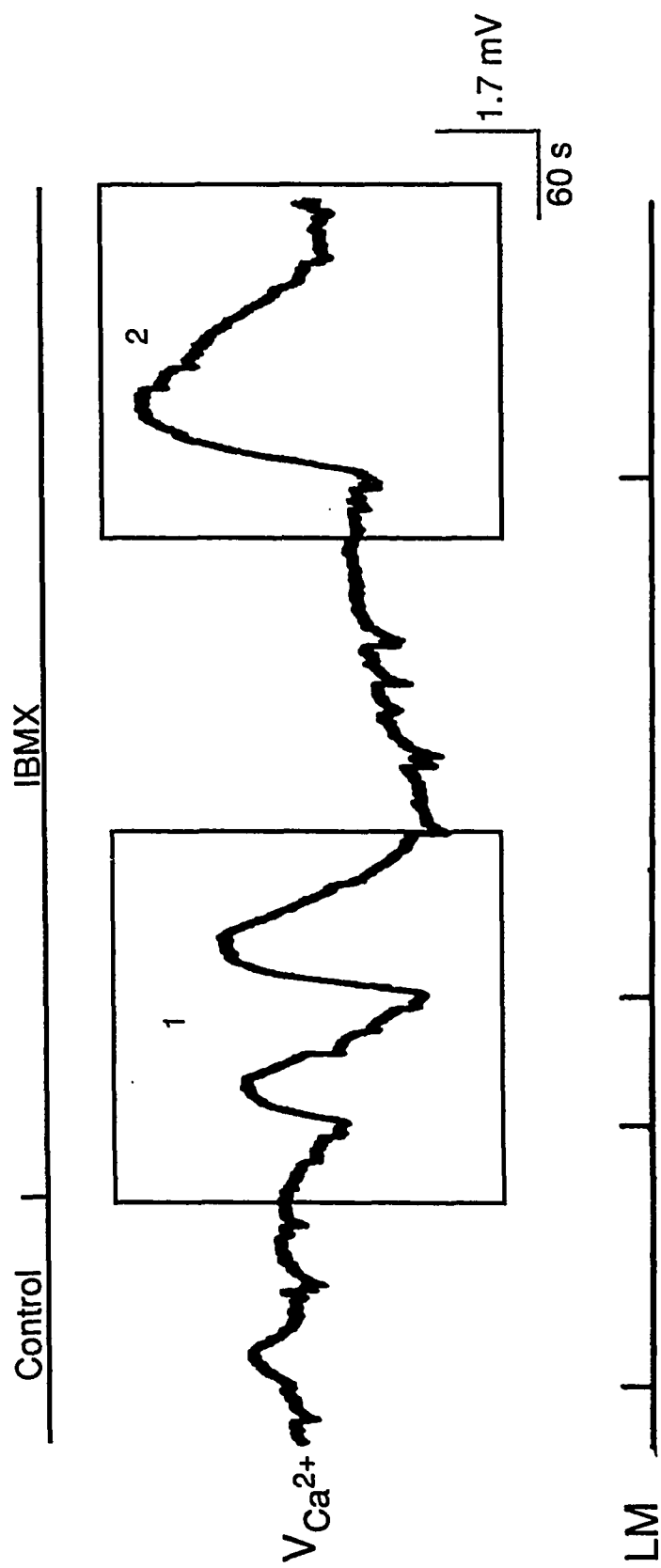


Fig. 13. Effects of stimulus interval on light-evoked  $V_{Ca^{2+}}$  responses in IBMX.

level well above that of the control responses (see Fig. 13, box 2). The duration of the  $V_{Ca^{2+}}$  photoresponse appeared to increase with increasing time of exposure to IBMX, although this was not explicitly quantified.

### 3.3.3 : *The effects of blocking $Na^+/K^+/Ca^{2+}$ exchange on $V_{Ca^{2+}}$ .*

Another mechanism by which colchicine could increase  $[Ca^{2+}]_i$  would be to block  $Na^+/K^+/Ca^{2+}$  exchange, and thus trap  $Ca^{2+}$  inside the rods, as previously discussed. The effects of blocking  $Na^+/K^+/Ca^{2+}$  exchange on interphotoreceptor  $V_{Ca^{2+}}$  have not, however, been previously measured. Therefore, it was necessary to measure  $V_{Ca^{2+}}$  during an experiment with an established method of blocking  $Na^+/K^+/Ca^{2+}$  exchange to compare to  $V_{Ca^{2+}}$  changes caused by colchicine.

Trivalent ions, such as  $La^{3+}$ , block  $Na^+/K^+/Ca^{2+}$  exchangers in  $\mu M$  doses, while the drug amiloride blocks these exchangers in mM doses. Unfortunately, the  $Ca^{2+}$  microelectrodes responded to the presence of these drugs, making their use for measurement of  $V_{Ca^{2+}}$  changes questionable.

Removing the  $Na^+$  gradient across the rod membrane can also effectively stop  $Na^+/K^+/Ca^{2+}$  exchange (Yau, 1984; Hodgkin 1987). A  $Li^+$  gradient will not support the  $Na^+/K^+/Ca^{2+}$  exchanger, but will, however, permeate  $g_{hV}$ . Therefore,  $Li^+$  substitution for  $Na^+$  in solutions bathing rods provides another means of selectively stopping  $Na^+/K^+/Ca^{2+}$  exchange, as previously discussed. Furthermore,  $Li^+$  substitution for  $Na^+$  neither produced extrinsic responses in the  $Ca^{2+}$  microelectrodes nor changed the calibration characteristics of the electrodes (see Section 2.4). Thus this technique provided the means of obtaining the necessary data.

Figure 14 shows the results of replacing  $Na^+$  with  $Li^+$  on  $V_{Ca^{2+}}$ . Replacing  $Na^+$  with  $Li^+$  prolonged the 1st subsequent  $V_{Ca^{2+}}$  photoresponse, then decreased dark-adapted  $V_{Ca^{2+}}$  and eventually abolished  $V_{Ca^{2+}}$  photoresponses after a few minutes (box 1). These results are consistent with the interpretation that replacing  $Na^+$  with  $Li^+$  stops extrusion of  $Ca^{2+}$  from rods (hence lowering  $V_{Ca^{2+}}$  while increasing  $[Ca^{2+}]_i$ ), which leads to a shutdown of the

**Figure 14.** *The effect of Li<sup>+</sup> replacement of Na<sup>+</sup> on V<sub>Ca<sup>2+</sup></sub> and V<sub>Ca<sup>2+</sup></sub> photoresponses.*

A Li<sup>+</sup>-based test solution superfused the retina where indicated. An equimolar amount of Li<sup>+</sup> replaced Na<sup>+</sup> (100% replacement). The superfusate additionally contained the phosphodiesterase inhibitor, IBMX (500 μM), where indicated. The Ca<sup>2+</sup> concentration in all solutions was 10<sup>-4</sup> M (Solutions B1, E10 and E11; Table 3). Flashes of light (100-ms, 26,000 quanta rod<sup>-1</sup> flash<sup>-1</sup>) stimulated the retina where indicated.

The superfusates were made by adding either 108 mM NaCl or 108 mM LiCl to a Ca<sup>2+</sup>-containing split sample. The pH was adjusted by adding either LiOH or NaOH as required. Control solution changes before and after the experiment showed no measurable differences in V<sub>Ca<sup>2+</sup></sub> between the various superfusates.

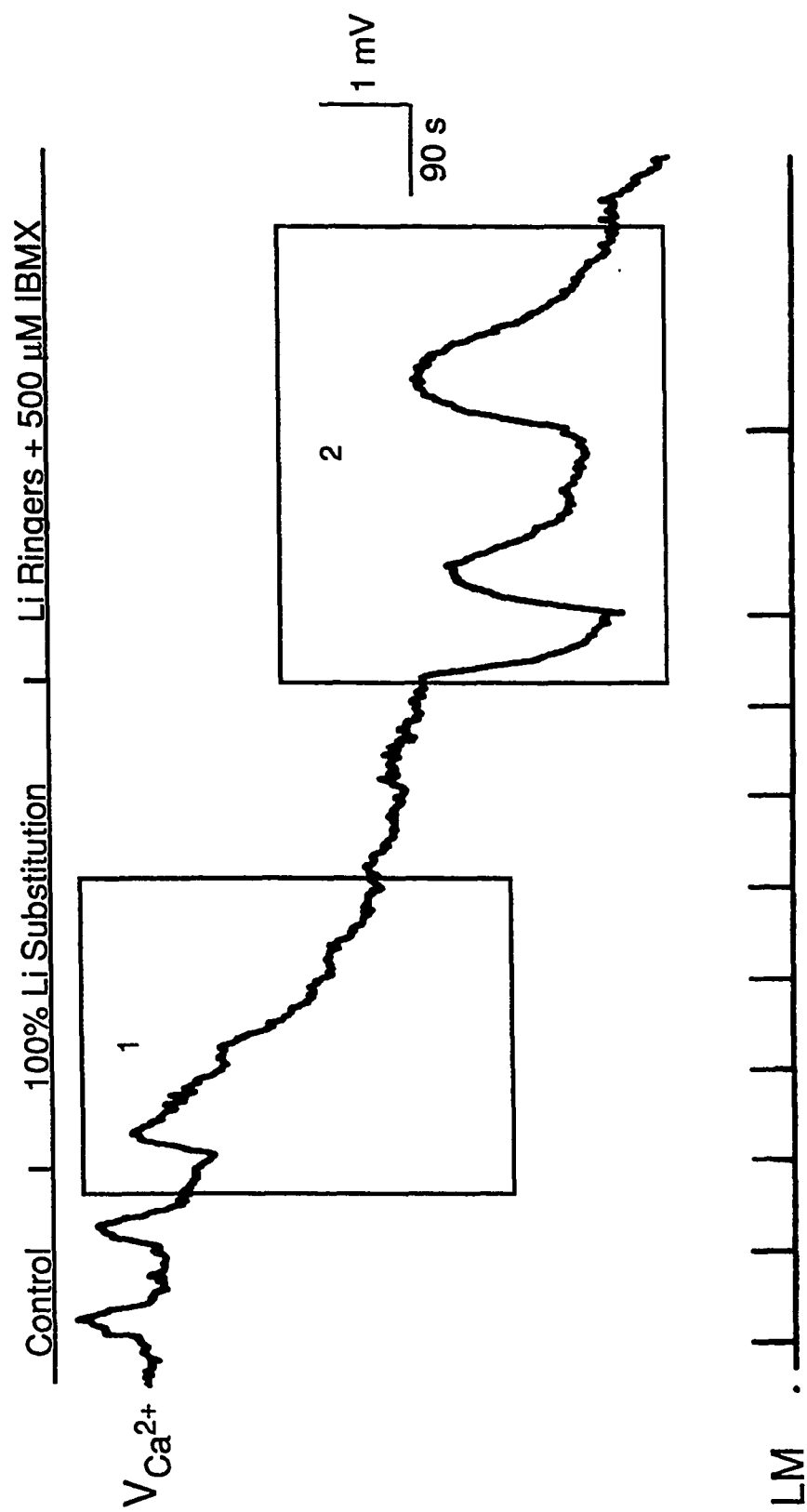


Fig. 14. The effect of  $Li^+$  replacement of  $Na^+$  on  $V_{Ca^{2+}}$  and  $V_{Ca^{2+}}$  photoresponses.

light-sensitive current. These results will be further discussed in Chapter 4.

Since blocking  $\text{Na}^+/\text{K}^+/\text{Ca}^{2+}$  exchange not only stops  $\text{Ca}^{2+}$  extrusion, but also shuts down the light-sensitive current, the effects of stopping  $\text{Na}^+/\text{K}^+/\text{Ca}^{2+}$  exchange on  $V_{\text{Ca}^{2+}}$  should be self-limiting. If the light-sensitive current could be restarted during blockade of the  $\text{Na}^+/\text{K}^+/\text{Ca}^{2+}$  exchanger,  $V_{\text{Ca}^{2+}}$  should again start to decline. Adding IBMX to increase  $[\text{cGMP}]_i$  and restart the light-sensitive current during  $\text{Li}^+$  superfusion achieved this condition (see box 2). Furthermore, it restored  $V_{\text{Ca}^{2+}}$  photoresponses. The recuperated  $V_{\text{Ca}^{2+}}$  photoresponses had amplitudes and durations noticeably longer than controls. Note, however, that the absolute  $V_{\text{Ca}^{2+}}$  level of the  $V_{\text{Ca}^{2+}}$  photoresponse peak did not exceed the bath  $V_{\text{Ca}^{2+}}$  level. Thus the  $V_{\text{Ca}^{2+}}$  photoresponse most likely resulted from the loss of a  $\text{Ca}^{2+}$  gradient between the interphotoreceptor space and the bath, rather than from a net efflux of  $\text{Ca}^{2+}$  from the photoreceptors. This will be discussed further in Chapter 4.

Figure 15 shows the effects of replacing  $\text{Na}^+$  with  $\text{Li}^+$ , and subsequently adding IBMX, on  $V_m$  and  $V_m$  photoresponses. The superfusates in this experiment also contained 0.1 mM  $\text{Ca}^{2+}$ , so that the results could be correlated with those just shown in Fig. 14. Note that during  $\text{Li}^+$  superfusion,  $V_m$  hyperpolarized, and the  $V_m$  photoresponses decreased in amplitude as previously described (compare Fig. 15 to Fig. 9). Introducing IBMX during the  $\text{Li}^+$  superfusion, however, reversed these effects: IBMX depolarized the rods and increased the  $V_m$  photoresponse amplitudes and durations. Returning  $\text{Na}^+$  for  $\text{Li}^+$ , but continuing IBMX superfusion, shortened the duration of the  $V_m$  photoresponses but hardly affected response amplitude. These results, which help to interpret the  $V_{\text{Ca}^{2+}}$  changes seen in the above experiment, will be discussed further in Chapter 4.

As stated previously, IBMX increases rod  $\text{Ca}^{2+}$  influx. Blocking  $\text{Na}^+/\text{K}^+/\text{Ca}^{2+}$  exchange in the presence of IBMX, then, provides a means of loading rods with  $\text{Ca}^{2+}$ . If rods are loaded with  $\text{Ca}^{2+}$  in this way, reactivating the  $\text{Na}^+/\text{K}^+/\text{Ca}^{2+}$  exchanger by returning  $\text{Na}^+$  to replace  $\text{Li}^+$  should provide a large efflux of  $\text{Ca}^{2+}$  into the interphotoreceptor space.

Figure 16 shows  $V_{\text{Ca}^{2+}}$  changes resulting from reactivating the  $\text{Na}^+/\text{K}^+/\text{Ca}^{2+}$  exchanger in rods loaded with  $\text{Ca}^{2+}$  in the manner just described. Note that the presence of IBMX



**Figure 15.** *Effects of replacing Na<sup>+</sup> with Li<sup>+</sup> and subsequent addition of IBMX on V<sub>m</sub> and V<sub>m</sub> photoresponses.*

A single barrel microelectrode recorded V<sub>m</sub> during Li<sup>+</sup> replacement of Na<sup>+</sup>, and during subsequent addition of 500 μM IBMX. The solution compositions were identical to those described in Fig. 14.

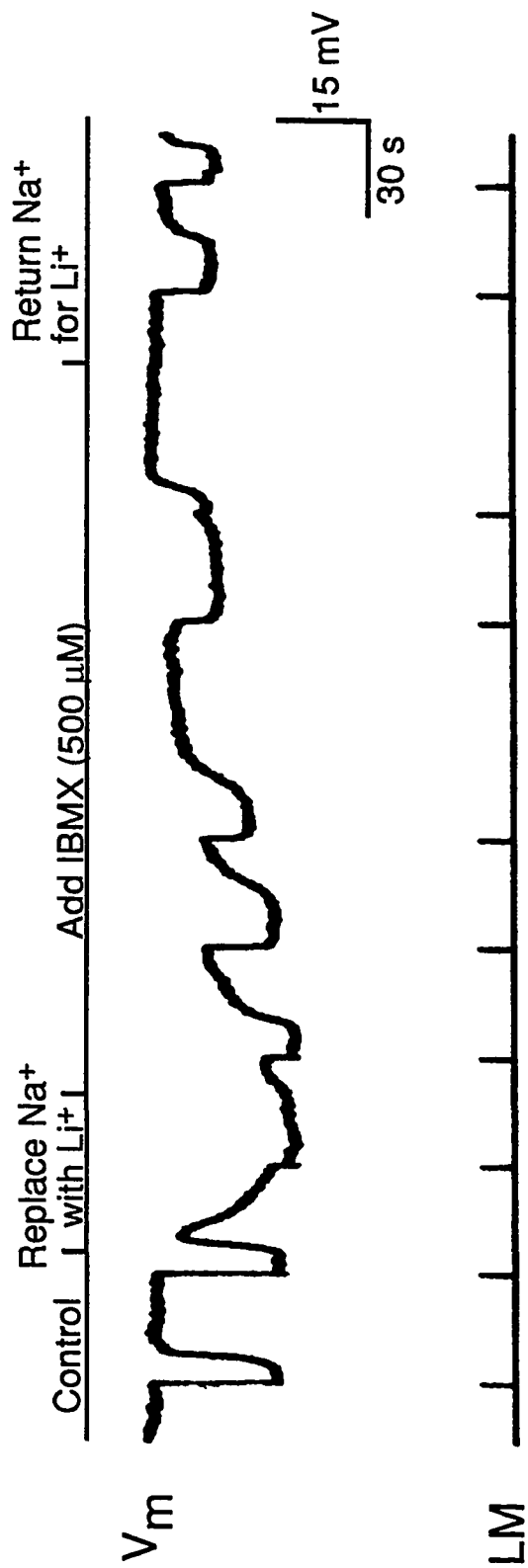


Fig. 15. Effects of replacing  $\text{Na}^+$  with  $\text{Li}^+$  and subsequent addition of IBMX on  $V_m$  and  $V_m$  photoresponses.

**Figure 16.** *Changes in  $V_{Ca^{2+}}$  evoked by  $Li^+$  replacement of  $Na^+$  and vis a' vis in the presence of IBMX.*

Solutions containing IBMX (500  $\mu$ M) superfused the retina where indicated. All solutions contained 0.1 mM  $Ca^{2+}$  as previously described (solutions B1, E10 and E11, Table 3). Light flashes (100-ms, 26,000 quanta rod $^{-1}$  flash $^{-1}$ ) and a light pulse (10-s, 260,000 quanta rod $^{-1}$  s $^{-1}$ ) stimulated the retina where shown.

IBMX

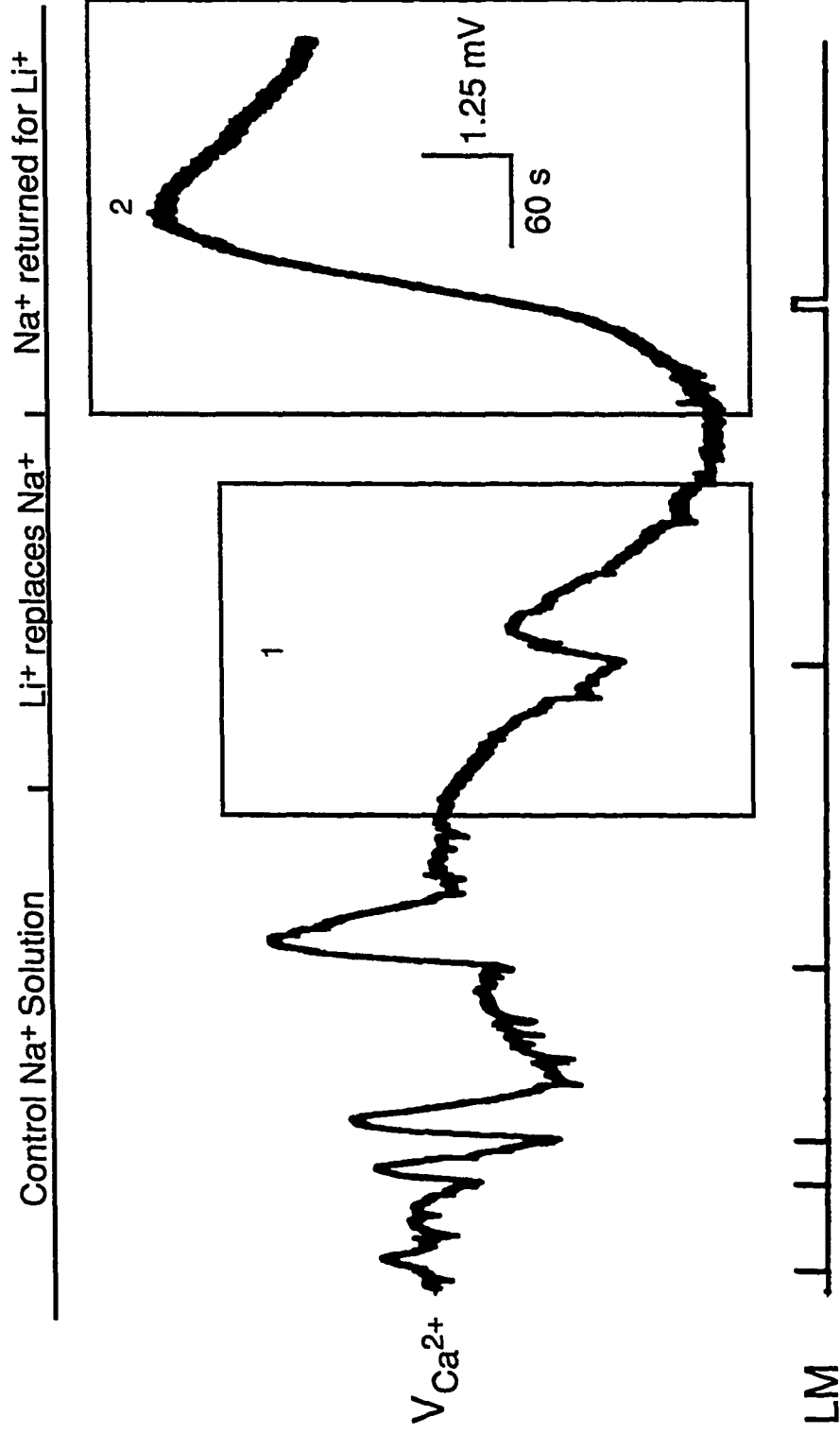


Fig. 16. Changes in  $V_{Ca^{2+}}$  evoked by Li<sup>+</sup> replacement of Na<sup>+</sup> and vis a' vis in the presence of IBMX

amplified the  $V_{Ca^{2+}}$  decline caused by stopping  $Na^+/K^+/Ca^{2+}$  exchange (compare box 1 of Fig. 16 to box 1 of Fig. 14). Stopping  $Na^+/K^+/Ca^{2+}$  exchange in the presence of IBMX decreased the  $V_{Ca^{2+}}$  photoresponse amplitude but increased its duration in the only photoresponse shown here. Note that the peak of the  $V_{Ca^{2+}}$  photoresponse again did not exceed the bath level. In other experiments, prolonged cessation of  $Na^+/K^+/Ca^{2+}$  exchange during IBMX superfusion eventually abolished the  $V_{Ca^{2+}}$  photoresponses.

Returning  $Na^+$  for  $Li^+$  in the superfusate dramatically increased  $V_{Ca^{2+}}$  (box 2), which transiently peaked at a level well above that of the bath. A 10-s light stimulus accelerated the  $V_{Ca^{2+}}$  increase after removal of IBMX. The  $V_{Ca^{2+}}$  level eventually returned to near its control value (not shown). Thus reactivating  $Na^+/K^+/Ca^{2+}$  exchange after loading the rods with  $Ca^{2+}$  gave the expected results:  $V_{Ca^{2+}}$  increased dramatically as a result of a large efflux of  $Ca^{2+}$  from the rods. This result can now be used to compare to the effects of colchicine applied and removed in the presence of IBMX.

#### 3.3.4. *The effects of colchicine on $V_{Ca^{2+}}$ .*

Now that the effects on  $V_{Ca^{2+}}$  of increasing rod  $Ca^{2+}$  permeability and of blocking  $Na^+/K^+/Ca^{2+}$  exchange are known, they can be compared to the effects of colchicine on  $V_{Ca^{2+}}$ . Figures 17-22 show the  $V_{Ca^{2+}}$  changes evoked by colchicine superfusion under various conditions. Figure 17 shows dark-adapted  $V_{Ca^{2+}}$ , dark-adapted  $V_m$ ,  $V_{Ca^{2+}}$  photoresponses and  $V_m$  photoresponses during simple colchicine superfusion and during superfusion with colchicine and IBMX. Colchicine superfusion increased dark-adapted  $V_{Ca^{2+}}$  and hyperpolarized rods (see box 1). Although the first  $V_{Ca^{2+}}$  photoresponse after the introduction of colchicine increased in duration, colchicine eventually abolished  $V_{Ca^{2+}}$  photoresponses and nearly abolished  $V_m$  photoresponses (see also Fig. 18). Adding IBMX to the superfusate reversed these effects; i.e., it decreased both  $V_{Ca^{2+}}$  and  $V_m$ , but increased both the  $V_{Ca^{2+}}$  photoresponses and the  $V_m$  photoresponses (box 2). When colchicine was then removed, but IBMX continued,  $V_{Ca^{2+}}$  again decreased while the  $V_{Ca^{2+}}$  photoresponse amplitudes became very large (Fig. 17B, box 3). Thus the effects of

**Figure 17.** *Effects of colchicine and colchicine + IBMX on  $V_{Ca^{2+}}$  and  $V_m$* 

Control superfusate and superfusates containing 10 mM colchicine and 10 mM colchicine + 500  $\mu$ M IBMX superfused the retina where indicated (solutions B1, B2 and B3 in Table 3). Periodic flashes of light (100-ms, 1/90 s, 26,000 quanta rod<sup>-1</sup> flash<sup>-1</sup>) assessed colchicine's effects on  $V_{Ca^{2+}}$  and  $V_m$  photoresponses.

**A.** Both  $V_{Ca^{2+}}$  and  $V_m$  were recorded for part of the record

**B.** A longer record of  $V_{Ca^{2+}}$  is shown. The intracellular electrode became dislodged during the later part of the record, and is therefore left out for clarity.

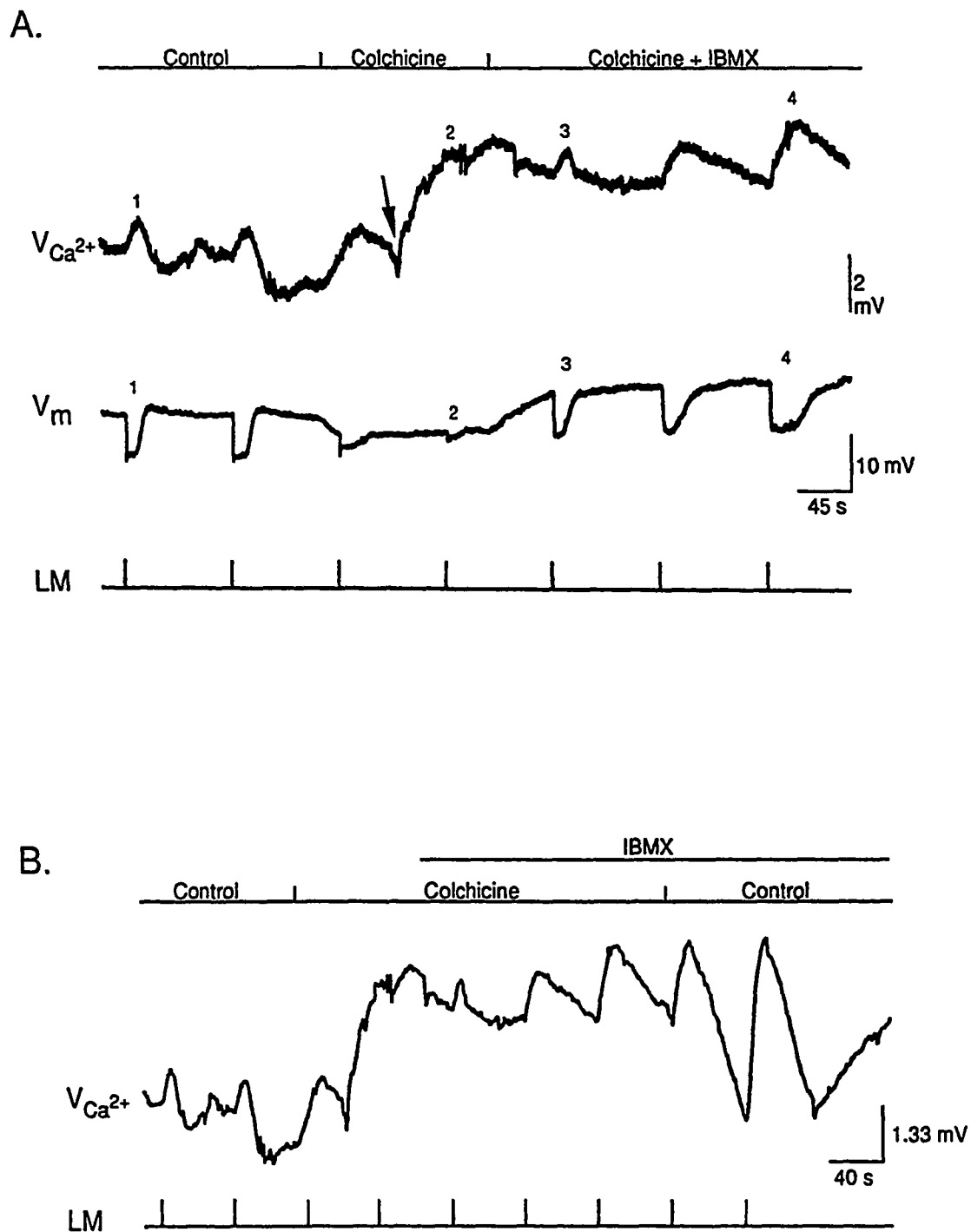


Fig. 17. Effects of colchicine and colchicine + IBMX on  $V_{Ca^{2+}}$  and  $V_m$ .

**Figure 18. Effects of colchicine on  $V_{Ca^{2+}}$  photoresponses.**

The  $V_m$  and  $V_{Ca^{2+}}$  photoresponses numbered in Fig. 17 are replotted on expanded time scales and decreased voltage scales:

- A.** control response.
- B.** response during 10 mM colchicine superfusion.
- C.** response shortly after adding 500  $\mu$ M IBMX to the superfusate (containing colchicine).
- D.** response after four-minute exposure to IBMX in the presence of colchicine.



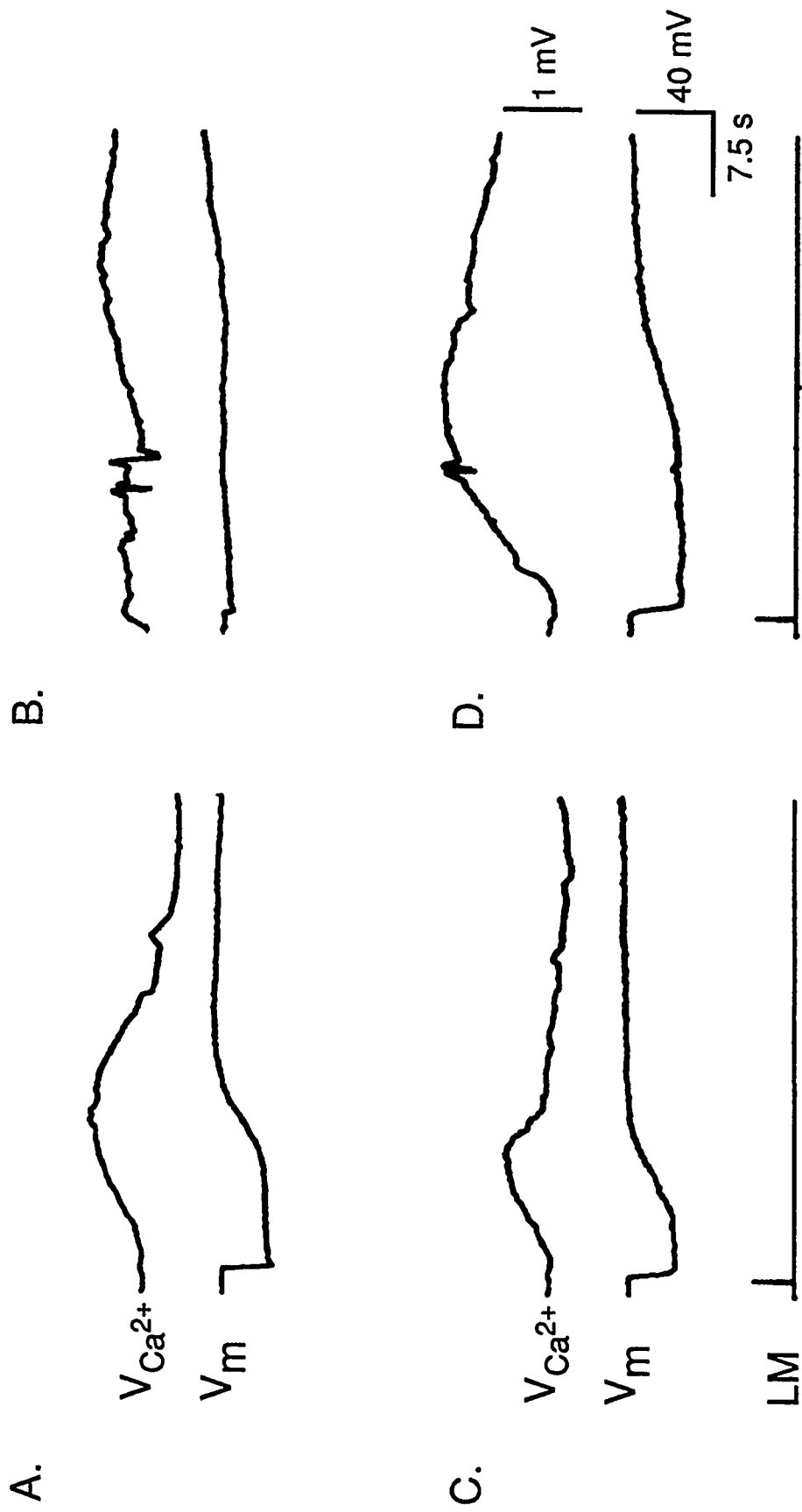


Fig. 18. Effects of colchicine on  $V_{Ca^{2+}}$  photoresponses.

colchicine and IBMX appear to be antagonistic.

Reversing the order of IBMX and colchicine application also demonstrates the antagonistic action of these two drugs, as shown in Fig. 19. Colchicine applied in the presence of IBMX again-increased  $V_{Ca^{2+}}$  and reduced the  $V_{Ca^{2+}}$  photoresponses (box 1), which had been substantially increased by the presence of IBMX.

These results, showing that colchicine and IBMX have antagonistic effects on  $V_{Ca^{2+}}$ , are inconsistent with the hypothesis that colchicine increases rod permeability to  $Ca^{2+}$ . Similarly, since blocking  $Na^+/K^+/Ca^{2+}$  exchange causes  $V_{Ca^{2+}}$  changes opposite to colchicine's, it also seems unlikely that colchicine actually blocks  $Na^+/K^+/Ca^{2+}$  exchange. Figure 19 contains further evidence against colchicine's blockade of  $Na^+/K^+/Ca^{2+}$  exchange. A previous experiment (shown in Fig. 16) demonstrated that blocking  $Na^+/K^+/Ca^{2+}$  exchange in the presence of IBMX loaded the photoreceptors with  $Ca^{2+}$ , which was rapidly extruded when the exchanger was reactivated, causing a large increase in  $V_{Ca^{2+}}$ . Applying colchicine and IBMX, however, did not appear to increase the  $Ca^{2+}$  load of the photoreceptors. Not only did applying colchicine in the presence of IBMX cause large increases in  $V_{Ca^{2+}}$ , rather than decreases (compare box 1 of Fig. 16 & 19), but removing colchicine from the superfusate caused  $V_{Ca^{2+}}$  to decrease, rather than to increase (compare box 2 of Fig. 16 & 19). Thus the inability of the combination of colchicine and IBMX to increase the  $Ca^{2+}$  load of rods is inconsistent with the hypothesis that colchicine blocks  $Na^+/K^+/Ca^{2+}$  exchange.

Colchicine, then, apparently neither increases  $Ca^{2+}$  influx into rods nor decreases  $Ca^{2+}$  efflux from rods, yet colchicine's ability to abolish  $V_{Ca^{2+}}$  photoresponses is still further evidence that colchicine blocks  $g_{h\nu}$ . Blocking  $Na^+/K^+/Ca^{2+}$  exchange, however, also abolished  $V_{Ca^{2+}}$  photoresponses, indicating again that increased  $[Ca^{2+}]_i$  has effects which resemble colchicine's.

The possibility remains that colchicine's effects could be mediated by a release of  $Ca^{2+}$  from internal stores. From Figs. 17 and 19, it is clear that the application of colchicine increases interphotoreceptor  $V_{Ca^{2+}}$ . This  $V_{Ca^{2+}}$  increase could reflect increased extrusion of

**Figure 19. Effects of colchicine on  $V_{Ca^{2+}}$  and  $V_{Ca^{2+}}$  photoresponses in the presence of IBMX.**

Solution compositions were the same as in Fig. 17, but the order of application was switched (solutions B1, B4, B3 and B2 in Table 3). Flashes of light (100-ms, 26,000 quanta rod<sup>-1</sup> flash<sup>-1</sup>) stimulated the retina where shown..

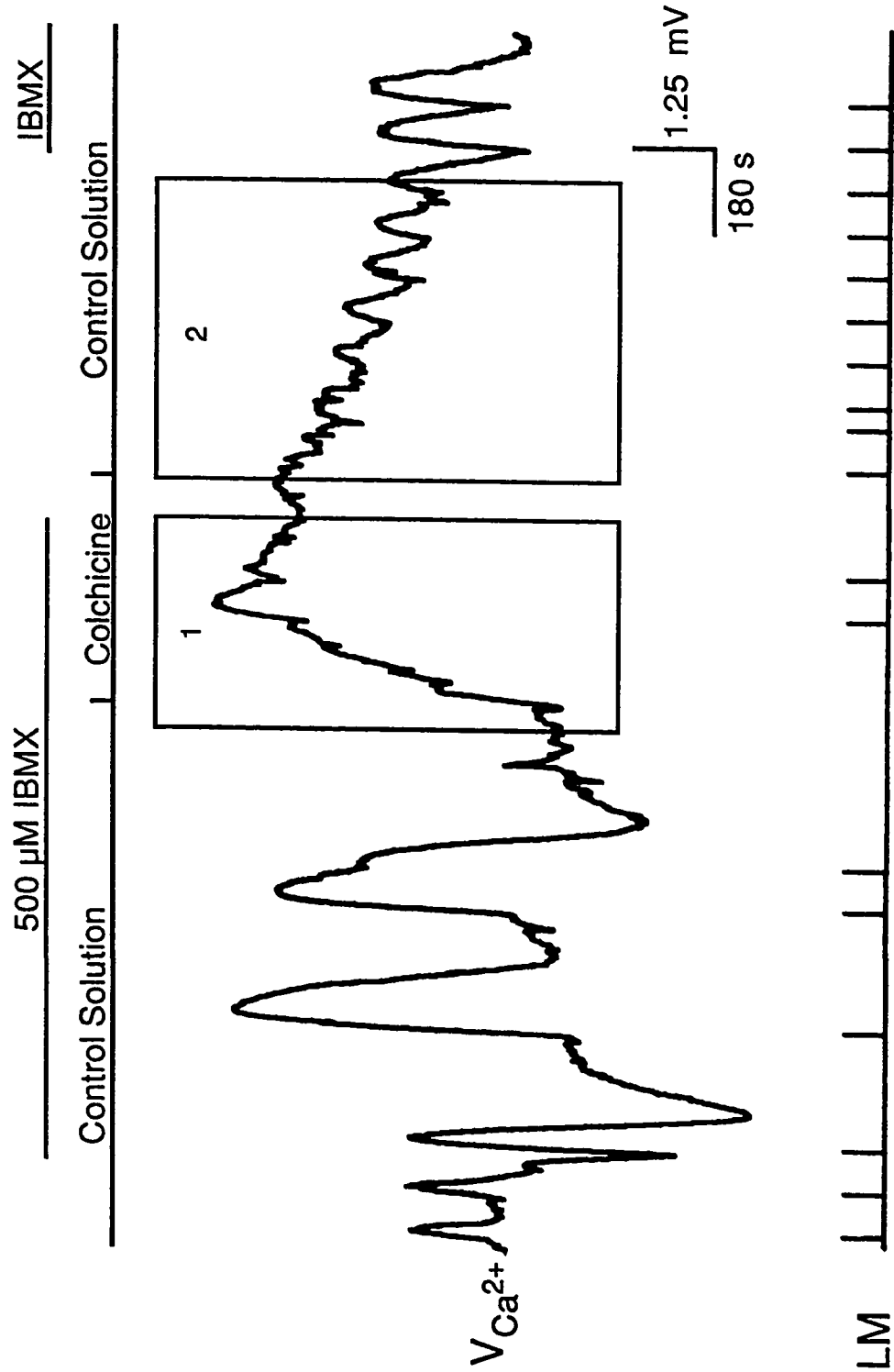


Fig. 19. Effects of colchicine on  $V_{Ca^{2+}}$  and  $V_{Ca^{2+}}$  photoresponses in the presence of IBMX.

$\text{Ca}^{2+}$  from rods, which results from an internal storage release of  $\text{Ca}^{2+}$ . Alternatively, the  $V_{\text{Ca}^{2+}}$  increase might simply reflect colchicine's closure of the  $g_{\text{hv}}$ .

In Figs. 17 and 19, the apparent increase in  $V_{\text{Ca}^{2+}}$  appeared to be larger and more prolonged than those induced by closing the  $g_{\text{hv}}$ , so it was hypothesized that colchicine releases  $\text{Ca}^{2+}$  from internal stores. The experiment shown in Fig. 20 tested this hypothesis. The  $V_{\text{Ca}^{2+}}$  response to a 2-min. step of light was compared to the  $V_{\text{Ca}^{2+}}$  response to a 2-min. light step of the same intensity which followed immediately after the initiation of colchicine superfusion. During a step of light,  $g_{\text{hv}}$  is closed and  $[\text{Ca}^{2+}]_i$  is pumped into the interphotoreceptor space, increasing  $V_{\text{Ca}^{2+}}$  (Figs. 11A & 20A). If colchicine releases  $\text{Ca}^{2+}$  from internal stores, applying colchicine just prior to a similar light step should cause an even greater increase in  $V_{\text{Ca}^{2+}}$ . Figure 20B shows the results obtained when 10 mM colchicine superfusion preceded a similar 2-min. light step. The  $V_{\text{Ca}^{2+}}$  and  $V_m$  records in Fig. 20B came from the same retina and cell as in Fig. 20A following a 3-minute intervening period of dark adaptation. There were marked differences between the  $V_{\text{Ca}^{2+}}$  waveforms obtained from the two light steps. In the control response in Fig. 20A,  $V_{\text{Ca}^{2+}}$  initially increased rapidly, peaked after about 20 s and then gradually declined to near bath level by the end of the 2-min. stimulus. In the test response shown in Fig. 20B, however,  $V_{\text{Ca}^{2+}}$  initially increased rapidly, and then continued to increase gradually throughout the period of light stimulation. The post stimulation portions of the  $V_{\text{Ca}^{2+}}$  waveforms also differed. The prominent post-illumination  $V_{\text{Ca}^{2+}}$  undershoot seen in the control waveform did not occur when the superfusate contained colchicine. Instead,  $V_{\text{Ca}^{2+}}$  remained elevated until control solution again superfused the retina (see also Fig. 20).

The two  $V_m$  waveforms also differed. The membrane voltage appeared to recover more quickly and completely in control solution than in solution containing colchicine. This result was unexpected, since colchicine did not clearly slow or reduce post-stimulus depolarization in previous experiments using higher concentrations of  $\text{Ca}^{2+}$  in the bath (see Fig. 6). This latter result was observed in four separate experiments, while the prolongation of the response in the lower  $[\text{Ca}^{2+}]$  bath was observed twice in the same retina.

**Figure 20.** Effects of colchicine on  $V_{Ca^{2+}}$  during constant illumination.

**A.** Control response. A two-minute step of light ( $26,000 \text{ quanta rod}^{-1} \text{ s}^{-1}$ ) stimulated the retina during superfusion with control solution (solution B1, Table 3). This is the same record shown in Fig. 10.

**B.** Responses during colchicine superfusion. A solution containing 10 mM colchicine began superfusing the retina about 10 s prior to light stimulation (solution B2, Table 3). The recordings are from the same retina and cell as in A. A five-minute dark period intervened between the two 2-minute steps of light.

**C.** A longer record of the experiment shown in B is replotted. This record illustrates the effects of colchicine on dark adaptation.

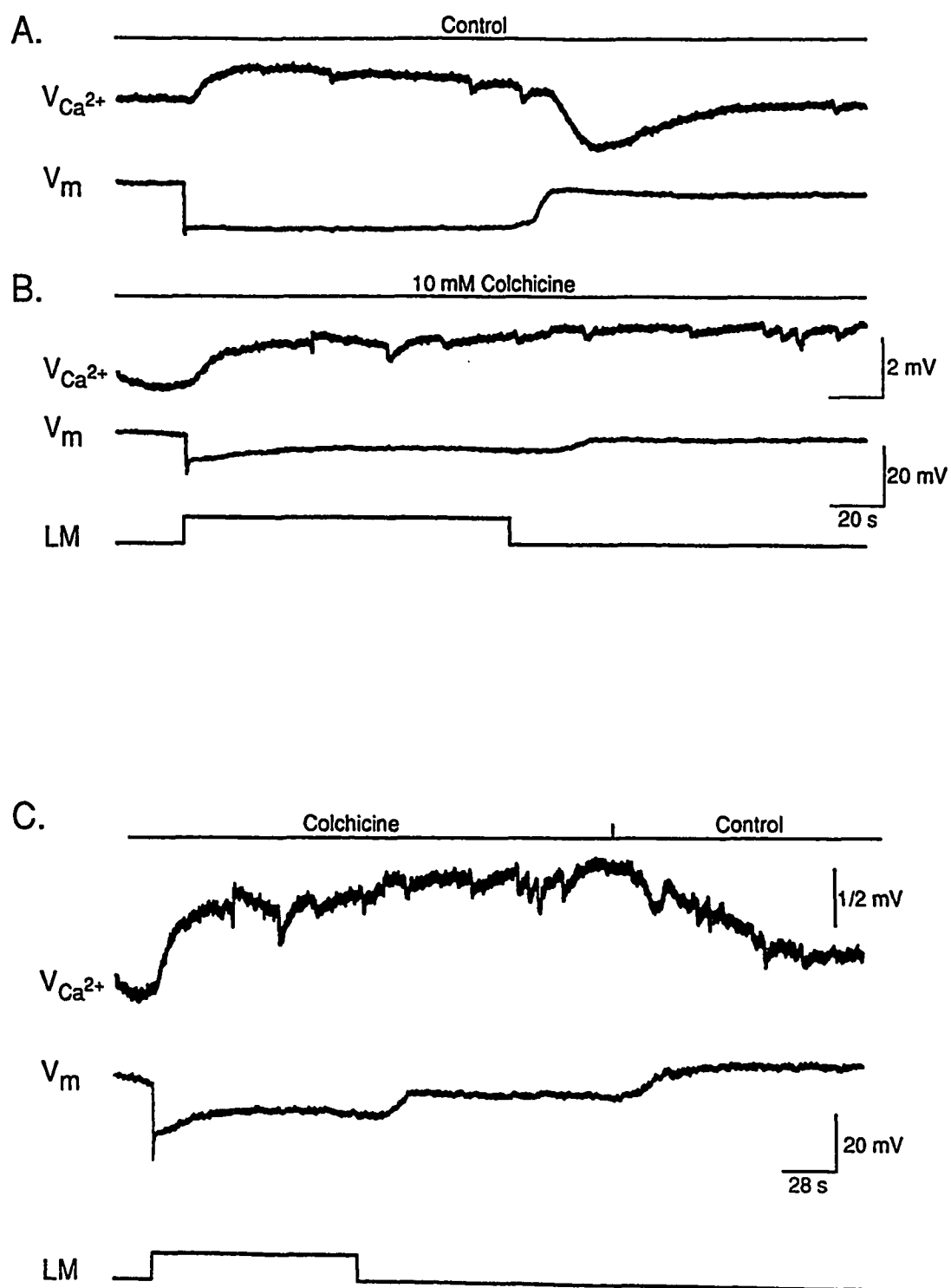


Fig. 20. The effects of colchicine on  $V_{Ca^{2+}}$  during constant illumination.

It is also interesting that even though  $V_m$  partially recovered after cessation of the light stimulus,  $V_{Ca^{2+}}$  continued to increase until colchicine was removed from the superfusate (see Fig. 20C), after which both  $V_m$  and  $V_{Ca^{2+}}$  returned to their dark-adapted values. The results from this experiment are consistent with the hypothesis that colchicine releases  $Ca^{2+}$  from internal stores, and will be discussed further in Chapter 4.

### **Section 3.4. *Effects of colchicine during alteration of $[Ca^{2+}]_o$ .***

Evidence has thus far been given to support the hypotheses that colchicine blocks the  $g_{hn}$  and that colchicine releases  $Ca^{2+}$  from internal stores. In addition, colchicine has thus far been shown to have effects on photoreceptor  $V_m$ ,  $V_m$  photoresponses and  $V_{Ca^{2+}}$  photoresponses that can be mimicked by increasing  $[Ca^{2+}]_i$ . It can be inferred from these results that some of colchicine's effects on  $g_{hv}$  could be mediated by the release of  $Ca^{2+}$  from internal stores, and this inference is now put forth as a hypothesis. Reversing the effects of colchicine by lowering  $[Ca^{2+}]_i$ , or conversely, reversing the effects of lowered  $[Ca^{2+}]_i$  with colchicine would provide supportive evidence for this hypothesis.

It is difficult, if not impossible to selectively lower  $[Ca^{2+}]_i$  in intact photoreceptors without altering other aspects of photoreceptor physiology. Common methods used to lower  $[Ca^{2+}]_i$  have side effects. These methods of lowering  $[Ca^{2+}]_i$  include lowering  $[Ca^{2+}]_o$  and injecting the  $Ca^{2+}$  chelator EGTA. The side effects caused by these two techniques are different. Lowering  $[Ca^{2+}]_o$  increases the unitary conductance of  $g_{hv}$  channels by reducing the inhibition of externally applied divalent cations (Matthews, 1986; Stern et al, 1986). This effect should depolarize rods but it is not as strong as the depolarizing effect resulting from the corresponding lowered  $[Ca^{2+}]_i$  (Detwiler, 1989). The binding of EGTA to  $Ca^{2+}$  releases protons, and could affect intracellular pH, which has been proposed to block  $g_{hv}$  (Pugh & Liebman, 1983). This effect is opposite, however, to the typical effects observed during EGTA injections (Oakley & Pinto, 1982). Furthermore, I have been unable to obtain any hyperpolarizing effects by injecting pure acetic acid, thus it seems unlikely that the protons released by EGTA significantly change intracellular pH. It seems likely, then, that



obtaining corroborative results from injecting EGTA and from lowering  $[Ca^{2+}]_o$  would indicate that lowering  $[Ca^{2+}]_i$  is responsible for the effects. The results from experiments using these two techniques to reverse colchicine's effects are shown below.

#### *3.4.1. Effects of lowering $[Ca^{2+}]_o$ in the presence of colchicine.*

Figure 21 shows the effects of lowering  $[Ca^{2+}]_o$  on rods that have been treated with colchicine. The initial application of colchicine (20 mM) hyperpolarized  $V_m$  as previously described. Lowering  $[Ca^{2+}]_o$  to  $10^{-6.4}$  M in the presence of colchicine depolarized  $V_m$ , which stabilized near its dark-adapted control value, as seen in Fig. 21A. Thus lowering  $[Ca^{2+}]_o$  reversed the colchicine-induced hyperpolarization. Lowering  $[Ca^{2+}]_o$  did not, however, reverse the effects of colchicine on the  $V_m$  photoresponses. Instead, the  $V_m$  photoresponses continued to decrease in amplitude and duration throughout colchicine superfusion. Removing colchicine allowed the  $V_m$  photoresponse amplitudes and durations to increase (see also Figs. 21B, 21C & 21D), as well as allowed further depolarization of  $V_m$ . Surprisingly, the time-to-peak of the  $V_m$  photoresponses remained delayed during low- $Ca^{2+}$  superfusion (Fig. 21D).

Figures 22A-22D show the results of a similar experiment, but emphasize the light adaptation-like effects of colchicine. Again, lowering  $[Ca^{2+}]_o$  reversed the effects of colchicine on  $V_m$ , but not on the  $V_m$  photoresponses. Control flashes again produced only greatly attenuated  $V_m$  photoresponses in the presence of colchicine and low- $[Ca^{2+}]_o$ . Brighter flashes, however, evoked responses with near-normal amplitudes (Fig. 22B) and with near-normal peak times (Fig. 22D), although the durations of the responses to the brighter flashes still remained shorter than the durations of control responses (Fig. 22C). The durations of the responses to the bright flashes lengthened after removing colchicine from the superfusate. In summary, lowering  $[Ca^{2+}]_o$  reversed colchicine's effects on  $V_m$  but not colchicine's effects on the recovery kinetics of the  $V_m$  photoresponses. It is interesting that the cells appeared to be desensitized when in the presence of colchicine and low- $[Ca^{2+}]_o$ . This effect will be discussed further in Chapter 4.

**Figure 21.** *The effects of lowering  $[Ca^{2+}]_o$  in the presence of colchicine.*

Solutions containing control (0.9 mM) and low ( $10^{-6.4}$  M)  $Ca^{2+}$  concentrations superfused the retina where indicated (solutions A1 and D3, Table 3). The solutions also contained 20 mM colchicine where indicated by the top bar (solutions A2a and D2a, Table 3). Flashes of light ( $100\text{-ms}$ ,  $260$  quanta  $\text{rod}^{-1}$  flash $^{-1}$ ) stimulated the retina where indicated. The different records in the figure are:

- A.** the superfusate record.
- B.** the numbered  $V_m$  photoresponses in A replotted on expanded time and voltage scales.
- C.** the normalized and superimposed responses shown in B.
- D.** the first 1.5 s of the records in C, replotted on further expanded time scales.

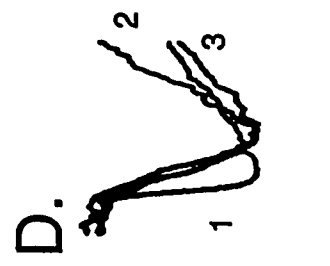
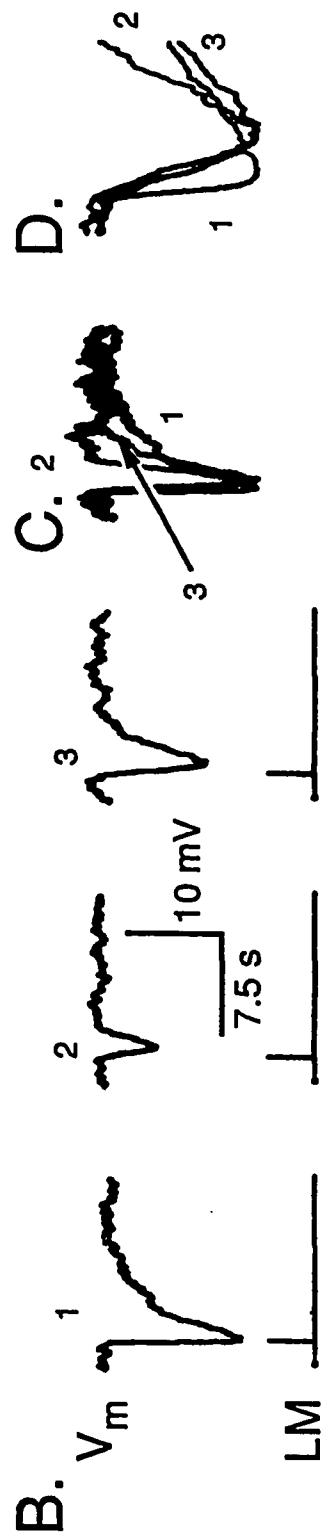
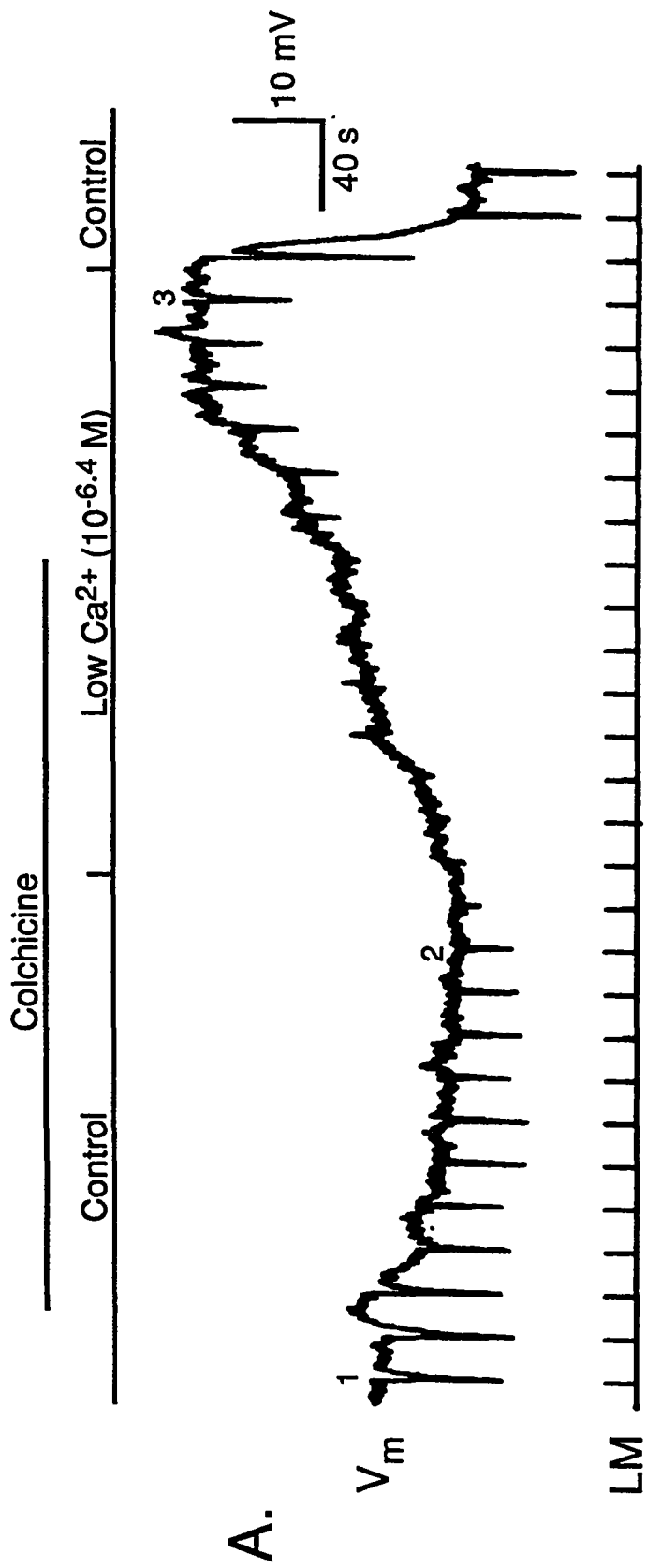


Fig. 21. The effects of lowering  $[Ca^{2+}]_o$  in the presence of colchicine.

**Figure 22.** *The adaptation-like effects of lowering  $[Ca^{2+}]_o$  in the presence of colchicine.* Solutions superfusing the retina were the same as those described in Fig. 21. Flashes of light (100-ms, 260 quanta rod<sup>-1</sup> flash<sup>-1</sup>) stimulated the retina where indicated by the short pulses in the LM record. Brighter flashes of similar duration but higher irradiance (100-ms, 2,600 quanta rod<sup>-1</sup> flash<sup>-1</sup>) stimulated the retina where indicated by the taller pulses in the LM record. A-D are the same as in Fig. 21.

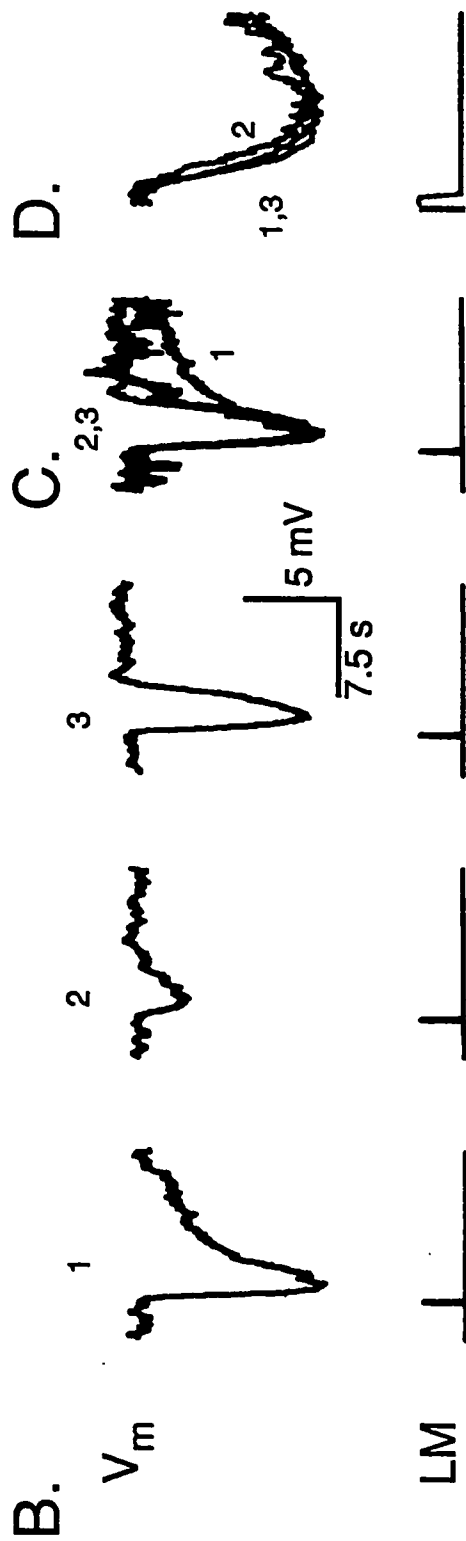
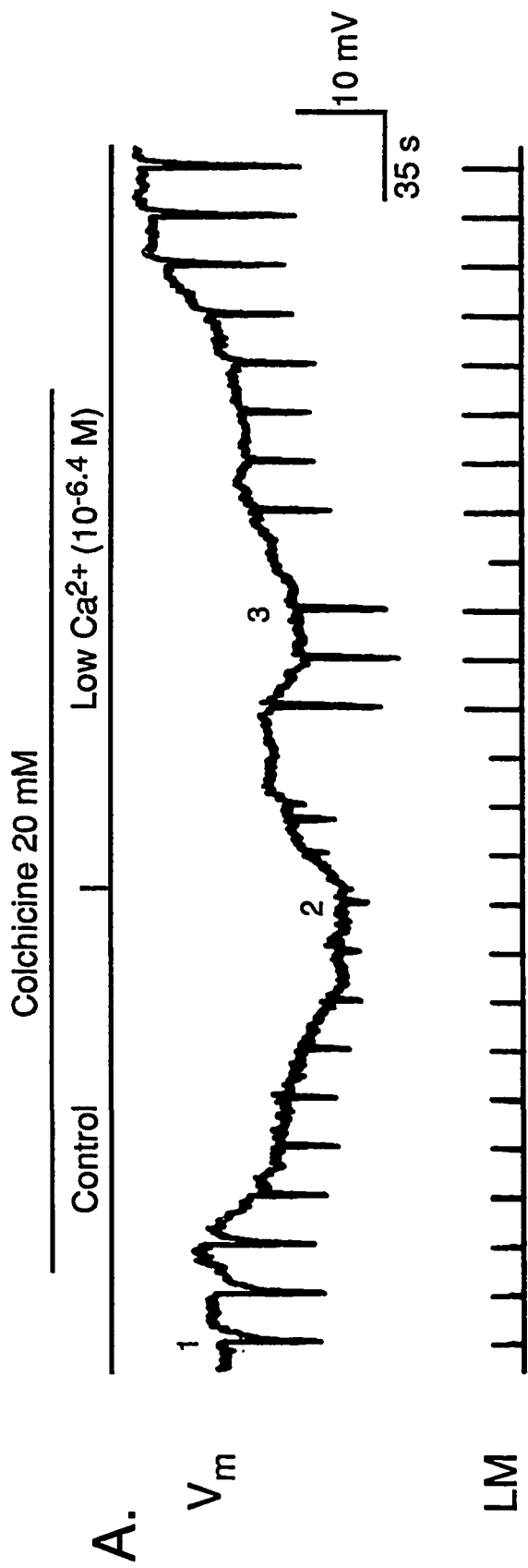


Fig. 22. The adaptation-like effects of lowering  $[\text{Ca}^{2+}]_o$  in the presence of colchicine.

### 3.4.2: Lowering $[Ca^{2+}]_i$ with EGTA injections reverses only some of colchicine's effects.

Pressure-injecting the specific  $Ca^{2+}$ -chelator, EGTA, into rods depolarizes them by increasing the light-sensitive current (Oakley & Pinto, 1982). This increase in the light-sensitive current presumably is mediated by lowered  $[Ca^{2+}]_i$ , as it depends only on the  $Ca^{2+}$ -chelating ability of EGTA (Oakley & Pinto, 1982). Therefore injecting EGTA provides a way to lower  $[Ca^{2+}]_i$  without altering external divalent ion concentrations. If colchicine's effects are mediated by  $Ca^{2+}$  released from internal stores, then it should be possible to reverse these effects by injecting EGTA. Likewise, injecting EGTA should reverse any effects mediated by increased  $[Ca^{2+}]_i$  in other treatments as well. The effects of increased  $[Ca^{2+}]_o$  on  $V_m$  and  $V_m$  photoresponses are at least partially mediated by increased  $[Ca^{2+}]_i$ . Therefore, the effects of increased  $[Ca^{2+}]_o$  on  $V_m$  and  $V_m$  photoresponses, too, should be at least partially reversed by injecting EGTA. The experiments described below compare the ability of injected EGTA to reverse colchicine's effects and to reverse the effects of increased  $[Ca^{2+}]_o$ . The latter is shown first.

Figure 23 shows a recording from a cell impaled during a period of high- $[Ca^{2+}]_o$  superfusion. The high  $[Ca^{2+}]_o$  (6x normal  $[Ca^{2+}]_o$ ) hyperpolarized the cell, and attenuated the  $V_m$  photoresponses. Injecting EGTA depolarized the rod, reversing the hyperpolarizing effect of increased  $[Ca^{2+}]_o$ . Injecting EGTA reversed the effects of high- $[Ca^{2+}]_o$  on  $V_m$  photoresponses as well, as shown in 23B, where the  $V_m$  photoresponses numbered 1\*, 2\* and 3\* in 23A are replotted on expanded time and voltage scales. The amplitude and duration of the  $V_m$  photoresponse during EGTA injection (2\*) compared more favorably with the amplitude and duration of the  $V_m$  photoresponses during superfusion with control solution (3\*), than with the  $V_m$  photoresponses during superfusion with high- $[Ca^{2+}]_o$  without injecting EGTA (1\*). This result is consistent with EGTA reversing the effects of increased  $[Ca^{2+}]_i$  on  $V_m$  photoresponses.

It now remains to be determined if injections of EGTA can reverse the effects of colchicine on  $V_m$  and  $V_m$  photoresponses. Following the experiment just described (see Fig. 23), control superfusate bathed the retina for several minutes, which allowed the

**Figure 23.** *The effects of EGTA injections on  $V_m$  and  $V_m$  photoresponses during superfusion with increased  $[Ca^{2+}]_o$ .*

**A.** The records are from a cell impaled during superfusion with high- $[Ca^{2+}]_o$  solution. The bar above the record indicates the period of high- $[Ca^{2+}]_o$  superfusion (6x control, solution C2, Table 3), and where the switch to control solution (solution A1, Table 3) occurred. Light flashes (100-ms, 653 quanta rod<sup>-1</sup> flash<sup>-1</sup>) stimulated the retina where indicated. A 10-s pressure pulse injected EGTA where indicated by the first pulse in the record labeled P. Shorter pulses (1-s) injected EGTA periodically (1/min.) after the switch to control superfusate. The last injection shown on this record had a 2-s pulse duration.

**B.** The starred numbered light responses shown in A are replotted on expanded time and voltage scales.

**C.** The numbered EGTA-evoked depolarizations shown in A are replotted on expanded time and voltage scales.

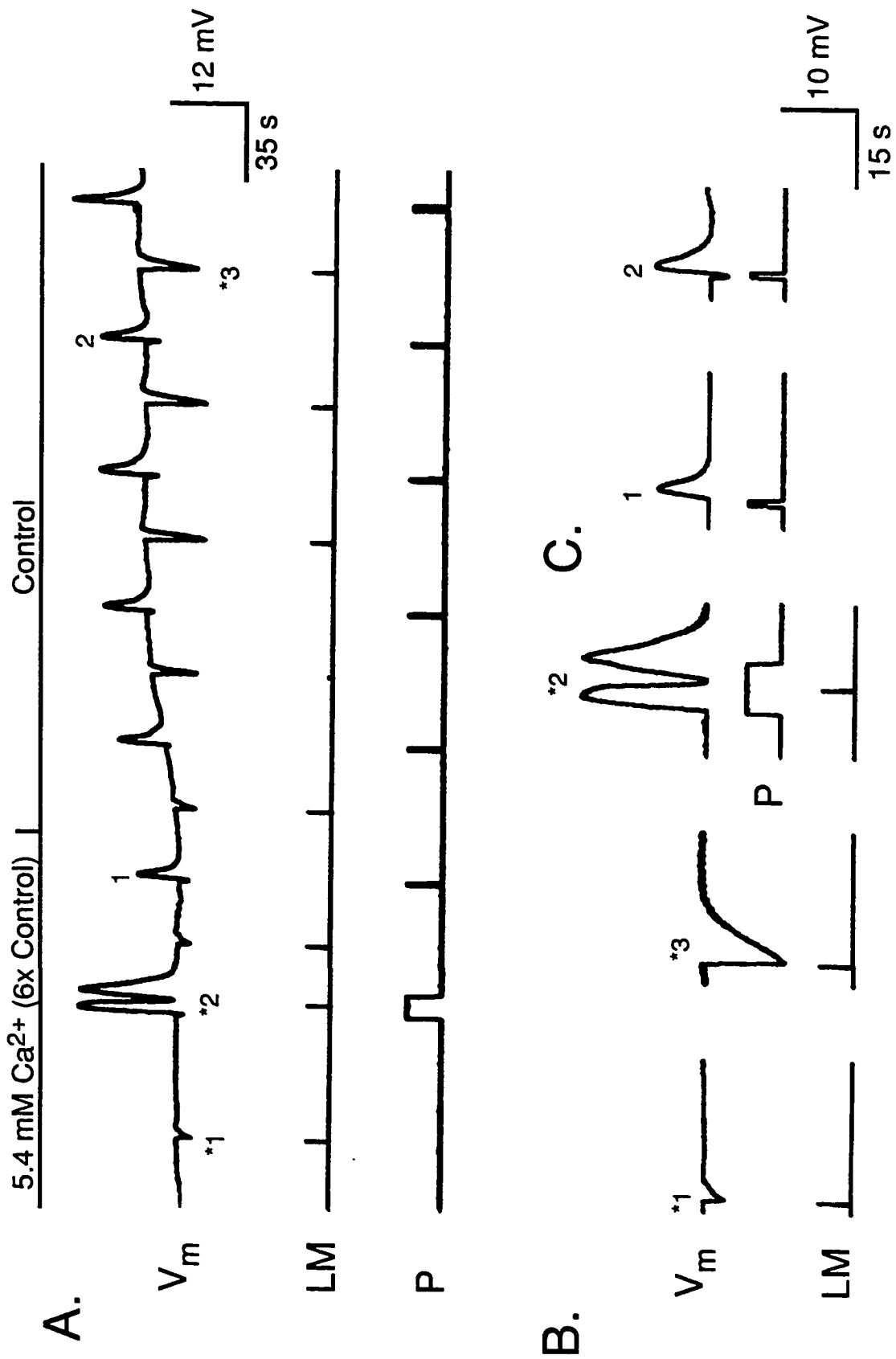


Fig. 23. The effects of EGTA injections on  $V_m$  and  $V_m$  photoresponses during superfusion with increased  $[Ca^{2+}]_0$ .



amplitude and durations of the  $V_m$  photoresponses to increase and to stabilize. Next, a solution containing 20 mM colchicine superfused the retina. Figure 24 shows the effects of EGTA injections during this period of colchicine superfusion. Long pulses of EGTA (20-s) depolarized the rod in the presence of colchicine, indicating that the hyperpolarizing effects of colchicine on  $V_m$  could be reversed by lowering  $[Ca^{2+}]_i$ . Light flashes presented to the retina during the depolarized time periods, however, did not regain their control amplitudes or durations, as they did when EGTA was injected during high  $[Ca^{2+}]_o$  superfusion (compare  $V_m$  photoresponses in Fig. 23B and 24B). Instead, the responses remained attenuated.

Lowering  $[Ca^{2+}]_i$  by either injecting EGTA or lowering  $[Ca^{2+}]_o$  reversed the hyperpolarizing effects of colchicine (i.e., it reversed the colchicine-evoked decrease in  $g_{hv}$ ), but failed to reverse the adaptation-like effects of colchicine.

### *3.4.3. Colchicine and elevated $[Ca^{2+}]_o$ have different effects on the kinetics of EGTA-evoked depolarizations.*

In addition to the effects described in Section 3.4.2, both elevated  $[Ca^{2+}]_o$  and colchicine had pronounced effects on the durations and amplitudes of the EGTA-evoked depolarizations. Figure 25 shows the effects of elevated  $[Ca^{2+}]_o$  on the kinetics of EGTA-evoked depolarizations. In Fig. 25A, six 1-s pulses of pressure injected EGTA during superfusion with 5.4 mM  $[Ca^{2+}]_o$  (6x normal). A 5-s injection pulse and a 10-s injection pulse then followed. The injections of EGTA depolarized the rod during both the control period and during the period of high- $[Ca^{2+}]_o$  superfusion. The amplitudes and recovery rates of the responses, however, increased during high- $[Ca^{2+}]_o$  superfusion. This is seen more clearly in Fig. 25B, which shows the individual EGTA-evoked depolarizations numbered 2 and 6 in Fig. 25A, replotted on expanded time and voltage scales. These two waveforms compare the voltage responses from 1-s pressure pulses during superfusion with control solution and with high- $[Ca^{2+}]_o$  solution.

The third waveform shown in Fig. 25B resulted from 10-s injection of EGTA, and

**Figure 24.** *The effects of EGTA injections on  $V_m$  and  $V_m$  photoresponses during superfusion with colchicine.*

**A.** The records are from the same cell as Fig. 23. Control solution (solution A1, Table 3) and a similar solution containing 20 mM colchicine (solution A2a, Table 3) superfused the retina where indicated. Light flashes identical to those in Fig. 22 (100-ms, 653 quanta rod<sup>-1</sup> flash<sup>-1</sup>) stimulated the retina where indicated. A 2-s pressure pulse injected EGTA where indicated by the first pulse in the record labeled P. Long pulses (20-s) injected EGTA during superfusion with colchicine.

**B.** Brief records containing the numbered light responses shown in A are replotted on expanded time and voltage scales.

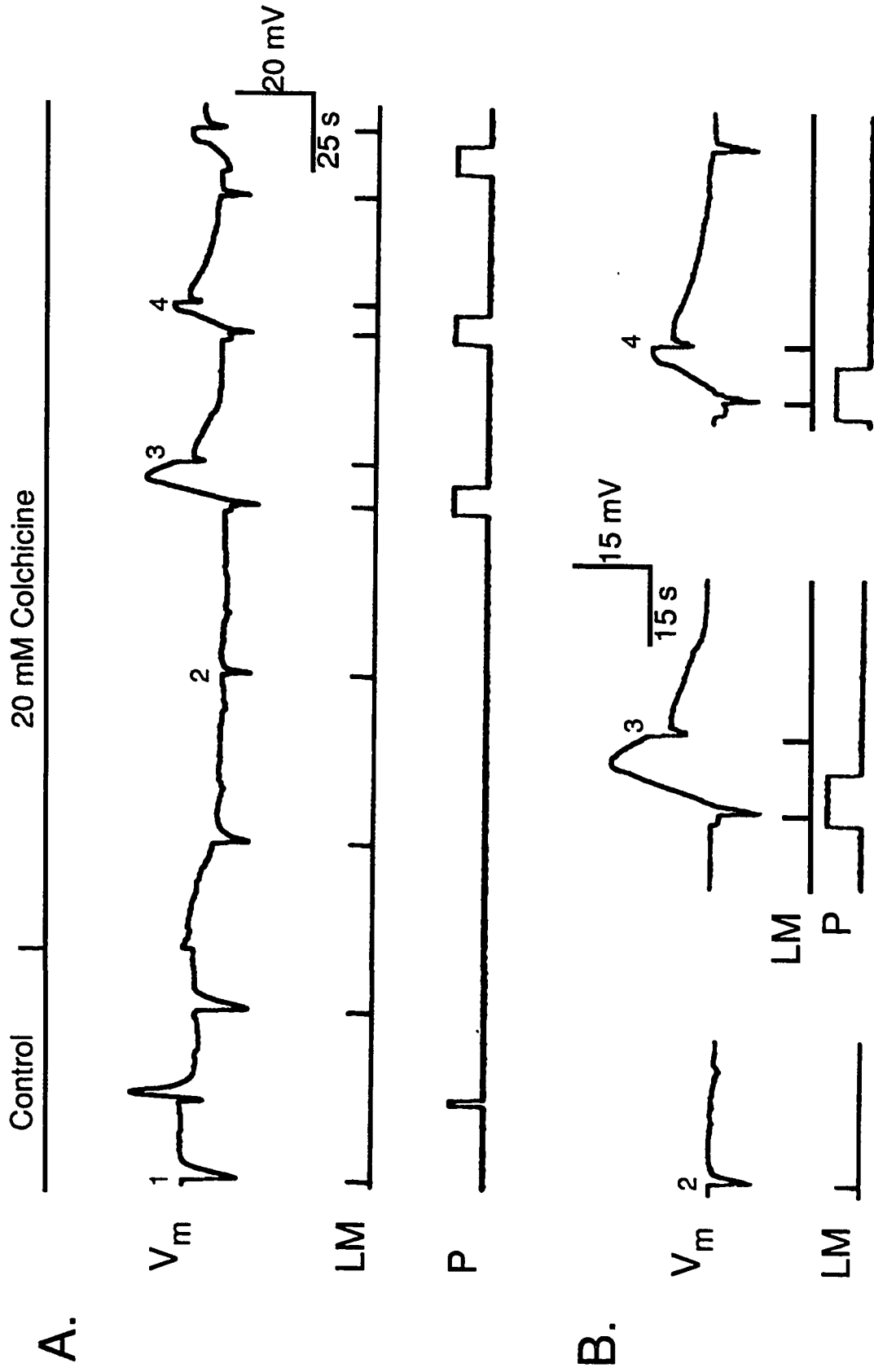


Fig. 24. The effects of EGTA injections on  $V_m$  and  $V_m$  photoresponses during superfusion with colchicine.

**Figure 25.** *The effects of increased  $[Ca^{2+}]_0$  on the kinetics of EGTA-evoked depolarizations.*

- A.** A high- $[Ca^{2+}]_0$  solution (6x control, solution C2, Table 3) superfused the retina where indicated by the bar above the  $V_m$  record. Light flashes (100-ms, 653 quanta rod<sup>-1</sup> flash<sup>-1</sup>) stimulated the retina where indicated by the pulse markers in the LM record. Six, 1-s pressure pulses, followed by a 5-s and a 10-s pressure pulse injected EGTA periodically (1 pulse/min.) where indicated by the pulse markers in the record labeled P.
- B.** Records containing the EGTA-evoked depolarizations numbered 2, 6 and 8 in A are replotted on expanded time and voltage scales. A light flash stimulated the retina during the recovery of the EGTA-evoked depolarization numbered 8, and is indicated by the pulse marker in the record labeled LM.

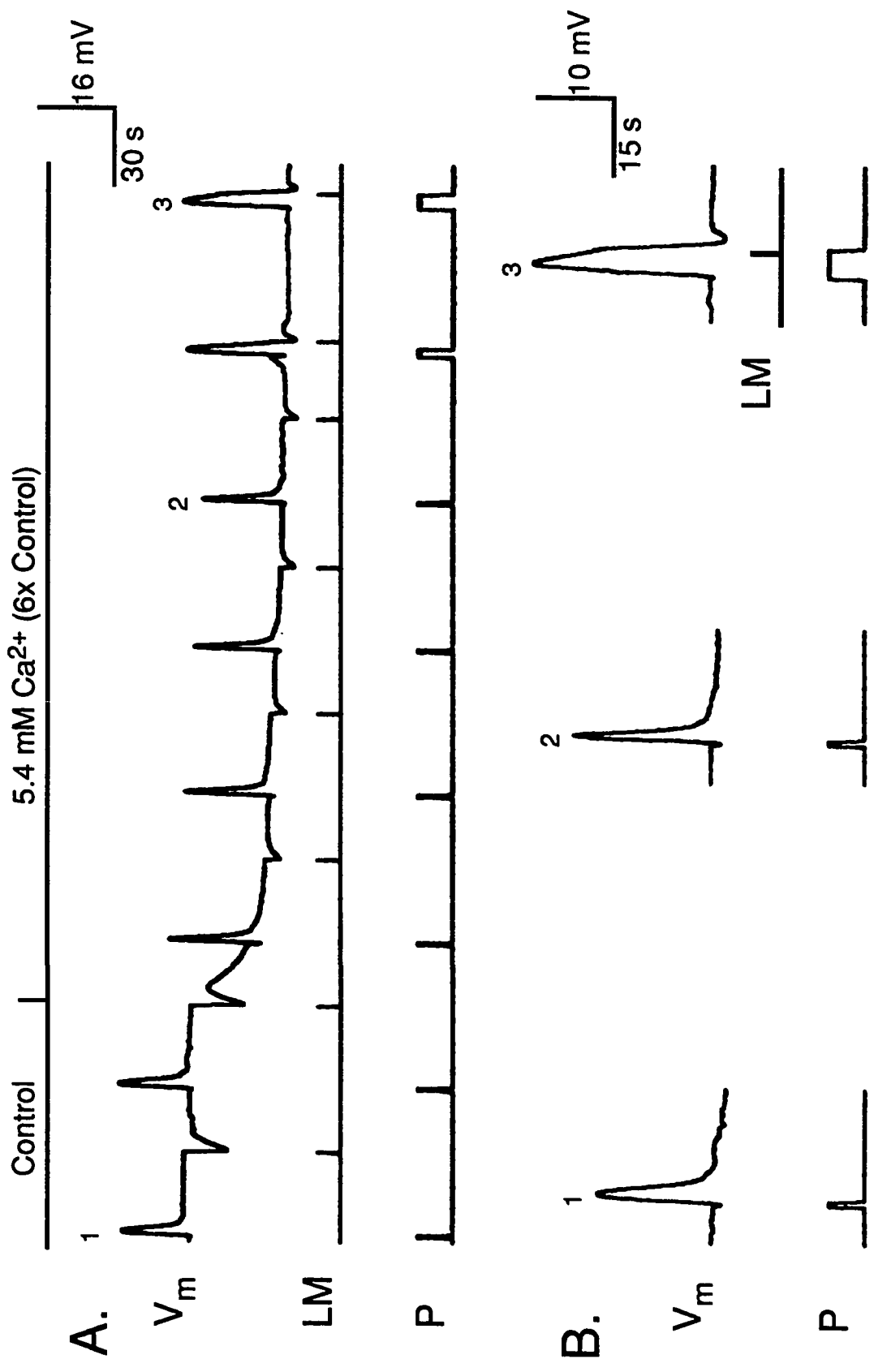


Fig. 25. The effects of increased  $[Ca^{2+}]_o$  on the kinetics of EGTA-evoked depolarizations.

thus had a longer duration. A flash of light stimulated the retina during the EGTA-evoked depolarization and promptly increased the  $V_m$  recovery rate. This light-evoked increase in the recovery rate is consistent with the recovery phase being controlled by declining cGMP levels, which in turn are controlled by  $[Ca^{2+}]_i$  in the dark but by phosphodiesterase activity during photostimulation. The factors contributing to the recovery rate and to the risetime of EGTA-evoked depolarizations will be discussed further in Chapter 4.

The results shown in Fig. 26 and Fig. 27 demonstrate the effects of colchicine on EGTA-evoked depolarizations. These separate experiments compared the the amplitudes and kinetics of the EGTA-evoked depolarizations in control and in colchicine-containing superfusates. Figure 26A shows that colchicine markedly reduced the amplitudes of the EGTA-evoked depolarizations (see also Fig. 26B) and slowed both the peak-times and the recovery rates of the EGTA-evoked depolarizations as well (see Fig. 26C). After returning to control solution, the amplitudes and kinetics of the EGTA-evoked depolarizations returned to control values, possibly before the kinetics of the  $V_m$  photoresponses returned to control values.

Figure 27 shows the results from a similar experiment that demonstrates other interesting aspects of colchicine's effects on the kinetics of EGTA-evoked depolarizations. The waveforms in Fig. 27B and Fig. 27C, taken from the first half of Fig. 27A, show that the peak-times of the EGTA-evoked depolarizations increased as the time of exposure to colchicine increased, but the waveform recovery rate transiently increased before it eventually decreased. The transient increase in the recovery rate correlated with a transient increase in the response amplitude. Figure 27A shows, however, that the absolute value of  $V_m$  reached during response #2 was not as great as the absolute value of  $V_m$  reached during response #1. The increase in the response amplitude, then, reflects the decreased  $V_m$  at the initiation of the injection and not an increase in the maximum  $V_m$  attained. The second half of the trace in Fig. 27A, and Figs. 27D and 27E show that the decreased recovery rate induced by colchicine again increased when control solution again superfused the retina. Finally, Fig. 27F shows that colchicine affected the recovery

**Figure 26.** *The effects of colchicine on the kinetics of EGTA-evoked depolarizations.*

- A.** A solution containing 10 mM colchicine (Solution A2, Table 3) superfused the retina where indicated. Light flashes (100-ms, 653 quanta rod<sup>-1</sup> flash<sup>-1</sup>) stimulated the retina where indicated by the short pulse markers in the P, LM record. Brief, 1-s pressure pulses injected EGTA periodically (1 pulse/min.) where indicated by the tall pulse markers in the P, LM record.
- B.** Records containing the EGTA-evoked depolarizations numbered in A are replotted on expanded time scales.
- C.** The EGTA-evoked depolarizations shown in B are replotted superimposed.

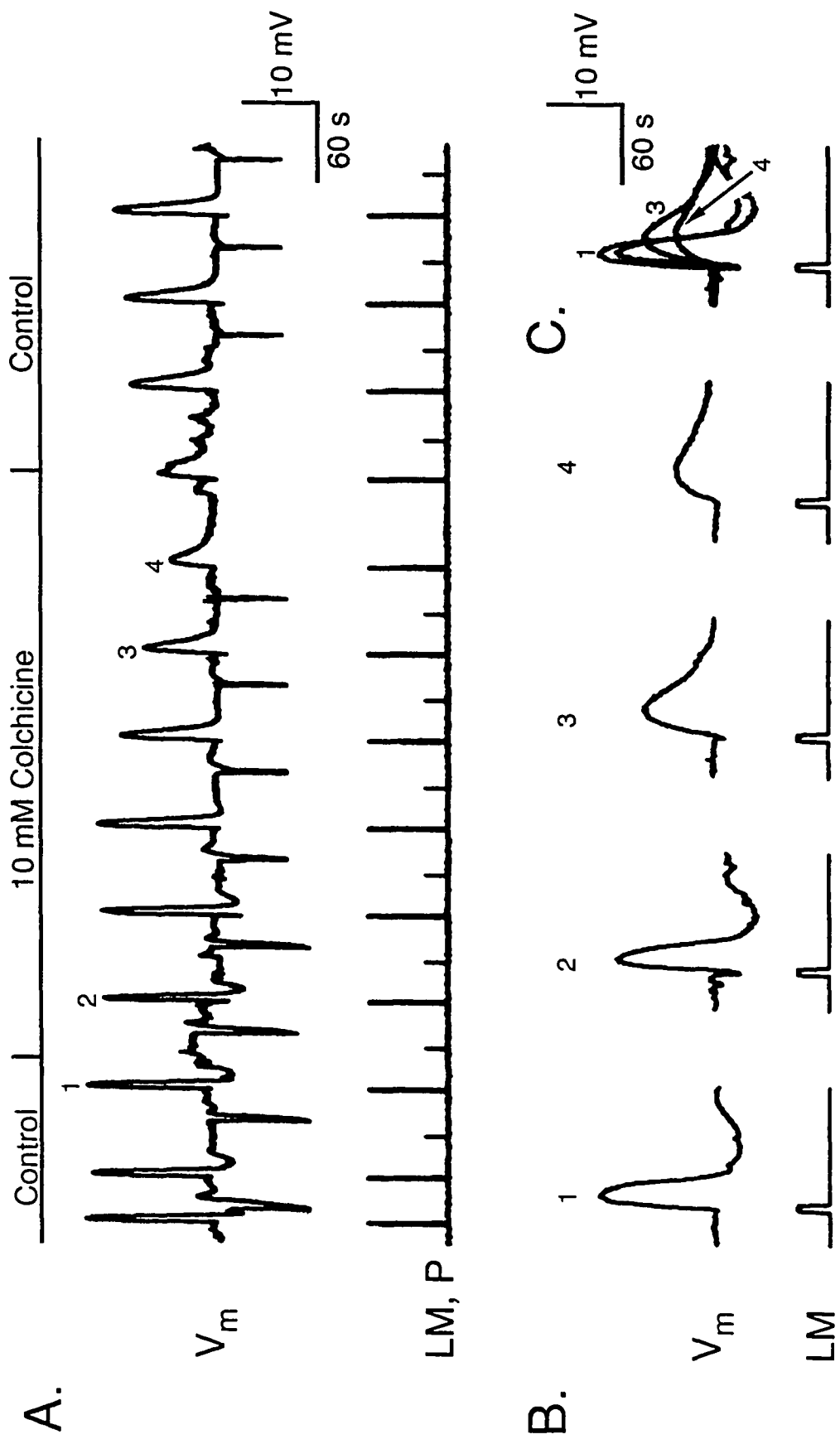


Fig. 26. The effects of colchicine on the kinetics of EGTA-evoked depolarizations.



**Figure 27.** *Further effects of colchicine on the kinetics of EGTA-evoked depolarizations.*

**A.** The two parts of the record are from different rods impaled during the same experiment. A second rod was impaled during the period of colchicine superfusion to assure that the effects attributed to colchicine were not due to loading the cell with the  $\text{Ca}^{2+}$  buffer. About 30 s elapsed between the recordings shown for the two cells. The solution containing 10 mM colchicine (Solution A2, Table 3) superfused the retina where indicated. Periodic light flashes (100-ms, 653 quanta rod<sup>-1</sup> flash<sup>-1</sup>, 1 flash/ min.) stimulated the retina where indicated by the pulse markers in the LM record. Note that the two halves of the record are plotted with different time scales. Brief, 1-s pressure pulses injected EGTA periodically (1 pulse/min.) where indicated by the narrow pulse markers in the P record. A longer pulse (3 s) provided a saturating response during colchicine superfusion where indicated by the wider pulse in the P record.

**B.** Records containing the EGTA-evoked depolarizations numbered 1, 2 and 3 in the 1st half-record in A are replotted on expanded time scales.

**C.** The EGTA-evoked depolarizations shown in B are replotted superimposed.

**D.** Records containing the EGTA-evoked depolarizations numbered 6 and 7 in the 2nd half-record in A are replotted on expanded time scales.

**E.** The EGTA-evoked depolarizations shown in D are replotted superimposed.

**F.** Records containing the EGTA-evoked depolarizations numbered 5 and 7 in the 2nd half-record in A are replotted on expanded time and voltage scales.

**G.** The recovery portions of the EGTA-evoked depolarizations numbered 5 and 7 in the 2nd half-record of A are replotted superimposed, but with the y coordinates of the records matched to the same absolute voltage.

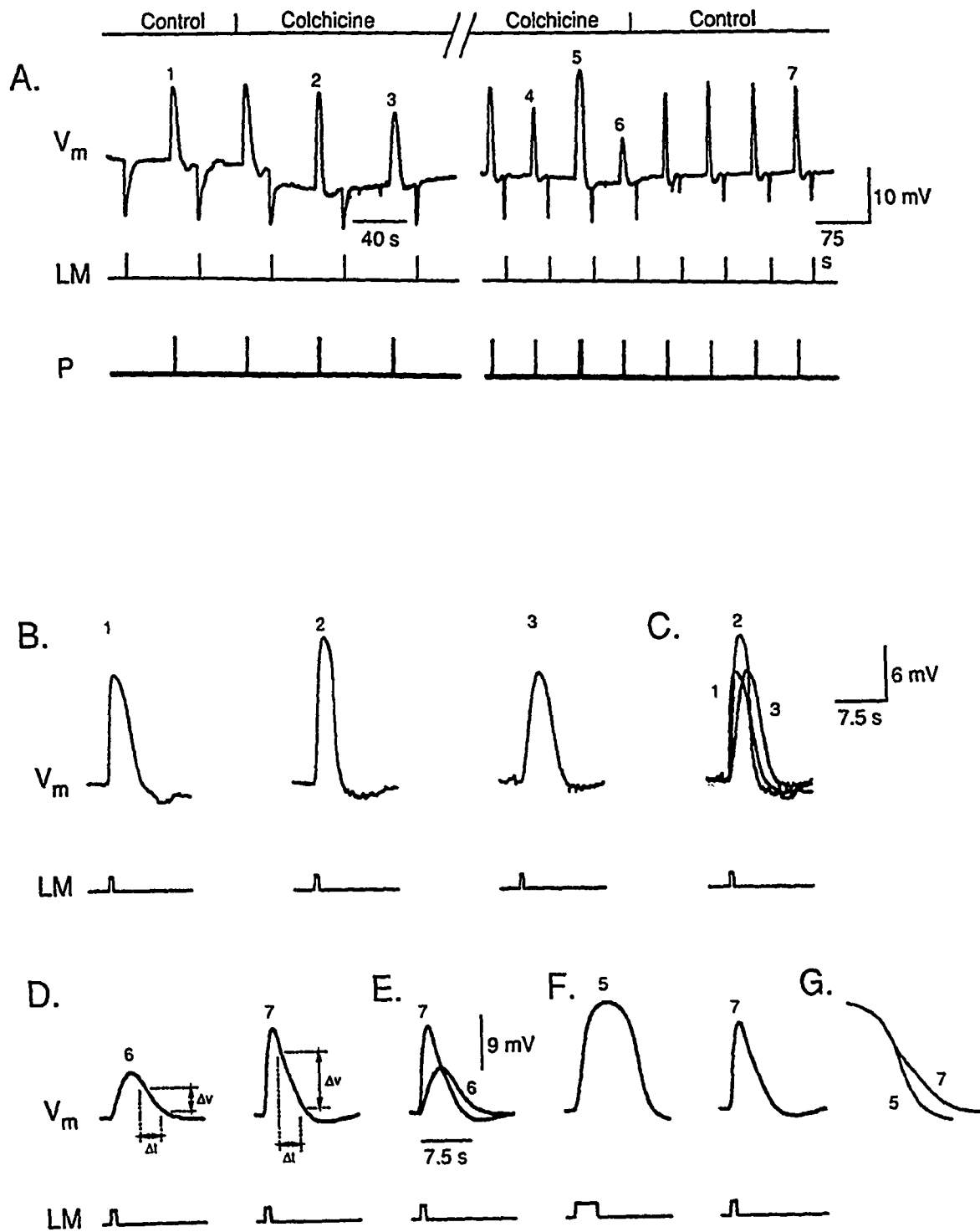


Fig. 27. Further effects of colchicine on the kinetics of EGTA-evoked depolarizations.

rate of the EGTA-evoked depolarizations independently of voltage. The declining portion of the records numbered 4, 5 and 7 in Fig. 27A are replotted superimposed, but with the values of the absolute voltages matched on the ordinate.

In summary, colchicine altered the effects of EGTA on the rod photoreceptors in the following ways: it reduced the amplitude of the EGTA-evoked depolarization; it increased the time-to peak of the EGTA-evoked depolarization; and it decreased the recovery rate of EGTA-evoked depolarization in a voltage-independent manner. These results are consistent with the hypothesis that colchicine affects  $\text{Ca}^{2+}$  regulation in rods, since colchicine alters the extent and timecourse by which a perturbation in  $[\text{Ca}^{2+}]_i$  changes rod voltage. A more extensive analysis of the effects of colchicine on the kinetics of the EGTA-evoked depolarizations is deferred to Chapter 4.

### **Section 3.5. Colchicine reverses many effects of low $[\text{Ca}^{2+}]_o$ .**

The above experiments demonstrated that colchicine increases the net efflux of  $\text{Ca}^{2+}$  from rods, that lowering  $[\text{Ca}^{2+}]_i$  reverses the effects of colchicine on rod  $V_m$  and that colchicine inhibits the ability of EGTA injections to depolarize rods. These results are consistent with colchicine releasing  $\text{Ca}^{2+}$  from internal stores and with the resulting increased  $[\text{Ca}^{2+}]_i$  inhibiting  $g_{hv}$ . If colchicine indeed releases  $\text{Ca}^{2+}$  from internal stores, then colchicine should temporarily reverse the effects of lowering  $[\text{Ca}^{2+}]_i$  in rods. The effects of lowering  $[\text{Ca}^{2+}]_o$  on rod  $V_m$  and on rod  $V_m$  photoresponses have been well-studied (Bastian & Fain, 1979, 1982a, b). Figure 28 illustrates important aspects of these effects. When  $[\text{Ca}^{2+}]_o$  is lowered, the  $V_m$  photoresponse amplitudes first increase dramatically. Over time, however, two different effects can occur, depending on the  $[\text{Ca}^{2+}]_o$  concentration. When  $[\text{Ca}^{2+}]_o$  remains above  $\sim 10^{-6.5}$  M, the  $V_m$  photoresponse amplitudes remain large. When  $[\text{Ca}^{2+}]_o$  is maintained below this, as in the experiments shown in Fig. 28, a phenomena known as desensitization occurs (Bastian & Fain, 1979). In general terms, desensitization is the requirement for greater stimulation to produce the same response in any type of neuron. In rods, this results in stimuli of equal strength (flashes of

**Figure 28.** *Effects of lowering  $[Ca^{2+}]_o$  below  $10^{-7}$  M on  $V_m$  and  $V_m$  photoresponses.*

A. Low- $[Ca^{2+}]_o$  solution ( $10^{-7.1}$  M, solution D7, Table 3) superfused the retina where indicated. Periodic flashes of light (100-ms, 1 flash/min., 1300 quanta rod<sup>-1</sup> flash<sup>-1</sup>) stimulated the retina where indicated by pulses in the LM record.

B. The  $V_m$  photoresponses numbered in A are replotted on expanded time and voltage scales.

C. The responses in B are superimposed.

D. The responses in B are normalized and superimposed.

E. Low- $[Ca^{2+}]_o$  ( $10^{-8}$  M solution D10, Table 3) superfused the retina in a separate experiment. Periodic flashes of light (100-ms flashes, 1 /min., 260 quanta rod<sup>-1</sup> flash<sup>-1</sup>) stimulated the retina where indicated by the short pulses in the LM record. A brighter flash (100-ms, 26,000 quanta rod<sup>-1</sup> flash<sup>-1</sup>) stimulated the retina where indicated by the tall pulse.

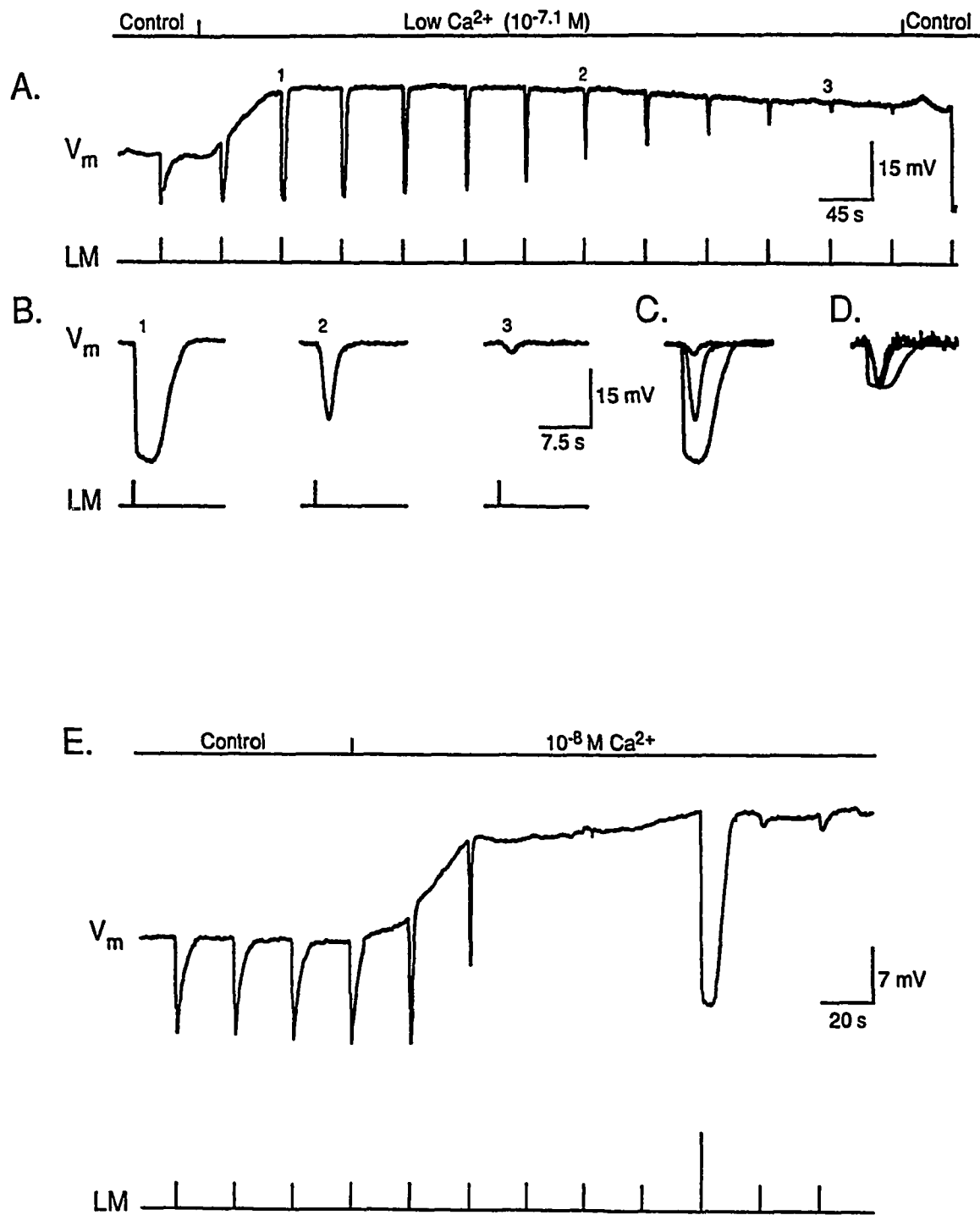


Fig 28. Effects of lowering  $[Ca^{2+}]_0$  below  $10^{-7}$  M on  $V_m$  and  $V_m$  photoresponses.

equal irradiance) producing  $V_m$  photoresponses with decreased amplitudes, decreased hyperpolarization rates and decreased durations when  $[Ca^{2+}]_o$  falls below  $\sim 10^{-7}$  M (see Fig. 28A). The changes in the responses when  $[Ca^{2+}]_o$  is lowered, then, mimic the changes in the responses when flash irradiance is decreased at constant  $[Ca^{2+}]_o$  (compare the first three responses of Fig. 1 to the responses in Fig. 28A). Furthermore, increasing flash irradiance reverses the effects of desensitization, i.e., the amplitudes, durations and hyperpolarization rates of the  $V_m$  photoresponses increase (Bastian & Fain, 1979). Figure 28E illustrates that a brighter flash can reverse the desensitizing effects of lowered  $[Ca^{2+}]_o$ .

Figures 29 -31 show effects of colchicine on desensitization. Figures 29A-D are controls showing the effects of lowering  $[Ca^{2+}]_o$  to  $10^{-7.1}$  M, while Figs. 29E-H show the results of lowering  $[Ca^{2+}]_o$  to  $10^{-7.1}$  M when the superfusate includes 10 mM colchicine. Comparing Figs. 29A-D and Figs. 29E-H shows that colchicine slowed the rate of desensitization. Furthermore, colchicine also affected the time required for rod hyperpolarization upon returning the superfusate to control solution. The rod hyperpolarized much more quickly in the presence of colchicine. This result is consistent with colchicine counteracting the effects of lowering  $[Ca^{2+}]_o$ , perhaps by releasing  $Ca^{2+}$  from internal stores.

In addition to inhibiting low- $[Ca^{2+}]_o$  induced desensitization, Fig. 30 shows that colchicine can reverse it. In this experiment, low- $[Ca^{2+}]_o$  solution containing 20 mM colchicine superfused the retina following desensitization. Adding colchicine to the superfusate partially and transiently reversed the desensitization, i.e., it increased the  $V_m$  photoresponse amplitudes. During the partial reversal of desensitization, colchicine simultaneously hyperpolarized  $V_m$  a few mV. These important results are consistent with colchicine having  $Ca^{2+}$ -like effects, and, in particular, releasing  $Ca^{2+}$  from internal stores. A thorough discussion of these results and the phenomena of low- $[Ca^{2+}]_o$  evoked desensitization is deferred to Chapter 4.

During low- $[Ca^{2+}]_o$  evoked desensitization, then, colchicine improved the light responsiveness of the photoreceptors, whereas in all previous experiments, colchicine only

**Figure 29.** *Effects of colchicine on low- $\text{Ca}^{2+}$  evoked desensitization.*

**A-D.** These records are the same as A-D in Fig. 27.

**E.** This record is from the same rod as in A-D. The second half of a split sample of the low- $[\text{Ca}^{2+}]_o$  solution described in Fig. 28, but additionally containing 10 mM colchicine (solution D8, Table 3), superfused the retina where indicated. A five minute recovery period of superfusion with control solution (0.9 M  $\text{Ca}^{2+}$ , solution A1, Table 3) intervened between the two low- $[\text{Ca}^{2+}]_o$  treatments. Light flashes of the same irradiance, duration and periodicity as in A-D stimulated the retina where indicated by the pulse markers in the LM record.

**F-H.** same as B-D in Fig. 27 and above.

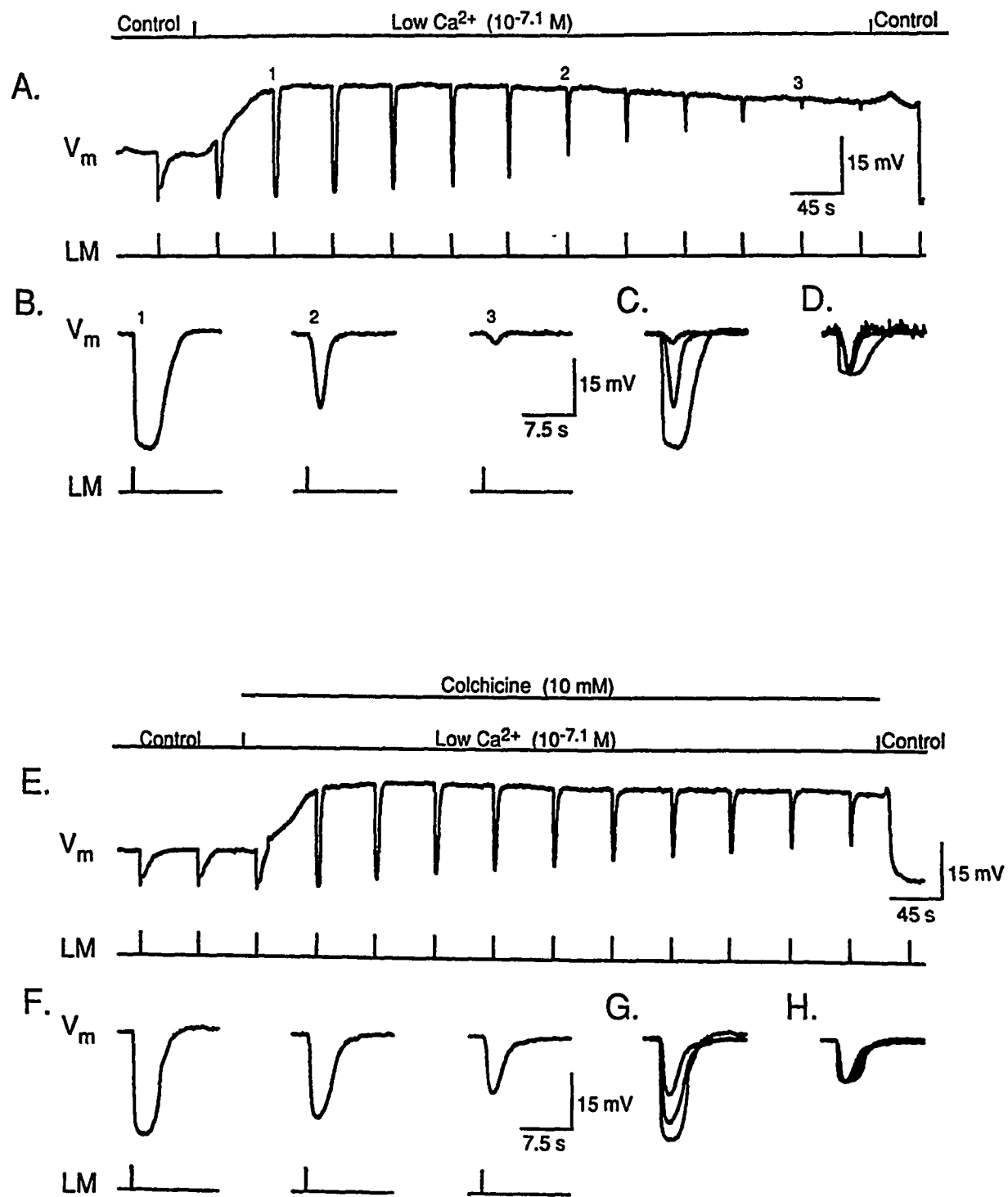


Fig 29. Effects of colchicine on low- $\text{Ca}^{2+}$  evoked desensitization.



**Figure 30.** *Effects of colchicine on rods desensitized with low  $\text{Ca}^{2+}$ .*

- A.** A solution containing low  $\text{Ca}^{2+}$  and  $\text{Cl}^-$  ( $10^{-8}$  M  $\text{Ca}^{2+}$ , solution D10, Table 3), superfused the retina where indicated. The second half of a split sample of the low- $\text{Ca}^{2+}$  solution that additionally contained 20 mM colchicine, and that was osmotically adjusted by reducing  $\text{NaCH}_3\text{SO}_3$ , superfused the retina during the period indicated by the top bar (solution D11, Table 3). Periodic light flashes (100-ms, 2 flashes/ min., 260 quanta  $\text{rod}^{-1}$  flash $^{-1}$ ) stimulated the retina where indicated.
- B.** This record contains the initial 1.5 s of the numbered  $V_m$  photoresponses from A replotted on expanded time and reduced voltage scales.
- C.** The responses shown in B are replotted superimposed.

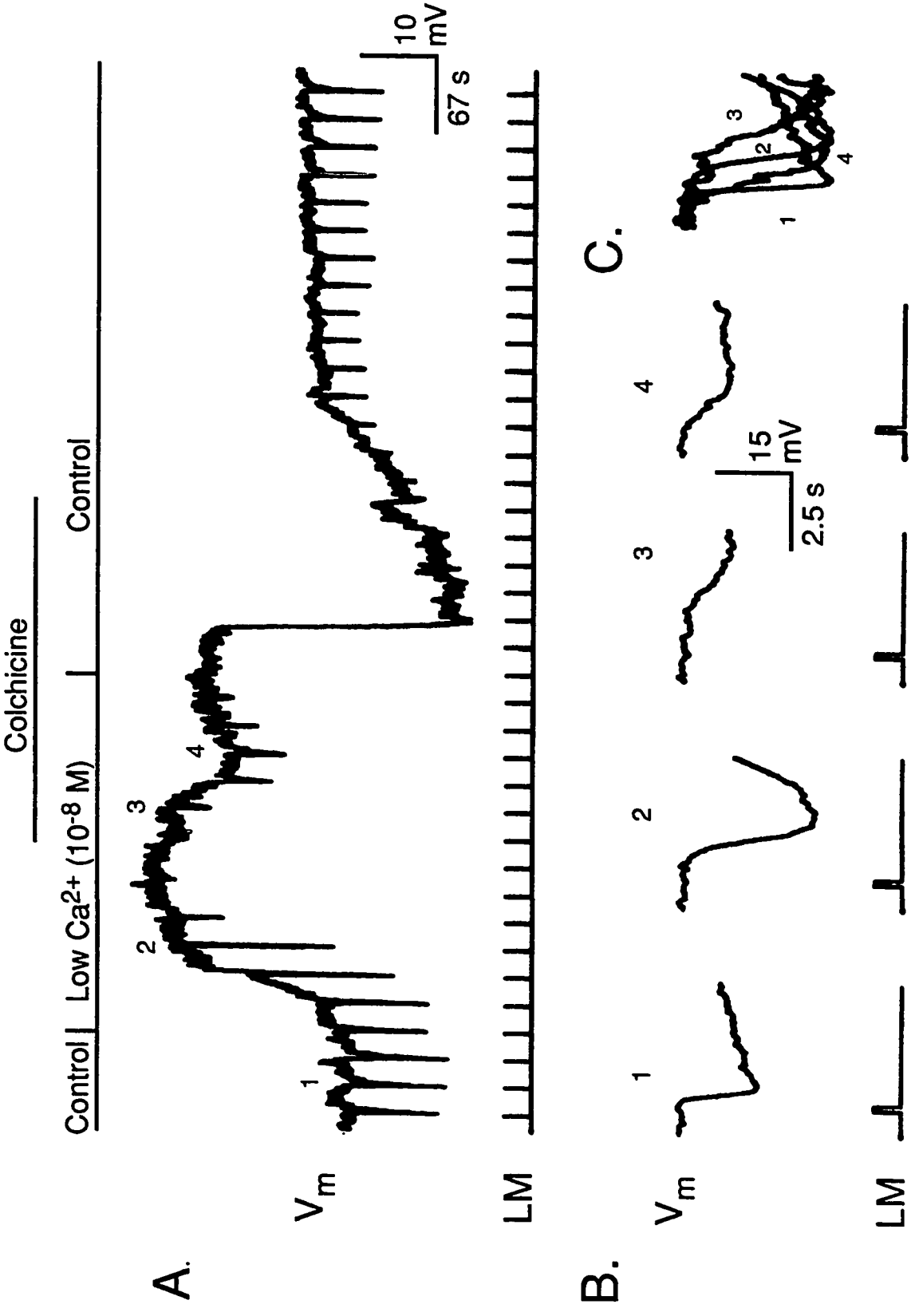


Fig. 30. Effects of colchicine on rods desensitized with low  $Ca^{2+}$ .

inhibited the light responsiveness of photoreceptors. It is important to note, however, that the  $V_m$  photoresponses never regained their control amplitudes or durations, and that eventually, the photoreceptors still lost their light responsiveness in the presence of colchicine and low- $[Ca^{2+}]_o$ . Furthermore, when  $Ca^{2+}$  was added back to the superfusate in the presence of colchicine, the cell hyperpolarized after ~40 s, but rod photoresponsiveness did not return until colchicine was removed from the superfusate. Similar results to these occurred repetitively in other experiments.

Finally, an experiment in which colchicine superfused the retina after lowering  $[Ca^{2+}]_o$  to only to  $10^{-6.4}$  M, to avoid desensitization is shown in Fig. 31. In this experiment, colchicine again reversed the depolarizing effects of lowered  $[Ca^{2+}]_o$ . Furthermore, colchicine decreased the  $V_m$  photoresponse amplitudes and durations. Returning the superfusate to the low- $[Ca^{2+}]_o$  control solution then reversed colchicine's effects, i.e.,  $V_m$  and  $V_m$  photoresponses approached pre-colchicine, low- $[Ca^{2+}]_o$  controls.

In summary, colchicine both slows and reverses low- $[Ca^{2+}]_o$  induced desensitization. Colchicine also reverses the non-desensitized, low- $[Ca^{2+}]_o$  evoked changes in  $V_m$  and  $V_m$  photoresponses produced when  $[Ca^{2+}]_o$  is lowered to concentrations that remain above  $10^{-6.5}$  M.

### **Section 3.6. Effects of colchicine on $V_m$ and $V_m$ photoresponses during increased $[Ca^{2+}]_i$**

If colchicine's effects result from increased  $[Ca^{2+}]_i$ , then other treatments that increase  $[Ca^{2+}]_i$  should enhance the effects of colchicine. Since lowering  $[Ca^{2+}]_o$  reversed many of colchicine's effects and *vis a vis*, raising  $[Ca^{2+}]_o$  should enhance the effects of colchicine. Moreover, raising  $[Ca^{2+}]_o$  is a plausible means of increasing  $[Ca^{2+}]_i$ .

Figure 32 shows the effects superfusing 10 mM colchicine in the presence of  $[Ca^{2+}]_o$  raised to 5x the typical control value. Figure 32A shows that the hyperpolarizing effects of colchicine and increased  $[Ca^{2+}]_i$  were additive, i.e., the addition of colchicine further hyperpolarized the rod when added to the high- $[Ca^{2+}]_o$  superfusate. The  $V_m$

**Figure 31.** *The effects of colchicine during superfusion with non-desensitizing low  $\text{Ca}^{2+}$  concentrations.*

- A.** A solution containing low  $\text{Ca}^{2+}$  and  $\text{Cl}^-$  ( $10^{-6}$ - $6.4$  M  $\text{Ca}^{2+}$ , solution D4a, Table 3), superfused the retina where indicated. The second half of a split sample of the low- $\text{Ca}^{2+}$  solution that additionally contained 20 mM colchicine, and that was osmotically adjusted by reducing  $\text{NaCH}_3\text{SO}_3$ , superfused the retina during the period indicated by the top bar. Periodic light flashes (100-ms, 2 flashes/ min., 260 quanta  $\text{rod}^{-1}$  flash $^{-1}$ ) stimulated the retina where indicated.
- B.** The numbered  $V_m$  photoresponses in A are replotted on an expanded time and a reduced voltage scale.
- C.** This record contains the initial 1.5 s of the numbered  $V_m$  photoresponses from B replotted superimposed.

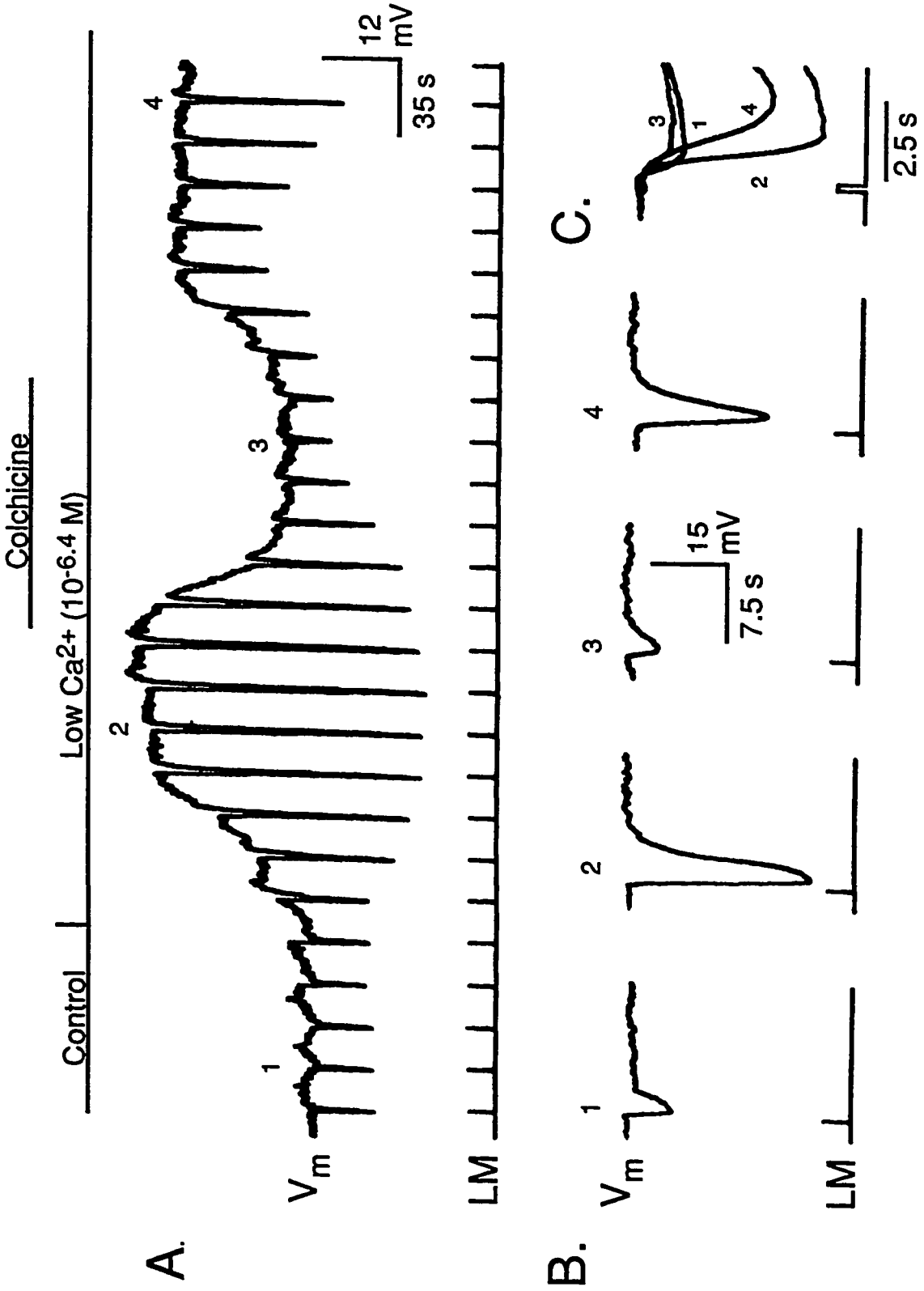


Fig. 31. The effects of colchicine during superfusion with non-desensitizing low- $Ca^{2+}$  concentrations.

**Figure 32.** *Effects of colchicine on  $V_m$  and  $V_m$  photoresponses during superfusion with increased  $[Ca^{2+}]_o$ .*

**A.** A solution containing 5x control  $[Ca^{2+}]$  (solution C1, Table 3) superfused the retina where indicated. A similar solution that also contained 10 mM colchicine superfused the retina where indicated by the top bar above the  $V_m$  record. Flashes of light (100-ms, 260 quanta rod<sup>-1</sup> flash<sup>-1</sup>) stimulated the retina where indicated by the pulse markers in the LM record.

**B.** The photoresponse waveforms numbered in A are replotted on expanded time and voltage scales.

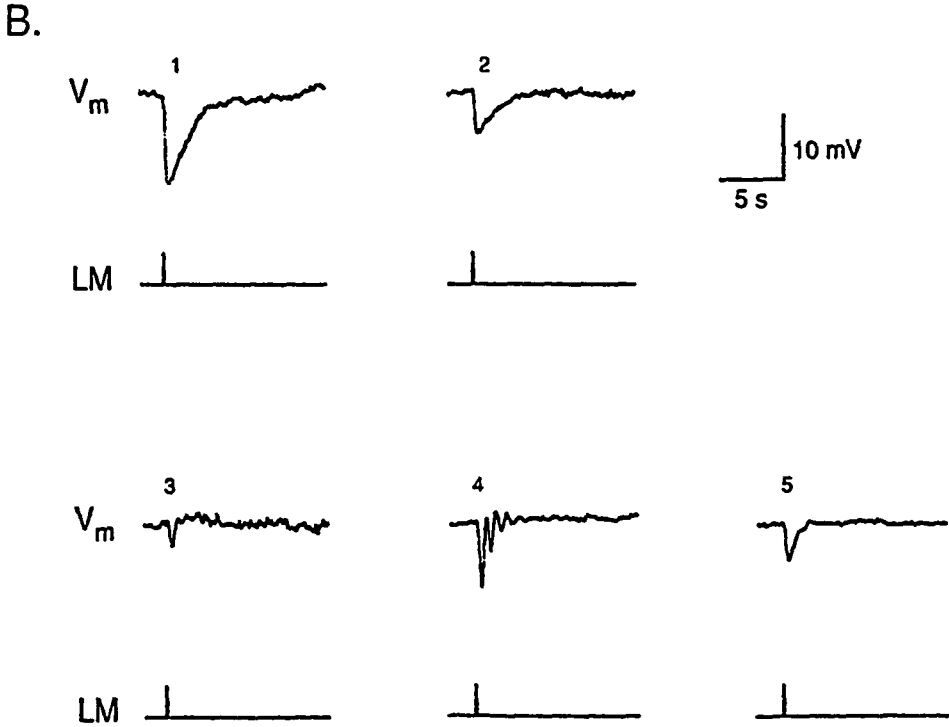
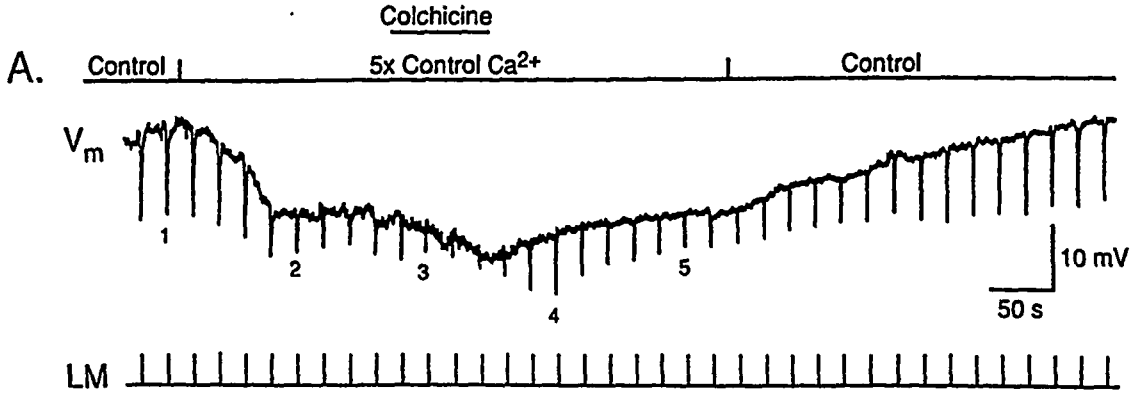


Fig. 32. Effects of colchicine on  $V_m$  and  $V_m$  photoresponses during superfusion with increased  $[Ca^{2+}]_o$ .

photoresponses were clearly more attenuated by the combination of 10 mM colchicine and 5x-normal  $[Ca^{2+}]_o$  than by either treatment alone (see Fig. 3 for the effects of 10 mM colchicine alone).

It is interesting that the response durations during the combination treatment, shown in Fig. 32B, were clearly shorter than in the treatments using colchicine alone. This is particularly interesting when it is remembered that increased  $[Ca^{2+}]_o$  typically increases response durations (see Fig. 8). Other unexpected effects occurred when colchicine was removed from the superfusate. Although  $V_m$  returned to the pre-colchicine level, the  $V_m$  photoresponse amplitudes transiently exceeded pre-colchicine levels before eventually declining back to pre-colchicine levels. Furthermore, oscillations occurred during photoresponse recovery. The recovery remained unusually rapid for several minutes, but response durations eventually began to lengthen, but the durations of the  $V_m$  photoresponses remained considerably shorter than pre-colchicine responses for the entire 12-min. period shown. These results are considered in detail in Chapter 4.

### **Section 3.7. Injections of cGMP during colchicine and high $[Ca^{2+}]_o$ superfusions.**

As discussed in Chapter 1,  $[Ca^{2+}]_i$  reduces the dark current by altering  $[cGMP]_i$ , an effect that results from calcium's alteration of the activities of guanylate cyclase and possibly cGMP phosphodiesterase. The results presented thus far in this thesis strongly support a  $Ca^{2+}$ -like effect of colchicine, so it may be argued that colchicine should have  $Ca^{2+}$ -like effects on these two enzymes. An *in situ* assay for phosphodiesterase activity using cGMP injections has been developed (Oakley et al, 1985; Proenza et al, 1986; Kawamura & Murakami, 1986), although it has limitations (see Section 4.5). Results from experiments applying this technique to compare the effects of colchicine and of increasing  $[Ca^{2+}]_i$  on phosphodiesterase activity are shown below. The assay technique itself is discussed in some detail in Chapter 4, Section 4.5.

In order to raise  $[Ca^{2+}]_i$ ,  $Na^+/K^+/Ca^{2+}$  exchange was blocked by replacing  $Na^+$  with  $Li^+$ . The results are shown in Fig. 33. The record in Fig. 33A are from an experiment where



cGMP injections were given during colchicine superfusion. Note that cGMP continued to depolarize the rods substantially in the presence of colchicine, which further supports the hypothesis that colchicine does not change the cGMP-sensitivity of the channel proteins. The  $V_m$  waveforms resulting from cGMP injections before, during and after colchicine superfusion are shown in Fig. 33B. These records were normalized and replotted superimposed in Fig. 33C. Note that the amplitude of the waveform increased during colchicine superfusion, while the duration of the response shortened a small, but noticeable amount.

Similar results are seen in Fig. 33D-6, which is taken from an experiment where  $\text{Na}^+/\text{K}^+/\text{Ca}^{2+}$  exchange was blocked in order to increase  $[\text{Ca}^{2+}]_i$ . The effects of blocking  $\text{Na}^+/\text{K}^+/\text{Ca}^{2+}$  exchange on the recovery rate of cGMP-evoked depolarizations are slightly more pronounced than the effects caused by colchicine. The changes in the recovery rates of cGMP-evoked depolarizations caused by both colchicine and increased  $[\text{Ca}^{2+}]_i$ , however, are small compared to the effects caused by modest illumination (shown in Figs. 33H-I).

### **Section 3.8. *Tests for possible tubulin or microtubule mediation of colchicine's effects.***

As discussed in Chapter 1, colchicine is best known as a tubulin-binding drug, and its tubulin-binding characteristics have been well-studied. Furthermore, as stated in Chapter 1, two labs have suggested that a membrane bound form of tubulin may play a role in the biochemistry of the G-protein mediated  $\alpha$ -adrenergic system (Lampedis et al, 1987; Rasenick et al, 1988). Since the biochemistry of the  $\beta$ -adrenergic system is very similar to the biochemistry of phototransduction, it is important to determine if the colchicine's effects on rods involve tubulin. Eventually, this question will need to be resolved using appropriate biochemical tests.

There are, however, some electrophysiological studies that could help assess the possibility that tubulin mediates colchicine's effects on rod physiology. Since the tubulin-binding properties of colchicine have been well-characterized (Garland, 1974; Borisy &

**Figure 33.** *Effects of colchicine and Na<sup>+</sup> replacement by Li<sup>+</sup> on V<sub>m</sub> recovery kinetics from pressure-injected cGMP.*

**A.** Thirty mM cGMP was pressure-injected where indicated by the pulse marks in the record labeled P (injection solution A, Table 4). Control and colchicine-containing solutions (solutions A1 & A2, Table 3) superfused the retina where indicated.

**B.** The numbered cGMP-evoked V<sub>m</sub> responses in A are replotted superimposed as labeled.

**C.** These records show normalized and superimposed cGMP-evoked V<sub>m</sub> responses (30 mM cGMP) from a separate experiment under control and light-exposed conditions. The cGMP response labeled hv occurred during exposure to 130 quanta/rod/s of light. The cGMP injection was initiated 30 s after the stimulus began. This record is superimposed on a control response to a similar pulse of cGMP injected before the light stimulus began. The latter two superimposed records show controls from before light stimulation and >1 1/2 min. after the stimulus ended.

**D.** Thirty mM cGMP was pressure-injected where depolarizations in the V<sub>m</sub> record occur. Unfortunately, no pulse record was kept during this experiment, but the pulse amplitude and duration was not changed during the course of this record. Control solution (solution A, Table 4) was switched to a Li<sup>+</sup>-based solution (solution E1, Table 3) to block Na<sup>+</sup>/K<sup>+</sup>/Ca<sup>2+</sup> exchange where indicated.

**E.** The cGMP-evoked V<sub>m</sub> responses numbered 1 and 2 in D are replotted superimposed.

**F.** The cGMP-evoked V<sub>m</sub> responses numbered 2 and 3 in D are replotted superimposed.

**G.** The cGMP-evoked V<sub>m</sub> responses numbered 1 and 4 in D are replotted superimposed.

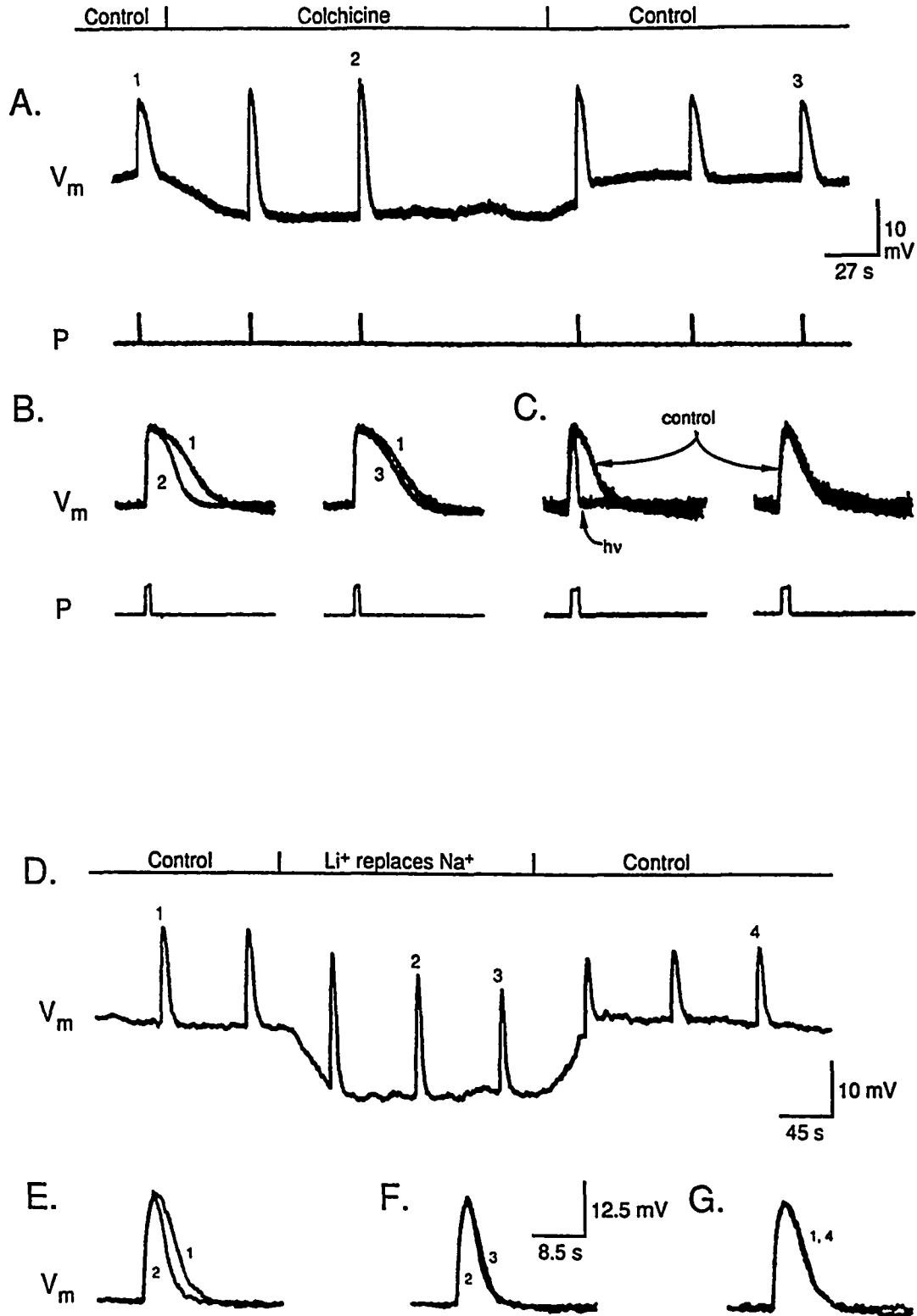


Fig. 33. Effects of colchicine and  $\text{Na}^+$  replacement by  $\text{Li}^+$  on  $V_m$  recovery kinetics from pressure-injected cGMP.

Taylor, 1976; Wilson, 1977; Andreau & Timasheff, 1986), the dose-response relationship between colchicine and its electrophysiological effects can be compared to the known tubulin-colchicine binding relationships. Also, the effects of the colchicine analog,  $\beta$ -lumicolchicine, can be compared to the effects of colchicine as a means of assessing the likelihood that colchicine's effects are tubulin-mediated, since  $\beta$ -lumicolchicine binds tubulin with a much lower affinity than colchicine. Finally, the effects of colchicine can be compared to the effects of other drugs with well-characterized tubulin-binding properties that resemble or that compete with colchicine's. The experiments described below provide preliminary data regarding: the dose-response relationship of colchicine superfusion and its resulting electrophysiological effects; colchicine's effects compared to  $\beta$ -lumicolchicine's effects; colchicine's effects compared to the effects of the tubulin-binding drugs vincristine and podophyllotoxin.

### *3.7.1. Dose-response relationship of superfused colchicine.*

Previous experiments showed how either 10 mM or 20 mM colchicine affected the electrophysiology of rods under various conditions. Ten and 20 mM concentrations of colchicine produced consistent, easily-recognized effects on rods, but these concentrations are quite large compared to the  $K_d$  of the tubulin-colchicine complex observed *in vitro*. It was important, then, to determine the concentration-dependency of colchicine's effects on rod electrophysiology. Figures 34 and 35 show the maximal effects of colchicine on  $V_m$  and  $V_m$  photoresponses at concentrations ranging from 0.1 to 20 mM. After beginning superfusion with colchicine at a given concentration, colchicine's effects typically increased for a period of time. The data shown in Fig. 35 are from maximal changes occurring at a given concentration, i.e., continued exposure to colchicine produced no further measurable changes in the parameter of interest.

Figure 35 shows typical  $V_m$  photoresponses from cells exposed to colchicine from 0.5 mM to 20 mM. Control responses are shown on the left, drug-associated responses are shown in the center, and the normalized drug-associated responses are shown on the right.

**Figure 34.** *The concentration-dependency of the effects of superfused colchicine on  $V_m$*

Colchicine superfused the retinas where indicated. Flashes of light (100-ms, 260 quanta rod<sup>-1</sup> flash<sup>-1</sup>, except C, which is 650 quanta rod<sup>-1</sup> flash<sup>-1</sup>) stimulated the retinas where indicated by the pulses in the LM record. Each record was obtained from a separate retina in a separate experiment. Colchicine concentrations in the superfusates for the various rows were:

- A. 0.5 mM
- B. 1.0 mM
- C. 10 mM
- D. 20 mM

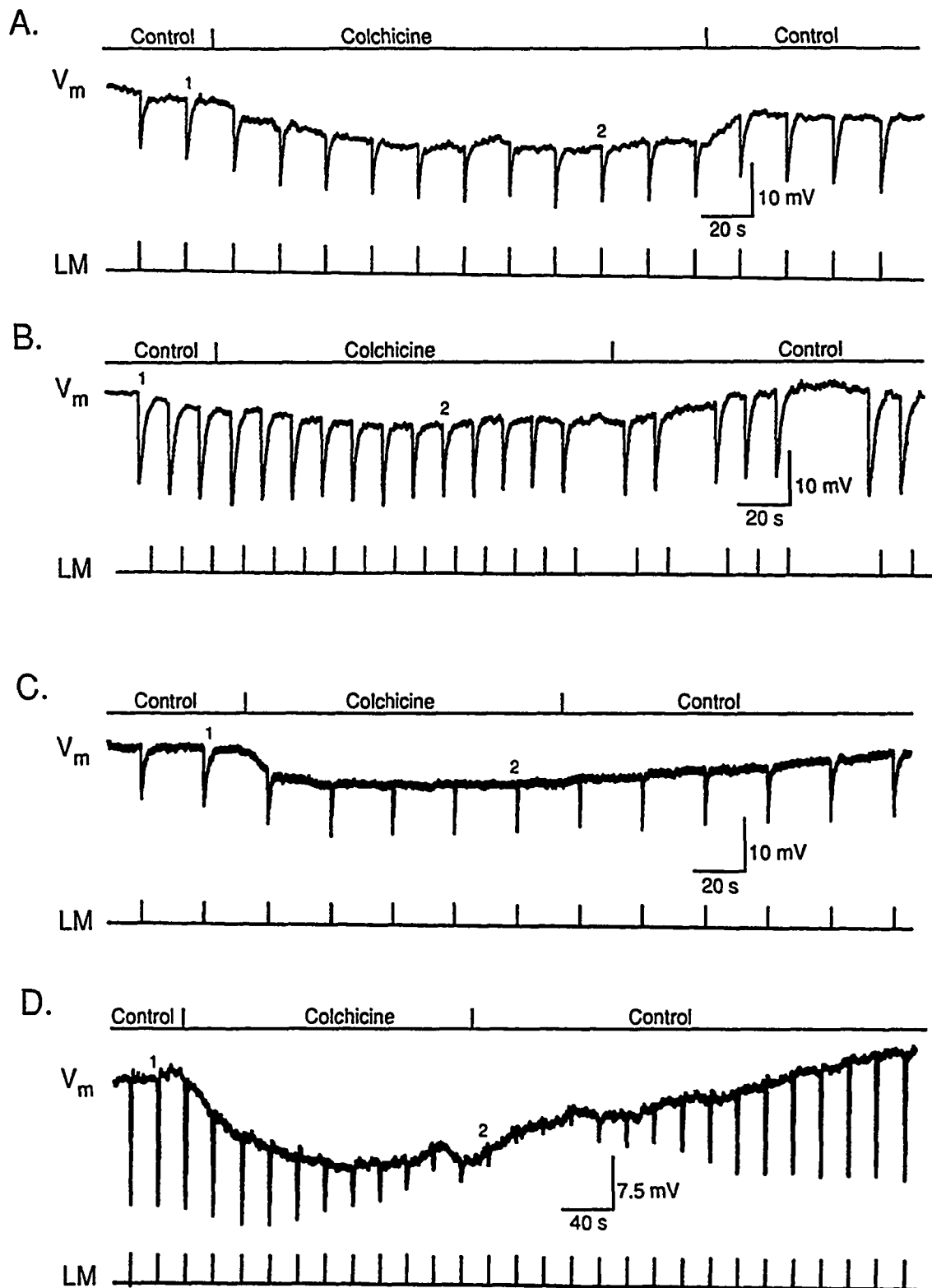


Fig. 34. The concentration-dependency of the effects of superfused colchicine on  $V_m$ .

**Figure 35.** *The concentration-dependency of the effects of superfused colchicine on  $V_m$  photoresponses.*

The numbered  $V_m$  photoresponses from Fig. 34 are replotted on expanded time and voltage scales. The column on the left shows the  $V_m$  photoresponses in the control solution. The middle column shows the photoresponses during colchicine superfusion, and the right column shows the normalized, superimposed records of A - D. Colchicine concentrations in the superfusates for the various rows were:

- A. 0.5 mM
- B. 1.0 mM
- C. 10 mM
- D. 20 mM

The short duration of the light response during control superfusion in row D resulted from previous exposure to 20 mM colchicine. The effects of 20 mM colchicine on shortening the duration of  $V_m$  photoresponses had persisted for a long period (over 15 min.) after the amplitudes of  $V_m$  photoresponses returned to control values.

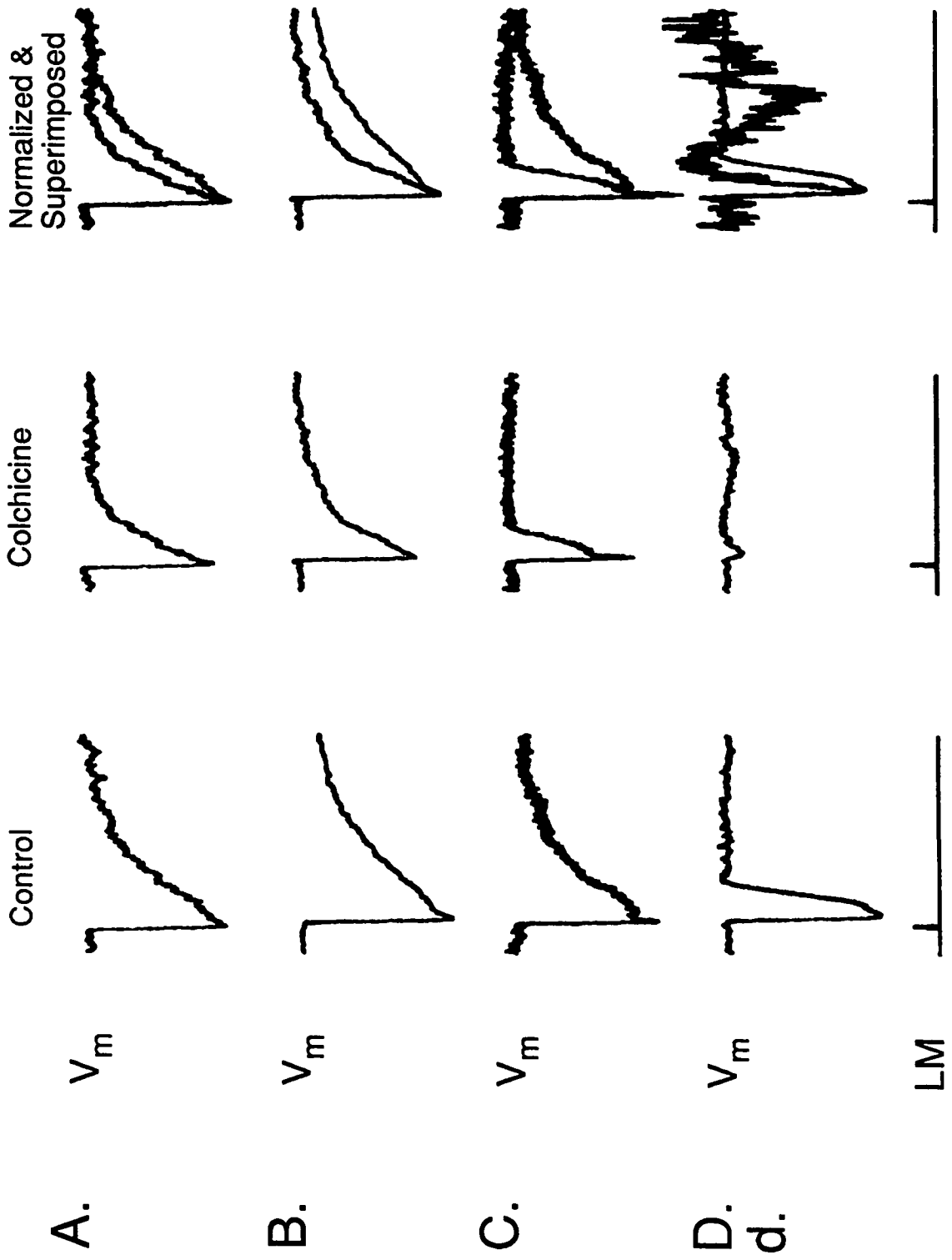


Fig. 35. The concentration-dependency of the effects of superfused colchicine on  $V_m$  photoresponses.



The responses shown are from rods in different retinas, and only a few records were obtained for each individual solution. The results, then, only show trends and can not be meaningfully quantitated.

From the trends, however, it is suggested that colchicine begins to have noticeable effects on both  $V_m$  and  $V_m$  photoresponses at a concentration of about 0.5 mM. These effects increased with concentration of the drug throughout the range studied. Due to variations in the solution exchange time and the unknown nature of colchicine permeation into the rods, meaningful data regarding the time-dependency of colchicine's effects could not be obtained. The effects of colchicine did, however, always appear to stabilize in less than 10 minutes.

### *3.7.2. Effects of $\beta$ -lumicolchicine compared to colchicine.*

Illumination with ultraviolet irradiation produces an isomer of colchicine,  $\beta$ -lumicolchicine, with a reduced affinity for tubulin. This colchicine isomer contains the trimethoxyphenol tubulin-binding ligand, but not the tropolone tubulin-binding ligand, of colchicine (see Illus. 5).

Since tubulin-binding requires higher concentrations of  $\beta$ -lumicolchicine than colchicine, effects produced by colchicine at low concentrations ( $<10^{-5}$ ) that are not reproduced by  $\beta$ -lumicolchicine at similar concentrations imply that the effects are likely to be tubulin-mediated (see Section 1.4 - 1.5). Since both colchicine and  $\beta$ -lumicolchicine share a common tubulin-binding ligand, comparable effects are produced by the two different drugs at high concentration application for short periods.

This knowledge may be useful in characterizing the biochemical action of colchicine, so the effects of  $\beta$ -lumicolchicine on rod photoreceptors are of interest. Unfortunately, the solubility of  $\beta$ -lumicolchicine is considerably lower than colchicine, and concentrations greater than 0.5 mM were unstable even when dissolved in DMSO prior to addition to the superfusates. Furthermore, the effects of colchicine only begin to be observed at 0.5 mM concentrations, which makes comparing the effects of  $\beta$ -lumicolchicine and colchicine

impossible over the entire colchicine ranges used.

Nevertheless, superfusion experiments tested the effects of  $\beta$ -lumicolchicine on rods. Figure 36 shows the results. Figures 36A-36C show the effects of 0.5 mM  $\beta$ -lumicolchicine, which can be compared to the effects of 0.5 mM colchicine shown in Figs. 34A and 35A. Figures 36D-36F show the effects of 3 mM  $\beta$ -lumicolchicine applied in a similar way. The effects produced are not measurably different than the effects of 0.5 mM  $\beta$ -lumicolchicine. The superfusate had to be supersaturated with  $\beta$ -lumicolchicine to produce this the 3 mM concentration.

Figure 37 compares the changes seen in a rod when the superfusate was switched between 0.5 mM colchicine and  $\beta$ -lumicolchicine. Superfusion with 0.5 mM  $\beta$ -lumicolchicine hyperpolarized  $V_m$  about 8 mV, and decreased the amplitudes of the  $V_m$  photoresponses. Switching the superfusate to one containing 0.5 mM colchicine changed the amplitudes of the  $V_m$  photoresponses only marginally. The  $V_m$  photoresponse durations did not change noticeably as shown in the normalized plots (Fig. 37C). Switching back to the  $\beta$ -lumicolchicine superfusion again (not shown) affected the durations of the  $V_m$  photoresponses only minimally.

Similar results occurred in other experiments, thus it appears that  $\beta$ -lumicolchicine is equally as effective as colchicine in hyperpolarizing  $V_m$  at 0.5 mM concentrations. These results are consistent with the trimethoxyphenol ligand causing the hyperpolarizing effects of colchicine. From the results shown here, however, it is not clear whether the effects of colchicine on  $V_m$  response durations can be solely attributed to the trimethoxyphenol ligand.

### *3.7.3 . Effects of nocodazole, vincristine and podophyllotoxin on rod $V_m$ and $V_m$ photoresponses.*

Section 1.6 of Chapter 1 describes the tubulin-binding characteristics of nocodazole, podophyllotoxin and vincristine. These drugs bind tubulin dimers, which leads to the

**Figure 36.** *The effects of  $\beta$ -lumicolchicine on  $V_m$  and  $V_m$  photoresponses.*

**A.** The colchicine derivative,  $\beta$ -lumicolchicine, superfused the retina (0.5 mM; solution A6, Table 3) where indicated. Flashes of light (100-ms, 260 quanta rod<sup>-1</sup> flash<sup>-1</sup>) stimulated the retina where indicated by the pulses in the LM record.

**B.** The numbered photoresponses in A are replotted on expanded time and voltage scales.

**C.** The responses in B are replotted normalized and superimposed.

**D.** This record shows the results of an experiment similar to the one shown in A, but with a supersaturated solution of 3 mM  $\beta$ -lumicolchicine as the test solution. Light flashes were of the same irradiance as in A.

**E-F.** These records are similar to C-D.

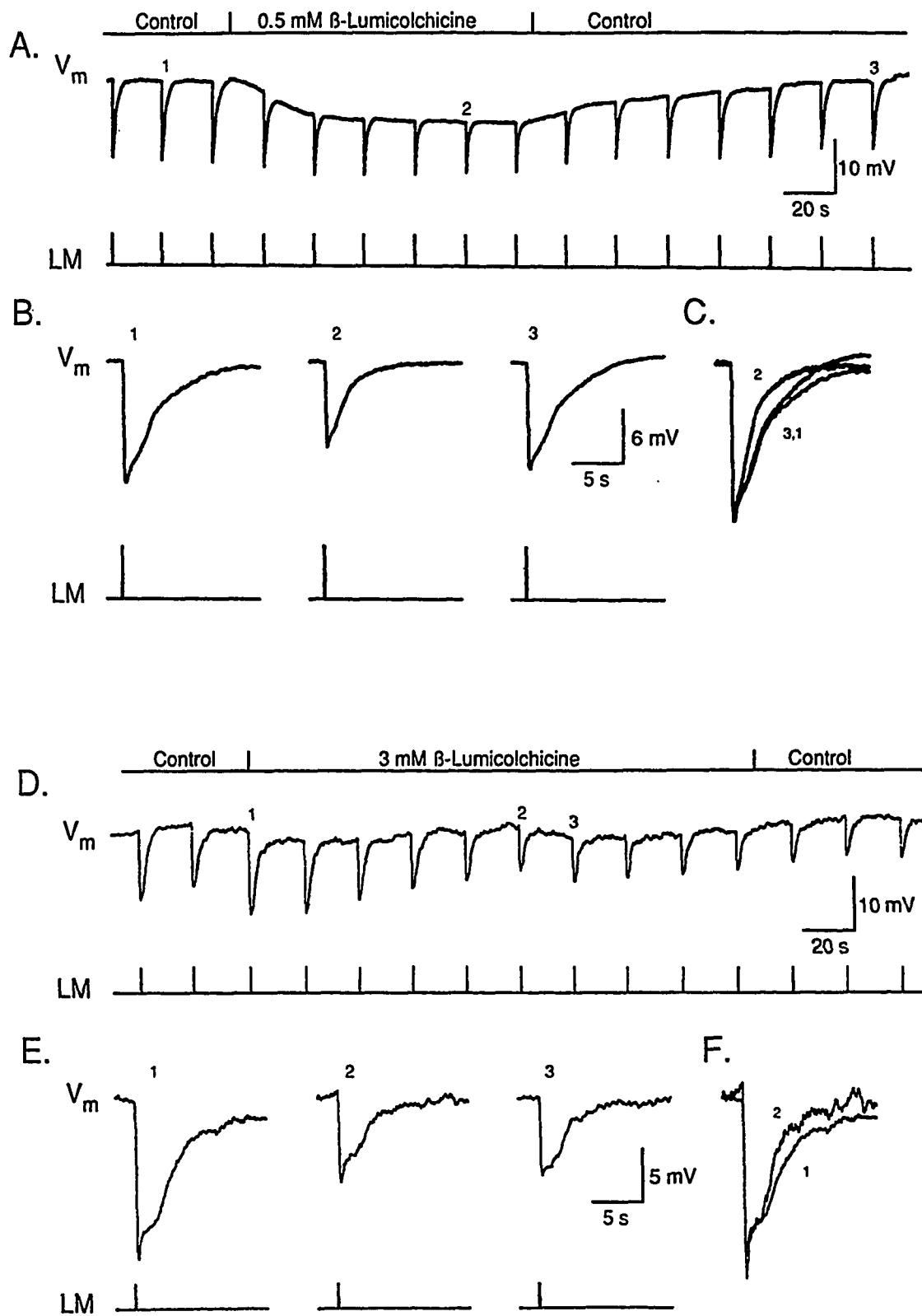


Fig. 36. The effects of  $\beta$ -lumicolchicine on  $V_m$  and  $V_m$  photoresponses.

**Figure 37. Comparative effects of  $\beta$ -lumicolchicine and colchicine on  $V_m$  and  $V_m$  photoresponses in the same rod.**

- A.** The colchicine derivative,  $\beta$ -lumicolchicine, superfused the retina (0.5 mM; otherwise identical to solution A6, Table 3) where indicated. The superfusate was switched to 0.5 mM colchicine, also indicated on the labeled bar above the  $V_m$  record. Flashes of light (100-ms, 260 quanta rod<sup>-1</sup> flash<sup>-1</sup>) stimulated the retina where indicated by the pulses in the LM record.
- B.** The  $V_m$  photoresponses numbered in A are replotted on expanded time and voltage scales. The record labeled C is a control response that occurred during superfusion in control solution (solution A1, Table 3) before the superfusate was switched to one containing  $\beta$ -lumicolchicine (not shown). An artifactual drift in the electrode voltage prevents a direct comparison of the voltages between the control and colchicine/ $\beta$ -lumicolchicine responses. The electrode drift did not appear to affect the time course of the responses.
- C.** The responses shown in B are normalized and superimposed as indicated by the labels. Results consistent with the time course changes of this experiment were obtained in two repetitions of this experiment in the same retina, and in two other separate experiments on successive days.

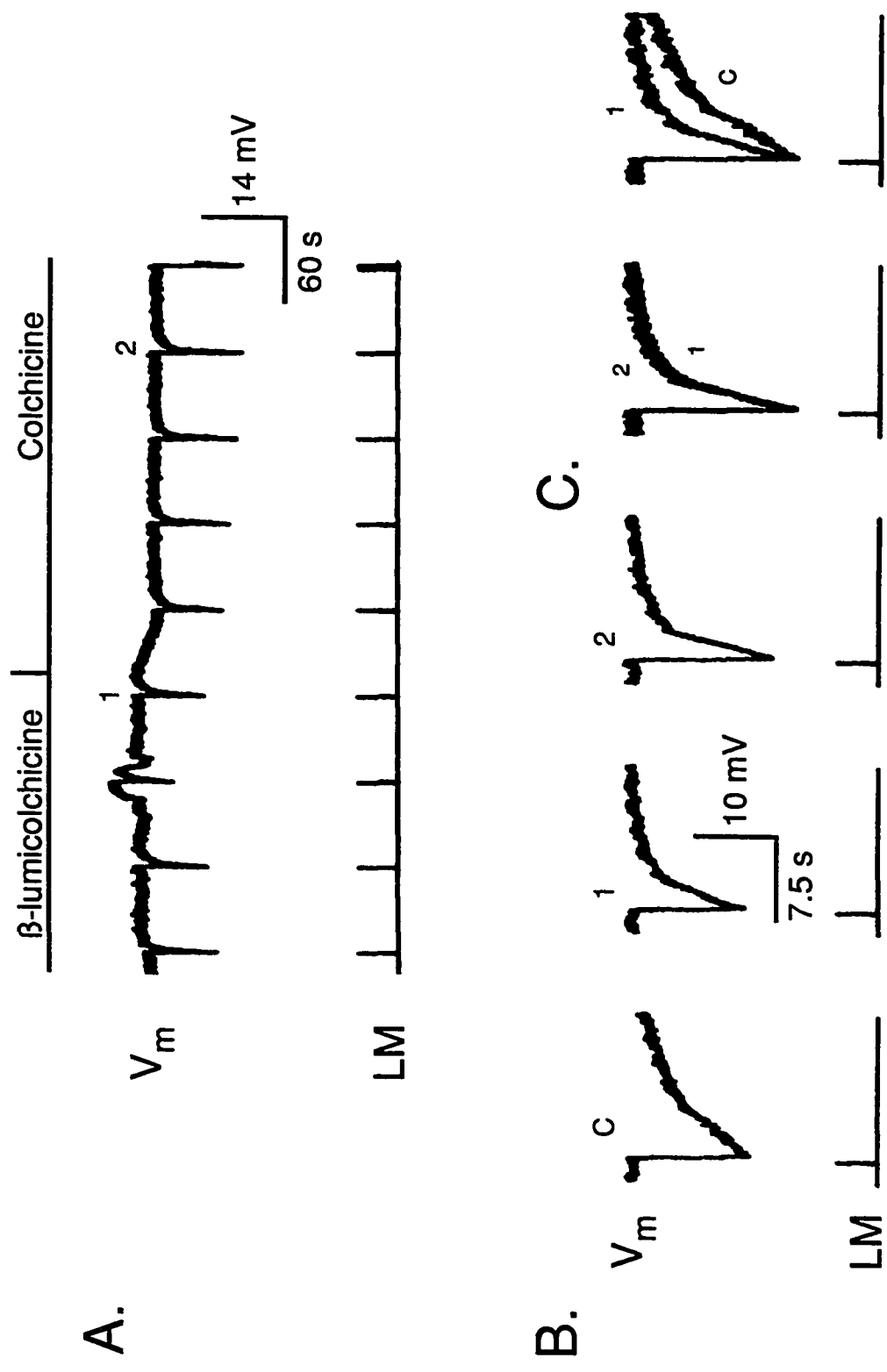


Fig. 37. Comparative effects of  $\beta$ -lumicolchicine and colchicine on  $V_m$  and  $V_m$  photoresponses in the same rod.

eventual dissociation of microtubules. Although these drugs bind to tubulin, they have different effects on the biochemistry of tubulin, including tubulin's ability to bind colchicine and other small molecules. Whenever treatments with these drugs produce similar effects on a system, it usually implies that the effects result from microtubule disruption. Whenever these drugs have different effects on a system, the meaning of the results is less clear. Most likely, however, the effects have not resulted from the disruption of microtubules. The effects of these drugs on rods, then, is of interest, since they may implicate microtubule involvement. Unfortunately, the low solubilities of these drugs limited the concentrations that could be used. Typically, 10-100  $\mu\text{M}$  concentrations were the highest used.

There were no clearly discernible effects from nocodazole or podophyllotoxin at these low concentrations. Vincristine had small effects on rods, as shown in Fig. 38. Vincristine depolarized  $V_m$ , and increased the  $V_m$  photoresponse amplitudes and durations. Vincristine had little effect, however, on the kinetics of cGMP-evoked depolarizations at these low concentrations. In other experiments, 10  $\mu\text{M}$  vincristine increased the hyperpolarizing transient (the nose) of bright flashes (not shown). Thus the effects of vincristine at these concentrations may be consistent with alteration of a voltage-sensitive conductance in the inner segment, rather than  $g_{hv}$ .

The effects of other tubulin-binding drugs were too small to clearly interpret at low concentrations, and low-solubility of these drugs (nocodazole & podophyllotoxin) prevented the study of effects at higher concentrations.

**Figure 38.** *The effects of vincristine on  $V_m$ ,  $V_m$  photoresponses and cGMP-evoked depolarizations.*

- A.** The tubulin-binding drug, Vincristine (25 $\mu$ M, solution F3, Table 3), superfused the retina where indicated. Pressure injections of cGMP (injection solution A, Table 4) stimulated the rod where indicated by the pulses in the record labeled P. Flashes of light (100-ms, 1000 quanta rod<sup>-1</sup> flash<sup>-1</sup>) stimulated the retina where indicated by the pulses in the LM record.
- B.** The  $V_m$  photoresponses in A are replotted on expanded time and voltage scales.
- C.** The  $V_m$  photoresponses in B are replotted normalized and superimposed.
- D.** The numbered cGMP responses in A are replotted on expanded time scales.
- E.** The cGMP responses in D are replotted normalized and superimposed.



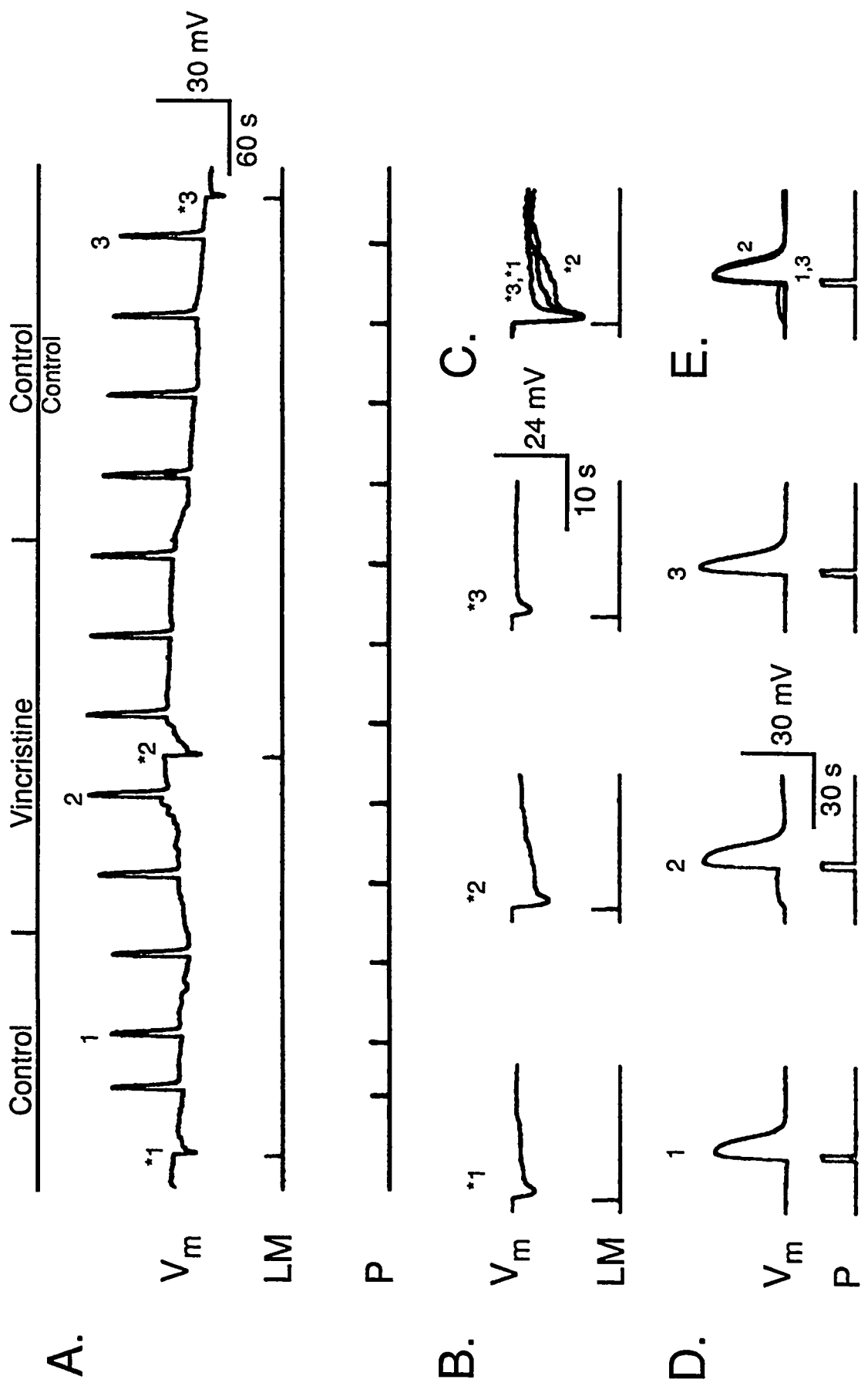


Fig. 38. The effects of vincristine on  $V_m$ ,  $V_m$  photoresponses and cGMP-evoked depolarizations.

## Chapter 4

### Discussion

#### Section 4.0 *Colchicine blocks $g_{hv}$ .*

Several results presented in Chapter 3 clearly support the hypothesis that superfusion with colchicine decreases  $g_{hv}$ . Colchicine superfusion hyperpolarizes rods, while increasing the input resistance to a current passed between an intracellular electrode and ground. This combination is consistent with the reduction of a conductance passing an inward, but not an outward current. In dark-adapted rods, the only inward current carrying more than a few pA is the light-sensitive current. Colchicine also reduces the amplitude of  $V_m$  photoresponses and alters the response recovery kinetics, which are effects essentially controlled by  $g_{hv}$ . This is discussed in the appendix under Derivation 4, and essentially follows from the discussion of Baylor et al (1984). The photocurrent, controlled by  $g_{hv}$ , can be considered a "driving current" that drives the inner segment, which can be modeled as a passive linear circuit over small voltage changes. The time-dependent effects of the inner segment conductances are minimal for the recovery part of the waveform. The steady-state voltage sensitivity of the inner segment conductances are approximately linear for voltages above -40 mV, and therefore do not contribute to the differences in kinetics attributable to colchicine. Furthermore, the effects of colchicine on recovery kinetics persisted when the inner segment conductances were blocked.

The blockade of nearly all conductances in rods other than  $g_{hv}$  enhances, rather than eliminates, the effects of colchicine, which is consistent with colchicine specifically blocking  $g_{hv}$ . If colchicine acted only on conductances other than  $g_{hv}$ , prior blockade of these conductances should have nullified further effects by colchicine. The enhancement of colchicine's effects, then, supports the hypothesis that colchicine's effects are specific for  $g_{hv}$ . This can be reasoned from the knowledge of the non-linear nature of the inner segment conductances. The rod inner segment voltage-sensitive potassium channels are

normally open in dark-adapted rods, and carry a significant amount of current (Oakley and Shimazaki, 1984; Bader et al 1982). This current shuts down during hyperpolarization induced by illumination. The inward-rectifier in the rod inner segment, however, is closed in dark-adapted rods, but opens on hyperpolarization during illumination (Bader et al, 1982; Hastrin, 1987). Thus an outward current closes while an inward current opens as a result of the hyperpolarization induced by the closing of  $g_{hv}$ . The action of both of these currents is to oppose hyperpolarization during illumination (Bader et al, 1982). It is the action of these channels that produces the non-linear voltage changes seen in Fig. 1. If colchicine also affected these currents in addition to the light-sensitive current, then the electrophysiological effects of colchicine alone should have been as effective as the channel-blocking cocktail and colchicine. Instead, the channel-blocking drugs enhanced colchicine's effects. This enhancement occurred when each drug was used individually with colchicine as well. The enhancement of colchicine's effects by these drugs can be explained by the inhibitions of the normal opposition to colchicine-evoked hyperpolarization by the non-adapting, voltage-sensitive currents.

Superfusion with colchicine during steps of illumination provides further evidence that colchicine's effects are relatively specific. Colchicine's effects during illumination are limited primarily to an inhibition of light-adaptation. If colchicine affected inner-segment conductances in addition to the blocking effects on  $g_{hv}$ , then shutting down  $g_{hv}$  should make rod voltage more sensitive to effects on other conductances, and effects of colchicine on these conductances should become pronounced. Instead, the hyperpolarizing effects of colchicine appear to be reduced. The most noticeable effect of colchicine application during a step of illumination, inhibition of light-adaptation, can be explained by effects on  $g_{hv}$ , which controls light adaptation (Matthews et al, 1987; Yau, 1987).

Finally, flashes of light closing  $g_{hv}$  cause transient increases in  $[Ca^{2+}]_o$  (Hagins and Yoshikami, 1980; Gold and Korenbrot, 1980; Gold, 1986; Miller and Korenbrot, 1987) which are demonstrated in Fig. 9. The data discussed below supports the hypothesis that these fluxes result from imbalances in  $Ca^{2+}$  influx and efflux, resulting from decreases in the  $Ca^{2+}$

influx through  $g_{hv}$ , in agreement with the results of others (Miller and Korenbrot, 1987; Gold, 1986; Yau and Nakatani, 1984a; Nakatani and Yau, 1988). Colchicine stops these light-evoked increases in  $[Ca^{2+}]_o$ , and strongly inhibits the light-evoked increased  $[Ca^{2+}]_o$  changes caused by IBMX. These results are consistent with the hypothesis that colchicine blocks  $g_{hv}$ , and can be explained by the inhibition of  $Ca^{2+}$  influx into rods, which raises  $[Ca^{2+}]_o$  and reduces light-evoked  $[Ca^{2+}]_o$  changes. It is concluded, then, that colchicine blocks  $g_{hv}$ .

**Section 4.1** *Colchicine probably is not a competitive or allosteric inhibitor of cGMP-channel binding.*

With the recent discovery of an integral membrane tubulin in the rod outer segment plasma membrane (Matesic and Liebman, 1989; Peter Stein, personal communication), the effects of colchicine on the rod outer segments need to be carefully examined, especially since these two groups of researchers contend that this membrane tubulin is the same protein that has been thought to be the cGMP-sensitive channel by others (Koch et al, 1987). It is important, then, to determine whether colchicine blocks  $g_{hv}$  by binding to the channel, or whether colchicine affects  $g_{hv}$  by lowering  $[cGMP]_i$ , which does bind to the channel and increases the channel conductance (Fesenko et al, 1985; Yau and Nakatani, 1985; Stern et al, 1986; Matthews, 1986; Matthew and Watanabe, 1987).

Several pieces of evidence shown in the results section of this thesis do not support a specific blocking action of colchicine at the channel level. First, addition of colchicine to superfusates during steps of illumination did not block post-stimulus recovery after the termination of light steps, despite continued exposure of the retina to colchicine. This result can be interpreted as showing that  $[cGMP]_i$  levels, which increase during the post stimulus period, can increase the conductance of  $g_{hv}$  in the presence of colchicine. If this interpretation is correct, then the corollary can be made that colchicine does not stop post-stimulus increases in  $[cGMP]_i$ , which presumably depend on guanylate cyclase activity (Oakley et al, 1985; Proenza et al, 1986; Kawamura and Murakami, 1986; Hodgkin and

Nunn, 1988; Detwiler and Rispoli, 1989). Likewise, superfusion with the phosphodiesterase inhibitor, IBMX, which also increases  $[cGMP]_i$ , reversed the effects of colchicine on cells. These results are further supported by the results shown in Figs. 32 and 33, which show clearly that colchicine does not block depolarizations resulting from injections of cGMP, nor does colchicine reduce the amplitude or slow the time-to-peak of the injection-evoked depolarizations. In fact, the amplitudes of the depolarizations increase.

If colchicine simply blocks cGMP activation of  $g_{h\nu}$ , colchicine should block or inhibit depolarization resulting from injected cGMP or post-stimulus increases in  $[cGMP]_i$  resulting from cGMP-evoked increases in  $g_{h\nu}$  (Waloga, 1983; Oakley et al, 1985; Kawamura and Murakami, 1986; Proenza et al, 1986; Matthews, 1986). In fact, the increased depolarization amplitudes resulting from injections of cGMP in the presence of colchicine are consistent with a colchicine-evoked decrease in  $[cGMP]_i$ . A model for the mechanism of voltage changes resulting from intracellular injections of cGMP is described in Subsection 4.2.4.

Although the  $[cGMP]_i$  - voltage relationship is quite complex, it has been shown empirically that depolarizing cells by lowering  $[cGMP]_i$  using the phosphodiesterase inhibitor IBMX lowers the amplitude of voltage depolarizations induced by cGMP injections due to compression (Oakley et al, 1985; Waloga, 1983), whereas lowering  $[cGMP]_i$  with increased  $[Ca^{2+}]_o$  increased the amplitude of cGMP-evoked depolarizations (see Fig. 32).

This evidence collectively supports the hypothesis that colchicine lowers  $[cGMP]_i$ , rather than the hypothesis that colchicine inhibits cGMP binding to the channel protein. Others have found that low doses of colchicine do not inhibit  $Ca^{2+}$  release from liposomes containing the rhodopsin-like cGMP-sensitive channel protein (Diane Matesic, personal communication), consistent with the above results. Effects of colchicine on tubulin-containing liposomes with the rhodopsin-like channel have not yet been assayed, but deserve investigation.

These results should not, however, be considered conclusive evidence that colchicine

does not act at the channel level. It is possible, for instance, that colchicine-binding to the channel proteins requires a conformation that exists only when cGMP is bound to the a protein. In this case, colchicine would be an allosteric inhibitor of cGMP-sensitive channels. Colchicine would then have no effects during bright steps of illumination, since the channels remain unbound to cGMP during such stimulation. Furthermore, the effects of colchicine would offset the effects of rising cGMP during light adaptation. Likewise, colchicine might not affect the rate of voltage increase during cGMP injections, since cGMP would act on the closed, non-colchicine bound channels. Colchicine might, however, be expected to affect the recovery kinetics if this model is correct, and a small effect on the recovery is observed, consistent with this idea.

It is more difficult, though, to explain then why the effects of colchicine are less dramatic when low  $[Ca^{2+}]_o$  is used to depolarize the rods. A calcium-sensitive binding of colchicine to the channels must also be proposed to explain these results. For the sake of argument, it should be restated that tubulin-colchicine binding is enhanced by  $Ca^{2+}$  (see Section 1.4.4.). Furthermore, the drug DCPA acts at the channel level to inhibit  $g_{hv}$  in a  $Ca^{2+}$  sensitive manner (see Section 1.1.2).

Other results are more difficult to explain with an allosteric inhibitory model of colchicine's action. The cGMP phosphodiesterase inhibitor, IBMX, reverses colchicine's effects when added to superfusates, presumably by increasing  $[cGMP]_i$ . Colchicine and IBMX are mutually inhibitory, but it is unusual that an allosteric inhibitor acting at the channel level, does not completely shut down  $g_{hv}$ . As cGMP increases during IBMX treatment and opens channels, colchicine should freely bind to the channels and close them. The mutual inhibition better fits a model of competitive inhibition, rather than the allosteric model described above. Thus, if colchicine's effects are at the channel level, a very unusual mechanism must be proposed: colchicine binds only to cGMP-bound channels, but in a competitive manner.

Since cGMP binds cooperatively at channels (see Section 1.1.2), it is possible that colchicine binds near a final cGMP binding site, and thus requires cGMP binding, yet is

competitively inhibitory. If this is true, then it is difficult to explain why colchicine does not inhibit the  $\text{Ca}^{2+}$  permeability of the purified rhodopsin-like channel. Either the doses studied in the purified protein preparation were too low ( $\mu\text{M}$  doses were used) or colchicine's effects require the presence of the membrane tubulin component as well, and the interactions are exceedingly complex.

In order to refute this channel-binding model completely, the effects of colchicine on isolated membrane patches will need to be studied, and the effects of colchicine on reconstituted systems containing both the purified rhodopsin-like channel and the membrane tubulin components will also need to be studied. Hopefully, such studies will use a wide range of colchicine concentrations (up to 20 mM) so that the results can be compared to those of this thesis.

Finally, a channel-blocking effect of colchicine alone cannot explain three important results: the inhibition of dark-adaptation in the presence of normal, dark-adapted voltages, the persistent light adaptation-like effects in the presence of lowered  $[\text{Ca}^{2+}]_i$  and the continued efflux of  $\text{Ca}^{2+}$  from rods during a step of light. When colchicine is superfused onto retinas that have been stimulated with a step of light, colchicine blocks light-adaptation (see Fig. 6), and also blocks dark-adaptation after stimulus termination. It does not stop  $V_m$  recovery to dark-adapted voltage levels. Colchicine's hyperpolarizing effects on dark-adapted rods can be reversed by lowering  $[\text{Ca}^{2+}]_i$ , either by injecting  $\text{Ca}^{2+}$  buffers or by lowering  $[\text{Ca}^{2+}]_o$ , but rods remain desensitized to light flashes. The depolarized  $V_m$  during these conditions is indicative of increased  $[\text{cGMP}]_i$ , yet colchicine's desensitizing effects persist. It is apparent, then that part of colchicine's effects are independent of  $[\text{cGMP}]_i$ , and probably affect the enzyme cascade sequence itself. These results make it difficult to argue that colchicine has a single effect on photoreceptors, since colchicine apparently inhibits light-evoked decreases in  $[\text{cGMP}]_i$ , yet colchicine appears to either lower  $[\text{cGMP}]_i$  or else it blocks  $g_{hv}$  in a complex way.

The increased efflux of  $\text{Ca}^{2+}$  from rods is also difficult to explain with a channel-blocking mechanism of action of colchicine. Although closing  $g_{hv}$  certainly leads to a  $\text{Ca}^{2+}$

efflux, the addition of colchicine prevented the decline of  $[Ca^{2+}]_o$  during illumination, which indicates an increase in  $Ca^{2+}$  available for extrusion from the cells; i.e., a release of  $Ca^{2+}$  from internal stores. Furthermore, the presence of colchicine caused  $[Ca^{2+}]_o$  to continue to increase after the light step ended, despite a partial depolarization of  $V_m$ . The prevention of the slow decline in  $[Ca^{2+}]_o$  observed during a light step by preventing a light adaptation-evoked opening of cGMP-sensitive channels might be considered consistent with colchicine acting on the channel proteins. This seems unlikely, however, since evidence is against adaptation being responsible for the slow decline of  $[Ca^{2+}]_o$  during the light step: This decline was independent of the irradiance of the light step (see Fig. 11C). More likely, the decline is the result of  $Ca^{2+}$  diffusion from the photoreceptor layer to the overlying bath.

Furthermore, colchicine actually caused  $[Ca^{2+}]_o$  to increase during steps of illumination. Considering the irradiance of the steps of light used,  $g_{hv}$  should have been completely closed down despite the presence of colchicine. Thus, the increasing  $[Ca^{2+}]_o$  during the light step more likely results from increased  $[Ca^{2+}]_i$  available for extrusion rather than further reduction of open cGMP-sensitive channels. Moreover, it is important to note that  $[Ca^{2+}]_o$  continued to increase for more than 2 min. after the light-stimulation was stopped. The membrane voltage depolarized a few mV during this same period, indicating an increase in  $g_{hv}$ . This increase in  $g_{hv}$  should have allowed  $Ca^{2+}$  influx into rods to increase, and resulted in a decline in  $[Ca^{2+}]_o$ . Instead,  $[Ca^{2+}]_o$  continued to stay elevated until colchicine was removed. This result is more consistent with colchicine increasing  $[Ca^{2+}]_i$  by releasing intracellularly stored  $Ca^{2+}$ , and thus keeping the rate of  $Ca^{2+}$  efflux elevated above the rate of  $Ca^{2+}$  influx.

In order to continue to argue that colchicine acts at the channel level, either two cGMP-sensitive channels or two channel conductance states would have to be proposed. One of these states, or channels, when bound to colchicine, would not allow  $Ca^{2+}$  to permeate the conductance in the absence of cGMP, but would allow other ions to permeate the conductance when cGMP becomes bound. The binding of cGMP to the other channel or the other conductance state would then promote colchicine binding to that channel or state,



which would reduce this second conductance state's permeability to cations other than  $\text{Ca}^{2+}$ .

Although this rather elaborate binding scheme is feasible, it seems much more plausible to postulate that colchicine has at least two major effects on photoreceptors: Colchicine lowers  $[\text{cGMP}]_i$  by releasing  $\text{Ca}^{2+}$  from bound intracellular reservoirs; Colchicine increases the rate of decay of activated G-Protein.

#### **Section 4.2 Colchicine releases $\text{Ca}^{2+}$ from intracellular stores**

The hypothesis that colchicine releases  $\text{Ca}^{2+}$  from intracellular stores must be examined critically because of the indirect nature of the evidence. Still, this hypothesis provides the simplest and most coherent explanation for many of colchicine's effects. It was previously mentioned that many of colchicine's effects resemble increased  $[\text{Ca}^{2+}]_i$ : Colchicine blocks  $g_{\text{hV}}$ , as does increased  $[\text{Ca}^{2+}]_i$ ; Colchicine causes a delay in the time-to-peak of  $V_m$  photoresponses, as does increased  $[\text{Ca}^{2+}]_i$ . Finally, both increased  $[\text{Ca}^{2+}]_i$  and colchicine cause small increases in the voltage recovery rate from injected cGMP (see Fig. 32). Indeed, these  $\text{Ca}^{2+}$ -like effects of colchicine lead to the hypothesis that colchicine increased  $[\text{Ca}^{2+}]_i$ , which, in turn, caused the effects on  $V_m$  and  $V_m$  photoresponses.

There are several mechanisms by which colchicine could increase  $[\text{Ca}^{2+}]_i$ . As previously stated, colchicine could act by releasing  $[\text{Ca}^{2+}]_i$  from the large intracellular stores of  $\text{Ca}^{2+}$  in the disk membranes (see Section 1.3). Alternatively, colchicine could increase the photoreceptor  $\text{Ca}^{2+}$  permeability in some manner, perhaps by acting as an ionophore, or colchicine could inhibit  $\text{Na}^+/\text{K}^+/\text{Ca}^{2+}$  exchange, thus trapping  $\text{Ca}^{2+}$  in rods. The experimental evidence is most consistent with a release of  $\text{Ca}^{2+}$  from internal stores. Each set of experiments is discussed individually below. The experiments measuring  $[\text{Ca}^{2+}]_o$  with  $\text{Ca}^{2+}$ -selective electrodes provided the most revealing information with respect to this hypothesis, but their interpretation requires that the mechanism of  $[\text{Ca}^{2+}]_o$  changes be firmly established. Experiments establishing the mechanism of  $[\text{Ca}^{2+}]_o$  efflux is discussed first.

*Section 4.2.1: The mechanism responsible for measured  $[Ca^{2+}]_o$  changes is disturbance of the equilibrium between  $Ca^{2+}$  influx and efflux into rod outer segments.*

Current theory states that there are continuous equal and opposite fluxes of  $Ca^{2+}$  across the plasma membrane in dark-adapted photoreceptors. Shutting  $g_{hv}$  leads to increases in  $[Ca^{2+}]_o$  by stopping  $Ca^{2+}$  influx into photoreceptors through  $g_{hv}$  while allowing  $Na^+/K^+/Ca^{2+}$  exchange to continue to extrude  $Ca^{2+}$ . Thus  $[Ca^{2+}]_o$  outside the rods increases. Although others have provided convincing evidence for this hypothesis (see Sections 1.2 and 1.3), the  $[Ca^{2+}]_o$  increases observed in this whole-retina preparation using double-barreled  $Ca^{2+}$ -selective microelectrodes had not yet been tested for conformity to the general  $Ca^{2+}$  flux theory. This was done in experiments shown in Figs. 9 - 16. The results of these experiments showed that:

1.  $V_{Ca^{2+}}$  changes always followed photoreceptor hyperpolarization.
2. The rate of the  $V_{Ca^{2+}}$  increase was constant for flash intensities that saturated the  $V_m$  photoresponse.
3. The amplitudes of the  $V_{Ca^{2+}}$  photoresponses saturated, but increased in duration as the duration of the  $V_m$  photoresponses increased.
4. Steps of illumination that continued to saturate the  $V_m$  photoresponses exhibited as slow decline in  $V_{Ca^{2+}}$  during stimulation.
5. This rate of decline was independent of intensity for flashes saturating  $V_m$  responses.
6. Flashes of sufficient irradiance to produce saturating  $V_m$  photoresponses produced post-stimulus  $V_{Ca^{2+}}$  undershoots with durations which do not correlate strongly with the durations of saturated  $V_m$  photoresponses.
7. Increasing  $g_{hv}$  by blocking cGMP phosphodiesterase activity with IBMX depolarized rods, decreased  $V_{Ca^{2+}}$  but increased  $V_{Ca^{2+}}$  photoresponses.
8. Blocking  $Na^+/K^+/Ca^{2+}$  exchange by substituting  $Li^+$  for  $Na^+$  in superfusates hyperpolarized rods while decreasing  $V_{Ca^{2+}}$ . Pretreatment with IBMX increased the magnitude, but not the direction of the changes observed.

9. Activating  $\text{Na}^+/\text{K}^+/\text{Ca}^{2+}$  exchange after loading photoreceptors with  $\text{Ca}^{2+}$  by blocking  $\text{Ca}^{2+}$  extrusion during superfusion with IBMX caused a large, transient increase in  $V_{\text{Ca}^{2+}}$ .

The first seven points listed above are consistent with results obtained by others using other types of  $\text{Ca}^{2+}$ -selective electrodes to measure  $\text{Ca}^{2+}$  extrusion from bovine (Gold, 1986) and salamander rods (Miller and Korenbrot, 1987). Originally, light-evoked increases in  $[\text{Ca}^{2+}]_o$  were considered as evidence supporting a light-evoked  $[\text{Ca}^{2+}]_i$  increase, which resulted from light-evoked  $\text{Ca}^{2+}$  release from disks. These results have been challenged, most seriously by the measurement of light-evoked  $[\text{Ca}^{2+}]_i$  decreases using photosensitive dyes (McNaughton et al, 1986; Ratto et al, 1988). Likewise, the results just presented, and those of others using  $\text{Ca}^{2+}$ -selective electrodes, are far more consistent with the hypothesis of continuous dark-adapted  $\text{Ca}^{2+}$  fluxes proposed by Yau and Nakatani (1985a).

The arguments that the results presented in 1 - 9 above support the  $\text{Ca}^{2+}$  flux hypothesis will be considered in some detail, since interpreting colchicine's effects on  $V_{\text{Ca}^{2+}}$  depend on the validity of the  $\text{Ca}^{2+}$  flux hypothesis.

First, the  $[\text{Ca}^{2+}]_o$  photoresponses always followed rod hyperpolarization. This is consistent with  $[\text{Ca}^{2+}]_o$  increase resulting from a  $\text{Ca}^{2+}$  influx reduction through  $g_{\text{hv}}$ . If the influx of  $\text{Ca}^{2+}$  in the dark is equal and opposite a  $\text{Na}^+/\text{K}^+/\text{Ca}^{2+}$  exchange-mediated efflux, the efflux of  $\text{Ca}^{2+}$  from cells becomes unopposed during photostimulation, and intracellular  $\text{Ca}^{2+}$  becomes transferred to the interphotoreceptor space, raising  $[\text{Ca}^{2+}]_o$ . If light-excitation leads to any increase in  $[\text{Ca}^{2+}]_i$ , which then acts to inhibit  $g_{\text{hv}}$ , one might well expect the action of  $\text{Na}^+/\text{K}^+/\text{Ca}^{2+}$  exchange, which is enzyme-like and responds very quickly, to be at least as fast as calcium's  $g_{\text{hv}}$ -inhibiting effects. It seems surprising, then, that the  $\text{Ca}^{2+}$  increase is always subsequent to the voltage change, even at very high light intensities.

Furthermore, the rate of increase in  $[\text{Ca}^{2+}]_o$  becomes saturated at much lower light irradiances than the rate of voltage hyperpolarizations. This is in conflict with what one

expects if a light-evoked  $[Ca^{2+}]_i$  increase inhibits  $g_{h\nu}$ . It would be expected that the rate of the  $[Ca^{2+}]_i$  increase would increase with stimulus irradiance, and that this rapid  $[Ca^{2+}]_i$  increase would increase the rate of  $Ca^{2+}$  efflux via the  $Na^+/K^+/Ca^{2+}$  exchanger, which is non-saturating over a large range (Gill et al, 1984; Miller & Korenbrot, 1987). The results shown in Fig. 9 are more consistent with the initial efflux rate being constant, as it would be if  $[Ca^{2+}]_i$  were relatively constant, and the rate of  $[Ca^{2+}]_o$  increase depended on this rate alone. This is exactly what is predicted by the  $Ca^{2+}$  flux hypothesis, since  $Ca^{2+}$  influx would be zero during saturating flashes (this argument ignores the small increase in efflux resulting from faster closure of  $g_{h\nu}$  at supersaturating irradiances).

Equally as inconsistent with a light-evoked increase in  $[Ca^{2+}]_i$  is the amplitude saturation of  $V_{Ca^{2+}}$  photoresponses while  $V_m$  photoresponses increase in duration. If  $[Ca^{2+}]_i$  increases contributed to  $g_{h\nu}$  inhibition, then the duration of responses resulting from flashes of increasing irradiance would require a super-saturating increase in  $[Ca^{2+}]_i$ , that would produce continued  $g_{h\nu}$  inhibition until  $[Ca^{2+}]_i$  fell below the saturating level. Calcium extrusion, then, would continue during the entire period of inhibition. Extracellular  $Ca^{2+}$  should continue to increase, since  $Ca^{2+}$  should continue to accumulate in the interphotoreceptor space. This clearly does not happen. Instead, the amplitude saturation of  $[Ca^{2+}]_o$  photoresponses is again more consistent with the extrusion of a finite amount of  $[Ca^{2+}]_i$  at a declining rate independent of flash irradiance. According to this latter model,  $[Ca^{2+}]_o$  would plateau when essentially all of the  $[Ca^{2+}]_i$  was pumped out of the cells, or at least where the rate of efflux from the cells equaled the rate of  $[Ca^{2+}]_o$  diffusion into the overlying unstirred bath layer.

The changes in  $[Ca^{2+}]_o$  resulting from steps of light also challenge the model of light-evoked increases in  $[Ca^{2+}]_i$ . If this model is correct,  $[Ca^{2+}]_i$  must stay elevated during the entire period of illumination in order to inhibit  $g_{h\nu}$ . Thus  $Ca^{2+}$  should continue to be extruded into the interphotoreceptor space, continually increasing  $[Ca^{2+}]_o$  until the rate of  $Ca^{2+}$  diffusion to the overlying unstirred layer equals the rate of efflux from the cells. The fact that  $[Ca^{2+}]_o$  declines during illumination contradicts the model of light-evoked  $[Ca^{2+}]_i$

calcium release.

A decline in  $[Ca^{2+}]_i$ , and thus reduce  $Ca^{2+}$  extrusion, resulting from adaptation might be proposed to account for the declining  $[Ca^{2+}]_o$ . The rate of decline, however, was independent of supersaturating irradiances that should have affected adaptation rates. Again, this phenomena was more consistent with the balance  $Ca^{2+}$  flux model, where a finite amount of  $[Ca^{2+}]_i$  is rapidly extruded into the interphotoreceptor space. In this model, the decline in  $[Ca^{2+}]_o$  with continued photostimulation results from  $Ca^{2+}$  diffusion into the overlying bath after the  $Ca^{2+}$  efflux from rods has approached zero.

During post-stimulus recovery,  $[Ca^{2+}]_o$  decreases below baseline levels in a prominent undershoot (see Figs. 9 & 10). In the light-evoked  $[Ca^{2+}]_i$  increase model, it was proposed that the integral of this undershoot equaled the integral under the increased light-evoked  $[Ca^{2+}]_o$  curve. This model proposed that  $Ca^{2+}$  extruded into the interphotoreceptor space during stimulation had to be replaced after stimulation. Postulating this mechanism to explain the undershoot required that all of the  $Ca^{2+}$  extruded from the photoreceptors diffuse out of the interphotoreceptor space prior to the end of stimulation. Clearly this does not happen, as the voltage traces in Fig. 9 clearly show voltage recovery preceding even the beginning of  $[Ca^{2+}]_o$  recovery by up to two seconds during brighter flashes. Furthermore, for steps of illumination, the areas under the increased  $[Ca^{2+}]_o$  curve greatly exceed the area under the undershoot curve. Furthermore, the area of the undershoot curve depends only weakly on the duration of the light step.

These results, too, are more consistent with a finite  $[Ca^{2+}]_i$  concentration being pumped into the extracellular space, which only slowly diffuses away. The undershoot, then, is still slightly dependent on stimulus duration, as the area under the undershoot part of the curve should equal the amount of  $Ca^{2+}$  which as diffused away during stimulation, which is far less than the area under the increased  $[Ca^{2+}]_o$  part of the  $[Ca^{2+}]$ -time curve.

The equal flux hypothesis can be directly tested in other ways. If  $g_{hv}$  can be increased, it should cause  $[Ca^{2+}]$  to decrease, as the  $Ca^{2+}$  influx into rods exceeds the  $Ca^{2+}$  efflux. This was accomplished by using the cGMP phosphodiesterase inhibitor, IBMX, to increase

$g_{hv}$ . The expected results occurred. Extracellular  $[Ca^{2+}]$  transiently decreased for a period of several minutes, before eventually returning to near baseline levels. Furthermore, the  $V_{Ca^{2+}}$  photoresponses increased greatly in magnitude, duration and rate of rise. The increased rate of rise and magnitudes are consistent with an increase in the  $Ca^{2+}$  efflux which occurs when  $Ca^{2+}$  influx through  $g_{hv}$  is decreased by photostimulation. The fall in dark-adapted  $V_{Ca^{2+}}$  is consistent with  $Ca^{2+}$  influx exceeding efflux during IBMX superfusion, and supports the claims that  $g_{hv}$  is both sensitive to IBMX (as a result of increased  $[cGMP]_i$ ) and permeable to  $Ca^{2+}$ . The increased  $V_{Ca^{2+}}$  photoresponses are inconsistent with IBMX inhibiting  $Ca^{2+}$  extrusion. Instead, IBMX appears to enhance  $Ca^{2+}$  extrusion by building up  $[Ca^{2+}]_i$ . Independent experiments by others using  $Ca^{2+}$ -sensitive dyes have shown that IBMX loads photoreceptors with  $Ca^{2+}$  (McNaughton et al, 1986), consistent with the above interpretation. The results just described provide evidence that the increase in  $[Ca^{2+}]_i$  caused by IBMX results primarily via an increase in  $g_{hv}$ . These results further support the dual  $Ca^{2+}$  flux model by showing that increasing  $g_{hv}$  decreases  $V_{Ca^{2+}}$ .

A large increase in the durations of both  $V_{Ca^{2+}}$  and  $V_m$  photoresponses occurred during IBMX superfusion. This duration increase probably results from the increased  $[Ca^{2+}]_i$  caused by IBMX. Increased  $[Ca^{2+}]_i$  has been shown to delay recovery from photostimulation by several groups (Bastian and Fain, 1979; Matthews et al, 1988; Nakatani and Yau, 1988b). This delay in recovery has been proposed to result from either an inhibitory action of  $[Ca^{2+}]_i$  on guanylate cyclase activity, or an inhibition of the decay of photoexcited phosphodiesterase (see Sections 1.1,1.3), and possibly both. The durations of the photoresponses continued to increase during the time  $V_{Ca^{2+}}$  remained below baseline. In other experiments, the response durations shortened when the intervals between flashes were decreased, thus allowing less time for  $Ca^{2+}$  accumulation in the cells, consistent with the duration increase being caused by increased  $[Ca^{2+}]_i$ .

These results provided some insight into IBMX effects on rod photoreceptors, which was an interesting aside to the thesis research. The above results combined with the

results of others cited, can be cast into the following model explaining the effects of IBMX in photoreceptors: IBMX decreases the basal activity of cGMP phosphodiesterase in dark adapted photoreceptors. Continued guanylate cyclase production out paces cGMP degradation by the phosphodiesterase, increasing  $[cGMP]_i$  and the cGMP-sensitive conductance,  $g_{hv}$ . The increase in this  $Ca^{2+}$  permeable conductance allows  $Ca^{2+}$  influx to exceed  $Ca^{2+}$  efflux temporarily. Since  $[cGMP]_i$  will continue to rise until its synthesis and degradation are equal, a new steady state will be reached only when  $[Ca^{2+}]_i$  inhibits guanylate cyclase sufficiently to match the IBMX-inhibited phosphodiesterase activity.

The drug IBMX is a competitive inhibitor of phosphodiesterase, so the increasing  $[cGMP]_i$  should increase the rate of cGMP degradation, helping to restore the equilibrium. Once  $[cGMP]_i$  has stabilized,  $[Ca^{2+}]_i$  can again reach a steady state when  $Ca^{2+}$  efflux again equals  $Ca^{2+}$  influx. The apparent equilibrium potential of  $g_{hv}$  is about 0 mV (Fesenko et al, 1985; Cervetto et al, 1977; Bader et al, 1979). With large increases in  $g_{hv}$ , rod  $V_m$  should stabilize at about this voltage. In actuality, it stabilized a few mV positive (see Fig. 12). With  $10^{-4}$   $[Ca^{2+}]_o$  bathing the retina,  $[Ca^{2+}]_i$  would have to reach nearly  $10^{-4}$  M before  $Ca^{2+}$  influx would cease. At this stable voltage,  $Ca^{2+}$  influx per unit conductance decreases logarithmically with intracellular concentration. If  $[cGMP]_i$  levels stabilize, the increasing  $[Ca^{2+}]_i$  contributes to reductions in the  $Ca^{2+}$  influx.

The photoreceptors should reach a new steady-state level of  $[Ca^{2+}]_i$  eventually, even if the negative feedback is insufficient to compensate for the IBMX-induced inhibition of phosphodiesterase. The large increase in  $[Ca^{2+}]_i$  resulting from the IBMX treatment then alters the photoresponses of the cells. Since 500  $\mu$ M IBMX does not completely inhibit phosphodiesterase, bright flashes can activate enough phosphodiesterase to hydrolyze the excess cGMP and produce a photoresponse. To decrease  $[cGMP]_i$ , the activity of the phosphodiesterase needs only to exceed the  $[Ca^{2+}]_i$ -inhibited activity of guanylate cyclase. The light-evoked increase in phosphodiesterase activity can apparently exceed guanylate cyclase activity and produce a photoresponse. The large amount of  $[Ca^{2+}]_i$  in the photoreceptors must be lowered substantially before guanylate cyclase activity can exceed

phosphodiesterase and allow the cell to begin to depolarize.

The results shown in Fig. 14 showed that stopping  $\text{Ca}^{2+}$  efflux by blocking  $\text{Na}^+/\text{K}^+/\text{Ca}^{2+}$  exchange decreased  $V_{\text{Ca}^{2+}}$  while eliminating  $V_{\text{Ca}^{2+}}$  photoresponses. The dual  $\text{Ca}^{2+}$  flux model predicts a decrease in  $V_{\text{Ca}^{2+}}$  when  $\text{Ca}^{2+}$  extrusion from rods is blocked, since it leaves  $\text{Ca}^{2+}$  influx into rods temporarily unopposed. The elimination of  $V_{\text{Ca}^{2+}}$  photoresponses, contrarily, requires a decrease in  $g_{\text{h}\nu}$ . Increasing  $[\text{Ca}^{2+}]_i$  by many methods has been shown to block  $g_{\text{h}\nu}$ . That this occurred under these experimental conditions is shown by the  $V_m$  record in Fig. 15. Others have shown that blocking  $\text{Na}^+/\text{K}^+/\text{Ca}^{2+}$  exchange leads to a buildup of  $[\text{Ca}^{2+}]_i$ , which then shuts down  $g_{\text{h}\nu}$  (Bastian & Fain, 1982b; Yau & Nakatani, 1984a).

Figures 14 and 15 also show that the effects of  $\text{Li}^+/\text{Na}^+$  replacement can be partially reversed by adding 500  $\mu\text{M}$  IBMX to the superfusate. Under these conditions,  $\text{Ca}^{2+}$  influx into photoreceptors is maintained, yet  $\text{Ca}^{2+}$  efflux is blocked. The dual flux model would predict a peculiar  $V_{\text{Ca}^{2+}}$  photoresponse under such conditions. Opening  $g_{\text{h}\nu}$  during blockage of  $\text{Ca}^{2+}$ -extrusion should turn the photoreceptors into  $\text{Ca}^{2+}$  sinks, decreasing  $V_{\text{Ca}^{2+}}$ . Closing  $g_{\text{h}\nu}$  again, then, by light stimulation, should stop the influx of  $\text{Ca}^{2+}$  into the photoreceptors, allowing  $V_{\text{Ca}^{2+}}$  to return to bath levels, but not to exceed it. This prediction is in approximate agreement with the results shown in Fig. 14.

The presence of IBMX during blockage of  $\text{Ca}^{2+}$  extrusion again greatly prolonged the durations of both  $V_m$  and  $V_{\text{Ca}^{2+}}$  photoresponses. Conversely reactivating  $\text{Ca}^{2+}$  extrusion by returning  $\text{Na}^+$  to replace  $\text{Li}^+$  in the superfusate shortened the duration of the photoresponses ( $V_m$  shown in Fig. 15;  $V_{\text{Ca}^{2+}}$  not shown).

Since IBMX increased  $\text{Ca}^{2+}$  fluxes, its presence amplified the effects of blocking  $\text{Na}^+/\text{K}^+/\text{Ca}^{2+}$  exchange, as was seen in Fig. 16. It enhanced the resulting decrease in  $V_{\text{Ca}^{2+}}$  caused by blocking  $\text{Ca}^{2+}$  efflux and leaving the  $\text{Ca}^{2+}$  influx unopposed. Blocking  $\text{Ca}^{2+}$  efflux in the presence of IBMX, then, turns the photoreceptors into a large  $\text{Ca}^{2+}$  sink. Reactivating  $\text{Ca}^{2+}$  efflux by returning  $\text{Na}^+$  for  $\text{Li}^+$  in superfusates caused a remarkable increase in  $V_{\text{Ca}^{2+}}$  as the large stores of  $[\text{Ca}^{2+}]_i$  were pumped into the interphotoreceptor



space (see Fig. 16, second box).

In summary, the data from  $\text{Ca}^{2+}$ -selective electrode measurements of  $[\text{Ca}^{2+}]_o$  are in good agreement with the dual  $\text{Ca}^{2+}$  flux model of photoreceptors. Extracellular  $\text{Ca}^{2+}$  measurements now provide a means of distinguishing changes in  $\text{Ca}^{2+}$  influx resulting from increased permeability, from changes in  $\text{Ca}^{2+}$  efflux resulting from blockade of  $\text{Na}^+/\text{K}^+/\text{Ca}^{2+}$  exchange, and thus provide a means of evaluating the effects of colchicine.

*Section 4.2.2. Colchicine-evoked increases in  $[\text{Ca}^{2+}]_o$  can be attributed to a release of  $\text{Ca}^{2+}$  from internal stores.*

The introduction of 10 mM colchicine increased  $V_{\text{Ca}^{2+}}$  and essentially eliminated  $V_{\text{Ca}^{2+}}$  photoresponses. Colchicine's effects on  $V_{\text{Ca}^{2+}}$  are not consistent with the drug having an ionophore-like action, which should have lowered  $V_{\text{Ca}^{2+}}$ , or with the drug blocking  $\text{Na}^+/\text{K}^+/\text{Ca}^{2+}$  exchange, which also should have lowered  $V_{\text{Ca}^{2+}}$ , as discussed in the preceding section. Colchicine's results are most consistent with colchicine blocking  $g_{\text{hV}}$ , thus stopping  $\text{Ca}^{2+}$  influx, raising  $V_{\text{Ca}^{2+}}$  and stopping  $V_{\text{Ca}^{2+}}$  photoresponses. Increasing  $\text{Ca}^{2+}$  fluxes by the addition of IBMX made colchicine's effects more pronounced, but did not alter the direction of the effects.

It still remains to be explained, then, why colchicine's effects resemble increased  $[\text{Ca}^{2+}]_i$ . As previously stated in Section 4.1, the effects of colchicine might be explainable by a release of  $\text{Ca}^{2+}$  from internal stores. It was previously stated that  $V_{\text{Ca}^{2+}}$  normally rises, then slowly decreases during light steps, but in the presence of colchicine, the rapid increase in  $V_{\text{Ca}^{2+}}$  is followed by a slow increase, that continues until colchicine is removed. As previously stated, this result is attributed to a colchicine-evoked release of  $\text{Ca}^{2+}$  from internal stores. This hypothesis will now be treated more quantitatively.

As described in Section 1.3, total intracellular  $\text{Ca}^{2+}$  in rod outer segments is more than 1 mM, yet  $[\text{Ca}^{2+}]_i$  is less than 1  $\mu\text{M}$ , and most intracellular  $\text{Ca}^{2+}$  remains bound and relatively non-exchangeable inside the lamellar disks. If colchicine has the effects of releasing significant amounts of  $\text{Ca}^{2+}$  from intracellular stores, it probably releases  $\text{Ca}^{2+}$

from the disks. Some estimates of the feasibility of this action by colchicine can be made.

The hyperpolarizing effects of colchicine have been observed for long periods of time, up to 20 minutes. Thus the reservoir of  $\text{Ca}^{2+}$  released by colchicine must be capable of supplying ample  $\text{Ca}^{2+}$  to inhibit  $g_{\text{hv}}$  for this length of time. An estimate of the  $\text{Ca}^{2+}$  efflux from toad rods can be made assuming  $\text{Ca}^{2+}$  influx and efflux are equal in dark adapted rods. Assuming the dark current in toads is 20 pA (see Korenbrot, 1985 for a review), and that 15% of this current is carried by  $\text{Ca}^{2+}$  (see Section 1.1 - 1.2), the efflux of  $\text{Ca}^{2+}$  from a rod is about 3 pA or  $9.36 \times 10^6 \text{ Ca}^{2+}$  ions/s. It is difficult to estimate the percentage of the dark current that 10 mM colchicine blocks from voltage measurements, but it is reasonable, from the experimental data presented, to assume a value between 30% and 50%. It is equally difficult to estimate the average  $[\text{Ca}^{2+}]_i$  required to produce this inhibition, but comparing the effects of 10 mM colchicine to the results using  $\text{Ca}^{2+}$  ionophores by others (Bastian & Fain, 1979), it is reasonable to estimate that at least  $10^{-5} \text{ M } [\text{Ca}^{2+}]_i$  is needed to produce the inhibitory effects of colchicine (**Note:**  $\text{Ca}^{2+}$  ionophores make the cell membrane essentially "transparent" to  $\text{Ca}^{2+}$ , such that  $[\text{Ca}^{2+}]_i \cong [\text{Ca}^{2+}]_o$ , and Bastian & Fain demonstrated attenuating effects with  $10^{-5} \text{ M } [\text{Ca}^{2+}]_o$  in the presence of ionophore similar to the effects of 10 mM colchicine. This would be a change in  $[\text{Ca}^{2+}]_i$  of 1-2 log units, which seems reasonable for this magnitude of attenuation, based on calcium's inhibitory effects on cGMP synthesis. see Chapter 1). From the data of others quantitating the  $\text{Ca}^{2+}$ -sensitivity of  $\text{Na}^+/\text{K}^+/\text{Ca}^{2+}$  exchange, (Gill et al, 1984), this increase in  $[\text{Ca}^{2+}]_i$  would increase  $\text{Ca}^{2+}$  efflux by ~50%, or raise total efflux to  $14 \times 10^6$  ions/s. Calcium influx falls to  $6.24 \times 10^6$  ions/s, leaving a net efflux of  $7.76 \times 10^6 \text{ Ca}^{2+}$  ions/s. Estimating rod size to be  $6 \mu\text{m} \times 60 \mu\text{m}$ , and assuming that one half of the rod volume is taken up by disks, this extrusion of  $\text{Ca}^{2+}$  ( $1.55 \times 10^{-17}$  moles  $\text{Ca}^{2+}$  /s +  $8.48 \times 10^{-13}$ ) leads to a decline in  $[\text{Ca}^{2+}]_i$  of  $15.2 \mu\text{M/s}$ . The hyperpolarizing effects of 10 mM colchicine in  $0.9 \text{ mM } \text{Ca}^{2+}$  have been observed to remain essentially stable for as long as 20 min. If colchicine's hyperpolarizing effects are attributable only to increased  $[\text{Ca}^{2+}]_i$  released from stores, the total  $\text{Ca}^{2+}$  content of rods during a 20 min. period would fall by 18.2 mM which exceeds the total  $[\text{Ca}^{2+}]_i$  in

rods (see Section 1.3; Schnetkamp, 1985). There are other mechanistic problems associated with colchicine's effects being solely due to  $\text{Ca}^{2+}$  released from stores. Colchicine reduces cGMP-sensitive ion permeabilities in plasma membranes, and does not act as a  $\text{Ca}^{2+}$  ionophore. How, then would colchicine release intradiskal  $\text{Ca}^{2+}$ , which is bound tightly to phosphatidyl serine, and can only be released by ion exchange when disk membranes are permeabilized? Furthermore, colchicine does not directly alter phospholipid membrane fluidity (see subsection 1.4.1), although  $\text{Ca}^{2+}$ -releasing effects of colchicine from phosphatidyl serine membranes have not been studied *per se*. Nevertheless, even if colchicine reduced the binding of  $\text{Ca}^{2+}$  to the membrane, the relative disk impermeability to  $\text{Ca}^{2+}$  must be overcome. Thus colchicine would have to increase disk permeability anyway, and would have to act on some as yet unidentified protein channel in the disk. Although the data above are consistent with a colchicine-evoked  $\text{Ca}^{2+}$  release from internal stores, this cannot be the only mechanism for colchicine's effects. Alternatively, colchicine could have  $\text{Ca}^{2+}$  agonistic effects on cellular proteins regulating cGMP or  $g_{\text{HV}}$ , and release a high percentage of bound non-diskal  $\text{Ca}^{2+}$ .

Because tubulin has both low and high affinity  $\text{Ca}^{2+}$  binding sites, it is reasonable to suspect that colchicine might release  $\text{Ca}^{2+}$  from tubulin. *In vitro* studies, however, have shown that colchicine does not affect  $\text{Ca}^{2+}$ -tubulin binding. Furthermore,  $\text{Ca}^{2+}$ -tubulin binding is virtually non-existent under *in vitro* conditions that resemble intracellular conditions ( $>100$  mM KCl,  $<1$  mM  $\text{Mg}^{2+}$ ). Finally, the amount of tubulin estimated to be in rod outer segments is about 0.01 mM. In order for tubulin to have enough bound  $\text{Ca}^{2+}$  to release for satisfying the electrophysiological effects of colchicine, it would have to have about all of the low-affinity binding sites saturated ( $K_{\text{d}} 2.5 \times 10^{-4}$  M), which could not occur under intracellular conditions ( $< 10^{-6}$  M  $\text{Ca}^{2+}$ ) without some unexplained major increase in the binding affinity of these sites.

The colchicine-evoked  $\text{Ca}^{2+}$  release from intracellular stores probably requires an action of colchicine on a  $\text{Ca}^{2+}$  binding site other than tubulin, or some *in vivo* condition that dramatically alters tubulin's pharmacology. The hypothesis that colchicine releases  $\text{Ca}^{2+}$

from internal stores, then, is not as gratifying or as interpretable as could be hoped. Because of the indirect nature of the evidence leading to a colchicine-evoked  $\text{Ca}^{2+}$  release, and the complexity in attributing a known action of colchicine to this effect, further evidence confirming these results should be pursued by biochemical and other physiological means.

The model just discussed estimates that the colchicine-evoked net efflux of  $\text{Ca}^{2+}$  is very near normal light-evoked net  $\text{Ca}^{2+}$  efflux, despite an approximately 10-fold increase in  $[\text{Ca}^{2+}]_i$ . This estimate can explain why the colchicine-evoked  $V_{\text{Ca}^{2+}}$  increases were not demonstrably larger than light-evoked  $V_{\text{Ca}^{2+}}$  increases. Release of  $\text{Ca}^{2+}$  from internal stores, however, would explain why  $V_{\text{Ca}^{2+}}$  increased during and after steps of illumination, when normally  $V_{\text{Ca}^{2+}}$  decreases during these periods. Calcium released from stores would maintain a more constant  $\text{Ca}^{2+}$  efflux during illumination, replacing extracellular  $\text{Ca}^{2+}$  that diffuses away into the overlying bath.

It is interesting to note that the post-stimulus recovery of  $V_m$  was slowed by 10 mM colchicine applied in 0.1 mM  $\text{Ca}^{2+}$ , whereas 10 mM colchicine had little effect on post-stimulus recovery when applied in 0.9 mM  $\text{Ca}^{2+}$  baths (compare Fig. 20 to Fig. 6). The experiments were not performed in the same retina, so a clear comparison cannot be made, but the differences might have resulted from the relative differences in the time of colchicine application. In the experiment shown in Fig. 20, colchicine was applied before the light-stimulus was introduced, whereas in Fig. 6, colchicine was applied after light stimulation. If colchicine's effects are  $\text{Ca}^{2+}$ -sensitive, then colchicine would be more likely to affect rod physiology when introduced before light stimulation, since during light stimulation  $\text{Ca}^{2+}$  falls to  $<10^{-8}$  M.

The absence of a post-stimulus undershoot of  $V_{\text{Ca}^{2+}}$  during colchicine superfusion should also be explained. The rapid post-stimulus decrease in  $V_{\text{Ca}^{2+}}$  requires  $\text{Ca}^{2+}$  influx to exceed  $\text{Ca}^{2+}$  efflux. Normally, after more than 20-s of stimulation,  $\text{Ca}^{2+}$  efflux is near zero (Miller and Korenbrot, 1987). Thus, the rapid opening of  $g_{\text{h}\nu}$  results in an unopposed  $\text{Ca}^{2+}$  influx. The presence of colchicine, however, could keep  $\text{Ca}^{2+}$  efflux

elevated (say 2 - 3 pA of  $\text{Ca}^{2+}$ ) while reducing the  $\text{Ca}^{2+}$  influx that occurs during post-stimulus recovery, leaving a small net efflux of  $\text{Ca}^{2+}$  that continues to elevate  $V_{\text{Ca}^{2+}}$ .

In summary, the results obtained measuring colchicine-evoked  $[\text{Ca}^{2+}]_o$  changes are consistent with a  $\text{Ca}^{2+}$  release from internal stores. The release of  $\text{Ca}^{2+}$ , however, is probably insufficient to account for colchicine's effects alone, although it may be contributory.

#### 4.2.3: Colchicine's effects on low $[\text{Ca}^{2+}]_o$ -evoked desensitization.

As shown in Fig. 29, lowering  $[\text{Ca}^{2+}]_o$  below  $10^{-6.5}$  M desensitizes rods after several minutes. Including colchicine in low- $[\text{Ca}^{2+}]_o$  baths clearly slows the desensitization process. Desensitization can be demonstrated in two ways: either the decline in photoresponse amplitude with a flash of constant irradiance, or the requirement for greater stimulation (high irradiance) to produce a photoresponse of the same amplitude. When flashes of equal irradiance are given, the time-to-peak of photoresponses are also slowed, while recovery from stimulation speeds up. Colchicine inhibits these effects as well (Fig. 29). Any effect of colchicine which inhibits the decline of  $[\text{Ca}^{2+}]_i$  should slow desensitization.

Since  $[\text{Ca}^{2+}]$  has a direct inhibitory action on  $g_{\text{hV}}$ , however, there is some concern about whether desensitization can be attributed to changes in  $[\text{Ca}^{2+}]_i$ , or whether it results from the channel inhibition of  $[\text{Ca}^{2+}]_o$ . The change in kinetics observed with desensitization are more consistent with desensitization resulting from  $[\text{Ca}^{2+}]_i$  effects. External effects of lowering  $[\text{Ca}^{2+}]_o$  result in the increase in unitary channel conductance. Channel opening is still controlled by  $[\text{cGMP}]_i$ , so although the current through the open channels in the dark increase, the mean number of open channels remains the same. These channels close when  $[\text{cGMP}]_i$  falls to sufficiently low levels such that the number of cGMP-bound channels is near zero. If  $[\text{cGMP}]_i$  were unaffected by  $[\text{Ca}^{2+}]_o$ , the rate of  $[\text{cGMP}]$  decrease would remain the same, leaving the time-to-peak unaltered. Furthermore, with a higher unitary conductance, the total current and voltage change for

closure of a given number of channels should increase, not decrease. Finally, desensitization requires up to 10 minutes for completion, yet measurements of solution change times showed solution changes to be 90% complete in less than 2 minutes. This means that desensitization lagged the solution change by several minutes. Thus, desensitization is most likely the result of decreased  $[Ca^{2+}]_i$ , not  $[Ca^{2+}]_o$ , and the inhibition of desensitization by colchicine is consistent with colchicine's inhibition of decreased  $[Ca^{2+}]_i$ .

The desensitization-inhibiting effects of colchicine may alternatively be partially explainable in terms of reduced  $g_{hv}$ . The low- $[Ca^{2+}]_o$  conditions required to produce desensitization actually reverse the  $Ca^{2+}$  gradient between the intracellular and extracellular environment. If colchicine blocks the channel, it would reduce  $Ca^{2+}$  efflux into the extracellular space through  $g_{hv}$  under these conditions. Coupled with a small release of  $Ca^{2+}$  from intracellular stores, colchicine could, then, slow the decline in  $[Ca^{2+}]_i$ .

The effects of colchicine on both kinetics and amplitudes at low  $[Ca^{2+}]_o$  are consistent with a colchicine-evoked increase in  $[Ca^{2+}]_i$ . Colchicine slows the low- $[Ca^{2+}]_o$  induced increase in time-to-peak, as does holding  $[Ca^{2+}]_o$  above  $10^{-6.5}$  M, and both treatments inhibit the decline in photoresponse amplitudes.

In several experiments, application of 20 mM colchicine partially and temporarily reversed some effects of desensitization. A typical example was shown in Fig. 30. Colchicine also hyperpolarized the rods a few mV as well. Colchicine's effects under these conditions are not consistent with a channel blocking effect of colchicine, alone. At these low extracellular  $Ca^{2+}$  concentrations, there should be no  $Ca^{2+}$  influx into rods, and intracellular  $Ca^{2+}$  was already low enough that desensitization had occurred. A simple reduction of  $Ca^{2+}$  efflux could not have increased  $[Ca^{2+}]_i$ , and subsequently, reversed desensitization. These results, then are consistent with a release of  $Ca^{2+}$  from internal stores, which may act synergistically with other actions of colchicine.

When  $[Ca^{2+}]_o$  is lowered to  $10^{-6}$  -  $10^{-6.5}$  M, rods depolarize but do not desensitize, thus producing large responses as shown in Fig. 31. Applying 10 mM colchicine to the retina

hyperpolarized the cells. The steady-state voltage reached during colchicine superfusion was depolarized slightly from control conditions, yet the  $V_m$  photoresponses were attenuated compared to control responses. The time-to-peak of the responses may have been delayed slightly compared to controls. This may be partially explained by external divalent ion effects as follows: lowering  $[Ca^{2+}]_o$  leads both to elevation of  $[cGMP]_i$ , increasing the number of open channels (Detwiler et al, 1989a), and to an increase in the unitary conductance (Matthews, 1986; Stern, 1986). If the effects of colchicine result from increased  $[Ca^{2+}]_i$  alone, then the  $[Ca^{2+}]_i$  required to reach a  $g_{hv}$  similar to control conditions under colchicine and low  $[Ca^{2+}]_o$  conditions would have to be elevated relative to control conditions. In other words, fewer channels would have to be opened relative to control conditions, to compensate for the greater unitary conductance. Thus  $[Ca^{2+}]_i$  would necessarily be greater than under control conditions, and the increased  $[Ca^{2+}]_i$  would cause a delay in the time-to-peak of responses. Alternatively, a non- $Ca^{2+}$  dependent  $g_{hv}$  decrease caused by lowering cGMP would have similar effects, whereas a direct channel-blocking effect by colchicine would tend to counter the requirement for sub-normal cGMP levels.

As a second alternative explanation, colchicine may simply inhibit light-evoked activation of phosphodiesterase, but this would not explain why colchicine speeds time-to-peak in low- $[Ca^{2+}]_o$  desensitized rods.

It is interesting to note that the photoresponse attenuating effects do not correlate with  $V_m$ . If colchicine's effects were solely attributable to increase  $[Ca^{2+}]_i$ , then one might expect that the attenuation would correlate with  $V_m$ . Actually, the attenuating effects of colchicine should correlate with  $[cGMP]_i$  and  $[Ca^{2+}]_i$ . Since lowering  $[Ca^{2+}]_o$ , as discussed above, not only raises  $[cGMP]_i$ , but also increases the unitary conductance, lower  $[cGMP]_i$  levels are required to produce the same  $V_m$ . It is possible that the attenuation of the responses results from lower  $[cGMP]_i$  levels. This can be seen from the differential equation governing  $[cGMP]$  changes:

$$\frac{d[\text{cGMP}]}{dt} = C1 - k2 [\text{PDE}^*] [\text{cGMP}]$$

(This equation is derived in the Appendix under Derivation 2. see also: Kawamura & Murakami, 1986; Hodgkin & Nunn, 1988. The grouping and labeling of constants is arbitrary, but reflects the authors preferences when this equation is derived from the chemical equations. See also Illus. 7). Where C1 is a constant rate of cGMP formation resulting from the saturating level of GTP in photoreceptors, and PDE\* is the active pool (concentration) of phosphodiesterase. For the sake of argument, C1 can be considered lower during colchicine superfusion than in control solution, leaving the steady state level of  $[\text{cGMP}]_i$  lower. The ramifications of this function can be understood using the rate plot in Illus. 7. The rate of change of cGMP is shown plotted vs. the level of cGMP. The slope of the line is  $k2[\text{PDE}^*]$ , while the intercepts are C1a and C1b, the rate of formation of cGMP by guanylate cyclase during control and colchicine superfusion. During steady-state conditions, the rate of change is, by definition, zero. A flash of light produces a sudden, step-like rise in PDE\*, changing the slope, but not the intercept of the curves. Curves representing the equation for the new level of PDE activity are shown by the dotted lines. The rate of change in  $[\text{cGMP}]_i$  at this time can be found by tracing a vertical line between the stability points of the original curves, and where they intersect the new curves. Following this point horizontally to the y axis gives the rate of change of  $[\text{cGMP}]_i$ . By comparing the similar triangles it is easy to see that during colchicine application, the rate of change is markedly reduced. Thus, integration over a constant time period will produce a greater change in  $[\text{cGMP}]_i$  under control conditions, provided that colchicine does not affect the amount or time course of phosphodiesterase activated by light.

#### *4.2.4: Colchicine's effects on the kinetics of depolarizations resulting from EGTA injections.*

Colchicine strongly inhibited the ability of EGTA injections to depolarize rods. As shown in Sub-section 3.3.3, colchicine reduced the amplitude of depolarizations caused by EGTA injections and slowed the recovery rate. It was shown in Figs. 26 & 27 that colchicine



**Illustration 7.** *Rate plots of the equation governing cGMP formation by guanylate cyclase and degradation by phosphodiesterase.*

The slope of the curve is  $k_2[\text{PDE}^*]$ , where  $\text{PDE}^*$  is phosphodiesterase activity and  $k_2$  is a rate constant. The line fits the nonhomogeneous equation (see text and Appendix, Derivation 2):

$$\frac{d[\text{cGMP}]}{dt} = C_1 - k_2 [\text{PDE}^*] [\text{cGMP}]$$

The equation is a parametrization of the more general form:

$$\frac{d[\text{cGMP}]}{dt} = g(t) - k_2 [\text{PDE}^*](t) [\text{cGMP}]$$

where guanylate cyclase activity and PDE activity are functions of time. At the steady state where the derivative is zero,  $[\text{cGMP}]$  is constant.

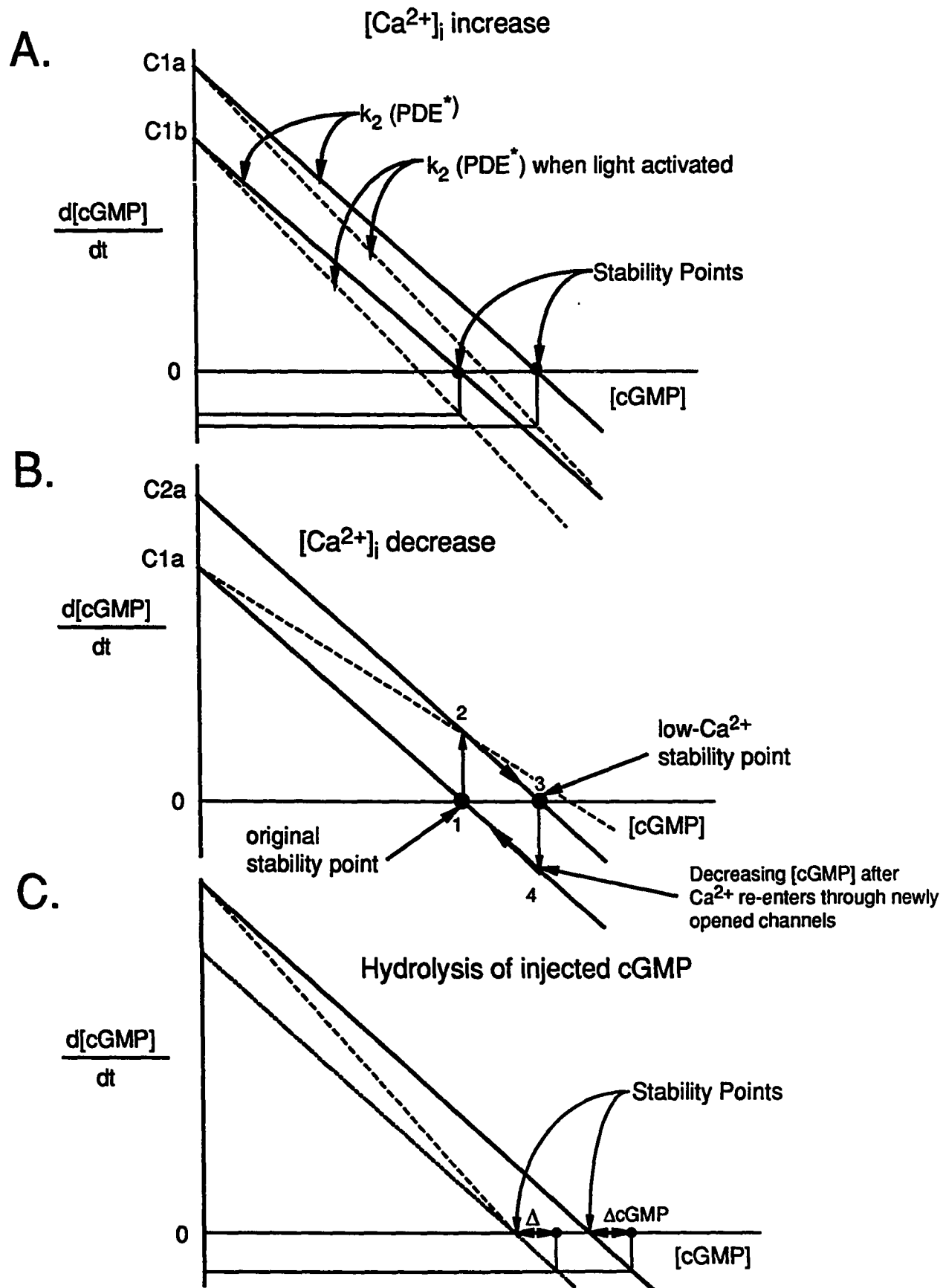


Illustration 7. Rate plots of the equation governing cGMP formation by guanylate cyclase and degradation by phosphodiesterase.

initially increased the rate of recovery before eventually slowing the recovery rate and attenuating the response.

Interpreting these results requires an understanding of the depolarizing effect of EGTA, which results from an increase in  $[cGMP]_i$ , which, in turn, results from a rate of cGMP synthesis that exceed degradation. A rate plot of the formula describing  $[cGMP]_i$  regulation is again useful in understanding the effects of colchicine. Illustration 7, together with Illus. 4, provide a pictorial means of understanding these results.

An injection of EGTA dramatically lowers a local concentration of  $[Ca^{2+}]_i$ , which causes a positive increase in the rate of  $[cGMP]$  formation, either by increasing guanylate cyclase activity or by decreasing phosphodiesterase activity. Either case leads to a net increase in  $[cGMP]_i$ , depolarizing the cell (point 3 on Illus. 7B). During the low- $[Ca^{2+}]_i$  condition,  $Ca^{2+}$  extrusion is essentially zero while  $Ca^{2+}$  influx is greatly increased, thus  $[Ca^{2+}]_i$  begins to accumulate and saturates the EGTA, resulting in decreased guanylate-cyclase activity or increased phosphodiesterase activity, which then begins to approach normal levels. Intracellular cGMP now exceeds the level required for stability (point 1 on Illus. 7B), thus  $[cGMP]_i$  levels decrease to the original stability point.

Intracellular buffering probably contributes negligibly to the effects of EGTA injections, as the  $K_d$  of the buffer sites is about the same as EGTA, and are saturated at normal  $[Ca^{2+}]_i$  (see Section 1.3). Furthermore,  $[Ca^{2+}]_i$  changes in rods appear to be almost exclusively controlled by  $Ca^{2+}$  fluxes across the membrane. Finally, increasing  $[Ca^{2+}]_o$ , which increases the rate of  $Ca^{2+}$  influx into rods, increases the recovery rate significantly, consistent with the proposition that EGTA saturation depends on  $Ca^{2+}$  influx.

The ability of a photostimulus to terminate EGTA-evoked depolarizations, when applied just after a pressure pulse, demonstrated that increased  $[cGMP]_i$  is responsible for the depolarizations. In the pulses shown in Fig. 25, injections during increased  $[Ca^{2+}]_o$  increased the depolarization caused by the injection. The rapid influx of  $Ca^{2+}$  during the depolarization appears to limit the extent of the depolarization, as judged by the narrowing of the depolarization peak (the depolarization does reach saturation). The larger voltage

responses obtained when EGTA is injected during increased  $[Ca^{2+}]_o$  can be attributed to non-linearities in the  $[Ca^{2+}]_i - V_m$  relationship. To understand this statement, one must first notice that the depolarizations in Fig. 25 do not reach saturation. The qualitative aspects of the relationship may be argued from the model discussed in the Appendix under Derivation 4 and in Baylor et al, 1984. The inner segment can be approximately described in this case as a passive circuit being driven by the dark current, which, in turn, is controlled by  $g_{hv}$ , which is, in turn, controlled by  $[cGMP]_i$ . Thus the change in voltage during EGTA injection,  $\Delta V$ , results from the change in  $g_{hv}$ ,  $\Delta g_{hv}$ . Although the passive circuit of the inner segment is time- and voltage-dependent, the changes resulting from EGTA injection are slow compared to the time constant of the conductances ( $> 10 \tau$ ), so the time-dependent aspects (modeled as an inductance in Baylor et al, 1984) may be ignored (consider  $L \cdot di/dt$  very small). The voltage-dependency of the conductances influences the waveform somewhat, but the effects are small above -40 mV, and a linear approximation can be made. Thus for a given  $\Delta g_{hv}$ , a given  $\Delta V$  should result. Since this is not the case, it is proposed that a given injection of EGTA,  $\Delta EGTA$ , produces a non-linear change in  $\Delta g_{hv}$ , which may result either from nonlinearities in the  $[cGMP]_i$  response to changes in  $[Ca^{2+}]_i$  or nonlinearities in the  $[cGMP]_i - g_{hv}$  relationship.

The results obtained from EGTA injection during increased  $[Ca^{2+}]_o$  help in interpreting the results observed when injections are made in the presence of colchicine. The first injection of EGTA following colchicine superfusion produced an increased voltage response, consistent with the response seen during increased  $[Ca^{2+}]_o$ . Likewise, the first EGTA injection following colchicine superfusion had a shortened duration and a slightly delayed peak time. Later EGTA injections had markedly attenuated responses with delayed peak times and increased durations.

The increased response during the first injection of EGTA, then, is similar to the change seen with increased  $[Ca^{2+}]_o$ , and both changes, then, might result from increased  $[Ca^{2+}]_i$  and non-linearities in the  $[Ca^{2+}]_i - V_m$  relationship as just discussed. The delay in peak-time during early colchicine superfusion could result from the inhibition of  $Ca^{2+}$  influx

resulting from the lower  $g_{hv}$  in the presence of increased  $[Ca^{2+}]_i$  caused by colchicine. This is in contrast with the more rapid influx of  $Ca^{2+}$  during increased  $[Ca^{2+}]_o$  superfusion. The increased recovery rate in the early EGTA injection, then, might result from an additional  $[Ca^{2+}]_i$  increase from internal storage release supplementing the influx of  $Ca^{2+}$  through  $g_{hv}$ .

As colchicine superfusion continued, the resulting depolarization caused by EGTA injections decreased, and the duration of the responses becomes increasingly longer. These results are more difficult to explain with a model using a release of  $[Ca^{2+}]_i$  from internal stores. The evolution of this pattern appears to coincide with colchicine's effects speeding the recovery of photostimulation, rather than the hyperpolarizing effect of colchicine. The slow recovery of the responses probably results from a reduced influx of  $Ca^{2+}$  that is not completely compensated for by the release of  $[Ca^{2+}]_i$  from internal stores, and the reduced  $Ca^{2+}$  influx is consistent with the reduced depolarization.

It was discussed previously that for colchicine's effects to be explainable by a release of internally stored  $Ca^{2+}$ , the rate of  $Ca^{2+}$  released by colchicine plus the entering  $Ca^{2+}$  would need to exceed the normal influx of  $Ca^{2+}$ . The minimal EGTA-evoked depolarization during colchicine superfusion should raise the  $Ca^{2+}$  influx to at least 1/2 the level of EGTA injections during control solutions. Assuming a factor of two increase in  $g_{hv}$  during EGTA injections in control solution, the total  $Ca^{2+}$  influx becomes the equivalent of 6 pA, whereas during colchicine superfusion, the total influx is 3 + 2.5 or 5.5 pA equivalents. Thus, the situation exists where the combined increase in  $[Ca^{2+}]_i$  resulting from colchicine-mediated  $Ca^{2+}$  release and from influx of  $Ca^{2+}$  through  $g_{hv}$  is less than the  $Ca^{2+}$  influx during control superfusion and EGTA injections. As long as the colchicine-evoked release of  $Ca^{2+}$  and the influx of  $Ca^{2+}$  through  $g_{hv}$  during the peak of the EGTA-evoked depolarization continue to exceed the  $Ca^{2+}$  influx during EGTA injections in control solutions, the recovery rate will continue to be greater under colchicine conditions than control conditions. Once the EGTA-evoked increase in  $g_{hv}$  during colchicine superfusion is insufficient to allow  $Ca^{2+}$  influx plus the colchicine evoked release of  $Ca^{2+}$  to be less than the  $Ca^{2+}$  influx during EGTA

injections in control solutions, the recovery rate would be slower than in the control conditions. This situation would occur when the colchicine-evoked release of  $\text{Ca}^{2+}$  begins to decrease. These results are consistent with a temporary release of  $\text{Ca}^{2+}$  from internal stores.

This argument hinges on the fact that the EGTA-evoked depolarization is slower in the presence of colchicine than control solutions, which is shown. Trying to interpret this effect in terms of increased  $[\text{Ca}^{2+}]_i$  is a more difficult process. It could be hypothesized that this effect results from nonlinearities in the  $[\text{Ca}^{2+}]_i$ -voltage relationship. There is as yet insufficient data to confirm or deny this. It is odd, however, that increased  $[\text{Ca}^{2+}]_i$  appears to increase the voltage response early during colchicine superfusion, but reduces the voltage response later. This result might be explainable if the range of the  $[\text{Ca}^{2+}]_i$  increase caused by colchicine were large, but this is unlikely, as it is inconsistent with the long-term effects of colchicine.

It is interesting that the varying effects of colchicine on EGTA-evoked voltage changes coincide with colchicine's duration-shortening effects, and it is interesting to speculate on a possible mechanism explaining the two effects. On one hand, colchicine reduces the ability of lowering  $[\text{Ca}^{2+}]_i$  to depolarize rods, which means that either colchicine acts at the channel level to reduce cGMP-sensitivity of the channels, or colchicine reduces cGMP formation in response to lowered  $[\text{Ca}^{2+}]_i$ . Arguments for and against the first hypothesis have been presented previously. The second hypothesis seems contradictory, in that colchicine speeds photoresponse recovery under normal under normal  $\text{Ca}^{2+}$  conditions, indicating colchicine frees rods from  $[\text{Ca}^{2+}]_i$  inhibition of  $[\text{cGMP}]_i$  increases, yet colchicine slows recovery from steps of illumination at lower  $\text{Ca}^{2+}$  concentrations, implying an inhibitory action by colchicine on  $[\text{cGMP}]_i$  increase.

Perhaps the most satisfying explanation for colchicine's effects on EGTA-induced depolarizations would be that colchicine causes a smaller change in  $[\text{Ca}^{2+}]_i$  caused by the EGTA injections. The easiest conceivable mechanism by which this could occur would be for colchicine to cause a significant change in internal buffering. Under such conditions,

the cell would be able to unload  $\text{Ca}^{2+}$  as it was extruded, and yet, injections of EGTA, instead of depleting all of the free  $[\text{Ca}^{2+}]_i$ , would acquire part of its  $\text{Ca}^{2+}$  from buffered  $[\text{Ca}^{2+}]_i$ , causing a smaller change in  $[\text{Ca}^{2+}]_i$ . Colchicine could change intracellular  $\text{Ca}^{2+}$  buffering either by altering the  $K_d$  of an existing buffer, or by making a previously inaccessible buffering site, such as the intradiskal space, accessible to cytoplasmic equilibration.

It is conceivable that a change in internal buffering caused by colchicine might explain the response shortening effect as well. Normally, during photostimulation,  $[\text{Ca}^{2+}]_i$  changes rapidly. Intracellular  $\text{Ca}^{2+}$  falls, resulting in an increased recovery rate, until entering  $\text{Ca}^{2+}$  slows the formation of cGMP by inhibiting guanylate cyclase, and perhaps maintaining PDE activity. Adding intracellular buffering to rods would lessen the fall in  $[\text{Ca}^{2+}]_i$ , and initially slow recovery. The buffer, on the other hand, would absorb entering  $\text{Ca}^{2+}$  late in recovery, and thus slow recovery inhibition by keeping  $[\text{Ca}^{2+}]_i$  temporarily lower than than normal. Unfortunately, this model cannot explain the persistent hyperpolarization caused by colchicine.

#### *4.2.5: Effects of colchicine on the recovery kinetics of cGMP-evoked depolarizations.*

The effect of colchicine, in some ways, resembles background illumination, which desensitizes photoresponses. This desensitization results from a simultaneous increase in both guanylate cyclase activity and phosphodiesterase activity. The increased guanylate cyclase activity actually results from lowered  $[\text{Ca}^{2+}]_i$  caused by the increase in phosphodiesterase activity, which lowers  $[\text{cGMP}]_i$ .

It seems plausible to consider whether colchicine's effects might result, then, from activation of phosphodiesterase. Several results, however, are inconsistent with this hypothesis. First of all, colchicine tends to increase the time-to-peak of photoresponses, which is opposite to the changes in time-to-peak caused by background illumination (Bastian and Fain, 1979). Furthermore, the colchicine-induced reduction in photoresponse recovery is little-affected by a 10-fold increase in irradiance, unlike background

illumination. Finally, an experiment performed to assay phosphodiesterase activity showed that colchicine affected this enzyme no more than blocking  $\text{Na}^+/\text{K}^+/\text{Ca}^{2+}$  exchange.

The results of this experiment were described in Section 3.7, and will be interpreted here with the assistance of the rate plot in Illus. 7C. It is helpful in understanding the results of cGMP injections by first considering the effects of phosphodiesterase and guanylate cyclase activities on  $[\text{cGMP}]_i$ . A lowered  $[\text{cGMP}]_i$  level can result from either an increase in phosphodiesterase activity, which affects the slope, but not the intercept of the rate plot, or reduced guanylate cyclase activity, which alters the intercept, but not the slope. Increased phosphodiesterase activity is indicated by the dashed line in Illus. 7C. Decreased guanylate cyclase activity is shown by the dotted line in Illus. 7C.

Injection of a constant number of moles of cGMP into rods results in a constant change in  $[\text{cGMP}]_i$  concentration in some localized area. This is shown by the  $\Delta [\text{cGMP}]$  marks beside the two stability points shown. The rate of decrease of  $[\text{cGMP}]_i$ , after an injection of  $\Delta \text{cGMP}$ , then, is located by moving vertically downward to the point of intersection with the curves. Since the decreased guanylate cyclase results in a parallel curve to the normalized curve, the rate at which the  $[\text{cGMP}]_i$  level recovers should be similar to the control injection, while the increase in phosphodiesterase activity results in a much faster rate of  $[\text{cGMP}]_i$  lowering.

There are some non-linearities to consider before applying these ideas to the data interpretation. First of all, the guanylate cyclase activity may not be constant during injection recovery, since the injected cGMP increases  $g_{\text{hv}}$ , resulting in  $\text{Ca}^{2+}$  influx into the cell which, in turn, inhibits guanylate cyclase activity. This results in an additional increase in the rate of change of  $[\text{cGMP}]_i$ . This increase will be the same at a given  $[\text{cGMP}]_i$  concentration regardless of whether phosphodiesterase activation or guanylate cyclase inhibition causes the original reduced steady-state  $[\text{cGMP}]_i$ . The result will, however, vary for different  $[\text{Ca}^{2+}]_i$  levels since the inhibitory action of  $[\text{Ca}^{2+}]_i$  is non-linear, and since the influx of  $\text{Ca}^{2+}$  depends on  $g_{\text{hv}}$ , which, in turn, depends on  $[\text{cGMP}]_i$ . This problem can be overcome partially by using saturating injections of cGMP, which would then assure that the



$\text{Ca}^{2+}$  influx is always the same. Unfortunately, the  $\text{Ca}^{2+}$  efflux will vary depending on the initial steady-state, so again different  $[\text{Ca}^{2+}]_i$  changes will be induced by the injections at different steady states.

One means of overcoming these difficulties is to compare effects at similar  $[\text{cGMP}]_i$  concentrations, which are reflected in similar voltages as long as the unitary conductances of  $g_{\text{hv}}$  remain fixed. The other non-linearity to consider in the recovery of cGMP injections is the cGMP-voltage relationship. The inner segment conductances are voltage-sensitive and thus influence the cGMP-voltage relationship. The net steady-state conductance of the inner segment currents map one-to-one with  $V_m$ , however; thus, at a given  $V_m$  their contribution is always the same, and thus  $g_{\text{hv}}$  sets the voltage of the cell (note, again, that the time-dependent effects of the inner segment conductances are ignored, as they are fast relative to the driving waveform. It may help to think of the outer segment as providing a driving voltage or current, that can be approximated by many small, voltage steps with durations of  $4\tau$ ,  $\sim 0.5$  s. Driving steps of this duration produce voltage changes approaching steady-state values. Thus the response is approximated by a series of voltage changes from one steady-state to another. Other arguments may be found under Derivation 4 in the Appendix.). Comparing  $[\text{cGMP}]_i$  recovery at similar steady-state voltages helps to overcome this problem, since  $[\text{cGMP}]_i$  maps one-to-one with  $g_{\text{hv}}$  and, thus, to  $V_m$  over nonsaturated ranges.

It is far more difficult to interpret the recovery to injections at different voltages, such as dark-adapted  $V_m$  in control solutions and  $V_m$  in light or colchicine-stimulation. Although constant phosphodiesterase activity at different voltages produces similar rates of  $[\text{cGMP}]_i$  decline, the rate of voltage change depends on the function of  $V_m$  (cGMP). Clear results can be interpreted only over the linear range (if there is one) of this relationship. This relationship has not been adequately determined to really justify quantitative comparison in this manner.

In Fig. 33, the effects on recovery of cGMP injections caused by activating phosphodiesterase with light are compared to the effects of colchicine and the effects of

blocking  $\text{Na}^+/\text{K}^+/\text{Ca}^{2+}$  exchange by replacement of  $\text{Na}^+$  with  $\text{Li}^+$ . Blocking  $\text{Na}^+/\text{K}^+/\text{Ca}^{2+}$  exchange enhanced recovery to about the same extent as 10 mM colchicine, whereas light stimulation dramatically increased the recovery rate. Guanylate cyclase activity has been shown to be very  $\text{Ca}^{2+}$ -sensitive, and it has been proposed that the activity of this enzyme increases as  $[\text{Ca}^{2+}]_i$  declines after photostimulation (see Section 1.3). After the initial increase in the injection recovery rate, prolonged stimulation caused the recovery rate to slow down, and  $V_m$  depolarized a few mV. This recovery of  $V_m$  has been attributed to increasing guanylate cyclase activity resulting from the light-evoked decrease in  $[\text{Ca}^{2+}]_i$ .

Importantly, the magnitude of this change, although opposite in direction, is roughly of the same magnitude as the changes in recovery rate caused by either blocking  $\text{Na}^+/\text{K}^+/\text{Ca}^{2+}$  exchange or by colchicine. All three change, then, might be attributable to  $\text{Ca}^{2+}$ -like changes. These results are consistent with the hypothesis that colchicine's effects on  $V_m$  recovery rate results from either increased  $[\text{Ca}^{2+}]_i$  or a  $\text{Ca}^{2+}$ -agonist effect of colchicine, rather than from a direct phosphodiesterase stimulatory effect by colchicine.

**Section 4.3:** *Effects of colchicine not attributable to increased  $[\text{Ca}^{2+}]_i$ ; colchicine may increase GTPase activity of transducin and inhibit the light-evoked enzymatic cascade.*

Still remaining unexplained, then, is why light responsiveness remains attenuated when  $[\text{Ca}^{2+}]_i$  is lowered in the presence of colchicine using intracellularly injected EGTA. This result probably suggests a separate effect by colchicine that does not result from increased  $[\text{Ca}^{2+}]_i$  or buffering changes. This effect is, in fact, more consistent with a colchicine-induced inhibition of PDE activation, which has been proposed by others (Caretta & Stein, 1986). These researchers used concentrations of colchicine similar to those used in this thesis, and they suspect that their results may have been caused by a direct action of colchicine on transducin (Peter Stein, personal communication). Evidence of colchicine binding to transducin has not been presented thus far.

Also of concern is the absence of any increase in the response duration caused by colchicine. Increases in  $[\text{Ca}^{2+}]_i$  typically cause an increase in the durations of responses,

as discussed previously. If colchicine caused  $[Ca^{2+}]_i$  to increase above normal levels, then it remains unanswered why the increased  $[Ca^{2+}]_i$  did not increase the response duration, which under these conditions, most likely results from reduced guanylate cyclase activity. Furthermore, under normal  $[Ca^{2+}]_o$  conditions, colchicine speeds response recovery, and under elevated  $[Ca^{2+}]_o$  conditions, this action is enhanced (compare Figs. 6 and 32). Even more puzzling is the fact that colchicine does not shorten the recovery from steps of illumination, but apparently, in fact, prolongs it during low  $Ca^{2+}$  superfusion (see Fig. 20). An attempt was made to explain this effect by changes in  $Ca^{2+}$  buffering, but these apparent contradictions might point to a second effect of colchicine that is  $Ca^{2+}$ -dependent, but not  $Ca^{2+}$  elicited.

The clearest evidence for a non- $Ca^{2+}$  mediated effect by colchicine comes from intracellular injections of EGTA during colchicine superfusion. This technique allows  $[Ca^{2+}]_i$  to be lowered in the presence of colchicine without the side effect of increasing the unitary conductance of cGMP-sensitive channels by lowering extracellular cations. Intracellular injections of EGTA were clearly capable of depolarizing rods in the presence of colchicine, although large doses were required. This depolarization should require that  $[cGMP]_i$  be raised to above normal levels if  $V_m$  is to be depolarized with respect to control conditions. Using arguments previously presented, this should enhance the photoresponses. Instead, it did not affect the response attenuating and recovery enhancing effects of colchicine. It might be argued that this result is an artifact resulting from network coupling, but the effects of network coupling are probably only noticeable at low flash irradiances under these conditions, where only a few photons/rod are administered. The hundreds of quanta per flash per rod administered during these mentioned experiments should have been enough to nearly shut down the dark current in each rod. Thus a rod whose voltage is elevated above the mean network voltage by increasing  $g_{hv}$  should have responded by marked hyperpolarization when  $g_{hv}$  was shut down. This was clearly accomplished in the very same rod when the retina was hyperpolarized by elevating  $[Ca^{2+}]_o$ . Chelating  $[Ca^{2+}]_i$  with EGTA reversed not only the hyperpolarizing effects of

elevated  $[Ca^{2+}]_o$ , but also reversed the photoresponse attenuating effects as well.

The inability of intracellularly injected EGTA to reverse colchicine's photoresponse attenuating effects was in agreement with the results obtained by lowering  $[Ca^{2+}]_o$ , which reversed the hyperpolarizing effects of colchicine, but not the response attenuating or shortening effects of colchicine (see Fig. 22). It was previously argued that the attenuating effects could have resulted from increased  $[Ca^{2+}]_i$  during colchicine and low  $[Ca^{2+}]_o$  superfusion. The results of EGTA injection, however, indicate that this is not the case. It can be seen that lowering  $[Ca^{2+}]_o$  and increasing flash irradiance did speed the time-to-peak of the responses, as well as increased the response amplitude to values near those of controls. Even the brighter flashes, however, did not increase response duration to control values, but removal of colchicine did. It is interesting that 10 fold brighter flashes, which normally increase the duration of the responses, had a relatively small effect, in this regard, during colchicine superfusion. It appears that colchicine, then, has a rate-limiting effect on the duration of the photoresponse that cannot be attributed to an increase in  $[Ca^{2+}]_i$ . These persistent effects of colchicine during low  $[Ca^{2+}]_o$  experiments also indicate that  $Ca^{2+}$  buffering may not be a satisfactory explanation for this effect.

It is also interesting to note that colchicine increases the GTPase activity of tubulin (see 1.4.4), a GTP-binding protein with inherent GTPase activity somewhat similar to transducin (Rasenick & Wong, 1988). It remains feasible, then, that colchicine may bind to transducin, and increase its GTPase activity. This is the rate-limiting step in the termination of phosphodiesterase activity, and thus such an effect by colchicine must remain a serious alternative explanation for the response-shortening action of this drug.

#### **Section 4.4** *Tubulin remains a plausible protein-mediator of colchicine's effects on rods.*

Because colchicine is best known for its tubulin binding characteristics, it is important to consider whether its effects on rods result from tubulin binding. It is almost certain that colchicine's effects are not mediated by microtubule disruption, since rod outer segment microtubules are resistant to this effect of colchicine (Kaplan, 1985; Besharse, 1988).

The concentration range of colchicine's effects on rods ( $10^{-4}$  -  $10^{-2}$  M) is large when compared to colchicine's tubulin-binding properties ( $K_d = 10^{-6}$  M). This result is difficult to interpret, since in these experiments there was no way of knowing the actual intracellular concentration of colchicine. With regard to this fact, it is interesting to note that the drug diltiazem has high-affinity effects on isolated membrane patches, yet mM doses are required to produce measurable effects *in situ* (see 1.1.2).

Furthermore, tubulin-binding by colchicine is very time and temperature dependent, and can take up to several hours to reach equilibrium (see Section 1.4, also Wilson, 1976; Borisy and Taylor, 1976). Optimum binding is typically at 37° C, which is more than 10° C higher than experimental conditions. As discussed in Section 1.4, the time dependency of colchicine's binding to tubulin results from a conformational change necessary for the binding of both ligands. Each independent ligand is capable of binding to tubulin with a low affinity. Normally, the tropolone ring binds to tubulin, and following a conformational change, the trimethoxyphenol ring becomes bound. If the binding of the trimethoxyphenol ring to tubulin alone produces the effects of colchicine on photoreceptors, then high concentrations of colchicine would produce time and temperature independent effects. The  $K_d$  for the trimethoxyphenol ring alone is  $\sim 10^{-4}$  M, which is in the neighborhood of the concentration range of colchicine-evoked photoreceptor effects. Alternatively, another protein with a low-affinity binding site for colchicine could mediate colchicine's effects.

In Fig. 36, the results using high concentrations of  $\beta$ -lumicolchicine compare, in some ways, to effects caused by similar concentrations of colchicine (compare Figs. 34, 35 & 36). In experiments where solutions containing these two drugs were alternately applied to a retina, slight differences in the effects of the two drugs were noted.  $\beta$ -lumicolchicine appeared to be more effective at hyperpolarizing rods than an equal dose of colchicine, but colchicine appeared to be more effective than  $\beta$ -lumicolchicine at altering the recovery kinetics of  $V_m$  photoresponses.  $\beta$ -lumicolchicine was also more effective than colchicine in reducing photoresponse amplitudes.

It seems likely that these results are consistent with there being two independent

actions by colchicine, since the effectiveness of the drugs coincides with other differences in colchicine's effects previously described, namely, the reversibility of the effects by lowering  $[Ca^{2+}]_i$ .

Both colchicine and  $\beta$ -lumicolchicine contain a trimethoxyphenol ring, but  $\beta$ -lumicolchicine does not contain a tropolone ring, which, then, reduces its overall affinity for tubulin (see Illus. 5). The effectiveness of both drugs is consistent with the trimethoxyphenol ring as being the ligand that induces colchicine's effects. Unfortunately, the effectiveness of  $\beta$ -lumicolchicine at these high concentrations cannot be considered evidence against tubulin mediating colchicine's effects, since both drugs bind tubulin with a  $K_d$  consistent with the action of these drugs on photoreceptors. The lack of high-affinity effects caused by colchicine has been previously discussed.

It is interesting to contemplate the reason for differences in the effectiveness of colchicine and  $\beta$ -lumicolchicine. The differences could be attributed to differences in the affinities of the binding sites of the proteins mediating the effects, or the differences could be attributed to a soluble versus a membrane associated form of the same protein. Colchicine is highly soluble, as previously stated, whereas  $\beta$ -lumicolchicine is nearly insoluble. In order to get  $\beta$ -lumicolchicine to mM levels, it had to be first dissolved in DMSO, then added to very warm salt solution and carefully cooled. It was then in a supersaturated state and often precipitated during experiments. Although data concerning the lipid partition coefficients of the two drugs was not found, it is likely that  $\beta$ -lumicolchicine is far more lipid soluble than colchicine, and might therefore be more effective in binding to integral membrane proteins. The kinetic effects of colchicine may be more prominent than  $\beta$ -lumicolchicine, and might, then, involve a soluble protein.

Conductance effects of colchicine on other neuronal systems was discussed in Section 1.5. It is interesting that, in most of these preparations, high concentrations of colchicine were used when rapid effects were being observed. High affinity effects of colchicine were found only in cultured cells, where incubation for several hours at low concentrations was feasible. When low concentrations of colchicine were used,  $\beta$ -lumicolchicine was typically

without effect at similar concentrations. Whereas when rapid, low-affinity effects were noted,  $\beta$ -lumicolchicine often gave results similar to colchicine.

The low affinity effects have been thought not to involve tubulin. Because of the time and temperature dependency of the high-affinity binding of colchicine, however, and the similarity of colchicine's effects on the different neuronal systems, it may be more reasonable to postulate that colchicine's effects on these channels does involve tubulin or a tubulin-like protein. The low-affinity for colchicine may result from the requirement for the effects to be rapid and from the low (room) temperature of the preparations. Under such conditions,  $\beta$ -lumicolchicine should be about as effective as colchicine in causing tubulin-mediated effects. It would be interesting to test cultured photoreceptor OS-1S fragments for high-affinity colchicine effects, since labs using these cells could incubate them for several hours with low concentrations of colchicine.

Vincristine is a tubulin-binding drug that does not share any binding sites with colchicine, but stabilizes colchicine and GTP binding by tubulin (see Section 1.4). Vincristine produces effects on  $V_m$  and  $V_m$  photoresponses that are in some ways opposite to the effects of colchicine: it depolarizes rods, increases photoresponse amplitudes and durations, and mildly increases the duration of depolarizations produced by injected cGMP. Its effects have not been exhaustively studied, but perhaps such studies are warranted given its "anticolchicine-like" effects. From the nature of vincristine's effects, one might suspect that these effects are attributable to an antagonistic action on the same protein that mediates colchicine's effects. These results are consistent consistent with vincristine affecting a tubulin-like protein. Alternatively, vincristine could bind to transducin, and inhibit its GTPase activity, an effect that is opposite to the effects on transducin previously proposed for colchicine.

Unfortunately, the present research leaves the question about tubulin-mediation of colchicine's effects unanswered. It is of interest that many of the neuronal systems which colchicine affects contain G-protein-related conductances: the  $\beta$ -adrenergic system in synaptosomes (Rasenick et al, 1988), heart muscle cells (Lampedis et al, 1986) and the

acetylcholine mediated system in *Aplysia* (Baux et al, 1981) and cultured neurons (Fukuda et al, 1981). At least two groups of researchers have proposed that the effects of colchicine in their systems are mediated by membrane tubulin (Rasenick, 1988; Lampedis, 1986). These latter two systems involve the G-protein-mediated,  $\beta$ -adrenergic drug receptor, which has a rhodopsin-like core. The  $\beta$ -adrenergic system is strikingly similar to the G-protein/rhodopsin system controlling transduction in rods. Moreover, the cGMP-binding channel in photoreceptors appears to be a form of rhodopsin that co-purifies with a membrane tubulin (Matesic and Liebman, 1989) that may alter the cGMP channel's characteristics (Paul Liebman, personal communication).

It is important to note that neither of the two cited reports of membrane tubulin's effects demonstrated channel-like activity of membrane tubulin, and mechanics of the effects of membrane tubulin and colchicine on channel conductance have not been determined.

Neither could the results presented in this thesis unambiguously state the mechanism causing colchicine's effects in rods. The results are consistent with colchicine causing at least three independent effects: a  $\text{Ca}^{2+}$ -agonistic action; an inhibition of light-evoked phosphodiesterase activation; a  $\text{Ca}^{2+}$ -dependent acceleration of response recovery, possibly a colchicine-evoked increase in the GTPase activity of transducin. Furthermore, colchicine appears to release  $\text{Ca}^{2+}$  from internal stores. It seems less likely, but still feasible, that colchicine might act at the channel level.

The effects of colchicine on the  $\beta$ -adrenergic system are consistent with those of this thesis: colchicine indirectly alters a G-protein system and channel activity. The similarity of the  $\beta$ -adrenergic and phototransduction systems makes tubulin-mediation of colchicine's effects in rods more plausible. The results discussed in this subsection should also be considered consistent with a tubulin-like protein mediating colchicine's effects. Much more research, using both biochemical techniques and other electrophysiological techniques, will be needed to unambiguously determine whether or not colchicine's effects are truly tubulin mediated. Should this not be the case, then much can be learned about the role in transduction played by the protein(s) that colchicine does affect by examining the results



described in this thesis.

**Section 4.5: *Future research concerning colchicine's effects: unanswered questions and plausible experiments.***

A great deal of work needs to be done to truly elucidate colchicine's mechanism of action. Patch clamp experiments could be used to conclusively test colchicine for effects at the channel level. Disk membrane suspensions could be used to assay for a colchicine-evoked  $\text{Ca}^{2+}$  release. Transducin needs to be assayed for a colchicine-induced increase in GTP hydrolysis and low affinity colchicine binding. Cultured OS-1S fragments could be used to study colchicine for high-affinity effects. The colchicine-binding affinities of membrane tubulin should be assayed, since this form of tubulin may have a reduced affinity for colchicine either when purified or when associated with membranes. Further studies of colchicine on phosphodiesterase activity and guanylate cyclase activity should be done to determine if this drug affects these enzymes directly or whether the effects result from  $\text{Ca}^{2+}$  release.

It is hoped that results from some of these experiments will shed further light on the intriguing action of this very old drug on its newly discovered effects on phototransduction. Personnel at laboratories at various locations have the equipment and expertise to perform these experiments. It is hoped that the arguments and results presented in this thesis are persuasive enough to encourage them to pursue these questions.

**Section 4.6: *Speculation regarding the consequences that these thesis results may have for other systems.***

Should membrane tubulin prove to mediate the electrophysiological effects of colchicine in photoreceptors, it may well prove to mediate the electrophysiological effects of colchicine in other systems. Why a form of a cytoskeletal protein should be involved in transduction is a very intriguing question, and one can only speculate about the

consequences. The results from this thesis would, then, support a hypothesis that membrane tubulin plays a role in regulating cytosolic  $\text{Ca}^{2+}$ , by regulating both the influx of  $\text{Ca}^{2+}$  and intracellular storage of  $\text{Ca}^{2+}$ . Since  $\text{Ca}^{2+}$  also plays an important role in microtubule assembly and stability, tubulin might play a feedback regulatory role in the formation of cytosolic structure such as synaptic boutons, and in cell differentiation, in addition to its previously known structural role. It would be interesting to propose a theory that tubulin, then, is part of a protein feedback control system that regulates cell differentiation. This might imply that tubulin regulation of  $[\text{Ca}^{2+}]_i$  plays a role in cell division and the cell life cycle itself. It is interesting that unusual quantities of membrane tubulin appear at the surface of oncogenic cells, and is associated with certain oncogenes. Thus loss of regulation of tubulin synthesis correlates with loss of growth regulation in these cells, which is consistent with tubulin playing a regulatory role in cell division.

These musings are certainly speculative at this time, but such speculation may be justified by the exhausted state of the thesis author.

## APPENDIX

Derivation 1. Successive approximation equations for determining free  $[Ca^{2+}]_f$  in solutions containing EGTA,  $Ca^{2+}$  and  $Mg^{2+}$ , modified from Caldwell.

The two independent equations governing the concentrations of the free cations,  $Mg^{2+}$  and  $Ca^{2+}$ , and EGTA may be expressed as:

$$1) \quad K_1 = \frac{[Ca^{2+} \cdot EGTA]}{[Ca^{2+}][EGTA]} \quad 2) \quad K_2 = \frac{[Mg^{2+} \cdot EGTA]}{[Mg^{2+}][EGTA]}$$

The total concentration of ions and EGTA added to the solutions are expressed below as:  $[EGTA_t]$ ,  $[Ca^{2+}_t]$  and  $[Mg^{2+}_t]$ . Realizing that the following substitutions may be made:

$$[EGTA] = [EGTA_t] - [Ca^{2+} \cdot EGTA] - [Mg^{2+} \cdot EGTA]$$

$$[Ca^{2+} \cdot EGTA] = [Ca^{2+}_t] - [Ca^{2+}]$$

$$[Mg^{2+} \cdot EGTA] = [Mg^{2+}_t] - [Mg^{2+}]$$

$$A = 1/K_1$$

$$B = 1/K_2$$

$$C = [Ca^{2+}_t] + [Mg^{2+}_t] - [EGTA_t]$$

The two equations above may be algebraically manipulated into the forms:

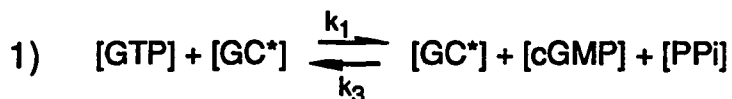
$$3) \quad [Ca^{2+}] = \frac{B([Mg^{2+}_t] - [Mg^{2+}])}{[Mg^{2+}]} + C - [Mg^{2+}]$$

$$4) \quad [Mg^{2+}] = \frac{A([Ca^{2+}_t] - [Ca^{2+}])}{[Ca^{2+}]} + C - [Ca^{2+}]$$

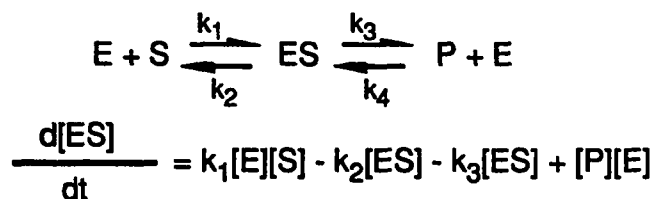
These two independent equations contain only two variables,  $[Ca^{2+}]$  and  $[Mg^{2+}]$ , once the amounts total amount of ions and EGTA added to the solution have been established. These two variables must have the same values in each of the equations. The solution is obtained by first estimating either the concentration of free  $Ca^{2+}$  or  $Mg^{2+}$ , and substituting this value into the equation that contains the estimated concentration on the left side of the equality. In solutions where the amount of EGTA added is  $\cong$  the amount of added calcium,  $[Mg^{2+}_t] \cong [Mg^{2+}]$ , which supplies a starting approximation. Equation 4 may then be rearranged into its quadratic form,  $ax^2 + bx + c = 0$ , and solved via the quadratic equation. The value of  $[Ca^{2+}]$  obtained is then substituted into equation 3, which is treated in the same fashion and solved for  $[Mg^{2+}]$ . The new value of  $[Mg^{2+}]$  is then used in equation 4, which is solved again for  $[Ca^{2+}]$ , etc. This technique converges rapidly (usually two iterations) to the solution. The rapid convergence offers an advantage over the technique suggested by Caldwell when hand calculations are done. These equations can be rearranged to solve for any two variables, e.g. added EGTA and  $[Mg^{2+}_t]$ , given design values of the other variables e.g.  $[Ca^{2+}]$ ,  $[Mg^{2+}_t]$  and  $[Ca^{2+}_t]$ .

Derivation 2. The rate equation governing the regulation of [cGMP]<sub>i</sub>.

The chemical equation governing the formation of cGMP from GTP, may be written as:



where the abbreviations are described in Table 1, and active forms of enzymes are designated by a \*. This equation follows from the application of the steady-state approximation to an enzymatic equation, of the form shown below, when the back reaction occurs to a significant extent, as it does in this reaction when all concentrations are std. at 1M:



and setting  $d[\text{ES}] = 0$

$$[\text{ES}] = \frac{(k_1[\text{S}] + k_4[\text{P}])[\text{E}]}{(k_2 + k_3)}$$

$$\frac{d[\text{S}]}{dt} = k_1[\text{E}][\text{S}] - k_2[\text{ES}]$$

substituting in the expression for [ES] and rearranging algebraically:

$$\frac{d[\text{S}]}{dt} = \left( k_1 - \frac{k_2 k_1}{k_2 + k_3} \right) [\text{E}][\text{S}] - \left( \frac{k_2 k_4}{k_2 + k_3} \right) [\text{P}][\text{E}]$$

where [E] is the enzyme concentration, [S] is the substrate concentration, and [P] is the product concentration. Note that this equation gives the same form as the depletion of substrate in equation 1, when the constants are renamed and the products in equation 1 are substituted for P.

Assuming that the back reaction in equation 1 is negligible under physiological conditions, where  $[\text{GTP}] \gg [\text{cGMP}]$ , equation 1 becomes:



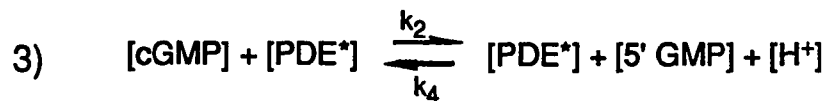
and

$$\frac{d[\text{cGMP}]}{dt} = k_1[\text{GC}^*][\text{GTP}]$$

The concentration of GTP falls only a few percent during illumination, and for practical purposes is considered a constant. [GC\*] can be treated parametrically, and lumped together with the constants to form the parameter C1. The formation of cGMP becomes:

$$2) \quad \frac{d[\text{cGMP}]}{dt} = C1[\text{GTP}]$$

The equation governing the degradation of cGMP may be treated in a similar fashion starting from the equation:



Again, the back reaction may be ignored as a result of the high energy barrier to this reaction and the low concentration of 5'GMP in the rod outer segment, maintained by endogenous nucleosidase activity (see Chapter 1). Thus:



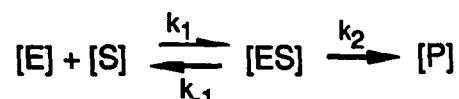
and the degradation rate equation becomes:

$$4) \quad \frac{d[cGMP]}{dt} = -k_2[PDE^*][cGMP]$$

Combining equations 2 and 4 gives the overall equation:

$$5) \quad \frac{d[cGMP]}{dt} = c_1[GTP] - k_2[PDE^*][cGMP]$$

A more traditional approach to the derivation, used by Kawamura and Murakami, starting with the Michaelis-Menton equation gives an identical equation using appropriate approximations. Note that the Michaelis-menton equation starts with the *a priori* assumption that the back reaction of products to enzyme-substate complex is negligible.



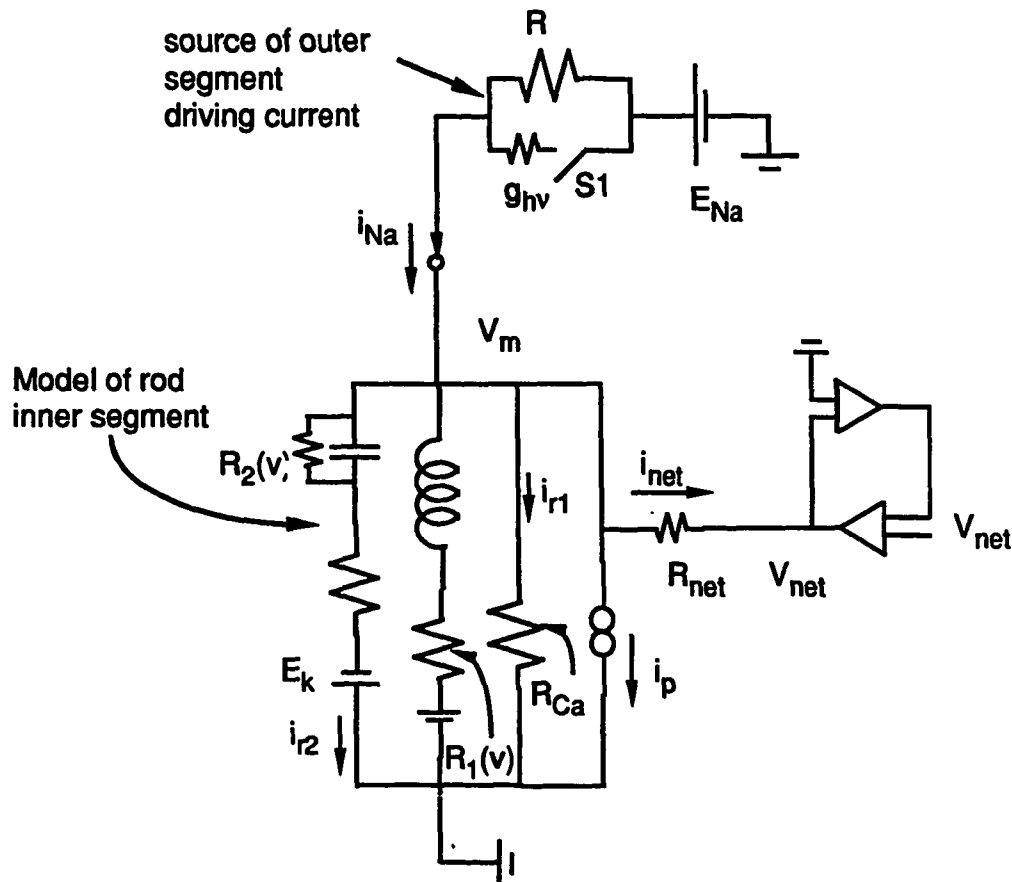
After making the steady-state approximation, and appropriate substitutions, this equation leads to the form:

$$\frac{d[P]}{dt} = \frac{k_2[E_0][S]}{K_m + [S]}$$

where  $[E_0]$  is the total amount of active enzyme,  $[E_0] - [ES] = [E]$ , and  $K_m$  is a lumping of rate constants. Note that when the substrate concentration is very large compared to  $K_m$ , as in the formation of cGMP (see Chapter 1 for values of  $K_m$ ), the right side of the equation reduces to a constant,  $k_2[E_0]$ , as  $K_m + [S] \equiv [S]$  (the equation becomes a zero order derivative). This occurs during enzyme saturation. When  $K_m$  is large compared to  $[S]$ , the equation becomes a first order derivative, as in the case of cGMP degradation by PDE, where the turnover number of PDE is very high (the enzyme becomes hard to saturate) and the substrate concentration is very low.

### Derivation 3. Effects of the photoreceptor network on a single depolarized cell.

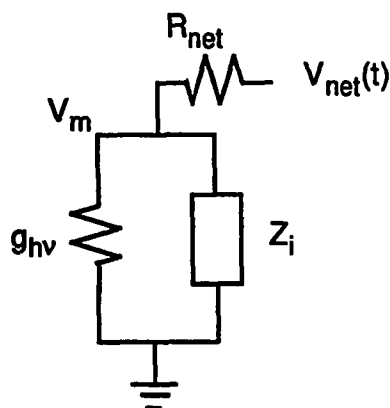
An individual photoreceptor cell can be approximately modeled by representing the inner segment as a passive circuit, and the outer segment as a driving circuit (Baylor et al, 1984). Such a circuit is shown below, where the outer segment driving current is derived from the  $\text{Na}^+$  battery circuit with the switch labeled S1 below. An approach to the network effects is described below, which treats the network as a voltage clamp attached to the inner segment.



When  $V_m = V_{net}$ , as in a dark-adapted retina or full-field illumination, the current  $i_{net} = 0$ . During injection of EGTA or cGMP, the switch S1 is closed, providing increased conductance across the cell membrane (opening cGMP-sensitive channels actually adds multiple such current paths in parallel, which add up to this increased conductance).  $V_m$  then increases and is  $\cong E_{Na} - i_{Na}/g_{hv}$ , and  $i_{net} = (V_m - V_{net})R_{net}$ . If  $V_{net}$  were to change while  $V_m$  remained constant,  $i_{net}$  would likewise change, and  $\Delta i_{net} = \Delta V_{net}R_{net}$ , but  $V_m$  also changes as  $i_{Na}$  increases.

In this model, a time-varying change in  $V_{net}$  estimates the effects of photostimulation of the network. For such a time varying change in  $V_{net}$ , the batteries and current pump are "transparent" to this "input" voltage signal, and the inner segment and outer segment form parallel paths for the transference of the voltage waveform. The model may be reconstructed as the one shown below, where the time and voltage varying conductances of the inner segment have been lumped together into a general transfer impedance.

Note that this is essentially a voltage divider circuit, except that  $Z_i$ , in its full form, is time and voltage dependent. Since  $Z_i$  is comprised of the inner segment conductances, which can be modeled with passive elements (see Baylor et al, 1984),  $V_m$  will always be attenuated with respect to the network signal. Furthermore, the transferred voltage will be less as  $g_{hv}$  and  $Z_i$  increase.



This essentially demonstrates that the large voltage responses observed in Fig. 23 result from closing the light-sensitive conductance, and not from network effects. The network responses can be assumed to be similar to the voltage responses seen in the impaled cell before EGTA was injected, and the voltage signal transferred to the impaled cell must be less than the network signal by the arguments just provided.

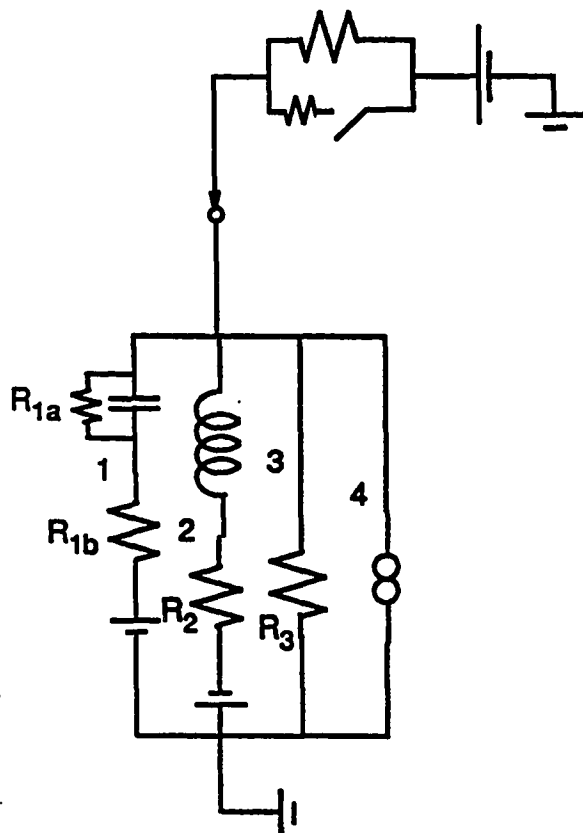
The actual strength of the network signal that is transferred to the rod depends, of course, on the ratio of the net resistance of the rod,  $1/(g_{hv} + g_z)$ , to  $[1/(g_{hv} + g_z)] + R_{net}$ . It will not be quantitated here, but it will be briefly described. Each rod is attached to ~6 other rods, and by assuming symmetry, each produces a voltage,  $V_{net}$ , that will be similar to the other five cells. Thus the network can be approximated by six parallel resistors, each with a resistance equal to the cell-to-cell resistance between two photoreceptors, attached to a voltage generator producing the signal  $V_{net}$ . As mentioned above,  $g_{hv}$  is large during injections of cGMP or EGTA. Furthermore, large depolarizations result in increases in the voltage-sensitive  $Ca^{2+}$  and  $K^+$  conductances, which also leads to increased  $Ca^{2+}$  sensitive conductance, shown as the parallel resistance in the first model. Thus the parallel rod conductances should be sufficiently large relative to  $R_{net}$  to produce some attenuation of the voltage transferred from the network.

The inductance branch in the first model shown results from an inward rectifier conductance in the inner segment, which essentially closes above -40 mV (see Chapter 1). The  $Ca^{2+}$  and  $K^+$  conductances close on hyperpolarization in a time-dependent way, and thus comprise the capacitive branch of the circuit in the first model. Note, then, that at depolarized states the circuit resembles a low-pass filter, as opposed to the high-pass filtering that occurs at more hyperpolarized voltages. This effect is important, in that it demonstrates that the peak hyperpolarization transferred from the network will be attenuated more than the recovery portion of the waveform.

Finally, this model does not take into account the lack of electrical buffering provided by the photoreceptor network to changes in  $V_m$ . The model shown, however, is conservative, in that the lack of buffering will allow the voltage difference between the injected rod and its neighbors to decrease, the lowering the parasitic current,  $i_{net}$ , that creates the voltage transference between the network and the impaled rod.

#### Derivation 4. Filtering effects of the inner segment on photoreceptor recovery.

As discussed in Derivation 3, the conductances of the inner segment can be modeled as passive elements, under some conditions, driven by a current provided by the outer segment (Baylor et al, 1984). A model approximating the inner segment was drawn in Derivation 3 and is redrawn below for convenience. At typical dark membrane voltages, the inner segment acts as a high-pass filter to changes in the photocurrent as a result of the rectifying conductance, modeled below as an inductance. At depolarized states  $> 40$  mV, the rectifying conductance is closed, and the circuit behaves more as a low-pass filter (see Derivation 3 for a discussion).



For time-varying current drives, the voltage drop across the "inductance" of the circuit is  $L \cdot di/dt$ . For slow signals, when  $di/dt$  approaches 0, the impedance provided by the inductance approaches 0, and the branch 2 impedance becomes the steady-state resistance of the voltage-gated channels. For such an approximation,  $L \cdot di/dt$  must be  $\ll \Delta V$  across  $R_2$ . At least in the salamander, the membrane voltage during the linear portion of the recovery curve from a saturating light flash is above  $-40$  mV, and  $R_2$  is very high, making  $i$  in branch 2, and thus  $di/dt$  during the voltage recovery, very small. Thus the time-varying part of the conductance is negligible in this branch. Similar results probably hold for the toad (see Torre & Owen, 1983).

In the capacitive branch, where the voltage drop across the membrane is  $1/C \int i dt$ , for slow, steady currents the voltage drop is  $\sim$  just  $V_m$ , and again is determined by the steady-state resistance in branch 1. Thus the time-varying contribution of inner segment conductances on the recovery part of waveforms from cGMP injections or light stimulation are minimal, as a result of their slow nature.

Another way of thinking about the time domain effects of the inner segment on the current signal is to realize that the voltage waveform caused by a time-varying current signal, such as the response of the photocurrent to a light flash, is the convolution of the photocurrent with the current impulse response of this linear approximation to the inner segment. Where the time constant the impulse response is fast relative to the driving signal, the waveform spreading effect of impulse response becomes small. Inner segment conductance time constants are on the order of  $100 \mu s$  (see Baylor et al, 1984; Bader et al, 1982), while the current changes to light flashes typical in these experiments are several seconds. A formal proof of this is beyond the scope of this thesis, but should be intuitive to those familiar with time-domain analysis of linear systems.



Handling the voltage-sensitivity of the conductances poses no more of a problem. The rectifying conductance is most easily handled, because it is essentially closed above -40 mV. Thus recovery waveforms from cGMP or EGTA injections should not be affected by the rectifying conductance unless the rod is hyperpolarized to  $<-40$  mV. This may be the case in cells during colchicine,  $\text{Li}^+$  or high  $\text{Ca}^{2+}$  superfusion, but the effects of the rectifying conductance should be most noticeable at the end of the injection recovery curves, and the peak of the voltage photoresponse curves, since these are the most hyperpolarized part of the respective responses.

The voltage dependency of the  $\text{Ca}^{2+}$  and  $\text{K}^+$  conductances of the inner segment can be approximated by linear functions over the range of -30 mV to -5 mV or even 0 mV without introducing too much error (see conductance vs. voltage curves of Bader et al, 1982). This includes the ranges of most of the responses characterized in this thesis.

Thus in the experiments of this thesis, the changes in the kinetics of the recovery curves from photostimulation or injection of cGMP or EGTA are more likely attributable to changes in the driving current (photocurrent) than the voltage and time-dependency of the channel conductances of the inner segment.

**BIBLIOGRAPHY**

- Abood, M.E., J.B. Hurley, M.-C. Pappone, H.R. Brown and L. Stryer (1982). Functional homology between signal coupling proteins: Cholera toxin inactivates the GTPase activity in Transducin. *J. Biol. Chem.* **257**:10540-10543.
- Alsteril, L.D. and F.R.Landsburger (1977). Interaction of colchicine with phosphatidylcholine membranes. *Nature.* **269**:70-72.
- Anderson, R.A. and V.T. Marchesi (1985). Regulation of membrane skeletal protein 4.1 with glycosphorin by a polyphosphoinositide. *Nature.* **318**:295-298.
- Andreu, J.M. and S.N. Timasheff (1986). Tubulin-colchicine interactions and polymerization of the complex. *Ann. N.Y. Acad. Sci.* **466**:676-689.
- Arai, T., Y. Ihara, K. Arai and Y. Kaziro (1975). Purification of tubulin from bovine brain and its interaction with guanine nucleotides. *J. Biochem. (Tokyo)* **77**:647-658.
- Arai, T. and Y. Kaziro (1977). Role of GTP in the assembly of microtubules. *J. Biochem. (Tokyo)* **82**:1063-1071.
- Arshavski, V.Y., A.M. Dizur, A.D. Kaulin, I.K. Shestakov and P.P. Filipov (1985). The effect of phosphorylation of rhodopsin on its interaction with transducin studied by the technique of light-scattering. *Biol. Membr.* **2**:1-11.
- Athanassious, R., M.A. Kylene and M.A. Ali (1984). Regulation of cyclic nucleotides in retinal photoreceptors: an ultracytochemical approach on the role of cyclases. *Cell Tissue Res.* **237**:95-101.
- Aton, B. and B.J. Litman (1984). Activation of rod outer segment phosphodiesterase by enzymatically altered rhodopsin: a regulatory role for the carboxyl terminus of rhodopsin. *Exp. Eye Res.* **38**:547-559.
- Bader, C.R., D. Bertrand and E.A. Schwartz (1982). Voltage-activated and calcium-activated currents studied in solitary rod inner segments from the salamander retina. *J. Physiol.* **331**:253-284.
- Bader, C.R., P.R. MacLeish and E.A. Schwartz (1978). Responses to light of solitary rod

- photoreceptors isolated from tiger salamander retina. *Proc. Natl. Acad. Sci.* **75**:3507-3511.
- Bader, C.R., P.R. MacLeish and E.A. Schwartz (1979). A voltage-clamp study of the light response in solitary rods of the tiger salamander. *J. Physiol.* **296**:1-26.
- Baehr, W., M.J.Devlin and M.L. Applebury (1979). Isolation and characterization of cGMP phosphodiesterase from bovine rod outer segments. *J. Biol. Chem.* **254**:11669-11677
- Barham, S.S. and B.R. Brinkley (1976). Action of rotenone and related respiratory inhibitors on mammalian cell division. 1. Cell kinetics and biochemical aspects. *Cytobios.* **15**:85-96.
- Barloff, A. and A.L. Norton (1965). Simultaneous recording of photoreceptor potentials and the PIII component of the ERG. *Vision Res.* **9**:1443.
- Bardoll, A.E., E.N. Pugh and A. Sitaramaya (1989). Calcium dependence of the activation and inactivation of the light-activated phosphodiesterase of retinal rods. *J. Gen. Physiol.* **93**:1091-1108.
- Baines, A.J. and V. Bennett (1986). Synapsin I is a microtubule-bundling protein. *Nature.* **319**:145-147.
- Bastian, B.L. and G.L. Fain (1979). Light adaptation in toad rods: requirement for an internal messenger which is not calcium. *J. Physiol.* **297**:493-520.
- Bastian, B.L. and G.L. Fain (1982a). The effects of low calcium and background light on the sensitivity of toad rods. *J. Physiol.* **330**:307-329.
- Bastian, B.L. and G.L. Fain (1982b). The effects of sodium replacement on the responses of toad rods. *J. Physiol.* **330**:331-347.
- Bauer, P.J. (1988). Evidence for two functionally different membrane fractions in bovine retinal rod outer segments. *J. Physiol.* **401**:309-327.
- Baux, G.M. Simonneau and L. Tanc (1981). Action of colchicine on membrane currents and synaptic transmission of Aplysia ganglion cells. *J. Neurobiol.* **12**:75-85.
- Bayior, D.A. and A. L Hodgkin (1974). Changes in time scale and sensitivity in turtle photoreceptors. *J. Physiol.* **242**:729-758.

- Baylor, D.A., T.D. Lamb and K.-W. Yau (1979). Response of retinal rods to single photons. *J. Physiol.* **288**:613-633.
- Baylor, D.A. and T.D. Lamb (1982). Local effects of bleaching in retinal rods of the toad. *J. Physiol.* **328**:49-71.
- Baylor, D.A., G. Matthews and B.J. Nunn (1984). Location and function of voltage-sensitive conductances in retinal rods of the salamander *Ambystoma tigrinum*. *J. Physiol.* **354**:203-223.
- Beahr, W., M.J. Devlin and M.L. Applebury (1979). Isolation and characterization of cGMP Phosphodiesterase from bovine rod outer segments. *J. Biol. Chem.* **254**:11669-11677.
- Beebe, D.C., D.E. Feagans, E.J. Blanchette-Mackie and M. Nau (1979). Lens epithelial cell elongation in the absence of microtubules: evidence for a new effect of colchicine. *Science.* **206**:836-838.
- Bennett, N. (1978). Evidence for differently protonated forms of metarhodopsin II as intermediates in the decay of membrane-bound cattle rhodopsin. *Biochem. Biophys. Res. Commun.* **83**:457-465.
- Bennett, N., M. Michel-Villaz and H. Kuhn. (1982). Light-induced interaction between rhodopsin and the GTP-binding protein: metarhodopsin II is the major photoproduct involved. *Eur. J. Biochem.* **127**:97-103.
- Bensch, K.G., R. Marantz, H. Wisniewski and M. Shelanski (1969). Induction *in vitro* of microtubular crystals by vinca alkaloids. *Science.* **164**:495-496.
- Bert, R.J. (1987). Colchicine's effects on the light-sensitive conductance in toad rods are due to inhibition of sodium-calcium exchange. *Invest. Ophthalmol. Vis. Sci. (suppl.)* **28**:353.
- Bert, R.J., R.R. Kuffel and B. Oakley II. (1986). Colchicine may effect the light-sensitive conductance in toad rods. *Invest. Ophthalmol. Vis. Sci. (suppl.)* **27**:241.
- Bert, R.J. and B. Oakley II. (1984). The effects of intracellularly-injected proteins and small molecules upon membrane potential in rod outer segments. *Carle Selected Papers. (Abstract)* **36**:60.

- Bert, R.J. and B. Oakley II. (1985). The cytoskeleton may affect rod membrane potential in the toad retina. *Invest. Ophthalmol. Vis. Sci. (suppl.)*. **26**:248.
- Besharse, J.C. (1986). Photosensitive membrane turnover: differentiated membrane domains and cell-cell interaction. *Adv. in Cell Neurobiol.*
- Besharse, J.C., D.M. Forestner and D.M. Defoe (1985). Membrane assembly in retinal photoreceptor. III. Distinct membrane domains of the connecting cilium of developing rods. *J. Neurosci.* **5**:1035-1048.
- Besharse, J.C. and D.A. Dunis (1982). Rod photoreceptor disc shedding *in vitro*: inhibition by cytochalasins and activation by colchicine. *Structure of the Eye.* Hollyfield. *Elsevier*. Chapter 10:85-96.
- Bhattacharyya, B. and J. Wolff (1975). The Interaction of 1-Amino-8-Naphthalene Sulfonate with Tubulin: A Site independent of the Colchicine-Binding Site. *Arch. Biochem. Biophys.* **167**:264-269.
- Bhattacharyya, B. and J. Wolff (1976). Stabilization of microtubules by Li<sup>+</sup> ion. *Biochem. Biophys. Res. Comm.* **73**:383-390.
- Bhattacharyya, B. and J. Wolff (1976). Anion-induced increases in the rate of colchicine binding to tubulin. *Biochem.* **15**:2283-2288.
- Bhattacharyya, B. and J. Wolff (1976). Tubulin aggregation and disaggregation: mediated by two distinct vinblastine-binding sites. *Proc. Natl. Acad. Sci. U.S.A.* **73**:2375-2378.
- Biernbaum, M.S. and M.D. Bownds (1979). Influence of light and calcium on guanosine 5'-triphosphate in isolated frog rod outer segments. *J. Gen. Physiol.* **74**:649-669.
- Blest, A.D., S. Stowe and W. Eddey (1982). A labile, Ca<sup>2+</sup>-dependent cytoskeleton in rhabdomeral microvilli of blowflies. *Cell Tissue Res.* **223**:553-573.
- Blitz, A.L. and R.E. Fine (1974). Muscle-like contractile proteins and tubulin in synaptosomes. *Proc. Natl. Acad. Sci. U.S.A.* **71**:4472-4476.
- Bodoia, R.D. and P.B. Detwiler (1984). Patch-clamp recordings of the light-sensitive dark noise in retinal rods from the lizard and frog. *J. Physiol.* **367**:183-216.
- Borisy, G.G. and J.B. Olmstead (1972). Nucleated assembly of microtubules in porcine

- brain extracts. *Science*. **177**:1196-1197.
- Borisy, G.G. and E.W. Taylor (1967). The mechanism of action of colchicine. Binding of  $^3\text{H}$  colchicine to cellular protein. *J. Cell Biol.* **34**:525-533.
- Borisy, G.G., J.M. Marcum, J.B. Olmstead, D.B. Murphy and K.A. Johnson (1975). Purification of tubulin and associated high molecular weight proteins from porcine brain and characterization of microtubule assembly *in vitro*. *Ann. N.Y. Acad. Sci.* **253**:107-132.
- Bownds, D., J. Daves, J. Miller and M. Stahlman (1972). Phosphorylation of frog photoreceptor membranes induced by light. *Nature New Biol.* **237**:125-127.
- Bretscher, A. (1984). Smooth muscle caldesmin rapid purification and F-actin cross-linking properties. *J. Biol. Chem.* **259**:12873-12880.
- Broekhuysse, R.M., E.F. Tolhuizen, A.P. Janssen and H.J. Winkens (1985). Light induced shift and binding of S-antigen in retinal rods. *Current Eye Res.* **4**:613-618.
- Brown, H.M. and D. Erne (1986). Effect of some divalent cations on pH regulation in *Balanus* photoreceptor. *Biophys. J. (suppl.)*. **49**:30a.
- Brown, J.E. and L.H. Pinto (1974). Ionic mechanism for the photoreceptor potential of the retina of *Bufo marinus*. *J. Physiol.* **236**:575-591.
- Brown, J.E. and L.H. Pinto (1977). Effects of injections of calcium and EGTA into the outer segments of retinal rods of *Bufo marinus*. *J. Physiol.* **236**:575-591.
- Brown, J.E., L.J. Rubin, A.P. Ghalagini, R.F. Tarver, M.J. Berridge and R.E. Anderson (1984). Myo-inositol polyphosphate may be a messenger for visual excitation in *Limulus* photoreceptors. *Nature*. **311**:160-163.
- Brown, K.T. and D.G. Flaming (1977). New microelectrode techniques for intracellular work in small cells. *Neurosci.* **2**:813-827.
- Bryan, J. (1972). Definition of three classes of binding sites in isolated microtubule crystals. *Biochem.* **11**:2611-2616.
- Burnside, M.B. and B. Nagle. (1983). Retinomotor movements of photoreceptors and retinal pigment epithelium: mechanisms and regulation. Prog. in Retinal Res. N. Osborne and G. Chader. *Pergamon Press. N.Y.* 67-109.

- Burnside, M.B. (1983). Regulation of photoreceptor cytoskeleton by  $\text{Ca}^{2+}$  and cyclic nucleotides. *Biophysical J.* **41**:378a.
- Caldwell, P.C. (1970). Calcium chelation and buffers. Calcium and Cellular Function. ed. Cuthbert, A.W. *London*. 10-16
- Capovilla, M., L. Cervetto, E. Pasino and V. Torre (1981). The sodium current underlying the responses of toad rods to light. *J. Physiol.* **317**:223-242
- Capovilla, M., L. Cervetto, A. Caretta and V. Torre (1983). Ionic movements through light-sensitive channels of toad rods. *J. Physiol.* **343**:295-310.
- Capovilla, M., L. Cervetto and V. Torre (1980). Effects of changing external potassium and chloride concentrations on the photoresponses of *Bufo bufo* rods. *J. Physiol.* **307**:529-551.
- Capovilla, M., L. Cervetto and V. Torre (1983). The effect of phosphodiesterase inhibitors on the electrical activity of toad rods. *J. Physiol.* **343**:277-294.
- Caretta, A. and P.J. Stein (1985). cGMP- and phosphodiesterase-dependent light-scattering changes in rod disk membrane vesicles: relationship to disk vesicle-disk vesicle aggregation. *Biochem.* **24**:5685-5692.
- Caretta, A. and P.J. Stein (1986). Light- and nucleotide-dependent binding of phosphodiesterase to rod disk membranes: correlation with light-scattering changes and vesicle aggregation. *Biochem.* **25**:2335-2341.
- Cervetto, L., E. Pasino and V. Torre (1977). Electrical responses of rods in the retina of *Bufo marinus*. *J. Physiol.* **267**:17-51.
- Cervetto, L., L. Lagnado, R.J.Perry, D.W. Robinson and P.A.McNaughton (1989). Extrusion of calcium from rod outer segments is driven by both sodium and potassium gradients. *Nature.* **337**:740-743.
- Chader, G., R. Fletcher, M. Johnson and R. Bensinger (1974a). Rod outer segment phosphodiesterase: factors affecting hydrolysis of cyclic AMP and cyclic GMP. *Exp. Eye. Res.* **18**:509-515.
- Chader, G., M. Johnson, R. Fletcher and R. Bensinger (1974b). Cyclic nucleotide phosphodiesterase of the bovine retina: activity, subcellular distribution and kinetic

- parameters. *J. Neurochem.* **22**:93-99.
- Chaitin, M.H., B.G. Schneider, M.O. Hall and D.S. Papermaster (1982):  
Immunocytochemical localization of actin at the EM level in photoreceptors and pigment epithelial cells of the retina. *J. Cell Biol.* **95**:14022.
- Chaitin, M.H. and D. Bok (1985). Immunoferritin localization of actin, myosin and calmodulin in photoreceptor outer segments. *Biophys. J.* **422**:114a.
- Chaitin, M.H., B.G. Schneider, M.O. Hall and D.S. Papermaster (1984). Actin in the photoreceptor connecting cilium: immunocytochemical localization to the site of outer segment disk formation. *J. Cell Biol.* **99**:239-246.
- Chanz, D.C. (1983). A voltage-clamp study of the effects of colchicine on the squid giant axon. *J. Cell Physiol.* **115**:260-264.
- Clack, J.W., B. Oakley II. and P.J. Stein (1983). Injection of GTP binding protein or cGMP phosphodiesterase hyperpolarize retinal rods. *Nature (London)*. **305**:50-52.
- Clack, J.W. and P.J. Stein (1988). Opsin exhibits cGMP-activated single-channel activity. *Proc. Natl. Acad. Sci. U.S.A.* **85**:9806-9810.
- Cohen, A.I. (1972). Rods and cones. Handbook of Sensory Physiology, VII/2. Springer-Verlag. N.Y. 63-110.
- Cook, N.J. and W.B. Kampp (1988). Solubilization, purification and reconstitution of the sodium-calcium exchanges from bovine retinal rod outer segments. *J. Biol. Chem.* **263**:11382-11388.
- Cook, N.J., G. Nullans and N. Virmaux (1985). Effects of fluoride on retinal rod outer segment cGMP phosphodiesterase and G-protein. *Biochem. Biophys. Res. Comm.* **131**:146-151.
- Cook, N.J., G. Nullans and N. Virmaux (1986). Interplay between calcium and activated cGMP phosphodiesterase from retinal rod outer segments. *Biochimica et Biophysica Acta.* **883**:63-68.
- Cone, R.A. (1973). The internal transmitter model for visual excitation: some quantitative implications. Biochemistry and Physiology of Visual Pigments. Langer, H. Springer-Verlag. Berlin. 275-283.



- Coquil, J.F., G. Brunelle and J. Guedon (1985). Occurrence of the methylisobutylxanthine-stimulated cyclic GMP binding protein in various rat tissues. *Biochem. Biophys. Res Comm.* **127**:226-231.
- Corey, D.P., J.M. Dubinsky and E.A. Schwartz (1984). The calcium current in inner segments of rods from the salamander (*Ambystoma tigrinum*) retina. *J. Physiol.* **354**:557-575.
- Cortese, F., B. Bhattacharyya and J. Wolff (1977). Podophyllotoxin as a probe for the colchicine binding site of tubulin. *J. Biol. Chem.* **252**:1134-1140.
- Cote, R.H., M.S. Biernbaum, G.D. Nicol and M.D. Bounds (1984). Light-induced decreases in cGMP concentration precede changes in membrane permeability in frog photoreceptors. *J. Biol. Chem.* **259**:9635-9641.
- Cote, R.H., G.D. Nicol, S.A. Burke and M.D. Bounds (1986). Changes in cGMP concentration correlate with some, but not all, aspects of light-regulated conductance of frog rod photoreceptors. *J. Biol. Chem.* **261**:12965-12975.
- Davidse, L.C. and W. Flach (1977). Differential binding of methyl benzimidazol-2-YL carbamate to fungal tubulin as a mechanism of resistance to this antimetabolic agent in mutant strains of *Aspergillus nidulans*. *J. Cell Biol.* **72**:174-193.
- Dawis, S.M., R.M. Graeff, T.F. Walseth, E.A. Butz and N.D. Goldberg (1987). Definition of the cyclic GMP metabolic events subserving photoexcited and attenuated states in toad photoreceptors. *Biophys. J.* **51**:270a.
- Deary, A. and B. Burnside (1984). Effects of extracellular  $Ca^{2+}$ ,  $K^{+}$  and  $Na^{+}$  on cone and retinal pigment epithelium retinomotor movements in isolated teleost retinas. *J. Gen. Physiol.* **83**:589-611.
- Defoe, D.M. and J.C. Besharse (1985). Membrane assembly in retinal photoreceptors. II. Immunocytochemical analysis of freeze-fractured rod photoreceptor membranes using anti-opsin antibodies. *J. Neurosci.* **5**:1023-1034.
- Del Priore, L.U., W.W. Carley, A. Lewis and W.W. Webb (1987). Actin three-dimensional organization in rod photoreceptors using a fluorescent toxin. *Invest. Ophthalmol. Vis. Sci.* **28**:633-639.

- Del Priore, L.U. and A. Lewis (1983). Calcium-dependent activation and deactivation of rod outer segment phosphodiesterase is calmodulin-independent. *Biochem. Biophys. Res. Comm.* **133**:317-324.
- Del Priore, L.U. and A. Lewis (1985a). Can mechanical coupling account for amplification in visual transduction? *Biophys. J.* **47**:103a.
- Del Priore, L.U. and A. Lewis (1985b). Vanadate, tungstate and molybdate activate rod outer segment phosphodiesterase in the dark. *Biochemica et Biophysica Acta.* **845**:81-85.
- Deterre, P.G., J. Bigay, F. Forquet, M. Robert and M. Chabre (1988). cGMP phosphodiesterase of retinal rods is regulated by two inhibitory subunits. *Biochemistry.* **85**:2424-2428.
- Detwiler, P.B. and G. Rispoli (1989). Phototransduction in detached rod outer segments: calcium control of the cGMP economy. *Invest. Ophthalm. and Vis. Sci. (suppl.).* **30**:162.
- Diamond, J., J.A.B. Gray and D.R. Inman (1958). The relation between receptor potentials and the concentration of sodium ions. *J. Physiol (London).* **142**:362-364.
- Dixon, R.A.F., I.S. Sigal, E. Rands, R.B. Register, M.R. Candelore, A.D. Blake and C.D. Strader (1987). Ligand binding to the beta-adrenergic receptor involves its rhodopsin-like core. *Nature.* **326**:73-77.
- Dowling, J.E. (1963). Neural and photochemical mechanisms of visual adaptation in the rat. *J. Gen. Physiol.* **46**:1287-1301.
- Downer, N.W. (1985). Cross-linking of dark-adapted frog photoreceptor disk membranes: evidence for monomeric rhodopsin. *Biophys. J.* **47**:285-293.
- Dratz, E.A. and P.A. Hargrave (1983). The structure of rhodopsin and the rod outer segment disk membrane. *Trends Biochem. Sci.* **8**:128-131.
- Ebrey, T.G. and B. Honig (1975). Molecular aspects of photoreceptor function. *Quarterly Reviews of Biophysics.* **8**:129-184.
- Edwards, C., C.A. Terzuolo and Y. Washizu (1963). The effects of changes of the ionic environment upon an isolated crustacean sensory neuron. *J. Physiol. (London).* **189**:351-356.

- Eigsti, O.J. and P. Dustin Jr. (1955). Colchicine in Agriculture, Medicine, Biology and Chemistry. Iowa State College Press.
- Fain, G.L. (1976). Sensitivity of toad rods: dependence of wave-length and background illumination. *J. Physiol.* **261**:71-101.
- Fain, G.L., H.M. Gerschenfield and F.N. Quandt (1980). Calcium spikes in toad rods. *J. Physiol.* **303**:495-513.
- Fain, G.L. and W. H. Schroder (1985). Calcium content and calcium exchange in dark-adapted toad rods. *J. Physiol.* **368**:641-665.
- Farber, D.B. and R.N. Lolley (1976). Calcium and magnesium content of rodent photoreceptor cells as inferred from studies of retinal degeneration. *Exp. Eye Res.* **22**:219-228.
- Faure, J.-P., M. Mirshahi, C. Dorey, B. Thillaye, Y. Kozak de and C. Boucheix (1984). Production and specificity of monoclonal antibodies to retinal S. antigen. *Current Eye Res.* **3**:867-872.
- Feit, H., P. Kelly and C.W. Cotman (1977). Identification of a protein related to tubulin in the postsynaptic density. *Proc. Natl. Acad. Sci. U.S.A.* **74**:1047-1051.
- Fesenko, E.E., S.S. Kolesnikov and A.L. Lyubarsky (1985). Induction by cyclic GMP of cation conductances in plasma membrane of retinal rod outer segments. *Nature.* **313**:310-313.
- Frigon, R.P. and S.N. Timasheff (1975). Magnesium-induced self-association of calf tubulin. *I. Stoichiometry. Biochem.* **14**:4559-4566.
- Fukuda, J., M. Kameyama and K. Yamaguchi (1981). Breakdown of cytoskeletal filaments selectively reduces Na and Ca spikes in cultured mammalian neurones. *Nature (London)*. **294**:82-85.
- Fukui, H. and H. Shichi (1982). Soluble 5'-nucleotidase: purification and reversible binding to photoreceptor membranes. *Biochem.* **21**:3677-3681.
- Fulton C. and P.A. Simpson (1979). Tubulin pools, synthesis and utilization. Microtubules. Hyams and Roberts, 72 ed. *Academic Press*. 117-174.
- Fung, B.K. and L. Stryer (1980). Photolyzed rhodopsin catalyzes the exchange of GTP for

- bound GDP in retinal rod outer segments. *Proc. Natl. Acad. Sci. U.S.A.* **77**:2500-2504.
- Fung, B.K., J.B. Hurley and L. Stryer (1981). Flow of information in the light-triggered cyclic nucleotide cascade of vision. *Proc. Natl. Acad. Sci. U.S.A.* **78**:152-156.
- Fung, B.K. (1983). Characterization of transducin from bovine retinal rod outer segments. I. Separation and reconstitution of the subunits. *J. Biol. Chem.* **258**:10495-10502.
- Fung, B.K. (1985). The light-activated cyclic GMP phosphodiesterase system in retinal rods. Molecular Mechanisms of Transmembrane Signalling. Elsevier Sci. Publ. Chapter 6:184-213.
- Fung, B.K. (1989). Transducin: Structure, function and role in phototransduction. *Progress in Retinal Research.* **8**:151-177.
- Fung, B.K. and C.R. Nash (1983). Characterization of transducin from bovine retinal rod outer segments: evidence for distinct binding sites and conformational changes revealed by limited proteolysis with trypsin. *J. Biol. Chem.* **258**:10503-10510.
- Furcht, L.T. and R.E. Scott (1975). Effect of vinblastine sulphate, colchicine and lumicolchicine on membrane organization of normal and transformed cells. *Exp. Cell Res.* **96**:271-282.
- Gadsby, D.C., R.F. Rakowski and P. DeWeer (1986). Voltage dependence of Na/K pump rate in squid giant axon. *Biophys. J.* **49**:36a.
- Garland, D.L. (1977). Evidence for colchicine induced protein conformational changes in tubulin. *Fedn. Proc. Fedn. Am. Soc. Exp. Biol.* **36**:899.
- Garland and Teller (1975). A reexamination of the reaction between colchicine and tubulin. *Ann. N.Y. Acad. Sci.* **253**:232-238.
- George and Hagins (1983). Control of Ca<sup>2+</sup> in rod outer segment disks by light and cGMP. *Nature.* **303**:344-348.
- George, J.S. (1987). Mechanism of cGMP stimulated Ca<sup>2+</sup> uptake by ROS disks. *Biophys. J.* **51**:272a.
- Gill, D.L., Ueda, T. and S.-H. Chueh (1985). Sodium-calcium exchange across the synaptic plasma membrane. *Ann. N.Y. Acad. Sci.* **456**:250-253.

- Gold, G.H. and J.I. Korenbrot (1980). Light-induced calcium release by intact rods. *Proc. Natl. Acad. Sci. U.S.A.* **77**:5557-5561.
- Gold, G.H. (1986). Plasma membrane calcium fluxes in intact rods are inconsistent with the "calcium hypothesis". *Proc. Natl. Acad. Sci. U.S.A.* **83**:1150-1154.
- Goldberg, N.D., A. Ames III, J.E. Gander and T.F. Walseth (1983). Magnitude of increase in retinal cGMP metabolic flux determined by  $^{18}\text{O}$  incorporation into nucleotide alpha-phosphoryls corresponds with intensity of photic stimulation. *J. Biol. Chem.* **258**:9213-9219.
- Goldman, D.E. (1965). The transducer action of mechanoreceptor membranes. *Symp. Quant. Biol.* **30**:59-68.
- Griff, E.R. and L.H. Pinto (1981). Interaction among rods in the isolated retina of *Bufo Marinus*. *J. Physiol.* **314**:237-254.
- Hadjian, A., C. Guidicelli and E.M. Chambaz (1977). Characterization of tubulin in the adrenal cortex cytosol. *FEBS Lett.* **77**:233-238.
- Hagins, W.A., R.D. Penn, R.D. and S. Yoshikami (1970). Dark current and photocurrent in retinal rods. *Biophys. J.* **10**:380-412.
- Hagins, W.A. and H. Ruppel (1971). Fast photoelectric effects and the properties of vertebrate photoreceptors as electrical cables. *Fed. Proc.* **30**:64-68.
- Hagins, W.A. and S. Yoshikami (1975). Ionic mechanisms in excitation of photoreceptors. *Ann. N.Y. Acad. Sci.* **264**:314-325.
- Hargrave, P.A., J.H. McDowell, D.R. Curtis, J.K. Wang and P. Argos (1983). The structure of bovine rhodopsin. *Biophys. Str. Mech.* **9**:235-244.
- Haynes, L.W., A.R. Kay and K.-W. Yau (1986). Single cyclic GMP-activated channel activity in excised patches of rod outer segment membrane. *Nature.* **321**:66-70.
- Hanke, W. and U.B. Kaupp (1984). Incorporation of ion channels from bovine rod outer segments into planar lipid bilayers. *Biophys. J.* **46**:587-595.
- Herzog, W. and K. Weber (1977). *In vitro* assembly of pure tubulin into microtubules in the absence of microtubule-associated proteins and glycerol. *Proc. Natl. Acad. Sci. U.S.A.* **74**:1860-1864.

- Hill, A.V. (1910). The possible effects of the aggregation of the molecules of haemoglobin on its dissociation curves. *J. Physiol.* **40**:IV-VII.
- Hinmann, N.D. and J.R. Cann (1976). Reversible binding of chlorpromazine to brain tubulin. *Molec. Pharmacol.* **12**:769-777.
- Hirokawa, N. and L.G. Tilny (1982). Interactions between actin filaments and between actin filaments and membranes in quick-frozen and deeply etched hair cells of the chick ear. *J. Cell Biol.* **95**:249-261.
- Hoebeke, J., G. Van Nijen and M. De Brabander (1976). Interaction of oncodazole (R 17934), a new antitumoral drug, with rat brain tubulin. *Biochem. Biophys. Res. Comm.* **69**:319-324.
- Hodgkin, A.L. and B.J. Nunn (1988). Control of light-sensitive current in salamander rods. *J. Physiol.* **403**:439-471.
- Hodgkin, A.L., P.A. McNaughton and B.J. Nunn (1987). Measurement of sodium calcium exchange in salamander rods. *J. Physiol.* **391**:347-370.
- Hodgkin, A.L. and B.J. Nunn (1987). The effects of ions on sodium calcium exchange in salamander rods. *J. Physiol.* **391**:371-398.
- Hollyfield, J.G., M.E. Rayborn, D.B. Farber and R.W. Lolly (1982). Selective photoreceptor degeneration during retinal development: the role of altered phosphodiesterase activity and increased levels of cyclic nucleotides. In The Structure of the Eye. Hollyfield, J.G. *Elsevier Biomedical*. Chapt. 11:97-114.
- Honig, B., U. Dinur, K. Nakanishi, V. Balogh-Nair, M.A. Gawinowicz, M. Arnaboldi and M. G. Motto (1979). An external point-charge model for wavelength regulation in visual pigments. *J. Am. Chem. Soc.* **101**:7084-7086.
- Honig, B. and T.G. Ebrey (1982). Protein-chromophore interactions as spectroscopic and photochemical determinants. *Methods in Enzymology.* **88**:462-470.
- Hotta, Y. and J. Shepard (1973). Biochemical aspects of colchicine action on mitotic cells. *Molec. Gen. Genet.* **122**:243-260.
- Hubbard, R. and A. Kropf (1958). The action of light on rhodopsin. *Proc. Natl. Acad. Sci. U.S.A.* **44**:130-139.

- Hudspeth, A.J. (1985). The cellular basis hearing: the biophysics of hair cells. *Science*. **230**:746-752.
- Hudspeth, A.J. and O.D. Corey (1977). Sensitivity, polarity and conductance changes in the response of vertebrate hair cells to controlled mechanical stimuli. *Proc. Natl. Acad. Sci. U.S.A.* **74**:2407-2411.
- Hurley, J.B. (1980). Isolation and recombination of bovine rod outer segment cGMP phosphodiesterase and its regulators. *Biochem. Biophys. Res. Comm.* **92**:505-510.
- Hurley, J.B., B. Barry and T.G. Ebrey (1981). Isolation of an inhibitory protein for the cyclic guanosine 3',5'-monophosphate phosphodiesterase of bovine rod outer segments. *Biochemica et Biophysica Acta.* **675**:359-365.
- Hurley, J.B. and L. Stryer (1982). Purification and characterization of the gamma subunit of cGMP phosphodiesterase from retinal rod outer segments. *J. Biol. Chem.* **257**:11094-11099.
- Jacobs, M. (1979). Tubulin and nucleotides. Microtubules. Hyams & Roberts. *Acad Press.* **255-277**.
- Jennings, J. (1985). Kinetics and mechanism of anion transport in red blood cells. *Ann. Rev. Physiol.* **47**:519-533.
- Julian, F.J. and D.E. Goldman (1962). The effects of mechanical stimulation of some electrical properties of axons. *J. Gen. Physiol.* **46**:297-313.
- Kaplan, M.W. (1984). Distribution and axial diffusion of retinol in bleached rod outer segments of frogs (*Rana pipiens*). *Exp. Eye Res.* **40**:721-729.
- Kaplan, M., R. Iwata and R. Sears (1986). Immunofluorescent staining of microtubules in frog rod outer segments. *Biophys. J. (suppl.)*. **49**:284a.
- Katz, N.L. (1975). Effects of antimitotic alkaloids on frog and rat neuromuscular junction. *Gen. Pharmacol.* **6**:267-270.
- Kaupp, U.B. (1984). The role of calcium in visual transduction. Information and Energy Transduction in Biological Membranes. A. R. Lias. N.Y. 325-339.
- Kaupp, U.B. and K.-Ukodi (1984). Cyclic GMP releases Ca<sup>2+</sup> from leaky rod outer segments. *Vision Res.* **24**:1477-1479.

- Kawamura, S. and M.D. Bownds (1981). Light adaptation of the cyclic GMP phosphodiesterase of frog photoreceptor membranes mediated by ATP and calcium ions. *J. Gen. Physiol.* **77**:571-591.
- Kawamura, S. and M. Murakami (1983). Intracellular injection of cyclic-GMP increases sodium conductance in *Gecko* photoreceptors. *Japan. J. Physiol.* **33**:789-800.
- Kawamura, S. and M. Murakami (1985). Functional role of phosphodiesterase in *Gecko* photoreceptors. *Neurosci. Res. (suppl.)*, **2**:S119-S125.
- Kawamura, S. and M. Murakami (1986). *In Situ* cGMP phosphodiesterase and photoreceptor potential in *Gecko* retina. *J. Gen. Physiol.* **87**:737-759.
- Keith, C.H., R. Ratan, F.R. Maxfield, A. Bajer and M.L. Shelanski (1985). Local cytoplasmic calcium gradients in living mitotic cells. *Nature*. **316**:848-850.
- Knowles, A. (1984). Rhodopsin bleaching intermediates and enzyme activation in the rod outer segment. *Biochem. Soc. Transactions.* **11**:672-674.
- Koch, K-W., N.J. Cook and U.B. Kaupp (1987). The cGMP-dependent channel of vertebrate rod photoreceptors exists in two forms of different cGMP sensitivity and pharmacological behavior. *J. Biol. Chem.* **262**:14415-14421.
- Koch, K-W. and L. Stryer (1988). Highly cooperative feedback control of retinal rod guanylate cyclase by calcium ions. *Nature*. **334**:64-66.
- Kohnken, R.E. and D.G. McConnell (1985). Use of 8-azidoguanosine 5'[gamma-<sup>32</sup>P]triphosphate as a probe of the guanosine 5' triphosphate binding protein subunits in bovine rod outer segments. *Biochem.* **24**:3803-3809.
- Kolesnikov, S.S., A.L. Lyubarsky and E.E. Fesenko (1984). Single anion channels of frog rod plasma membrane. *Vis. Res.* **24**:1295-1300.
- Korenbrod, J.I. (1985). Signal mechanisms of phototransduction in retinal rod. *Critical Rev. in Biochem.* **17**:223-256.
- Korenbrod, J.I. and R.A. Cone (1972). Dark ionic flux and the effects of light in isolated rod outer segments. *J. Gen. Physiol.* **60**:20-45.
- Korenbrod, J.I., D.T. Brown and R.A. Cone (1973). Membrane characteristics and osmotic behavior of isolated rod outer segments. *J. Cell Biol.* **56**:389-398.



- Kornguth, S.E. and E. Sutherland (1975). Isolation and partial characterization of a tubulin-like protein from human and swine synaptosomal membranes. *Biochimica et Biophysica Acta.* **393**:100-114.
- Krishna, G., N. Krishnan, R.T. Fletcher, and G. Chader (1976). Effects of light on cyclic GMP metabolism in retinal photoreceptors. *J. Neurochem.* **27**:717-722.
- Kishnan, N., R.T. Fletcher, G.J. Chader, and G. Krishna (1978). Characterization of guanylate cyclase of rod outer segments of the bovine retina. *Biochimica et Biophysica Acta.* **523**:506-515.
- Kuhn, H. (1976). Light-regulated binding of rhodopsin kinase and other proteins to cattle photoreceptor membranes. *Biochem.* **17**:4389-4395.
- Kuhn, H. (1980). Light and GTP-regulated interaction of GTPase and other proteins with bovine photoreceptor membranes. *Nature.* **283**:587-589.
- Kuhn, H. (1981). Interactions of rod cell proteins with the disk membrane: influence of light, ionic strength and nucleotides. *Curr. Topics in Membranes Transport.* **15**:171-200.
- Kuhn, H. (1984). Interactions between photoexcited rhodopsin and light-activated enzymes in rods. *Prog. Retinal Res.* **3**:123-256.
- Kuhn, H. and W.J. Dreyer (1972). Light dependent phosphorylation of rhodopsin by ATP. *FEBS Lett.* **20**:1-6.
- Kuhn, H., S.W. Hall, and U. Wilden (1984). Light-induced binding of 48-kDa protein to photoreceptor membranes is highly enhanced by phosphorylation of rhodopsin. *FEBS Lett.* **176**:473-479.
- Kupchan, S.M., Y. Komoda, A.R. Franfman, R.G. Dailey and V.A. Zimmerly (1974). Novel maytansinoids: structural interrelation and requirements for antileukemic activity. *J. Am. Chem. Soc.* **96**:3706-3708.
- Lagnado, L., L. Cervetto and P.A. McNaughton (1988). Ion transport by the Na-Ca exchange in isolated rod outer segments. *Proc. Natl. Acad. Sci.* **85**:4548-4552.
- Lamb, T.D., H.R. Matthews and V. Torre (1986). Calcium and light-adaptation in retinal rod photoreceptors. *Biophys. J.* **49**:408a.

- Lamb, T.D. (1986). Transduction in vertebrate photoreceptors: the roles of cyclic GMP and calcium. TINS. Elsevier Sci. Publ., B.V. Amsterdam. 224-228.
- Lamb, T.D. and H.R. Matthews (1988). External and internal actions in the response of salamander retinal rods to altered external calcium concentrations. *J. Physiol.* **403**:473-494.
- Lampedis, T.J., K.W. Trevorrow and R.W. Rubin (1986). Effects of colchicine on cardiac cell function indicate possible role for membrane surface tubulin. *Exp. Cell Res.* **164**:463-470.
- Lassing, I. and U. Lindberg (1985). Specific interaction between phosphatidylinositol 4,5-bisphosphate and profilactin. *Nature*. **316**:472-474.
- Lee, J.C., R.P. Frigon and S.N. Timasheff (1975). Structural stability of calf brain microtubule protein. *Ann. N.Y. Acad. Sci.* **253**:284-291.
- Leeper, H.F., R.A. Norman and D. Copenhagen (1978). Evidence for passive electronic interactions in red rods of toad retina. *Nature (London)*. **275**:234-236.
- Lerea, C.L., D.E. Somer, J.B. Hurley, I.B. Klock and A.H. Bunt-Milam. (1986). Identification of specific transducin alpha-subunits in retinal rod and cone photoreceptors. *Science*. **234**:77-80.
- Liebman, P.A. and E.N. Pugh (1979). The control of phosphodiesterase in rod disk membranes: kinetics, possible mechanisms and significance for vision. *Vis. Res.* **19**:375-380.
- Liebman, P.A. and A. Sitaramayya (1984). The role of G-protein-receptor interaction in amplified phosphodiesterase activation of retinal rods. Adv. in Cyclic Nucleotide and Protein Phosphorylation Research. **17**:215-225.
- Lipton, S.A. (1985). Conditioning hyperpolarization reveals a property of the light-sensitive current in photoreceptors that is modified by cGMP and EGTA. *Brain Research*. **341**:337-349.
- Loike, J.D. and S.B. Horwitz (1976). Effects of podophyllotoxin and VP-16-213 on microtubule assembly *in vitro* and nucleotide transport in HeLa cells. *Biochem.* **15**:5435-5443.

- Ludueña, R.F., M.C. Roach and P. McAda (1978). Competing effects of maytansine and vinblastine on microtubule disassembly. *Fedn. Proc. Fedn. Am. Soc. Exp. Biol.* **37**:1791.
- Ludueña, R.F. (1979). Biochemistry of tubulin. Roberts and Hyam. Microtubules. *Academic Press*. Chapter 2:65-116.
- MacLeish, P.R., E.A. Schwartz and M. Tachibana (1984). Control of the current in solitary rods of the *Ambystoma tigrinum* retina. *J. Physiol.* **348**:645-664.
- Maldow, R.P. and S. Yazulla (1986). Separation and light adaptation of rod and cone signals in the retina of the goldfish. *Vis. Res.* **26**:1655-1666.
- Mao, B., M. Tsuda and T.G. Ebrey (1981). Flash photolysis and low temperature photochemistry of bovine rhodopsin with a fixed 11-ene. *Biophys. J.* **35**:543-546.
- Marantz, R., M. Ventilla and M. Shelanski (1970). Structure of microtubular crystals induced by vinblastine *in vitro*. *J. Cell Biol.* **44**:234-238.
- Marcum, M. J.R. Dedman, B.R. Brinkley and A. Means (1978). Control of microtubule assembly-disassembly by calcium-dependent regulator protein. *Proc. Natl. Acad. Sci. U.S.A.* **75**:3771-3775.
- Matesic, D. and P. A. Liebman (1987). cGMP-dependent channel of retinal rod outer segments. *Nature.* **326**:600-603.
- Matesic, D. and P.A. Liebman (1989). Characterization of rod putative cGMP-cation channel proteins. *Invest. Opthal. and Vis. Sci. (suppl.)*. **30**:172.
- Matsumoto, G., H. Murofushi and H. Sakai (1980). The effects of reagents affecting microtubules and microfilaments on the excitation of the squid giant axon measured by the voltage-clamp method. *Biomed Res.* **1**:355-358.
- Matsumoto, G. and H. Sakai (1979). Microtubules inside the plasma membrane of squid giant axons and their physiological function. *J. Membrane Biol.* **50**:1-14.
- Matthews, G., V. Torre and T.D. Lamb (1985). Effects on the photoresponse of calcium buffers and cyclic GMP incorporated into the cytoplasm of retinal rods. *Nature.* **313**:582-585.
- Matthews, G. and S.-I. Watanabe (1987). Comparison of light-sensitive and cGMP-

- activated conductances of rod photoreceptors at the single-channel level. *Biophys. J.* **51**:16a.
- Matthews, G. (1986). Comparison of light-sensitive and cGMP-sensitive conductances of the rod photoreceptors: noise characteristics. *J. Neurosci.* **6**:2521-2526.
- Matthews, G. and S-T. Watanabe (1988). Activation of single ion channels from toad retinal rod inner segments by cyclic GMP: concentration dependence. *J. Physiol.* **403**:389-405.
- Matthews, H.R., R.L.W. Murphy, G.L. Fain, and T.D. Lamb (1988). Photoreceptor light adaptation is mediated by cytoplasmic calcium concentration. *Nature.* **334**:67-69.
- Matthews, R., R. Hubbard, P.K. Brown and G. Wald (1963). Tautomeric forms of metarhodopsin. *J. Gen. Physiol.* **47**:215-240.
- McClure, W.O. and J.C. Paulson (1977). The interaction of colchicine and some related alkaloids with rat brain tubulin. *Molec. Pharmacol.* **13**:560-575.
- McDonough, A. (1985). Immunodetection of Na,K-ATPase in guinea-pig retinal layers, cornea and lens. *Exp. Eye Res.* **40**:667-674.
- McNaughton, P.A., L. Cervetto and B.J. Nunn (1986). Measurement of the intracellular free calcium concentration in salamander rods. *Nature.* **322**:261-263.
- Meech, R.W. (1972). Intracellular calcium injection causes increased potassium conductance in *Aplysia* nerve cells. *Comp. Biochem. Physiol.* **42a**:494-499.
- Meech, R.W. (1974). The sensitivity of *Helix Aspersa* neurons to injected calcium ions. *J. Physiol.* **237**:259-277.
- Miki, N., J.M. Baraban, J.J. Kerns, J.J. Boyce, M.W. Bitenski (1975). Purification and properties of the light-activated cyclic nucleotide phosphodiesterase of rod outer segment. *J. Biol. Chem.* **250**:6320-6327.
- Milder, S.L. and D.S. Kliger (1986). A new approach to understanding the initial step in visual transduction. *Biophys. J.* **49**:567-570.
- Miller, D. and Korenbrot, J.I. (1987). Kinetics of light-dependent Ca<sup>2+</sup> fluxes across the plasma membrane of rod outer segments. A dynamic model of the regulation of the cytoplasmic Ca<sup>2+</sup> concentrations. *J. Gen. Physiol.* **90**:397-425.

- Miller, W.H. (1982). Physiological evidence that light-mediated decrease in cyclic GMP is an intermediary process in retinal rod transduction. *J. Gen. Physiol.* **80**:103-123.
- Miller, W.H. and G.D. Nicol (1981). Cyclic-GMP-induced depolarization and increased response latency of rods: antagonism by light. Current Topics in Membranes and Transport. chapter 24. 417-436.
- Mitranic, M.M., J.M. Boggs and M.A. Moscarello (1981). An effect of colchicine on galactosyl- and sialyltransferases of rat liver golgi membranes. *Biochimica et Biophysica Acta.* **672**:57-64.
- Mizel, S.B. and L. Wilson (1972). Nucleoside transport in mammalian cells. Inhibited by colchicine. *Biochem.* **11**:2573-2578.
- Molday, R.S. (1988). Monoclonal antibodies to ROS proteins. Prog. in Retinal Res. **8**:173-205.
- Mueller, P. and E.N. Pugh Jr. (1983). Protons block the dark current of isolated retinal rods. *Proc. Natl. Acad. Sci. U.S.A.* **80**:1892-1896.
- Musser, G.L. and S. Rosen (1973). Localization of carbonic anhydrase activity in the vertebrate retina. *Exp. Eye Res.* **15**:105-119.
- Nagle, B.W. and B. Burnside (1984). Calmodulin-binding proteins in teleost retina, rod inner and outer segments and rod cytoskeletons. *European J. Cell Biol.* **33**:248-257.
- Nakatani, K. and K.-W. Yau (1987). A magnesium component in the dark current in retinal rods. *Biophys. J.* **51**:18a.
- Nakatani, K. and K.-W. Yau (1988a). Calcium and magnesium fluxes across the plasma membrane of the toad rod outer segment. *J. Physiol.* **395**:695-729.
- Nakatani, K. and K.-W. Yau (1988b). Calcium and light adaptation in retinal rods and cones. *Nature.* **334**:69-71.
- Nakao, M. and D.C. Gadsby (1986). Voltage dependence of Na<sup>+</sup> translocation by the Na/K pump. *Nature.* **323**:628-630.
- Nicol, G.D., P.P.M. Schnetkamp, Y. Saimi, E.J. Cragoi Jr. and M.D. Bownds (1987). An amiloride derivative blocks the light- and cGMP-regulated conductance in frog rod photoreceptors. *Biophys. J. (suppl.)* **51**:272a.

- Norman, R.A. and I. Periman (1979). The effects of background illumination on the photoresponses of red and green cones. *J. Physiol.* **286**:491-507.
- Oakley, B. II. (1983). Effects of maintained illumination upon  $[K^+]_o$  in the subretinal space of the isolated retina of the toad. *Vision Res.* **23**:1325-1337.
- Oakley, B. II. and L.H. Pinto (1983). Modulation of membrane conductance in rods of *Bufo marinus* by the intracellular calcium ion. *J. Physiol.* **339**:273-298.
- Oakley, B. II. (1987). Measurement of potassium turnover in retinal rod photoreceptors using ion-selective microelectrodes. *Canadian J. of Physiol. Pharmacol.* **65**:1018-1027.
- Oakley, B. II, R.J. Bert and Proenza-Mueller (1985). Electrophysiological assessment of phosphodiesterase activity in rod photoreceptors. *Invest. Ophthalmol. Vis Sci. (suppl.)*. **26**:333.
- O'Connor, P. and B. Burnside (1981). Actin-dependent cell elongation in teleost retinal rods: requirement for actin filament assembly. *J. Cell Biol.* **89**:517-524.
- O'Connor, P. and B. Burnside (1982). Elevation of cyclic AMP activates an actin-dependent contraction in *Teleost* retinal rods. *J. Cell Biol.* **95**:445-452.
- Ohara, S. (1968). Effects of some organic cations on generator potential of crayfish stretch receptors. *J. Gen. Physiol.* **52**:363-386.
- Ohmori, H. (1985). Mechano-electrical transduction currents in isolated vestibular hair cells of the chick. *J. Physiol.* **359**:189-217.
- Olive, J. (1980). The structural organization of mammalian retinal disk membranes. *Int. Rev. Cytol.* **64**:107-169.
- Ostwald, T.J. and J. Heller (1972). Properties of a magnesium- or calcium-dependent adenosine triphosphatase from frog rod photoreceptor outer segment disks and its inhibition by illumination. *Biochem.* **11**:4679-4686.
- Ovchinnikov, Y.A., N.G. Abdulaev, M.Y. Feigina, I.D. Artamonov, A.S. Zolotarev, M.B. Kostina, A.S. Bogachuk, A.I. Moroshnikov, V.I. Martinov and A.B. Kudelin (1982). The complete amino acid sequence of visual rhodopsin. *Bioorg. Khim. (U.S.S.R.)*. **8**:1011-1014.

- Ovchinnikov, Y.A. (1982). Rhodopsin and Bacteriorhodopsin: Structure-function relationships. *FEBS Lett.* **148**:179-191.
- Ovchinnikov, Y.A., V.M. Lipskin, T.M. Shuvawa, A.A. Bogachuk and V.V. Shimyakin (1985). Complete amino acid sequence of gamma-subunit of the GTP-binding protein from cattle retina. *FEBS Lett.* **179**:107-110.
- Owëllen, R.J., D.W. Donigan, C.A. Hartke, R.M. Dickerson and M.J. Kuhar (1974). The binding of vinblastine to tubulin and to particulate fractions of mammalian brain. *Cancer Res.* **34**:3180-3186.
- Papermaster, D.S., B.G. Schneider, D. Defoe and J.C. Besharse (1986). Biosynthesis and vectorial transport of opsin on vesicles in retinal rod photoreceptors. *J. Histochem. Cytochem.* **34**:5-16.
- Papermaster, D.S., B.G. Schneider, N.A. Zorn and J.P. Kraehenbuhl (1978). Immunocytochemical localization of a large intrinsic membrane protein to the incisures and margins of frog rod outer segment discs. *J. Cell Biol.* **78**:415-425.
- Parker, K.R., L.E. Schaechter, J.W. Lewis, K.L. Zeman, D.S. Kliger and E.A. Dratz (1987). Mg<sup>2+</sup>-ATP induces filament growth from retinal rod outer segments with disrupted plasma membranes. *FEBS Lett.* **211**:35-40.
- Parkes, J.H., A. Sitaramayya, J. Harkness and P.A. Liebman (1985). Mechanism of light activation of PDE in rod disk membranes. *Invest. Ophthalmol. Visual Sci. (suppl.)* **26**:45.
- Pech, I.V. and W.L. Stahl (1984). Immunocytochemical localization of Na<sup>+</sup>, K<sup>+</sup>-ATPase in primary cultures of rat retina. *Neurochem. Res.* **9**:759-769.
- Pearce, L.B., R.D. Calhoon, P.R. Burn, A. Vincent and S.M. Goldin (1988). Two functionally distinct forms of guanosine 3', 5'-Phosphate stimulated channels in bovine rod photoreceptor disk preparation. *Biochemistry.* **27**:4396-4406.
- Pellicone, C., N.J. Cook, G. Nullans and N. Virmaux (1985a). Light-induced conformational change in rhodopsin detected by modification of G-protein binding, GTP-gamma-S binding and cGMP phosphodiesterase activation. *FEBS Lett.* **181**:184-188.

- Pellicone, C., G. Nullans and N. Virmaux (1985b). Localization of light-induced conformational changes in bovine rhodopsin. *FEBS Lett.* **181**:179-183.
- Pepe, I.M., I. Panfoli and C. Cugnoli (1986). Guanylate cyclase in rod outer segments of the toad retina: effect of light and  $Ca^{2+}$ . *FEBS Lett.* **203**:73-76.
- Pfister, C., H. Kuhn and M. Chabre (1983). Interaction between photoexcited rhodopsin and peripheral enzymes in frog retinal rods: influence on the postmetarhodopsin II decay and phosphorylation rate of rhodopsin. *FEBS Lett.* **136**:489-499.
- Pfister, C., M. Chabre, J. Plouet, V.V. Tuyen, Y. De Kozak, J.P. Faure and H. Kuhn (1985). Retinal S antigen identified as the 48K protein regulating light-dependent phosphodiesterase in rods. *Science.* **228**:891-893.
- Pierce, M.E. and J.C. Besharse (1985). Regulation of cone retinomotor movements: effects of melatonin, dopamine and GABA. *Invest. Ophthalmol. Vis. Sci. (suppl.)*. **26**:248.
- Poffenbarger, M. and G.M. Fuller (1976). Is melatonin a microtubule inhibitor? *Exp. Cell Res.* **103**:135-141.
- Poffenbarger, M. and G.M. Fuller (1977). Effects of psychotropic drugs on neurotubule assembly. *J. Neurochem.* **28**:1167-1174.
- Proenza, C.A., Bert, R.J. and B. Oakley II. (1986). Phosphodiesterase activity may control dark adaptation in rods. *Invest. Ophthalmol. Vis. Sci. (suppl.)*. **27**:299.
- Pugh, E.N. (1987). The nature and identity of the internal excitational transmitter of vertebrate phototransduction. *Ann. Rev. Physiol.* **49**:715-741.
- Puckett, K.L., E.T. Aronson and S.M. Goldin (1985). ATP-dependent calcium uptake activity associated with a disk membrane fraction isolated from bovine retinal rod outer segments. *Biochem.* **24**:390-400.
- Rasenick, M.M. and N. Wang (1988). Exchange of guanine nucleotides between tubulin and GTP-binding proteins that regulate adenylate cyclase: cytoskeletal modification of neuronal signal transduction. *J. Neurochem.* **51**:300-311
- Rasenick, M.M. (1986). Regulation of neuronal adenylate cyclase by microtubule proteins. *Ann. N.Y. Acad. Sci.* **466**:794-797.



- Rasenick, M.M., P.J. Stein and M.W. Bitensky (1981). The regulatory subunit of adenylate cyclase interacts with cytoskeletal components. *Nature*. **294**:560-562.
- Ratto, G.M., R. Payne, W.G. Owen, and R.Y. Tsien (1988). The concentration of cytosolic free calcium in vertebrate rod outer segments measured with Fura-2. *J. Neurosci.* **8**:3240-3246.
- Regula, C.S., P.R. Sager and R.D. Berlin (1986). Membrane tubulin. *Ann. N.Y. Acad. Sci.* **466**:832-842.
- Rembold, H. and T. Langenbach (1978). Effect of colchicine on cell membrane and on biopterin transport in *Crithidia fasciculata*. *J. Protozool.* **25**:404-408.
- Rispoli, G. and A. Menini (1988). The blocking effect of l-cis-diltiazem on the light-sensitive current of isolated rods of the tiger salamander. *Eur. Biophys. J.* **16**:65-71.
- Robinson, W.E. and W.A. Hagins (1979). GTP hydrolysis in intact rod outer segments and the transmitter cycle in visual excitation. *Nature*. **280**:398-400.
- Rodieck. 1973. The Vertebrate Retina. W.A. Freeman.
- Rodriguez, J.A. and H.S. Berra (1983). Tubulin and tubulin-colchicine complex bind to brain microsomal membrane *in vitro*. *Molecular and Cellular Biochem.* **56**:49-53.
- Roof, D.J. and M.L. Applebury (1985). Cytoskeletal specializations of the vertebrate rod outer segment. *Biolphys. J.* **421**:114a.
- Roof, D. and M. Applebury (1984). Localization of calmodulin and characterization of calmodulin binding proteins in the vertebrate rod outer segment. *Biolphys. J.* **45**:1a.
- Roof, D.J. and J.E. Heuser (1982). Surfaces of rod photoreceptor disk membranes: integral membrane components. *J. Cell Biol.* **95**:501-509.
- Roof, D.J., J.I. Korenbrot and J.E. Heuser (1982). Surfaces of rod photoreceptor disk membranes: light activated enzymes. *J. Cell Biol.* **95**:501-509.
- Rosenfeld, A.C., R.V. Zackroff and R.C. Weisenberg (1976). Magnesium stimulation of calcium binding to tubulin and calcium induced depolymerization of microtubules. *FEBS Lett.* **65**:144-147.
- Rosner, H. and M. Schonharting (1977). Binding of colchicine to isolated gangliosides and ganglioside-containing membranes. *Hoppe-Seyler's Z. Physiol. Chem.* **358**:915-

919.

- Ross, F. and P. Newell (1985). Streamers: chemotactic mutants of *Dictyostelium discoideum* with altered cyclic GMP metabolism. *J. Gen. Microbiol.* **127**:339-350.
- Rushton, W.A.H. (1965). The sensitivity of rods under illumination. *J. Physiol.* **178**:141-160.
- Rushton, W.A.H. (1981). Visual adaptation. Physiology of the Eye. Alder. Ed Moses, R.A. 650-663.
- Rybin, V.O. (1986). Influence of GDP on interaction of transducin with cyclic nucleotide phosphodiesterase and rhodopsin from bovine retinal rods. *Biokhimiya.* **51**:1035-1041.
- Ryips, H., R.E. Carr, I.M. Siegel and V.C. Greenstein (1984). Functional abnormalities in vincristine-induced night blindness. *Invest. Ophthalmol. Vis. Sci.* **25**:787-794.
- Saibil, H.R. (1982). An ordered membrane-cytoskeleton network in squid photoreceptor microvilli. *J. Mol. Biol.* **158**:435-456.
- Sale, W.S., J.C. Besharse and G. Piperno (1988). Distribution of acetylated  $\alpha$ -tubulin in retina and in *in vitro*-assembled microtubules. *Cell Motility and the Cytoskel.* **9**:243-253.
- Scheele, R.B. and G.G. Borisy (1979). *In vitro* assembly of microtubules. Microtubules. Hyams and Roberts. 217-277.
- Schnetkamp, P.P.M. (1987). Sodium ions selectively eliminate the fast component of guanosine cyclic 3', 5'-phosphate-induced  $Ca^{2+}$  release from bovine rod outer segment disks. *Biochemistry.* **26**:3249-3253.
- Schnetkamp, P.P.M. (1979). Calcium translocation and storage in isolated intact cattle rod outer segments in darkness. *Biochem. Biophys. Acta.* **554**:441-459.
- Schnetkamp, P.P.M. (1986). Sodium-calcium exchange in the outer segments of bovine rod photoreceptors. *J. Physiol.* **373**:25-45.
- Schnetkamp, P.P.M. and M.D. Bownds (1987).  $Na^{+}$  and cGMP-induced  $Ca^{2+}$  fluxes in frog rod photoreceptors. *J. Gen. Physiol.* **89**:481-500.
- Schnetkamp and Kamp (1985). Ca-H exchange in isolated bovine rod outer segments.

*Biochemistry*. **24**:723-777.

- Schnetkamp, P.P.M. (1985a). Ionic permeabilities of the plasma membrane of isolated intact bovine rod outer segments as studied with a novel optical probe. *J. Membrane Biol.* **88**:263-275.
- Schnetkamp, P.P.M. (1985b).  $\text{Ca}^{2+}$  buffer sites in intact bovine rod outer segments: introduction to a novel optical probe to measure ionic permeabilities in suspensions of small particles. *J. Membrane Biol.* **88**:249-262.
- Schwartz, E.A. (1977). Voltage noise observed in rods of the turtle retina. *J. Physiol.* **272**:217-246.
- Schwartz, E.A. (1985). Phototransduction in vertebrate rods. *Ann. Rev. of Neurosci.* **8**:339-367.
- Sherline, P., J.T. Leung and D.M. Kipnis (1975). Binding of colchicine to purified microtubule protein. *J. Biol. Chem.* **250**:5481-5486.
- Shichi, H., K. Yamamoto and R.L. Somers (1984). GTP binding protein: properties and lack of activation by phosphorylated rhodopsin. *Vis. Res.* **24**:1523-1531.
- Shichi, H. and R.L. Somers (1984). Regulation of rod GTP binding protein by guanine nucleotides. *J. Biochem.* **96**:1633-1636.
- Shimazaki, H. and B. Oakley II (1984). Reaccumulation of  $[\text{K}^+]_o$  in the Toad Retina during maintained illumination. *J. Gen. Physiol.* **84**:475-504.
- Shimazaki, H. and B. Oakley II (1986). Decline of electrogenic Na/K pump activity in rod photoreceptors during maintained illumination. *J. Gen. Physiol.* **87**:633-647.
- Sillman, A.J., H. Ito and T. Tomita (1969). Studies on the mass receptor potential of the isolated frog retina. II. On the basis of the ionic mechanism. *Vis. Res.* **9**:1443-1451.
- Sitaramayya, A., J. Harkness, J.H. Parkes, C. Gonzalez-Oliva and P.A. Liebman (1986). Kinetic studies suggest that light-activated cyclic GMP phosphodiesterase is a complex with G-protein subunits. *Biochem.* **25**:651-656.
- Sitaramayya, A., C. Casadevall, N. Bennett and S.I. Hakki (1988). Contribution of the guanosine triphosphatase activity of G-Protein to termination of light-activated guanosine cyclic 3', 5'-phosphate hydrolysis in retinal rod outer segments.

*Biochemistry*. **27**:4880-4887.

- Sitaramayya, A. and P. Liebman (1983). Mechanism of ATP quench of phosphodiesterase activation in rod disc membranes. *J. Biol. Chem.* **258**:1205.
- Smith, H.G. and P.M. Capalbo (1985). External calcium inhibits the efflux of calcium from isolated retinal rod outer segment disks. *Biochemistry*. **24**:4233-4239.
- Solomon, F. (1977). Calcium binding activity of tubulin. *Biochemistry*. **16**:358-363.
- Spira, A.W. and G.E. Milman (1982). Filament arrays in the photoreceptor cell of the human, monkey and guinea pig retina. Structure of the Eye. Hollyfield. Elsevier. Chapter 1: pp.1-40.
- Stadler, J. and W.W. Franke (1972). Colchicine-binding proteins in chromatin and membranes. *Nature*. **237**:237-238.
- Stadler, J. and W.W. Franke (1974). Characterization of the colchicine binding of membrane fractions from rat and mouse liver. *J. Cell Biol.* **60**:297-303.
- Stein, P.J., K.R. Halliday and M.M. Rasenick (1985). Photoreceptor GTP binding protein mediates fluoride activation of phosphodiesterase. *J. Biol. Chem.* **260**:9081-9084.
- Stein, P.J., M.M. Rasenick and M.W. Bitensky (1982). Biochemistry of the cyclic nucleotide-related enzymes in rod photoreceptors. Progress in Retinal Research. Pergamon Press. N.Y. Chapter 1:222-238.
- Steinberg, R.H., B. Oakley II. and G. Niemyer (1980). Light-evoked changes in  $[K^+]_o$  in retina of intact cat eye. *J. Neurophysiol.* **44**:897-921.
- Steinberg, R.H. and I. Wood (1975). Clefs and microtubules of photoreceptor outer segments in the retina of the domestic cat. *J. Ultrastruct. Res.* **51**:397-403.
- Stern, J.H., U.B. Kaupp and P.R. Mac Leish (1986). Control of the light-regulated current in rod photoreceptors by cyclic GMP, calcium and l-cis diltiazem. *Proc. Natl. Acad. Sci. U.S.A.* **83**:1163-1167.
- Stern, J.H., H. Knutson and P.R. MacLeish (1987). Divalent cations directly affect the conductance of excised patches of rod photoreceptor membranes. *Science*. **236**:1674-1678.
- Stirling, C.E. and A. Lee (1980).  $^3H$  ouabain autoradiography of frog retina. *J. Cell Biol.*

85:313.

Stryer, L. (1986). Cyclic GMP cascade of vision. *Ann. Rev. Neurosci.* **9**:87-119.

Stryer, L., J.B. Hurley and K.-K. Fung, (1981). Transducin: an amplifier protein in vision. *Trends Biochem. Sci* **6**:245-247.

Summers, K.E. and M.W. Kirschner (1977). The effect of polarity and capping on microtubule stability *in vitro* as observed by darkfield light microscopy. *J. Cell Biol.* **75**:296a.

Swartz, E.A. (1977). Voltage-noise observed in rods of turtle retina. *J. Physiol.* **272**:217.

Szuts, E.Z. (1985). Light stimulates phosphorylation of two large membrane proteins in frog photoreceptors. *Biochem.* **24**:4176-4184.

Tan, L.P. and J.R. Lagnado (1975). Effects of indole alkaloids and related compounds on the properties of brain microtubular proteins. *Biochem. Soc. Trans.* **3**:121-124.

Tanaka, J.C., R.E. Furman, W.H. Cobbs and P. Mueller (1987). Incorporation of a retinal rod cGMP-dependent conductance into lipid bilayers. *Proc. Natl. Acad. Sci. U.S.A.* **84**:724-728.

Tasaki, I., K. Swasa and R.C. Gibbons (1980). Mechanical changes in crab nerve fibers during action potential. *Japan J. Physiol.* **30**:897-905.

Terakawa, S. and T. Nakayama (1985). Are axoplasmic microtubules necessary for membrane excitation? *J. Membrane Biol.* **85**:65-77.

Terakawa, S. and A. Watanabe (1976). Effects of colchicine and other antimetabolic drugs on the electrophysiological properties of a crayfish axonal membrane. *Proc. Jpn. Acad. Sci.* **52**:82-85.

Torre, V. and W.G. Owen (1983). High-pass filtering of small signals by the rod network in the retina of the toad, *Bufo Marinus*. *Biophysical J.* **41**:305-324

Townes-Anderson, E., P.R. MacLeish and E. Raviola (1985). Rod cells dissociated from mature salamander retina: ultrastructure and uptake of horseradish peroxidase. *J. Cell Biol.* **100**:175-188.

Toyoda, J., H. Hashimoto, H. Anno and T. Tomita (1970). The rod response in the frog as studied by intracellular recording. *Vision. Res.* **10**:1983.

- Troyer, E.W., I.A. Hall and J.A. Rerrendelli (1978). Guanylate cyclases in CNS: enzymatic characteristics of soluble and particulate enzymes from mouse cerebellum and retina. *J. Neurochem.* **31**:825-833.
- Tyminski, P.N. and D.F. O'Brien (1984). Rod outer segment phosphodiesterase binding and activation in reconstituted membranes. *Biochem.* **23**:3986-3993.
- Ueno, S., H.J. Bambauer, H. Umar and M. Ueck (1984a). A new histo- and cytochemical method for demonstration of cyclic 3',5'-nucleotide phosphodiesterase activity in retinal rod photoreceptor cells of the rat. *Histochemistry.* **81**:445-451.
- Ueno, S., H.J. Bambauer, H. Umar and M. Ueck (1984b). Localization and function of cyclic guanosine monophosphate-phosphodiesterase activity in the retinal rods of the rat by means of a newly developed cytochemical method. *Cell Tissue Res.* **238**:453-457.
- Ueno, S., H.J. Bambauer, H. Umar, M. Ueck and K. Ogawa (1984c). Ultracytochemical study of Ca<sup>2+</sup>-ATPase and K<sup>+</sup>-NPPase activities in retinal photoreceptors of the guinea pig. *Cell Tissue Res.* **237**:479-489.
- Usukura, J. and E. Yamada (1981). Molecular organization of the rod outer segment in deep-etching study with rapid freezing using unfixed frog retina. *Biomedical Res.* **7**:177-193.
- Usukura, J. and D. Bok (1986). Immunocytochemistry and ultrastructure of freeze-substituted photoreceptor cells. *Proc. Int. Soc. for Eye Research.* **IV**:R-P18.
- Valeton, J.M. and D. Van Noeren (1983). Light adaptation of primate cones: an analysis based on extracellular data. *Vis. Res.* **23**:1539-1548.
- Van Reempts, J.L., M. Borgers, S.R. De Nollin, T.C. Garrevoet and W.A. Jacob (1984). Identification of calcium in the retina by the combined use of ultrastructural cytochemistry and laser microprobe mass analysis. *J. Histochem. Cytochem.* **32**:788-792.
- Virmaux, N., V.V. Tuyen and J.E. Hesketh (1980). Myosin in bovine retinal photoreceptors. *Ophthalmic Res.* **12**:151.
- Volotovski, I.D. and V.I. Khovratovich (1986). Coupling between transmembrane calcium

- transport and membrane potential in retinal rod discs. *Proc. R. Soc. Lond.* **228**:97-108.
- Volpe, P., C. Salvati, F. DiVirgilio and T. Pozzan (1985). Inositol 1,4,5-trisphosphate induces calcium release from sarcoplasmic reticulum of skeletal muscle. *Nature*. **316**:347-349.
- Waloga, G. (1983). Effects of calcium and guanosine-3'5'-cyclic-monophosphoric acid on photoreceptor potentials of toad rods. *J. Physiol.* **341**:341-357.
- Waloga, G. (1985). Inositol-1,4,5-triphosphate may be a messenger for vertebrate phototransduction. *Invest. Ophthalmol. Vis. Sci. (suppl.)*. **26**:167.
- Watkins, P.A., J. Moss, D.L. Burns, E.L. Hewlett and M. Vaughan (1984). Inhibition of bovine rod outer segment GTPase by *Bordetella pertussis* toxin. *J. Biol. Chem.* **259**:1378-1381.
- Wheeler, C.L. and M.W. Bitensky (1977). A light-activated GTPase in vertebrate photoreceptors: regulation of light-activated cyclic GMP phosphodiesterase. *Proc. Natl. Acad. Sci. U.S.A.* **74**:4238-4242.
- Wilden, U. and H. Kuhn (1982). Light-dependent phosphorylation of rhodopsin: number of phosphorylation sites. *Biochem.* **21**:3014-3022.
- Wilden, U., S. Hall and H. Kuhn (1986). Phosphodiesterase activation by photoexcited rhodopsin is quenched when rhodopsin is phosphorylated and binds 48 Kda-protein. *Proc. Natl. Acad. Sci. U.S.A.* **83**:1174-1178.
- Wilson, L. (1970). Properties of colchicine binding protein from chick embryo brain. Interactions with vinca alkaloids and podophyllotoxin. *Biochem.* **9**:4999-5007.
- Wilson, L., J.R. Bramburg, S.B. Mizel, L.M. Brishham and K.M. Creswell (1974). Interaction of drugs with microtubule proteins. *Fedn. Proc. Fedn. Am. Soc. Exp. Biol.* **33**:158-166.
- Wilson, L. (1975). Microtubules as drug receptors: pharmacological properties of microtubule protein. *Ann. N.Y. Acad. Sci.* **253**:213-231.
- Winston, M., E. Johnson, J.K. Kelleher, S. Banerjee and L. Margulis (1974). Melatonin: cellular effects on live *Stentors* correlated with the inhibition of colchicine-binding to

- microtubule protein. *Cytobios.* **9**:237-243.
- Wistrand, P.J., M. Schenholm and G. Lonnerholm (1986). Carbonic anhydrase isoenzymes CA I and CA II in the human eye. *Invest. Ophthalmol. Vis. Sci.* **27**:419-428.
- Witkovski, P., F.E. Dudek and H. Ripps (1975). Slow P III component of the carp electroretinogram. *J. Gen. Physiol.* **65**:119-134.
- Witkovski, P., J. Nelson and H. Ripps (1973). Action spectra and adaptation properties of carp photoreceptors. *J. Gen. Physiol.* **61**:401-423.
- Woodruff, M.L. and M.D. Bownds (1979). Amplitude, kinetics and reversibility of a light-induced decrease in guanosine 3',5'-cyclic monophosphate in frog photoreceptor membranes. *J. Gen. Physiol.* **73**:629-653.
- Woodruff, M.L., B.L. Bastian and G.L. Fain (1982). Light-dependent ion influx into toad photoreceptors. *J. Gen. Physiol.* **80**:517.
- Wormington, C.M. and R.A. Cone (1978). Ion blockage of the light-regulated sodium channels of isolated rod outer segments. *J. Gen. Physiol.* **71**:657-681.
- Yahara, I. and G.M. Edelman (1975). Modulation of lymphocyte receptor mobility by concanavalin A and colchicine. *Ann. N.Y. Acad. Sci.* **253**:455-469.
- Yamazaki, A., F. Bartucca, A. Ting and M.W. Bitensky (1982). Reciprocal effects of an inhibitory factor on catalytic activity and noncatalytic cGMP binding sites of rod phosphodiesterase. *Proc. Natl. Acad. Sci. U.S.A.* **79**:3702-3706.
- Yamazaki, A., I. Sen and M.W. Bitensky (1980). Cyclic GMP-specific, high-affinity, non-catalytic binding sites on light-activated phosphodiesterase. *J. Biol. Chem.* **255**:11619-11624.
- Yamazaki, A., P.J. Stein, N. Chernoff and M.W. Bitensky (1983). Activation mechanism of rod outer segment cyclic GMP phosphodiesterase: release of inhibitor by the GTP/GDP-binding protein. *J. Biol. Chem.* **258**:8188-8194.
- Yamazaki, A., K.R. Halliday, J.S. George, S. Nagao, C-H. Kuo, K.S. Ailsworth and M.W. Bitensky (1985). Homology between light-activated photoreceptor phosphodiesterase and hormone-activated adenylate cyclase systems. *Adv. Cyclic*



*Nucleotide and Protein Phosphorylation Res.* **19**:113-124.

- Yang, X., F. Guhuray and F. Sachs (1986). Mechanotransducing ion channels: ionic selectivity and coupling to viscoelastic components of the cytoskeleton. *Biophys. J.* **49**:373a.
- Yau, K.W. and L. Haynes (1986). Effect of divalent cations on the macroscopic cGMP-activated current in excised rod membrane patches. *Biophys. J.* **49**:33a.
- Yau, K.W., P.A. McNaughton and A.L. Hodgkin (1981). Effect of ions on the light-sensitive current in retinal rods. *Nature.* **292**:502-505.
- Yau, K.W. and K. Nakatani (1984a). Electrogenic Na-Ca exchange in retinal rod outer segment. *Nature.* **311**:661-663.
- Yau, K.W. and K. Nakatani (1984b). Cation selectivity of light-sensitive conductances in retinal rods. *Nature.* **309**:352-354.
- Yau, K.W. and K. Nakatani (1985a). Light-induced reduction of cytoplasmic free calcium in retinal rod outer segments. *Nature.* **313**:579-582.
- Yau, K.W. and K. Nakatani (1985b). Light-suppressible, cyclic GMP-sensitive conductance in the plasma membrane of a truncated rod outer segment. *Nature.* **317**:252-255.
- Yee, R. and P.A. Liebman (1978). Light-activated phosphodiesterase of the rod outer segment: kinetics and parameters of activation and deactivation. *J. Biol. Chem.* **253**:8902-8909.
- Yoshikami, S. and W.A. Hagins (1971). Light, calcium and the photocurrent of rods and cones. Abstracts of the Biophys. Soc. Meeting. 47a.
- Yoshikami, S. and W.A. Hagins (1973). Control of the dark current in vertebrate rods and cones. Biochemistry and Physiology of Visual Pigments. Langer, H. *Springer-Verlag. Berlin.* 245-256.
- Yoshikami, S., J.S. George and W.A. Hagins (1980). Light-induced calcium fluxes from outer segment layer of vertebrate retinas. *Nature (London).* **286**:395-397.
- Zimmerman, A.L. and D.A. Baylor (1986). Cyclic GMP-sensitive conductance of retinal rods consists of aqueous pores. *Nature.* **321**:70-72.
- Zimmerman, A.L. and D.A. Baylor (1987). Interactions of cations with the cyclic GMP-

- sensitive channel of retinal rods. *Biophys. J.* **51**:17a.
- Zimmerman, A.L. and D.A. Baylor (1988). Gating kinetics of the cGMP-activated channel of retinal rods. *Biophys. J.* **53**:37a.
- Zuckerman, R. (1973). Ionic analysis of photoreceptor membrane currents. *J. Physiol.* **235**:333-354.
- Zuckerman, R., G.J. Schmidt and S.M. Dacko (1982). Rhodopsin-to-metarhodopsin II transition triggers amplified changes in cytosol ATP and ADP in intact retinal rod outer segments. *Proc. Natl. Acad. Sci. U.S.A.* **79**:6414-6418.
- Zuckerman, R., B. Buzdygon, P. Liebman and A. Sitaramayya (1985). Arrestin: An ATP/ADP exchange protein that regulates cGMP phosphodiesterase activity in retinal rod disk membranes (RDM). *Biophys. J.* **47**:37a.
- Zurer, P.S. (1983). The chemistry of vision. *Chemical & Engineering News.* **61**:24-35.

## VITA

Robert Bert, born on May 7, 1954, in Perryville, Missouri, received his Bachelor's Degree in Civil Engineering from the University of Missouri, Rolla in December of 1976. From January of 1977 - January of 1982, he was employed by the Wisconsin Power & Light Company. In January, 1981, he received his Wisconsin Professional Engineers license after fulfilling the required four years as an Engineer in Training. Robert attended the University of Wisconsin during his last two years of employment, where he fulfilled his premedical requirements in biology and chemistry. He began the Master's Degree Program in Biomedical Engineering at the University of Wisconsin in January, 1982, but he left this program before completing his thesis to attend the Medical Scholars Program at the University of Illinois in August of 1983. While pursuing his PhD, degree, he was the recipient of 3 University of Illinois College of Medicine Summer Research Fellowships (1984, 1985 & 1986), and a University Fellowship for the 1988 - 1989 school year. He successfully defended his PhD thesis in Neurobiology in August, 1989. He has finished two and one-half years of training in medicine and he passed the National Boards Part I exam in 1988. He started his medical clerkships in August of 1989, and has completed his clerkships in Psychiatry and Obstetrics & Gynecology.